TERVALENT NICKEL AND COPPER

IN AQUEOUS SOLUTION

by

Kevin Douglas WHITBURN
B.Sc.(Hons), Adelaide, 1972

Thesis presented for the degree of

Doctor of Philosophy

Department of Physical and Inorganic Chemistry

UNIVERSITY of ADELAIDE

November, 1976

Awarded August 1977

This thesis contains no material previously submitted for a degree or diploma in any University, and, to the best of my knowledge contains no material previously published or written by another person, except where due reference is made in the text.

Kevin D. Whitburn
November, 1976.

ACKNOWLEDGEMENTS

I wish to sincerely thank my supervisor, Dr. Gerald S. Laurence, for his help and encouragement throughout this project. I express my gratitude to Dr. A. T. Thornton and the other members of the staff and fellow students for their help with this work.

I acknowledge with thanks the financial assistance of a Commonwealth Postgraduate Scholarship, and of the Australian Research Grants Committee. I express gratitude to the Australian Institute of Nuclear Science and Engineering in making available their facilities at the Australian Atomic Energy Commission Research Establishment.

Finally, I wish to thank Mrs. J. B. Schilling for typing this manuscript, and Mr. Barry Hibble for his assistance in copying of the thesis. Also, I wish to thank my wife Judith for her tolerance and patience during the trying periods of this work.

ABSTRACT

1. The unusual tervalent oxidation states of nickel and copper were generated by inorganic free radical oxidations of the corresponding bivalent states using mainly the flash photolysis technique, and to a small extent pulse radiolysis.

The trans [14] - series of 'Curtis' macrocyclic complexes were used in this work, varying from the fully unsaturated to the fully saturated complex; viz. the tetene, diene and tetramine. All three complexes were used for the nickel study, whereas only the diene complex was used for the copper.

Hydroxyl radical attack on the bivalent Ni tetramine and diene complexes involved simultaneous reaction with both the metal centre and the ligand. The proportion of each oxidation product was very pH dependent in the range 0 - 5. Only metal centre attack occurred on the unsaturated tetene complex. No evidence for simultaneous OH attack on the Cu(II)diene complex was obtained, with Cu(III)being the only oxidized product. The dihalogen radical-anions Cl_2^- and Br_2^- oxidized the three Ni(II) complexes to the tervalent state; $(SCN)_2^-$ oxidized only the tetramine and diene complexes, whilst I_2^- oxidized none of the bivalent complexes at an observable rate. Of the X_2^- radicals, only Cl_2^- oxidized Cu(II)di to tervalent copper.

At near neutral pH, the conversion of the tervalent nickel tetramine and diene complexes to a coordinated ligand-radical intermediate, $Ni(II)L^{\bullet}$, was observed. The observed second-order decomposition of M(III)L in acidic halide solutions was determined to be an anion-bridged electron-transfer mechanism;

$$M(III)L.X^{-}\ M(III)L \longrightarrow M(II)L + M(II)L_{ox} + X^{-} + 2H^{+}$$

where the $M(II)L_{ox}$ product contained no evidence of further ligand unsaturation. This product is considered to be the hydroxy-substituted macrocyclic complex.

The decay of NI(III)L, Ni(II)L$^{\bullet}$, Cu(III)diene with the hydroperoxy radical was studied in detail over the pH range 0 - 5. The transient complex oxidations of H_2O_2, Fe^{2+} and Mn^{2+} were investigated. A decay process believed to involve ligand fragmentation was observable under conditions of very low halide concentration and absence of recognized reductants.

2. Relevant rate constants are listed below:

		$k(M^{-1}sec^{-1})$ pH 2.0
OH + Ni(II)	tetene	$1.2\ (\pm 0.2) \times 10^{10}$
	diene	$6\ (\pm 2) \times 10^{9}$
	tetramine	$4.3\ (\pm 1.5) \times 10^{9}$
Cu(II)	diene	$1.5\ (\pm 0.3) \times 10^{10}$

		$k(M^{-1}sec^{-1})$ pH 1.0
Cl_2^{-} + Ni(II)	tetene	$1.2\ (\pm 0.2) \times 10^{10}$
	diene	$1.0\ (\pm 0.2) \times 10^{10}$
Cu(II)	diene	$1.5\ (\pm 0.2) \times 10^{8}$

		$k(M^{-1}sec^{-1})$ pH 1.0
Br_2^{-} + Ni(II)	tetene	$2.6\ (\pm 0.6) \times 10^{9}$
	diene	$2.2\ (\pm 0.7) \times 10^{9}$
	tetramine	$\sim 4 \times 10^{9}$
Cu(II)	diene	$\lesssim 10^{5}$

		$k(M^{-1}sec^{-1})$ pH 1.0
$(SCN)_2^-$ + Ni(II)tetene		~2 x 10^8
	diene	~6 x 10^8
	tetramine	$\lesssim 10^8$
I_2^- + Ni(II)L		$\lesssim 5 \times 10^7 M^{-1}sec^{-1}$
HO_2 + Ni(II)tetramine	(0.1M Br^-, pH 1.0)	$1.1(\pm 0.2) \times 10^7 M^{-1}sec^{-1}$

	$k(M^{-1}sec^{-1})$ pH 6.3
Ni(III)L + O_2^-	1 - 2 x 10^9

		$k(sec^{-1})$ pH 4.0
Ni(III)L ⟶ Ni(II)L•diene		~100
	tetramine	~150

		$k(M^{-1}sec^{-1})$ pH 1.0
Ni(III)L.Br^-. Ni(III)L (0.1M Br^-)	tetene	1.4 x 10^8
	diene	4.8 x 10^6
	tetramine	2.5 x 10^5

Ni(III)tam + Br^- ⟷ Ni(III)tam. Br^- $\quad K = 14\ M^{-1}$

Cu(III)di.Cl^-. Cu(III)di $\quad$ (313nm) $\frac{k}{\varepsilon l} \simeq 29sec^{-1}$ at pH 1.0

Ni(III)tam.HO_2.Ni(III)tam (pH 0.3) $\quad k = 1.2 \times 10^7 M^{-1}sec^{-1}$

		$k(M^{-1}sec^{-1})$ pH 1.0
Ni(III)L + H_2O_2		
	tetene	3.3 (±0.4) x 10^3
	diene	2.3 (±0.3) x 10^3
	tetramine	1.2 (±0.3) x 10^2

$Ni(III)L + Fe^{2+}$		$k(M^{-1}sec^{-1})$ pH 1.0
	tetene	$3.6\ (\pm0.4) \times 10^{4}$
	diene	$2.1\ (\pm0.5) \times 10^{8}$
	tetramine	$4.2\ (\pm0.6) \times 10^{4}$

$Ni(III)L + Mn^{2+}$		$k(M^{-1}sec^{-1})$ pH 1.0
	tetene	$1.5\ (\pm0.2) \times 10^{2}$
	diene	$\lesssim 10$
	tetramine	$\lesssim 10$

$Ni(III)L + Co^{2+}$ $\lesssim 1\ M^{-1}sec^{-1}$

TABLE of CONTENTS

Page

II EXPERIMENTAL

I INTRODUCTION

1. TERVALENT NICKEL AND COPPER

1.1 General

The metals of the first transition series from titanium to copper are noted for the variable valence which they display in their simple salts and complexes. This behaviour arises from the presence of an incomplete 3d shell of electrons. With the availability of d orbitals for bond formation, these elements form a large number of compounds with various stereochemical arrangements. There is an established trend towards decreased stability for high oxidation states across the period, with the high oxidation states having powerful oxidizing properties.(1)

In terms of variable valence, Ni is more conservative than the other transition elements. The only important and extensively studied oxidation state of Ni that occurs in aqueous solution is Ni(II), and the (III) and (IV) states appear in only a few compounds and complexes. The solution chemistry of these higher oxidation states is mostly non-aqueous. Ni(0) and Ni(I) are also very scarce.(1) Historically, the reluctance to accept the possibility of valence states other than the common one Ni(II) was reflected in the gross structural misinterpretations of $Ni(CO)_4$(2) - formally a Ni(0) complex, and of oxides which varied in composition from Ni_2O_3 to NiO_2.(3)

The most common oxidation states of copper are the (II) and (I) states. The relative stabilities of the aquated cuprous and cupric states are indicated by the equilibrium

$$2\ Cu^{+} = Cu^{2+} + Cu$$

for which $K = [Cu^{2+}] / [Cu^{+}]^2 \sim 10^6$.[1] The comparative stability of each state depends on several parameters; the nature of anions or other ligands present, on the dielectric constant of the solution, and on the nature of neighbouring atoms in a crystal. The Cu(II)/Cu(I) couple plays an important role, probably second only to iron among the transition metals, in biological redox processes. The tervalent state for Cu is unusual, and, while stable in the solid state, is unstable even in aprotic solvent.[1]

The general acceptance of the Ni(III) state over the years has been gradual. Reported compounds containing the Ni(III) state include halides and oxides,[4] and complexes with a variety of ligands; amines[6-9] arsines,[10-12] phosphines,[13-15] bidentate ligands containing two -NH- functions,[16-17] two -S- functions[18,19] (1,2-dithiolates), one -NH- and one -S- function,[20] monoacido ligands such as fluorides,[21] and tetradentate macrocyclic ligands having saturated nitrogen donors.[22] It has also been suggested that certain naturally occurring ores of Ni contain the metal in the trivalent state.[3] Much of the controversy in the past has centred around the problem of whether the oxidation of the Ni(II) compound actually involved the ligand rather than the metal centre. Detailed studies of several of these compounds have been made in an attempt to unequivocally establish the trivalent state of the metal.

In earlier investigations, most authors have based their claims of authenticity of the (III) state on the results of magnetic moment measurements which have been consistent with the presence of one unpaired electron in the d^7 structure. However, such measurements corresponding

to one unpaired electron can also be interpreted as Ni(II)-stabilized ligand cation radicals in which the unpaired electron is localized on the ligands. Such was the case when the presumed Ni(III) complex [Ni(O - phenylenebisdimethylarsine)$_2$Cl$_2$] Cl was re-examined by X-ray diffraction and e.p.r. spectroscopy,[23] where it was concluded that indeed this complex would be more properly described as a Ni(II) - stabilized ligand cation radical. In the light of these results the authenticity of certain presumed Ni(III) complexes is considered suspect. Only detailed ESR spectral studies will distinguish between the two possibilities.

There is enough evidence now available in the literature[6,7,9] to prove that at least the oxidized form of Ni complexes with saturated aliphatic amines do contain a central Ni ion in its trivalent state. Such complexes have been shown to be stable in the solid state and in solution in different organic solvents. These complexes, as with all the known trivalent Ni complexes, are unstable in aqueous solution (with the possible exception of the di-oxime complexes in strong alkaline solutions[24]). Cu(III), which is isoelectronic with Ni(II), occurs in several crystalline compounds. Among them are alkali and alkali-earth cuprates (e.g. Na Cu O_2),[1] and complexes; $[Cu(biuret)_2]^{+}$[16], $[Cu(IO_6)_2]^{7-}$[73] and $[Cu(HTeO_6)_2]^{7-}$[74], K_3CuF_6[71], and Cu $Br_2S_2CN-(n-C_4H_9)_2$, an orgonometallic complex.[72] The Cu(III) species were unstable in aqueous solution.

1.2 Previous inference to M(III)

Inferences of the Ni(III) state have been made in various chemical redox reactions. It has been postulated that Ni(III) complexes were

formed as intermediates in the spontaneous oxidation of mono-, di-, and triaminoguanidine Ni(II) compounds by atmospheric oxygen.[25] This spontaneous exothermic absorption of oxygen illustrated the ease with which some square-planar Ni(II) compounds could undergo oxidation. The tervalent state of copper was suggested as an intermediate in the copper-catalyzed oxidations of oxalate[75] and diethylamine[76] by $S_2O_8^{2-}$. The formation of Cu(III) as intermediate was suggested to account for the Cu - catalyzed oxidation of Mn^{2+} to MnO_4^- by OBr^-[77]. More recently, it has been proposed that the radiolytic induced oxidative deamination of amino acids, peptides, and ethylenediamine is catalyzed by Cu^{2+} via the formation of trivalent copper which oxidizes its ligands.[62, 79-81]

In basic aqueous media, oxygen and other oxidizing agents oxidized an aliphatic α-amine - oxime Ni(II) complex, leading to aromatization of the complex.[26] The four electrons ultimately removed from the organic part of the complex were presumed to be transferred through the metal ion centre, involving a (III) (or (IV)) oxidation state as an intermediate. Although no evidence for such intermediates was found, it was presumed that the oxidizing agent associated at the metal ion axial positions and transferred electrons through the metal ion.

It has been suggested that trivalent Ni,[27] and Cu[28] complexes of ethylenidiamine are formed as an intermediate in the electrocatalytic oxidation of ethylenediamine on platinum electodes. Very recently it has been reported that the tervalent state of Ni is involved as an intermediate in alkoxy radical oxidations of Ni(II) di-n-butyl-dithiocarbamate and diisothiophosphate complexes in non-aqueous solvents.[5]

1.3 Biological Models

To a large degree, the significant chemical behaviour of naturally occurring macrocyclic ligand transition metal complexes of biological interest such as the porphyrin and corrin ring systems, and the industrially important metal phthalocyanine complexes, depends on their facile redox properties.[29] The synthesis and properties of simpler inorganic systems, namely the square-planar tetradentate macrocyclic amino ligands, which can imitate certain of the properties of the naturally occurring complexes, have been described in an extensive review published by Curtis.[30] There are two major features distinguishing the tetra-aza macrocycles used in this study from the other classes of macrocyclic complexes; the absence of conjugation involving the donor nitrogen atoms, and the absence of fused ring systems. These complexes can serve as models for the biological systems to the extent that their properties are characteristic of metal ions coordinated to the tetra-aza macrocycles, but the greater flexibility of the macrocycles, and the limited ability to transmit electronic effects through the ligand because of lack of conjugation restrict their usefulness as models.

The natural and synthetic complexes can undergo a diverse array of chemical reactions, including ligand oxidative dehydrogenation,[30-34] metal alkylation,[35-37] ligand substitution,[38-40] and hydrogenation[41-43]. The very occurrence of some of these reactions is intimately linked with the ability of higher and lower oxidation states of the metal centre of these complexes to function as reactive intermediates. The remarkable kinetic inertness of the macrocyclic complexes to hydrolysis and substitution, even for normally considered labile metal ions, affords them the ability to stabilize a wide range of oxidation states of a

coordinated metal ion. This has been amply demonstrated for Ni and Cu by the studies of Olson and Vasilevskis.[9, 44] More recently Ni(III) complexes with macrocyclic ligands of the cyclic tetramine series have been reported.[22] The redox behaviour of the nickel cyclic amines was found to be a unique property of their cyclic nature, since a non-cyclic square-planar (Ni(II) saturated amine complex did not undergo one-electron redox reactions.[9] The overall redox behaviour of a range of such macrocyclic complexes in a given solvent was found to be a composite function of various factors including ring size, ring substituents, degree and type of unsaturation, charge type, and co-ordination number. It has been possible to document, in a semi-quantitative manner, the effects of such factors, and a concept of additivity of structural contributions to redox behaviour has been proposed.[29]

1.4 The Macrocyclic Effect

The considerable stability (both thermodynamically and kinetically) of the macrocyclic ligands in aqueous solution with respect to dissociation of the ligand from the metal, over the corresponding open-chain analogues, is referred to as the macrocyclic effect. This effect is distinct from the normal chelate effect because there is an additional enhancement in stability beyond that expected for the gain in translational entropy when chelates replace coordinated solvent around metal ions. The effect has been assigned[45] to a more negative ΔH^{o} for the complexation of the macrocycle compared with the open-chain ligand because it is less solvated by water than the latter due to its lack of open structure in the uncomplexed form. The macrocycle is not able to

accommodate as many H-bonded water molecules with its nitrogen donors because of steric hindrance. Thus, less enthalpic energy need be expended in breaking H-bonds with the solvent and a more favourable ΔH^{o} is found for macrocycle complexation. It should be noted that there is an associated effect of less positive ΔS^{o} for macrocycle complexation because less water molecules are released from the ligand.

It is the strong ligand field exerted by these macrocyclic ligands on the Ni(II) ion that raises antibonding orbital energies sufficiently to allow removal of an electron as a low energy process.[46] The charge placed on the metal ion centre by the four planar nitrogen σ-donors stabilizes the resultant trivalent oxidation state. (This argument accounts also for the formation and stabilities of Cu(III),[44] Ag(II),[47] and Ag(III)[48] complexes of these ligands.)

1.5 The 'Cyclam' macrocycles.

The most stable and best characterized complexes of the cyclic tetramine (or cyclam) class are those containing the 14-membered macro rings, with the trans- diene complex, viz. 5,7,7,12,14,14 - hexamethyl - 1, 4,8,11, tetraazacyclotetradeca - 4,11 - diene, being of most synthetical interest.[30] The structure of the diene complex is shown on the following page. (Forms of the ligand with varying degrees of saturation can be derived from this complex by simple chemical reactions). Complexes of these particular ligands generally have the nitrogen atoms almost co-planar, with the removal of the metal centre from coordination to the cyclic ligand being a relatively slow process. (It is notable, however, that macrocyclic complexes having chelating derivatives coordinated to a Ni(II) centre have been prepared in which the ligand can buckle

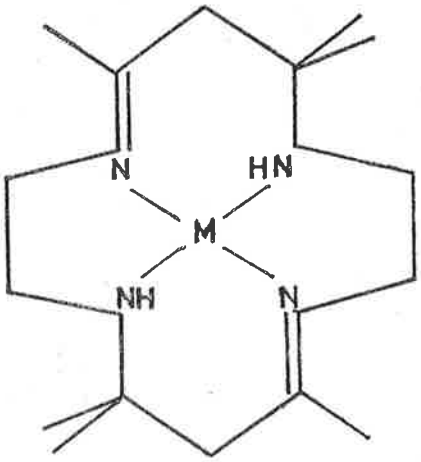

trans[14]diene

to create cis coordination sites on the octahedral metal centre.[49] (The degree of strain in the folded configuration depends on the actual macrocycle used.) The Ni(II) and Cu(II) complexes of trans-diene class are all kinetically stable in aqueous acidic solution (at room temperature) and such complexes show only weak interaction with solvent along the axial coordination positions.[30] These ligands can thus exercise the tendency to 'trap' the metal ion in a particular coordination geometry, even though the metal centre may change its oxidation state. That square planar geometry has been found for the trans-diene complex of Cu(I),[50] which is normally tetrahedral, is a good example of this. Macrocyclic complexes of Ni(III) have been shown to retain for the most part, the tetragonally distorted octahedral geometry of the original bivalent complexes.[22] Similar evidence has been found for trivalent complexes of Ni bis(ethylenediamine) and related complexes.[51]

The macrocyclic complexes used in this study are known to exist in a number of isomeric modifications.[43, 68] Isomerism in the trans [14]-

diene complexes is due to the presence of two asymmetric secondary amine nitrogens, N-meso or N-racemic, corresponding to the two amine protons being on the same or opposite sides of the N_4- coordination plane, respectively. The racemic and meso isomers of the Ni(II) complex are interconvertible in solution, the rate of hydrogen exchange depending on pH and temperature. Little is known about the Cu system, but it is likely that similar changes occur in solution. Isomerism in the trans [14] tetramine complex is due to the presence of two asymmetric carbon atoms (non-interconvertible C- meso and C- racemic) and four asymmetric coordinated secondary amine nitrogens.(69) The effects of complex isomerism have not been considered in this redox study of the tervalent macrocyclic complexes of Ni and Cu.

1.6 Means of M(III) production

The aquo or hydroxyaquo Ni(III) ion has not been detected in solution. The standard reduction potential (E^o) for the $Ni^{3+}aq/Ni^{2+}aq$ couple cannot be estimated with any real certainty, but it is probable that if it were <2.4 volts, $Ni^{3+}aq$ would be observable at least as a transient. $Cu^{3+}aq$ (or $CuOH^{2+}$), having an E^o of 2.4 volts, has been observed.(52) When strongly complexing ligands are coordinated to M(II) (M = Ni, Cu), the E^o of the resulting M(III)L/M(II)L couple (where L = ligand) is reduced, so that oxidation of the metal centre by chemical or electrochemical means to produce the trivalent state becomes possible. Bivalent Ni macrocyclic tetramine complexes have been oxidized by $S_2O_8^{2-}$ in aqueous solution(22) and by $NOClO_4$ in CH_3CN.(46) The Ni(II) and Cu(II) biuret complexes were oxidized by $S_2O_8^{2-}$ in strongly basic solutions,(16) while the Ni en_3X_2 (and related pn) complexes were oxidized by Cl_2 and Br_2 in methanol and CCl_4.(6,51) Oxidation of the

organo-metallic $CuS_2CN\ (n\text{-}C_4H_9)_2$ complex was achieved with Br_2 in CS_2.[72] Electrochemical oxidations of M(II) complexes have been studied for macrocyclic tetramine complexes in CH_3CN[9,29,44], and for the tris(ethylenediamine) complexes in water.[27,28] The Ni(III) state was stable in the aprotic solvent, but both this and the Cu(III) existed only as electro-chemical intermediates to ligand oxidation in the aqueous system. The Cu(III) complexes were unstable in CH_3CN at room temperature, undergoing spontaneous reduction to the bivalent state. The polarographic evidence in the CH_3CN systems indicated that the redox reaction did involve primarily the metal and not the ligand. The elecrochemically determined reduction potentials of the M(III)L/M(II)L couple for the macrocycles used in this study are shown below. These values were determined in CH_3CN relative to a Ag/Ag^+ (0.1M) reference electrode.

Complex	E^o(volts)
Ni tetramine	+ 0.87 (29)
Ni diene	+ 0.98 "
Ni tetraimine	+ 1.05 "
Cu diene	~+ 1.18 (44)

Thus, Ni(III) tetraimine is a more powerful oxidizer than the tetramine complex by +0.18V, while the Cu(III) diene is ~+0.13 volts more oxidative than the Ni(III) tetraimine.

Oxidation of M(II) complexes in aqueous solution by radical species has been reported in pulse radiolytic studies on dimethylglyoxime,[55] EDTA[56] (M = Ni), ammonical, ethylenediamine, glycine, (M = Ni, Cu)[53,54,78] and aquo,[52] amino acid [78] (M = Cu) complexes. In all these studies, except for the ammonia solutions, oxidation of the M(II) complex was achieved via the highly oxidizing OH radical (or O^- in basic

solution), which has an E^o of 2.8 volts. In NH_3 solution, the oxidizing species was considered to be the NH_2 radical formed by OH attack on NH_3. As yet, no investigations of the tervalent states of Ni and Cu have been attempted using the dihalogen radical anion species, X_2^- where X = Cl,Br,I, as the precursor oxidizing species. The E^o's for the $X_2^-/2X^-$ couples are +2.3, +1.8, +1.0 volts for X = Cl,Br,I respectively.[57] Nor have the trivalent Ni, Cu tetra-aza macrocycles been investigated using oxidizing radical species. The investigation presented in this thesis is a study of the Ni(III) (and to a lesser extent, Cu(III)) tetra-aza macrocyclic complexes of the trans [14]- class, using OH and X_2^- radicals as oxidizing species in aqueous solution. These radicals are generated in this work mainly by the flash photalysis technique.

1.7 Comparisons to related systems

The Cotrans [14] diene, X_2^- system has been investigated in terms of both X_2^- oxidation of the Co(II) complex, and X_2^- reduction of the tervalent complex.[58] The oxidations were diffusion controlled, while evidence for X_2^- reduction was found only for I_2^-. Analogy between the tervalent state of Co and that of Ni and Cu is limited however, since Co(III) is quite stable.

Unstable oxidation states have been suggested as intermediates for several reactions in which the metal ion inherently undergoes a two-electron transfer redox reaction. The highly reactive transient states of Tl(II) and Pt(III) have been well characterized as intermediates in the redox reactions involving the Tl(III)/Tl(I)[59] and Pt(IV)/Pt(II)[60]

couples, even though these oxidation states have not been formally characterized in isolatable compounds.[1] Mechanistic analogies between these powerfully oxidizing intermediate states and those of Ni(III) and Cu(III) cannot be made, since Ni and Cu do not have a stable state accessible to them in the (IV) state. The redox chemistry of the M(III) species is thus restricted to the return of the Ni and Cu centres to the bivalent state. Although there are several reports of compounds believed to contain Ni(IV) (stabilized by coordination with highly electronegative elements),[1] and the state has been suggested in redox reactions of Ni complexes in non-aqueous solvents[26,61], its existence as an intermediate in water is unknown and considered to be quite unlikely.[59] Thus, the point is made that in the general field of unusual oxidation state chemistry of metals, the states Ni(III) and Cu(III) are inherently different from Tl(II), Pt(III), Au(II)[67].

2. M(III) DECOMPOSITION IN SOLUTION

2.1 General

The electronic interaction between metal ions and ligands is well known to affect the reactivity of a complex towards redox reagents.[62] If the electron affinity of a ligand bound to a central metal atom is less than that of the metal centre, ligand oxidation is likely; alternatively, if the ligand electron affinity is substantially higher than that of the central atom, oxidation of the metal ion may occur. In general ligands must undergo a two equivalent change in their oxidation state before reaching a stable state, whereas metal ions, in most cases, may change their oxidation state in single equivalent steps without necessarily forming intermediates of high reactivity. This difference in redox behaviour between metal ions and ligands results in the great complexity of redox reactions between the two species. It is notable that polyatomic ligands may undergo redox reactions which involve bond cleavage in the ligand group, and which are not electron transfer processes in the narrow sense. Unstable systems produced by interaction of stable complexes with redox reagents, leading to redox changes in the ligand, have been discussed in a review by Anbar.[62]

2.2 Ligand Redox

Metal ions have been found to catalyse the oxidative dehydrogenation of coordinated amines to imines.[29,31,33,34,63,64] The oxidation of macrocyclic amine complexes to imine complexes was studied by Curtis, and Busch, and their studies have provided some insight into the mechanism of oxidative dehydrogenation. The reverse process of imine hydrogenation

to an amine is also a facile process for many cyclic complexes.[65] The Ni complexes of a range of Curtis macrocycle derivatives containing from zero to four imine groups have been isolated as products from a series of selected redox reactions. There is evidence that the redox reactions of this type are metal-ion dependent in the ease with which a reaction takes place as well as in the nature of the product formed.[65] It is generally true that the Fe(II) complexes undergo more facile oxidative dehydrogenation than the Ni(II) analogues, which react more readily in this way than the Cu(II) complexes. The complexes of Co(III) are resistant to oxidation. This trend suggests that the net reaction involves prior oxidation of the metal ion followed by oxidation of the ligand and reduction of the metal. Moreover it is apparent that there is a clear preference for Fe(II) macrocycles to form the α-di-imine linkage,[33] which is not found for the Ni(II) analogues. The introduction of unsaturation between adjacent carbon atoms in the backbone of a chelate ring is not known for the Curtis 'cyclam' series.[66] Strong chemical oxidants such as acid permanganate and peroxydisulphate can cause bond cleavage in the ligand, destroying the macrocyclic nature of the complex.[30]

2.3 Modes of M(III) decomposition

A number of macrocyclic Ni(III) complexes have been isolated from oxidation reactions on selected corresponding Ni(II) species.[8,22] The tervalent complexes were found to be indefinitely stable in the solid state, but decompose in solution,[22] the rate depending on the nature of the solvent.[46] Water is not unique in causing this decomposition as most solvents which are more basic than acetonitrile induce decomposition.

Barefield's recent work[46] on the mechanism of decay of Ni(III) complexes of saturated macrocyclic tetramines in various solvents is the only publication to date in this area. This study proposed a mechanism of base promoted reduction of the Ni(III) complex to produce a coordinated ligand radical intermediate;

where B is a basic solvent. This type of radical species was suggested as an intermediate in the oxidative dehydrogenation of Fe(III) trans [14]- diene in aqueous solution.[33] Depending on the solvent, 1-25% of the radical species formed decomposed with rupture of the macrocyclic ring; the remainder were converted back to the Ni(II) tetramine complex by hydrogen atom abstraction from ligand fragments, or produced the mono-imine complex from a bimolecular reaction with a second radical species. Under certain conditions the monoimine product was also formed by oxidation of the Ni(II) ligand radical by the Ni(III) complex. A similar mechanism was proposed to explain the introduction of an imine function into the ligand upon the decomposition of Cu(III) trans-[14] tetramine in CH_3CN.[44]

The decomposition of the Ni(II) ligand radical intermediate in water was first order, and analysis of the products suggested that the decay process involved both ring rupture and H-atom capture. There was no evidence in aqueous solution for the second order process

$$Ni(II)L^{\bullet} + Ni(II)L^{\bullet} \longrightarrow Ni(II)L + Ni(II)L_{OX},$$

in which the imine function would be introduced into the ligand.

Considerable work by Meyerstein et.al has been done on the decom-

position, and spectral properties of various non-cyclic complexes of trivalent Ni and Cu in aqueous solution.[27,28,53-56] The oxidation procedures used in attaining the trivalent state included both radiolytically produced radical oxidation, and electrochemical oxidation on platinum electrodes. In the electrolytic studies of the oxidation of Ni(II) en_3 and Cu(II) en_2 complexes, it was established that the mode of decay of the tervalent species was via a second-order rate determining step in which oxidation of the en occurred as a result in the Ni system,[27] while oxidation of water was considered operative in the Cu analogue.[28] The formation of H_3O^+ as a product of either en or water oxidation explained the observed pH effects in unbuffered solutions. The disappearance of the NH_3 and en complexes of Ni(III)[53, 54] and Cu(III)[78] generated by pulse radiolysis of N_2O-saturated solutions, was also found to obey a second-order rate law, The reaction mechanism proposed was analogous to the rate determining step of the electrolytic reactions. While Ni(III) gly decayed by the second-order process,[54] Cu(III) gly had a first-order intramolecular rate determining step.[78] This difference in behaviour is due to the higher redox potential of the Cu(III) amine complexes compared with that of the Ni(III) analogues, The aquo Cu(III) complex was rather unique in its decay mode due to its large E^o value of +2,4 volts. In neutral solution it was concluded that the Cu(III) exists in the form $CuOH^{2+}_{aq}$ (or $Cu(OH)^{+}_{2}aq$) and decomposes via $2CuOH^{2+} \longrightarrow 2Cu^{2+} + H_2O_2$. In acid solutions, the mechanism involved the formation of OH radicals probably via Cu^{3+}_{aq} $Cu^{2+} + OH$.[52]

A complicated decay mechanism has been proposed for the Ni(III) EDTA complex disappearance in pulse radiolysed aqueous solution.[56]

The initially formed unstable trivalent complex is transformed within milliseconds into a stable form. The forms are spectrally quite similar. The difference between the forms was suggested as being in the number of coordination sites occupied by the EDTA, or by an addition of OH^-. In the absence of oxidizable substrates, the stability of the re-arranged trivalent complex suggested that the metal centre is not strong enough to oxidize its ligand by a one equivalent process yielding a radical, and that a bimolecular two-electron process was most likely. The specific rate of such a reaction was proposed to be very slow due to poor overlap of the metal centred orbitals in the two ions. In aerated, or iodide solution, however, the trivalent complex can decay by the reactions,

$$Ni(III)EDTA + O_2 \longrightarrow Ni^{2+} + \text{products}$$

$$Ni(III)EDTA + I^- \longrightarrow Ni(II)EDTA + \tfrac{1}{2}I_2$$

In the EDTA work, as with the other complexes, Meyerstein has suggested that tetravalent Ni complexes might be formed as intermediates in the second-order disappearance reactions of the trivalent complexes. However, no kinetic or spectral evidence for its formation was found.

2.4 M(III) spectral properties

The identity of the oxidized form as the Ni(III) species in the aqueous pulse radiolysis studies has been reasonably attributed to the similarity of the absorption spectra of the NH_3, en, gly, and EDTA complexes.[56] These transient spectra are also comparable to the Ni(III) macrocyclic complex spectra determined in electrochemical studies in acetonitrile.[9] The Cu(III) spectra in the region 240-400 nm were similar for the aquo, NH_3, en, gly and α-alanine complexes in aqueous

solution. These spectra bore no close resemblance, however, to the Cu(III) macrocyclic complexes in CH_3CN. There was a significant difference between the trans-diene and tetramine complexes in fact. The spectra of some of the known M(III) complexes are shown in figure I 2.4.

2.5 Summary

The known mechanisms of Ni(III) complex decomposition in aqueous solution can thus be summarized accordingly:

(i) The non-cyclic complexes decay by a second-order process to produce a Ni(II) complex and oxidized ligand products.

(ii) The saturated macrocyclic tetramine complex decays by first-order ring fragmentation and H-atom capture, after the initial conversion of Ni(III)L to a coordinated ligand radical. It is to be noted that this decay mode is at variance with the decay in less basic solvents, and with the normal mode of ligand unsaturation determined by chemical oxidations of the bivalent complex. The Cu(III) complex would be expected to follow similar decay patterns to those of Ni(III), except, perhaps, that intramolecular electron-transfer from the ligand might be expected to be more facile for the copper, due to its higher oxidizing power.

More specific aspects of the known modes of Ni(III) complex decomposition will be discussed in relation to results presented in this thesis in the discussion sections. The compatability of the known mechanisms with the anion-assisted electron transfer through direct ligand interaction proposed in this thesis will be discussed. The results obtained for Cu(III) complex decay are used to complement the mechanisms derived for the Ni systems.

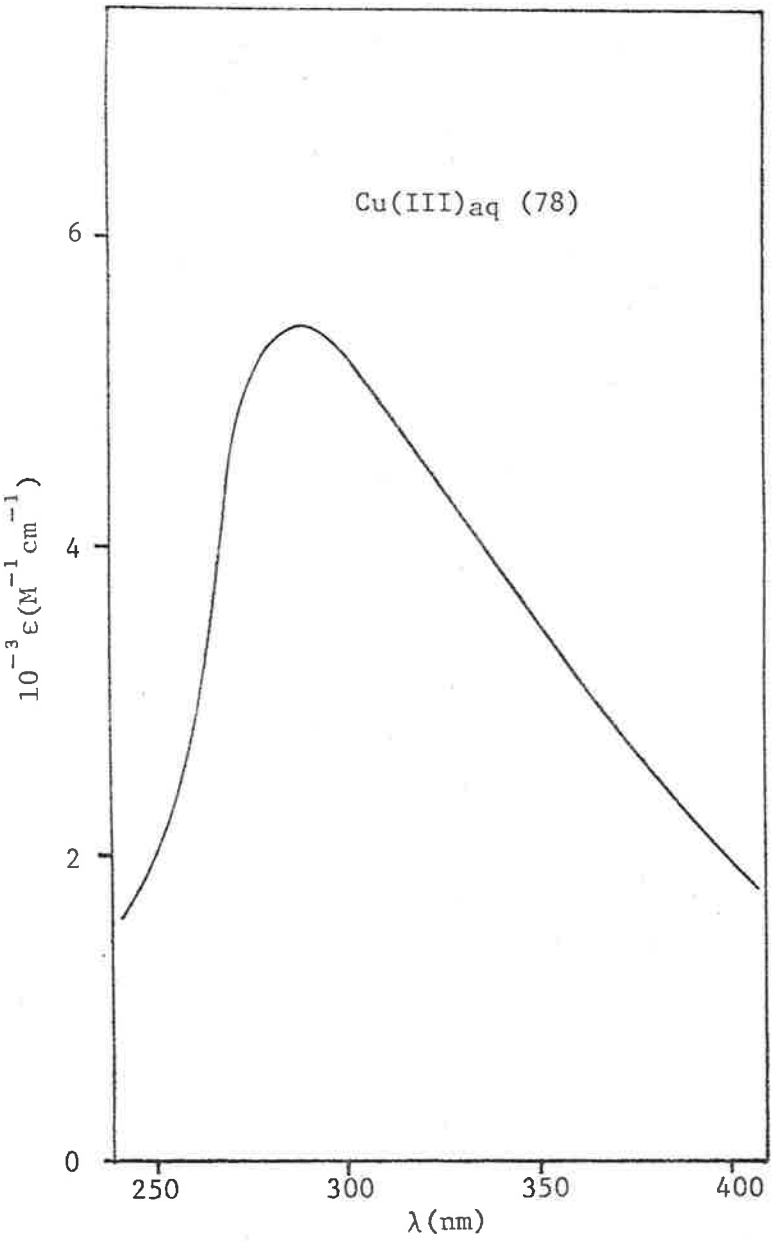
Cu(III)aq (78)
6
4
2
0
250
300
350
400
λ(nm)
$10^{-3}\varepsilon(M^{-1}cm^{-1})$

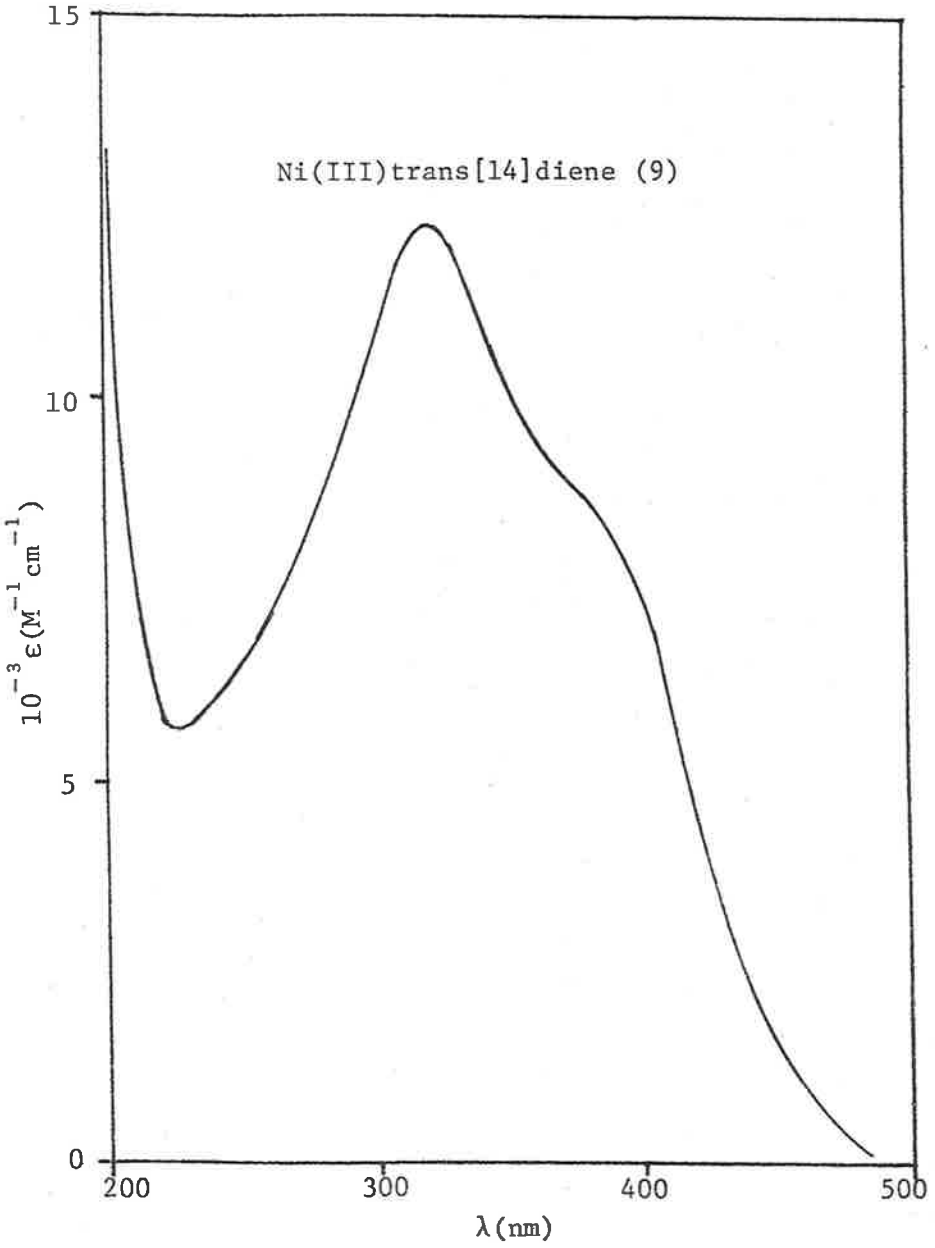
Ni(III)trans[14]diene (9)
15
10
5
0
200
300
400
500
λ(nm)
$10^{-3}\varepsilon(M^{-1}cm^{-1})$

FIGURE I 2.4

3. RADICAL CHEMISTRY

3.1 The hydroxyl radical

The properties of the hydroxyl radical, OH, and its reactivity toward organic and inorganic compounds have been the subject of numerous reviews and monographs for over ten years.[82] It is well established that OH is formed in the U.V. photolysis of H_2O_2 and H_2O, and in the radiolysis of aqueous solutions.[101] The information, particularly on the kinetic behaviour of this most important oxidizing free radical has become extensive and reliable.

The OH radical in water does not exhibit conveniently accessible spectrophotometric absorption, with the result that its reactivity has not been determined by direct observation of the species itself.[83] The rates of OH reaction have been determined by observation of product formation, or by competitive kinetics using a reference OH reaction whose rate is absolutely known.[84,85]

3.2 Dihalogen radical - ions

The dihalogen radical anions, X_2^- (X = Cl,Br,I and the pseudohalide SCN) have been invoked as reactive intermediates in reactions involving halogens or halide ions for many years.[87,88,127] Unstable species, believed to be the X_2^- radicals were observed in flash photolysis studies of aqueous halide solutions.[89] The reaction scheme proposed was

$$X^- \xrightarrow{h\nu} X + e^-aq$$

$$X + X^- \rightleftharpoons X_2^-$$

where e^-aq is the aquated electron and X = Cl,Br,I,SCN, the energy absorp-

tion being in the far U,V, region. The photochemically active absorption band of aqueous halide ions in the region below about 250nm has been interpreted as a charge-transfer-to-solvent (CTTS) excitation.[90] The e^-aq species has been observed for this system under conditions of extreme water purity.[91] The forward rate of the X/X_2^- equilibrium, under conditions of excess halide is very rapid, The value of the equilibium constant is $\sim 10^5$ for all the X (= Cl,Br,I,SCN)[92,93] so that by far the predominant radical species in halide solution is the X_2^- radical ion. Although the radical anions are present in only μM concentration in solution, they are readily observable because of their large absorption coefficients (ε max $\sim 10^4$ M^{-1} cm^{-1}) in the 300-400nm (X = Cl,Br,I)[89] and ~500 nm (X = SCN)[94] regions of the spectrum. Unlike the halide ions, the SCN^- ion is capable of photo-induced S-C bond dissociation attributed to the de-activation of a $\pi^* \leftarrow n$ excitation in the anion. In solutions <0,5mM in SCN^-, this mode of primary absorption is minimal. The absorption spectra of the X_2^- species are shown in figure I 3.2.

3.3 Dihalogen radical formation and decay

The identity of these transient species was verified by pulse radiolysis of aqueous halide solutions.[95-97] The primary absorption of high energy radiation is almost exclusively by the solvent to produce decomposition products of water, viz, e^-aq, OH and H atoms, along with other secondary species (H_2, H_2O_2). The mechanism proposed was

$$H_2O \rightsquigarrow OH,\ e^-aq,\ H \text{ etc.}$$

$$OH + X^- \longrightarrow OH^- + X$$

$$X + X^- \rightleftharpoons X_2^-$$

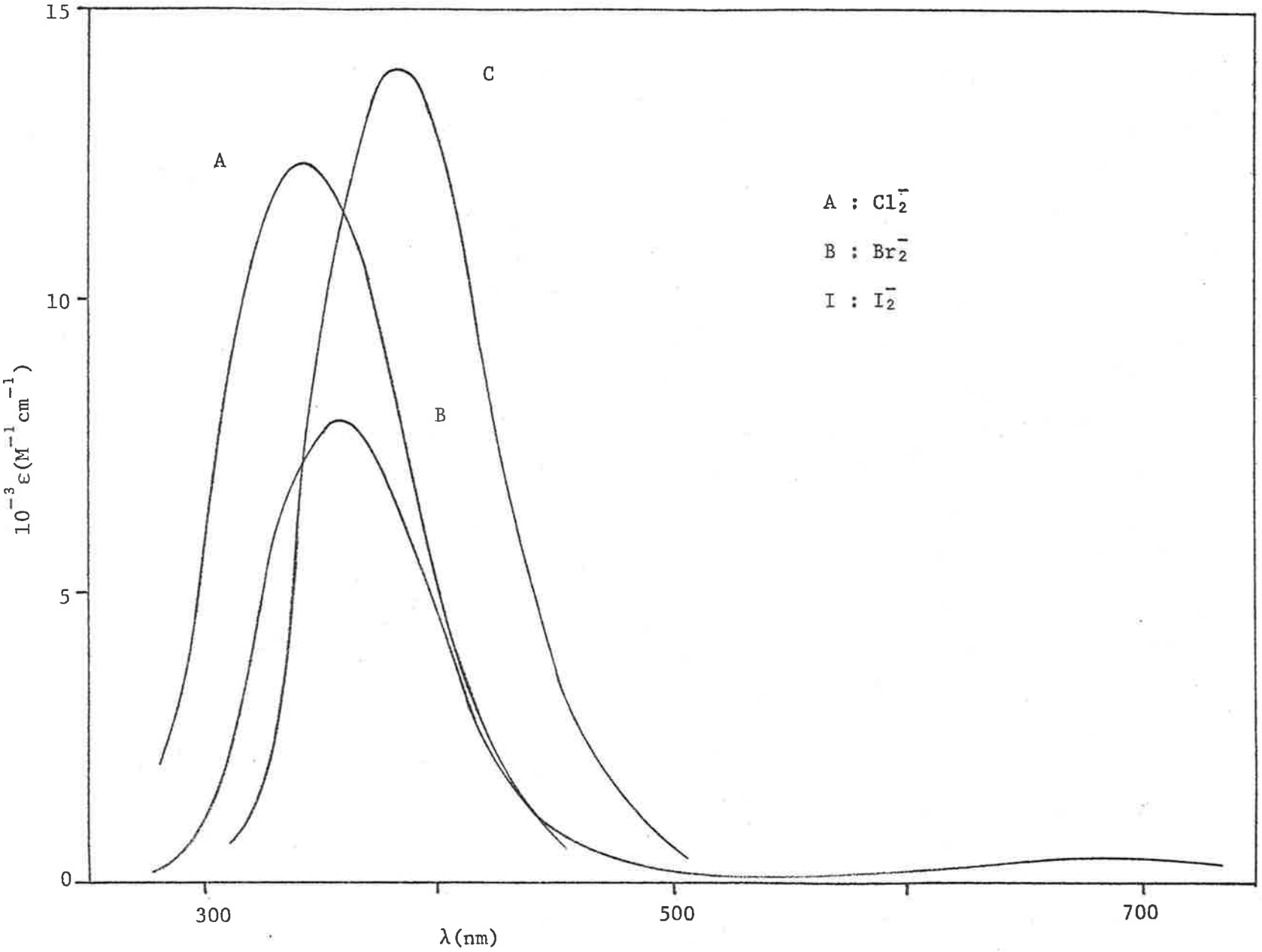
15
10
5
0
300
500
700
λ(nm)
$10^{-3}\varepsilon(M^{-1}cm^{-1})$
A
B
C
A : Cl_2^-
B : Br_2^-
I : I_2^-

FIGURE I 3.2

Later publications by Behan[98,99] reported the absorption spectra of precursor species to the X_2^- radical anions. It was concluded that the reaction of OH radical with halide ions produced the XOH^- intermediate in neutral and acidic solutions;

$$OH + X^- \rightleftharpoons XOH^-$$

$$XOH^- \longrightarrow X + OH^-$$

These reactions are very rapid, so that under normal experimental conditions (neutral to acidic solution, and excess halide ion) the half-lives for X_2^- formation are less than 1 μsec. Hence, complications due to XOH^- need not be considered when X_2^- decay reactions are of interest. The principle mode of X_2^- decay in the absence of substrates in solution is by disproportionation, having second-order rate constants in the region 2-5 x $10^9 M^{-1}$ sec^{-1} [89,96] for the X considered in this study;

$$X_2^- + X_2^- \longrightarrow X_3^- + X^- \quad \text{for X = Cl,Br,I}$$

$$\longrightarrow 2X^- + \text{products of } (SCN)_2 \text{ hydrolysis for X = SCN}$$

The apparent decay rate of X_2^- in the absence of added substrates can vary with the actual means of the radical production depending on the relative importance of possible side reactions with other radical species in solution viz. e^-aq, H, HO_2 etc.[92]

Apart from the already mentioned CTTS photochemically induced production of X_2^- from aqueous halide solution, there are several other photochemical means of the radical anion production. The systems used in this study include those in which the X_2^- are produced directly as a result of the primary photolysis and indirectly by secondary reactions of OH, which is itself photolytically produced. The actual nature of the photochemical act can be classified as either direct bond dissociation or a charge-transfer process. Only those techniques actually used

in this work will be introduced here.

One efficient means of X_2^- production, which probably involves the formation of the XOH^- intermediate, is the flash photolysis of H_2O_2 solutions containing halide ion. H_2O_2 undergoes photochemical bond cleavage to produce two OH radicals

$$H_2O_2 \xrightarrow{h\nu} OH + OH$$

The quantum yield for the photolysis, which involves light absorption below about 250nm, is independent of $[H_2O_2]$ and light intensity over wide ranges of concentration and intensity.(100) This method of radical production is used in this work for studying the M(II) complex oxidation with OH as the precursor radical. In halide solutions, the OH radicals which escape primary geminate recombination are then capable of reaction with halide ion, leading to X_2^- formation. Any simultaneous absorption in the CTTS of the halide ion leads to a further increase in X_2^- yield without complications due to the concomitant production of e^-aq. This follows since,

$$X^-aq \xrightarrow{h\nu} X + e^-aq$$

$$e^-aq + H_2O_2 \longrightarrow OH + OH^- \quad k \sim 10^{10} M^{-1} sec^{-1}$$

$$OH + X^- \longrightarrow X + OH^- \quad \text{(simplified)}$$

$$X + X^- \longrightarrow X_2^-$$

A complication arises when using this method of OH production if the $[H_2O_2]$ is too high; in such a case, the OH radicals may react with H_2O_2 by H-atom abstraction to produce the secondary radical species, HO_2, the hydroperoxy, or superoxy radical:

$$OH + H_2O_2 \longrightarrow HO_2 + H_2O$$

Side reactions involving this species may then become significant, and indeed dominant.

3.4 The hydroperoxy radical

The HO_2 radical can be readily generated by both photochemical and radiation-induced reactions.[101] In solution it is produced by the secondary reactions of e^-aq, H atoms, as well as OH radicals;

$$e^-aq + O_2 \rightarrow O_2^-$$

$$H + O_2 \rightarrow HO_2$$

$$HO_2 \rightleftharpoons H^+ + O_2^-$$

The radical is known to exist in an acid-base equilibirium, whose pKa has been determined to be 4.88.[102] Several studies have suggested the existence of $H_2O_2^+$ in acid solutions,[103-106] while no such evidence was found by other authors.[102,107,108] The proposed pKa was about 1.5.[104]

$$H_2O_2^+ \rightleftharpoons HO_2 + H^+$$

It is now accepted that evidence for the existence of $H_2O_2^+$ is very weak, since in almost all cases proposing its existence, the results have been re-interpreted satisfactorily without the necessity of proposing a new species. However, for some results, no alternative explanation is apparent. This point of controversy is mentioned here because results in this thesis support the argument against its existence.

The chemical properties of HO_2 in aqueous solution have been of chemical interest for many years, since its transient existence was postulated as one of the early examples of radical participation in redox reactions in solution.[109-111] The possibility that HO_2 (or O_2^-) may occur as intermediates in reactions of biological interest like photosynthesis, oxygen fixation, and biological oxidations has been suggested.[101] This has been demonstrated for certain enzymatic and non-enzymatic

oxidation reactions involving molecular oxygen. The HO_2 radical, which is intermediate in oxidation state between oxygen and H_2O_2 can behave both as an oxidizing agent and as a reducing agent. Estimates[114] of the E^o values for the HO_2 and O_2^- redox couples are shown below:

	E^o(volts)	
	pH 1 (HO_2)	pH 5 (O_2^-)
$'HO_2' + H^+ + e \rightleftharpoons H_2O_2$	1.5	1.2
$O_2 + H^+ + e \rightleftharpoons 'HO_2'$	.05	-0.2

The standard reduction potentials shown here are in reasonable agreement with particular values calculated thermodynamically and obtained by kinetic means,[133-136] (The kinetic redox potentials of Hayon[137] were claimed to be incorrect by Czapski,[136] since these were not equilibrium potentials).

3.5 Halide complex photolysis

The addition of excess halide ion to aqueous halogen solution produces the trihalide ion, X_3^- (X = Cl,Br,I)[115]

$$X_2 + X^- \rightleftharpoons X_3^-$$

In acid solution, the undersirable halogen hydrolysis reaction can be suppressed;

$$X_2 + H_2O \longrightarrow X^- + OX^- + 2H^+$$

The trihalide anions exhibit intense absorption bands in the U.V. region, the energies of which can be correlated with the bond strengths in the X_3^- and the gas phase spectra of the halogens. The X_2^- radical species have been observed in flash photolysed trihalide solutions, for which the primary photolysis step is bond dissociation. The stoichiometric

equation for the photolysis[89] is

$$X_3^- + X^- \xrightarrow{h\nu} 2X_2^-$$

The distinction between the two possible dissociation mechanisms,

(i) $X_3^- \xrightarrow{h\nu} 2X + X^-$

$2X + 2X^- \rightleftharpoons 2X_2^-$

(ii) $X_3^- \xrightarrow{h\nu} X^- + X_2$

$X + X^- \rightleftharpoons X_2^-$

has not been made, because of the speed of the common equilibirum step.

Strong absorption bands in the U.V. region of certain labile and inert metal complexes have been attributed to ligand-to-metal-charge-transfer (LMCT) excitations. It is a common observation that the energies of the band maxima increase as the central metal ion becomes more oxidizing and the ligand more reducing. When all the ligands are equivalent, there is no preference for electron transfer from any particular one; the electron is considered to come from a delocalized ligand molecular orbital. In a mixed-ligand complex with one ligand more reducing than the others, it is considered that the electron is transferred from that specific ligand to the central metal.[116] In halide complexes, it was found that the difference in energy of band maxima for the chloro-, bromo-, and iodo- complexes could be directly correlated with the electron affinity of the respective halogen atom of the complex.[117] The LMCT transition has been established as the process responsible for the photochemically induced reduction of transition metal complexes of labile systems, including FeX^{2+},[118,119,124] $PtCl_6^{2-}$[120], HgX_4^{2-}[121], and of inert systems, including $Co(NH_3)_5X^{2+}$[122] and $Rh(NH_3)_5X^{2+}$.[123]

Labile ferric ions in aqueous solution containing halide ions show a great tendency to form the halopentaquo complexes.(140)

$$Fe^{3+}_{aq} + X^- \rightleftharpoons FeX^{2+}$$

Irradiation of the complexes leads to X_2^- formation after primary absorption in the complex LMCT band, i.e.(126,125)

$$FeX^{2+} \xrightarrow{h\nu} [Fe^{2+} X] \text{ solvent cage}$$

$$[Fe^{2+} \cdot X] \longrightarrow FeX^{2+}$$

$$[Fe^{2+} \cdot X] \longrightarrow Fe^{2+} + X$$

$$X + X^- \rightleftharpoons X_2^-$$

$$X_2^- + Fe^{2+} \longrightarrow FeX^{2+} + X^-$$

In this system (as in labile systems in general) low overall quantum yields of radical formation are found due to the existence of fast secondary back reactions. The value of $\phi = 0.13$ in the wavelength range 300-400 nm has been found for the $FeCl^{2+}$ system.(126) It is noteworthy that X = OH^-, H_2O, undergoes the same LMCT type transition to produce the OH radical,(116) capable of X_2^- formation in halide solution. Radical formation via this type of complex photolysis is unsatisfactory for the iodide system, since Fe^{3+}_{aq} undergoes efficient thermal reduction by I^-, viz;(87)

$$2Fe^{3+} + 2I^- \longrightarrow 2Fe^{2+} + I_2$$

It is notable that I_2^- is considered to be an intermediate in this process. Such thermal reduction occurs more slowly for the thiocyanate complex.(127)

The mechanism of X_2^- formation from LMCT excitation in the inert CoA_5X^{2+} (A=NH_3) series of complexes in aqueous halide solution can be represented as,(92,129)

$$CoA_5X^{2+} \xrightarrow{h\nu} [CoA_5^{2+} \cdot X] \quad \text{solvent cage}$$

$$[CoA_5^{2+} \cdot X] \longrightarrow CoA_5X^{2+}$$

$$[CoA_5^{2+} \cdot X] \longrightarrow CoA_5^{2+} + X$$

$$CoA_5^{2+} \longrightarrow Co^{2+} + 5A$$

$$X + X^- \rightleftharpoons X_2^-$$

In this system the CoA_5^{2+} entities which escape primary geminate recombination in the solvent cage undergo very rapid ligand dissociation from the labile high-spin Co(II) metal centre, making secondary recombination of the type

$$CoA_5^{2+} + X_2^- \longrightarrow CoA_5X^{2+} + X^-$$

impossible. Also, the scavenging of X_2^- by Co^{2+}_{aq} is known to be too inefficient to effect the overall quantum yield.[128] If the photolysis radiation is not filtered, the process of photoaquation can simultaneously occur, leading to a reduced quantum yield of X_2^-.

$$CoA_5X^{2+} \xrightarrow{h\nu} CoA_5OH_2^{3+} + X^- \quad \text{for } X = Br^- \quad (130)$$

$$\xrightarrow[H^+]{h\nu} CoA_4(OH_2)X^{2+} + NH_4^+$$

$$\text{for } X = Cl^- \quad (131)$$

It is notable that the Co(III) macrocyclic complexes Co(trans[14]diene)$(OH_2)_2^{3+}$ and Co(trans[14]diene)Cl_2^+ undergo photoreduction with low quantum yields to produce the Co(trans[14]diene)$^{2+}$ complex.[138] The square planar coordination remains intact as a result of the low spin nature of the d^7 complex produced.[139]

3.6 Dihalogen radical reactions

The reactions of the X_2^- radical ions with a variety of oxidizable

substrates,[121] including transition metal ions, have been previously investigated. Oxidations of aquated transition-metal ions by these anions have provided a means of testing current theories of oxidative electron-transfer reactions of metal ions over a large range of substitution rate and free energy change.[128,133] These radicals, being among the simplest oxidizing radicals in aqueous solution, (apart from the OH radical), were thus considered an ideal choice for the attempted M(II) → M(III) oxidations investigated in this work.

3.7 Research Aims

In this thesis is presented a systematic investigation of the effects of differing the precursor radical on the mechanisms of formation and decay of the presumed Ni(III) entity in aqueous solution. The effects of ligand environment on the mechanistic and spectral properties of the tervalent state are examined by changing the degree of saturation of the macrocyclic ligand. It was found that the changes in experimental conditions for precursor radical production provided considerable insight into the various modes of disappearance available to the transient complex species. Mechanistic considerations of the tervalent Cu species are based on the more rigorous investigations of the Ni analogue.

II EXPERIMENTAL

1. REAGENTS AND STANDARDIZATION

1.1 The sodium salts of chloride, bromide and iodide were AnalaR or BDH A.R. grade. Ammonium thiocyanate and sodium azide were BDH A.R. grade chemicals. These halides and pseudo-halides were generally taken as primary standards. Where necessary the stock solutions were analyzed by potentiometric titration against standard silver nitrate solution.

BDH (A.R.) bromine was used to make up the aqueous tribromide solutions. The halogen concentration was estimated spectrophotometrically by conversion to I_3^- in excess iodide. The stock hydrogen peroxide solution was made up from A.R. 27.5% W/W H_2O_2 (Laporte Chemicals) and standardized by redox titration against standard potassium permangamate solution.

To adjust acidities, G.F. Smith A.R. 70% W/W and Fluka puriss grade perchloric acid were used. This was standardized against sodium tetraborate by pH titration (using a Horiba, type F-5 pH meter). The stock sodium perchlorate solution, used to adjust solution ionic strength, was made up using the Fluka A.R. salt, and taken as a primary standard.

The metal ion solutions were prepared from A.R. grade perchlorate salts (Fluka) without further purification. (Perchlorate counter-ions were used throughout in this work because of the inertness of this anion to radical attack). Acidified ferric perchlorate solution was analyzed by potentiometric titration against standard sodium ethylenediaminetetraacetic acid solution. Stock ferrous perchlorate in acidic

solution was shaken vigorously with Zn/Hg amalgam to reduce any Fe^{3+} impurity, and then stored under oxygen-free nitrogen to prevent aereal oxidation. (The presence of Zn^{2+} in solution was determined in a preliminary experiment to be inert to reaction with the photo-produced transients in this work). Concentrations of $Fe^{3+} < 10^{-4}$ of the Fe^{2+} concentration could be obtained (as analyzed by adding strong ammonium thiocyanate solution). The stock Fe^{2+} solution was analyzed by redox titration against potassium permangamate solution. The stock manganous perchlorate solution was analyzed by permanganate redox titration in strong pyrophosphate solution. (All standard analyses were performed according to Vogel[141]).

The tetranitromethane (TNM) was Fluka puriss grade, The stock TNM solution was analyzed spectrophotometrically after total reduction to the highly absorbing nitroform product by sodium sulphite (ε_{350} = 1.47×10^4 M^{-1} cm^{-1})[142]

Once recrystallized chloro- and bromo- pentammine cobalt (III) perchlorates had been previously prepared in the laboratory using published procedures.[143, 144] Freshly prepared solutions were always used because of the slow aquation of these complexes i.e.

$$Co(NH_3)_5X^{2+} + H_2O \longrightarrow Co(NH_3)_5OH_2^{3+} + X^-$$

The freshly made stock solutions were analyzed spectrophotometrically using[145]

X^-	λ(nm)	$\varepsilon(M^{-1}cm^{-1})$
Cl^-	530	47.3
Br^-	551	53.0

CIG high purity dry nitrogen was purged of any oxygen impurity in a chromous chloride scrubbing column. Nitrous oxide was once vacuum distilled medical grade (CIG). The oxygen used to fill flash lamps was

CIG medical grade and Xenon was grade X, 99.999% from British Oxygen.

1.2 All solutions were made up using deionized water which was twice distilled from neutral permanganate and acidic dichromate solutions under an atmosphere of oxygen in an all glass still. This procedure ensures the absence of any organic material that may act as a radical scavenger. The stock reagent solutions were stored in stoppered glass vessels.

2. PREPARATIONS OF COMPLEXES

2.1 The derivative 5,5,7,12,12,14-hexamethyl-1,4,8,11-tetraaza-cyclotetradeca-1,7-diene nickel (II) perchlorate was prepared following a method based on that of Curtis,[146] and Busch.[147] This complex is referred to as Ni(II) diene or Ni(II)di in the text of this thesis. The process involves the condensation of tris(ethylenediamine) nickel(II) perchlorate with acetone (3 ml/gm) by refluxing with a few drops of pyridine as catalyst for several hours until the solution is yellow-brown in colour. This mixture is evaporated down to an oil, and ethanol (2 ml/gm) is added to dissolve the polymeric side-products and to precipitate the required complex. The yellow product is isolated, washed with ethanol and dried in a vacuum dessicator. The product obtained is a mixture of the meso- and racemic isomeric forms. Separation of the isomers was not performed in this work. The ultra-violet (U.V.) and infra-red (I.R.) analyses of the product suggested that the complex was mainly in the so-called Aβ isomeric form.[146] The U.V. spectrum is shown in figure II2.1. Analysis of the stock complex solution was carried out spectrophotometrically using the molar absorbance values;[146]

FIGURE II 2.1

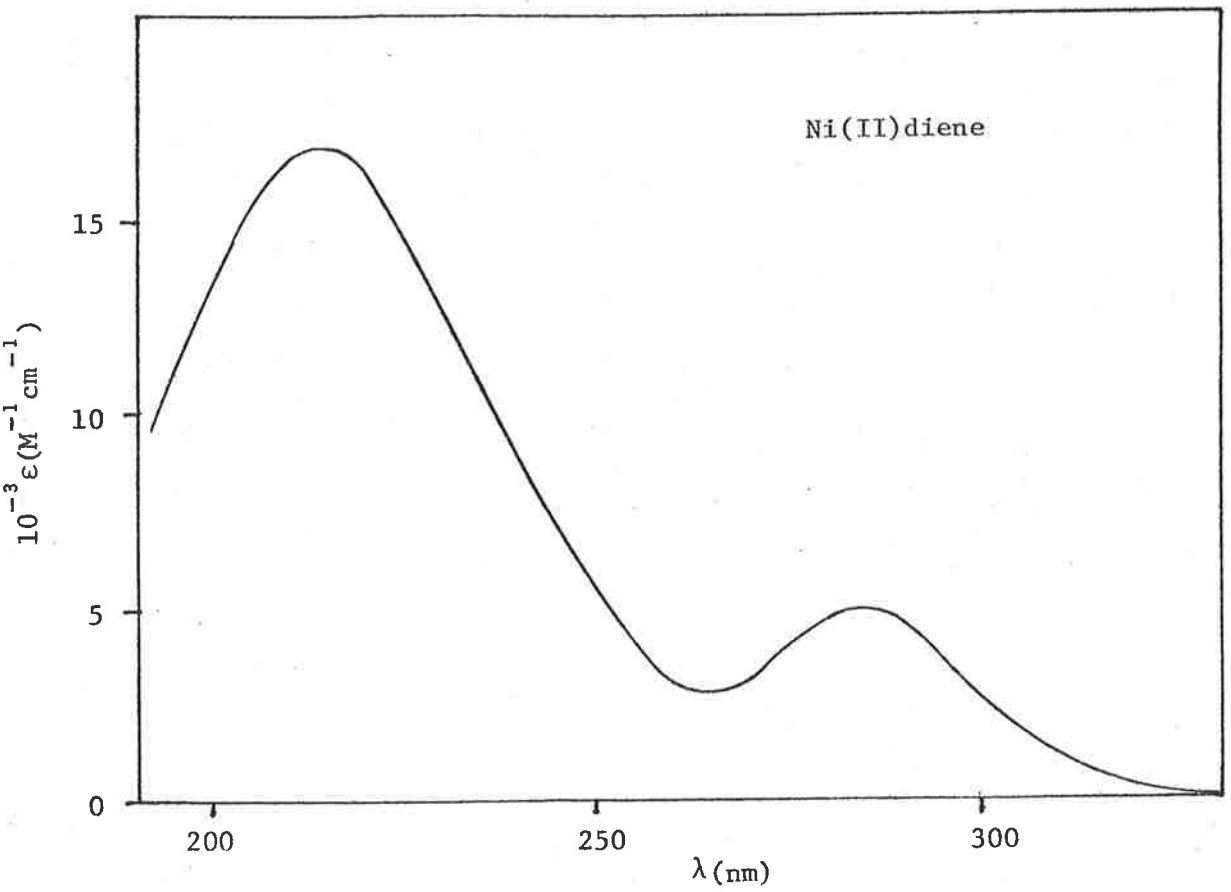

FIGURE II 2,2

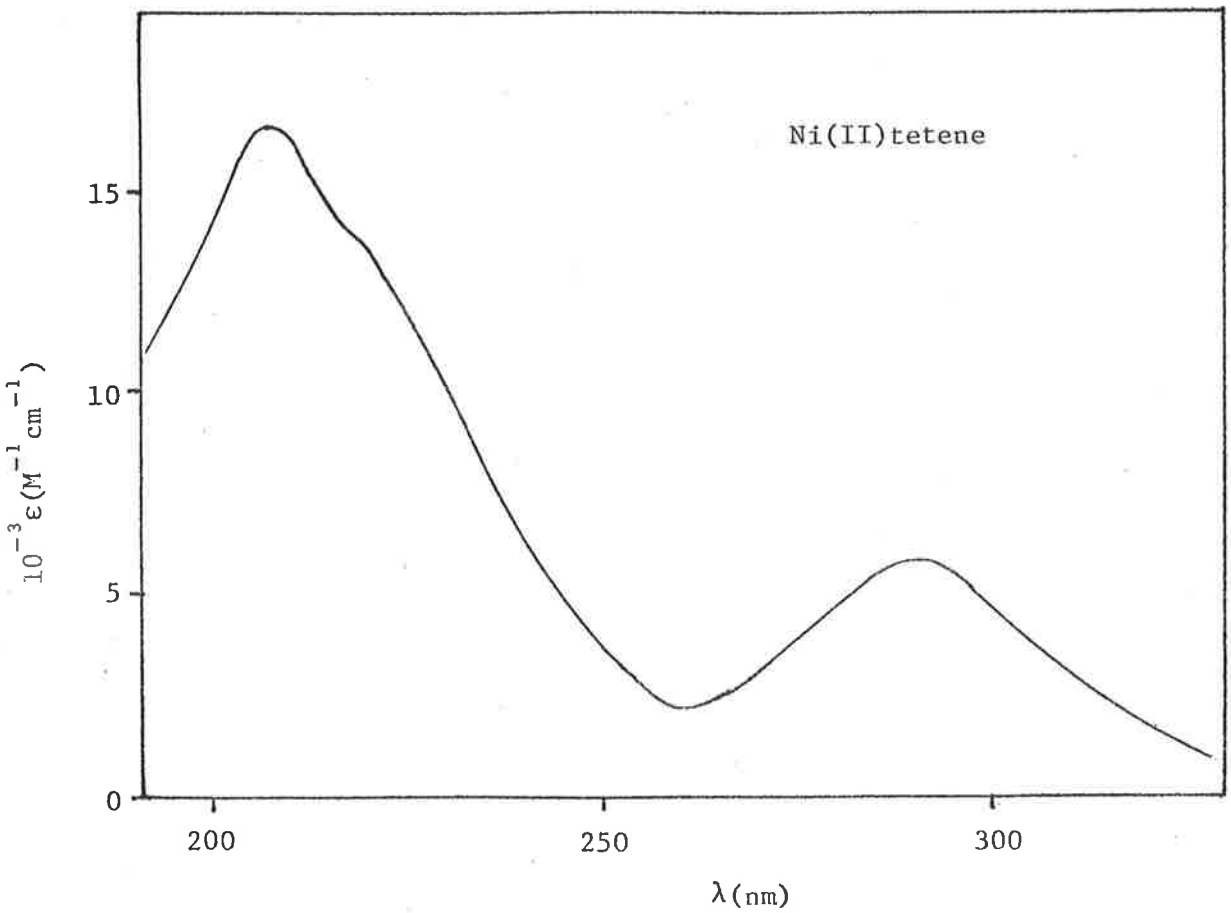

λ(nm)	ε(M^{-1} cm^{-1})
216	17000
282	5000
438	93

The identity of this complex was also confirmed by proton magnetic resonance spectroscopy (p.m.r.)[148]

This preparation is an example of the 'template' action of a metal ion in complex synthesis.[30] The usual reaction of acetone with ethylene diamine produces tarry polymeric material. In the presence of the nickel(II) ion, the cyclic Schiff-base amine complex is produced by a complicated series of reactions in which the nickel ion holds the diamine molecules in a suitable orientation for the cyclic condensation. The cyclic Schiff-base amine is stabilized by coordination, permitting oxidation/reduction to the cyclic tetraimine/tetraamine complexes.

2.2 The perchlorate complex of 5,5,7,12,12,14-hexamethyl 1,4,8,11 tetraazacyclotetradeca, 1,4,8,11, tetraene nickel(II) (referred to as Ni(II) tetene or Ni(II)tet) was prepared by nitric acid oxidation of the diene complex according to the method of Curtis.[148] Excessive oxidation of the diene complex should be avoided, since further oxidation beyond the formation of the tetraimine derivative can occur under the strongly oxidizing conditions. The point at which all the starting material has been oxidized can be detected by removal of a small sample of the reaction solution, which is then precipitated with sodium perchlorate. The presence of the diene complex can be detected using IR spectroscopy by the νNH peak at 3180 cm^{-1}. If this absorption persists, further oxidation is performed. The complex was characterized by its UV (figure II2.2) IR and pmr spectra.[148] Spectrophotometric analysis

of the stock solutions was obtained using the literature molar absorbance values;[148]

λ(nm)	ε(M^{-1} cm^{-1})
208	17000
291	6000
444	82

2.3 The 5,5,7,12,12,14 hexamethyl-1,4,8,11,-tetraazacyclotetradecanenickel(II) perchlorate complex (referred to as Ni(II) tetramine or Ni(II)tam) was prepared by the method of Curtis[149] via the reduction of the diene complex. The reduction was achieved using nickel-aluminium alloy in alkali medium. The complete reduction of the imine functions was indicated by the loss of the νC=N peak at 1670cm^{-1} in the IR spectrum. U.V. analysis suggested that the major conformational isomeric form of the product complex was the Curtis a isomer.[149] The analysis of the stock solutions of this complex was performed spectrophotometrically using[149]

λ(nm)	ε(M^{-1} cm^{-1})
206	10 500
235	15 600
462	79

The IR spectrum agreed well with the literature.

2.4 The preparation of 5,5,7,12,12,14-hexamethyl-1,4,8,11-tetraazacyclotetradeca-4,11,-diene dihydrogen perchlorate (referred to as 'free' diene or diene ligand) was based on a note in the Curtis review of macrocyclic complexes.[30] The procedure used to make 0.1 mole follows; the preparation was particularly water and impurity sensitive, so that only dry AR reagents were used. 14 ml of ethylenediamine was slowly added to a stirred refluxing solution of 90 gms of magnesium

perchlorate in 250 ml of acetone. A highly exothermic reaction occurred, and the solution turned yellow in colour. After the complete addition of the ethylenediamine, the reaction solution was refluxed for a further 30 minutes. 1M perchloric acid was added until the pH was ~5. This acidified solution was filtered, leaving a white product with traces of yellow impurity. The impure solid was warmed and stirred in 1M $HClO_4$ (40°C), in which the more buoyant particles of yellow impurity could be decanted off. This procedure was repeated until the traces of impurity were eliminated. The white product was washed several times with 1M $HClO_4$ and then with water. The white powdered crystals were air-dried then vacuum dried in a P_2O_5 dissicator. The compound was characterized by IR analysis.(150)

The dihydroperchlorate diene compound is relatively insoluble in hot and cold water and is remarkably resistant to imine hydrolysis. The stability of the macrocycle has been attributed to $N\text{-}H^{+}\text{-}N$ hydrogen-bonding between the acidic protons and the central nitrogen atoms, which, together with the geometrical constraints of the structure, combine to protect the imine linkages from rapid hydrolysis.(150)

2.5 The 5,5,7,12,12,14-hexamethyl-1,4,8,11-tetraazacyclotetradeca-4,11,- diene dopper(II) perchlorate complex (referred to as Cu(II) diene or Cu(II)di) was prepared by the method of Sadasivan and Endicott(150) in which copper(II) carbonate was heated with an excess of the diene ligand in a 1 : 1 methanol-water mixture. (This alternative method for the macrocyclic complex formation can be used for Ni(II) also, for which the carbonate or acetate is used). The product was characterized by UV(149) and IR(150) spectrophotometry. The stock solutions were

analyzed by UV-visible spectrophotometry using

λ(nm)	$\varepsilon(M^{-1}\ cm^{-1})$
<200	>10000
262	5900
507	110

2.6 The visible spectra of the Ni(II) and Cu(II) tetra-amine complexes show a single band (ε<100) and a broad asymmetric band (ε>100) characteristic of singlet ground state d-d transitions of Ni(II) and Cu(II) square planar compounds, respectively. The metal ion spectra of the complexes indicate that there is little variation in the ligand field strength of the hetero-cycle when amine and imine donor groups are interchanged, all having ligand field strengths comparable with bisethylenediamine.[30]

2.7 The UV-visible, and IR analyses were performed on Perkin-Elmer 402 and 457 spectrophotometers, respectively. The pmr characterizations were carried out on a Varian T60 spectrometer.

3. PREPARATION OF SOLUTIONS

Dilutions of stock solutions were carried out accurately using aerated doubly-distilled water. The glassware used was cleaned in either chromic acid or DECON 90 solution.

In the flash photolysis experiments, aerated solutions were transferred from the volumetric preparation flask directly into the flash cell. Syringes were used to admit solutions to the irradiation cell in the pulse radiolysis work. In cases where the presence of oxygen in solution either oxidized a reagent or could act as a reactant in tran-

sient decay processes, the solutions had to be deaerated before irradiation. This was necessary for solutions containing ferrous ion and for those where the Ni(III)L decay in the absence of oxygen was to be studied.

The rigorous method of degassing, involving freezing of the solution in liquid nitrogen under vacuum was not used in this work. A more convenient method was to evacuate a vessel containing the solution, which effectively released the dissolved gases in solution, and then allow oxygen-free nitrogen to bubble through for about five minutes. The vessel used in the flash experiments was a round-bottom flask with a 10 cm quartz flash cell attached via a graded-seal side-arm. Another side-arm, equipped with a tap and joint for connection to a vacuum pump, and an inlet tube for the nitrogen were also attached to the flask. The de-oxygenated solution was transferred to the flash cell via the side-arm by appropriate orientation of the vessel. Approximately μM concentrations of oxygen in solution can be obtained by this method.[151] This degassing technique does have the disadvantage, however, of a small loss of solution volume. This loss is small enough (<2%) to be neglected in most cases,

Nitrous oxide saturated solutions were prepared in the flash system by introducing high purity N_2O, instead of nitrogen, into the degassed solution. For the pulse radiolysis experiements, the solutions underwent ten minutes bubbling of the pure N_2O from the base of the syringe. In this procedure the dissolved air is replaced by N_2O.

The concentrations of the gases dissolved in solution were taken as the saturation solubilities at 1 atmos. pressure in pure water at 20°C.[152] viz.

gas	concentration
N_2	0.7 mM
O_2	1.4 mM
N_2O	30 mM

N_2O is aqueous solution has the useful property of the conversion of the highly reducing e^-_{aq} species to the oxidizing OH radical via a series of fast reactions represented as

$$N_2O + e^-_{aq} \xrightarrow{H_2O} OH + N_2 + OH^-$$

for which the specific rate is $\sim 10^{10} M^{-1}\ sec^{-1}$.(151)

All solutions were irradiated at ambient temperature (22 ± 5^oC). The error involved in rate determination over this temperature range is considered to be small, since low energies of activation can be assumed for the reactions of the very reactive intermediates used in this system.

4. THE IRRADIATION TECHNIQUES

The considerable majority of the work presented in this thesis was performed using the flash photolysis technique. Some data was obtained using the pulse radiolysis facilities of the A.A.E.C. Research Establishment at Lucas Heights, N.S.W.

The two techniques have been recently well reviewed.(153,154) The important characteristics of these methods are the nature of the energy deposition in the system, and the time scale of this deposition. In order to study fast reactions initiated by energy deposition, it is necessary that the reaction be initiated in a time that is short in comparison with the overall reaction time. The time resolution of these methods is typically in the microsecond range, but nanosecond and even picosecond

resolution has been achieved.

In pulse radiolysis, excitation and ionization by energy deposition via a pulse of high energy electrons replaces the process of photo-excitation by a photoflash. With these techniques the rapid absorption of energy serves to produce unstable species generally very far from their equilibrium states. The fate of these transients can be studied spectrophotometrically. The primary unstable species can be used to initiate reactions of interest.

Whilst for photoexcitation in solution the solvent is transparent to the wavelengths of photoexciting light, no substances are transparent to the absorption of energy from high-energy electrons. In this case the deposition of energy in the absorber system is Coulombic and therefore depends on the electron density of the absorber molecules. In dilute solutions therefore, the electron energy is given almost entirely to the solvent molecules and not to the solute,

i.e. $H_2O \rightsquigarrow OH, e^-_{aq}, H$ etc.

for which the yield in molecules/100 eV of electron dose (the G value) is $G_{OH} \simeq G_{e^-aq} \simeq 2.6$, $G_H \simeq 0.6$, for irradiation of energy > 1 MeV.(151)

The dose of OH radicals per pulse in N_2O-saturated solution was conveniently measured in this work by complete conversion to $(SCN)_2^-$ radical anions by

$$OH + SCN^- \xrightarrow{SCN^-} OH^- + (SCN)_2^-$$

for which $\varepsilon_{485}\ (SCN)_2^-$ is 7100 $M^{-1} cm^{-1}$.(94)

5 APPARATUS

5.1 The flash photolysis apparatus used in this work has been

previously described.[155] The flash of light was produced by the discharge of a 4.25μF high energy storage capacitor across the electrodes of a flash lamp. This lamp consisted of a T-shaped silica tube ≃16 cm long and ≃1 cm in diameter. The tube was sealed with two sharpened tungsten electrodes, and a vacuum tap for filling on a vacuum line. The lamp contained a 5 : 1 xenon-oxygen mixture at a pressure of 2-5 cm of Hg. The maximum energy input to the flash lamp was 1000J at 20 kV; in most experiments 500 J flashes were used. The flash profile had a typical half-width at half-height of ~8μsec with the overall duration of the intensity being ~30μsec. During the discharge of the lamp, observation of reaction is difficult because transient species are forming throughout this time, and stray light from the flash can interfere with the monitoring light signal. The emission spectrum of the flash is a continuum over a large range of the UV-visible spectrum, and is most intense around the 300 nm region. The discharge was triggered by the rapid earthing of an ignitron firing circuit either by manual triggering or via a trigger pulse from an external trigger source.

Flash solutions were contained in 10 cm quartz cylindrical cells, which were supported close to the flash lamp. The lamp and cell were enclosed by polished aluminium reflectors. When fast transient decay was observed, or when transient yields were large, 20 mm diameter cells could be used. However, for low yields and for very slow transient decays ($t_{\frac{1}{2}}$ >10 sec), thinner 6 mm cells were used. Almost homogeneous light absorption could be achieved in the thinner cell, resulting in higher transient concentrations being observable through the middle of the cell, and negligible diffusion effects,

5.2 The pulse source was a Van de Graaf electron accelerator, operated to give ~2μsec pulses having an average energy of 1 MeV and a typical pulse current of 10 mA. The pulse profile was approximately rectangular. The electron beam was focussed with magnets before leaving the exit window of the accelerator in order to cover the irradiation cell efficiently. A 1cm-square quartz cell was used. The penetration of the electron beam into the aqueous solutions was ~3 mm. The cell assembly was equipped with a two-way tap input, connected to the solution syringe and a source of high purity nitrogen. Irradiated solutions were flushed from the cell by the pressure of the nitrogen flow, and subsequently refilled by exchanging the phase of the tap.

5.3 In both techniques the fast spectro-photometric method was used to monitor the irradiated solutions. A block diagram of this apparatus, along with the irradiation source set-up is shown in figure II5.3. The flash photolysis arrangement consisted of a 100 W Xe : Hg lamp whose output was focussed onto a Baush and Lomb high intensity grating monochromator, having adjustable inlet and outlet slits, and an adjustable iris aperture on the outlet collimator. The light of selected wavelength passed through the solution cell and then through the long inlet collimator of a second monochromator. This collimator contained several discs with small concentric holes to greatly deplete the stray light pickup from the flash into the collecting monochromator. Two sets of monochromators were used, one each for the UV and visible regions. These were finely adjusted at the observation wavelength to allow maximum light passage through the detection system. The relative amount of stray light pick-up could be reduced by working at wave-lengths correspond-

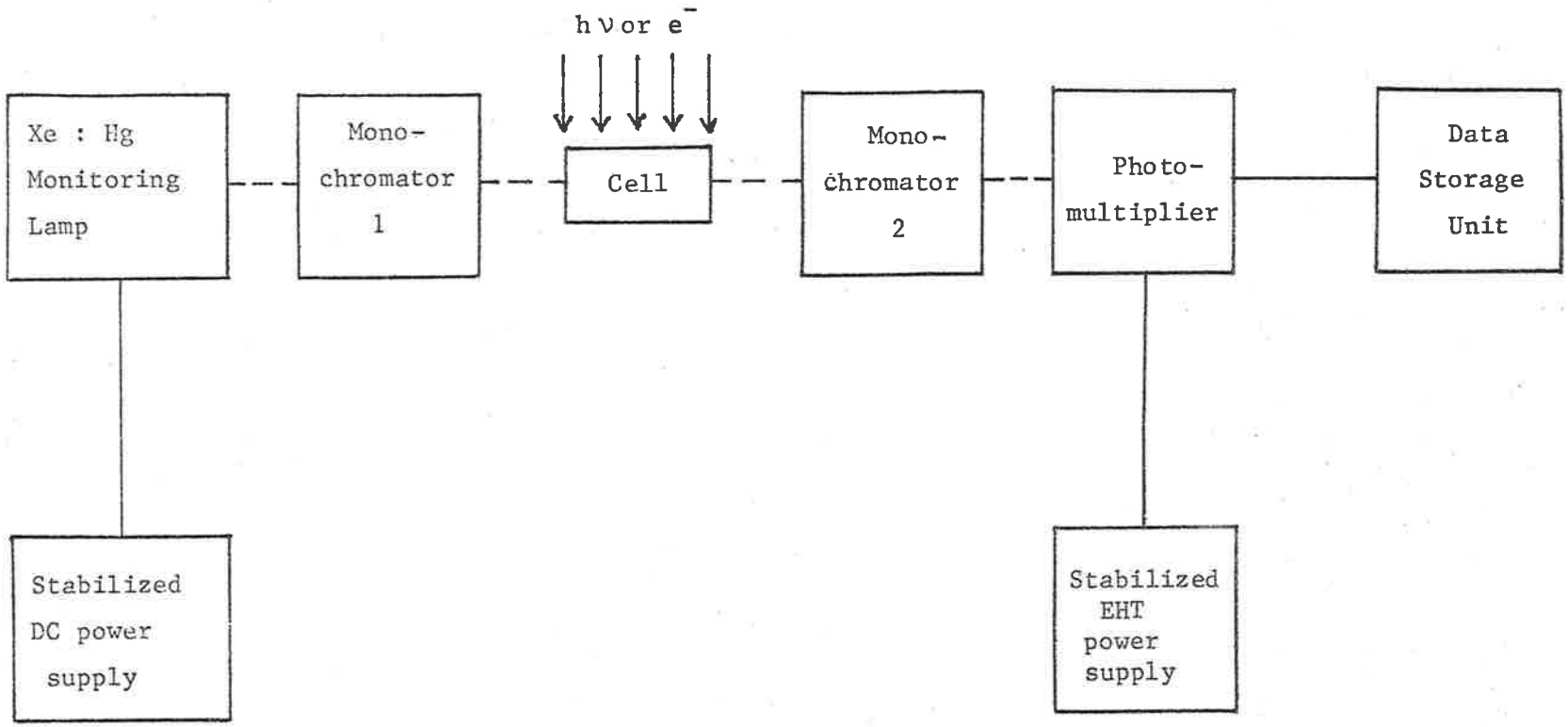

SPECTROPHOTOMETRY

APPARATUS

FIGURE II 5,3

ing to the most intense Hg lines of the monitoring lamp.

The detector system was an EMI 9558 QB photomultiplier (with an associated stabilized EHT power supply) followed by an integrated-circuit voltage follower. The photomultiplier output voltage, which could be filtered by an adjustable R-C filter circuit, was recorded as a function of time in one of several ways.

6. DATA STORAGE

6.1 In the pulse radiolysis work the voltage versus time data was photographed directly from an oscilloscope display, using a Polaroid camera attachment. The camera aperture was opened just prior to the pulse triggering and was left open for the entire duration of the transient reaction. The amount of monitoring light passing through the system initially was determined by a peak-peak measurement of the 'chopped' beam. This intensity value was given to the small 'lead-in' on the photographed reaction trace.

6.2 For the flash system the photomultiplier output was recorded as a function of time on a Tetronix 564 storage oscilloscope (prior to recent extensive updating of the storage and analysis systems). The time base of the oscilloscope was triggered externally by the initial triggering of the flash firing circuit. Accurate base-lines for absorbance measurement were obtained by using a delayed pulse generator. This device was connected between the ignitron firing circuit and the external trigger input of the oscilloscope. It triggered the oscilloscope once when the flash was fired, and again after the transient reaction was completely over.

The sensitivity of the measurement was increased by balancing a voltage source from the oscilloscope with the output of the photomultiplier in a differential comparator amplifier in the oscilloscope. This voltage was almost invariably set at 4.0 volts by prior adjustment of the EHT supply, and of the light output of the first monochromator. Transient absorption then resulted in a voltage change about this balance value. The stored trace on the oscilloscope display was photographed using 'Polaroid' film.

In highly absorbing solutions and at wavelengths corresponding to the continuum of the monitoring beam, it was necessary to apply high EHT levels to the photomultiplier in order to balance the 4.0 volt oscilloscope source. This resulted in lower signal-to-noise ratios. Lower signal-to-noise values were also inherent when observing reactions with half-lives ~10msec due to the resonance "bounce" of the spectrophotometer set-up induced in the initial flash noise shock.

6.3 This method of data storage utilized a digital transient recorder (Biomation 610B, Biomation Inc.). The 610B converts all analog input voltage signals to an accuracy of six binary bits. This means that the resolution is no better than 1 : 64, or 1.5%. The voltage sample input range was from 50 mV to 50 V full scale. The time resolution contained 250 words of information. The sample time interval which could be usefully employed was from 1 μsec (smaller times are possible, but the system is limited by the flash duration) to 50 msec. The data stored in the Biomation memory was displayed on an oscilloscope. If the data generated in a particular run was satisfactory for kinetic analysis, the digital output was transferred to a PDP - 11/10 computer for

the subsequent data analysis. The computer had a 16 k core memory. The data was conveniently transferred to the computer within 0.25 sec. A teletype, interfaced to the computer, was used for operator instructions and data input/output interactions. Punched tape recording of the digital data was possible through the teletype. Raw and processed data in the computer memory could be displayed on an interfaced oscilloscope.

Greater sensitivity in data storage could be achieved by an analog real-time subsystem of the computer. This AR11 module was capable of data storage by setting amplitude and time sampling specifications directly through the teletype. The AR11 converted the analog input signals to an accuracy of 10 binary bits, so that resolution of ~0.1% could be obtained. The amplitude range was program selectable between -2.5 to + 2.5 volts, this range being attenuable X1, X3, and X10 via an external amplifier. The programmable clock in the subsystem could be set to cover sample intervals from 50 μsec to 2 sec (so that very slow transient reactions ($t_{\frac{1}{2}}$ ~ min) could be recorded). 250 sample intervals were again covered per run.

The spectrophotometer beam could be monitored at any time before and after the flash by connection of the photomultiplier output to two digital volt meters (DVM). One meter could be triggered to hold a voltage sample just prior to the flash (to give initial transmittance data) and the other at any time interval (up to 1.1 sec) after the flash. This facility enabled convenient transient spectral measurements, by taking transmittance data before, and at a specified time after the flash, over a range of wavelengths. The constancy of the flash output was monitored by the DVM output of a photocell at the end of a perspex 'light-pipe',

collecting adjacent to the flash lamp.

The setting-up of the spectrophotometer and digital storage systems to receive transient data induced by the flash was as follows. After placing the sample cell in the monitoring beam, the photomultiplier output was adjusted to be about 2.0 volts, as shown on the DVM display. This voltage was fed as the negative input into either the Biomation 610B or AR11 recording systems. A back-off voltage was fed into the positive input of the recorder until the point of balance was within the voltage range of the transient recorder. The specifications of the data collection were then set, and the systems made ready to accept data when triggered. The time setting was arranged to cover the whole of the reaction when possible. A delay between the initial triggering of the recorder and the flash (to allow 'lead-in') was set by one of a series of electronic delay boxes. The initial output voltage through the system was sampled by triggering of the DVM during the lead-in period. The resultant kinetic data were displayed on an attached oscilloscope for the 610B and on the computer interfaced oscilloscope for the AR11, ready for rejection if unsatisfactory, or transferred to the computer memory for further analysis. A schematic representation of this is shown in figure II6.3.

7. TREATMENT OF DATA

7.1 For reactions which are simple first- or second- order processes (equal concentrations), the integrated rate expressions $\ln C_t$ or $^1/C_t$ (where C_t is the concentration of the reagent species at time t) give straight lines when plotted against time. The slopes of such plots are

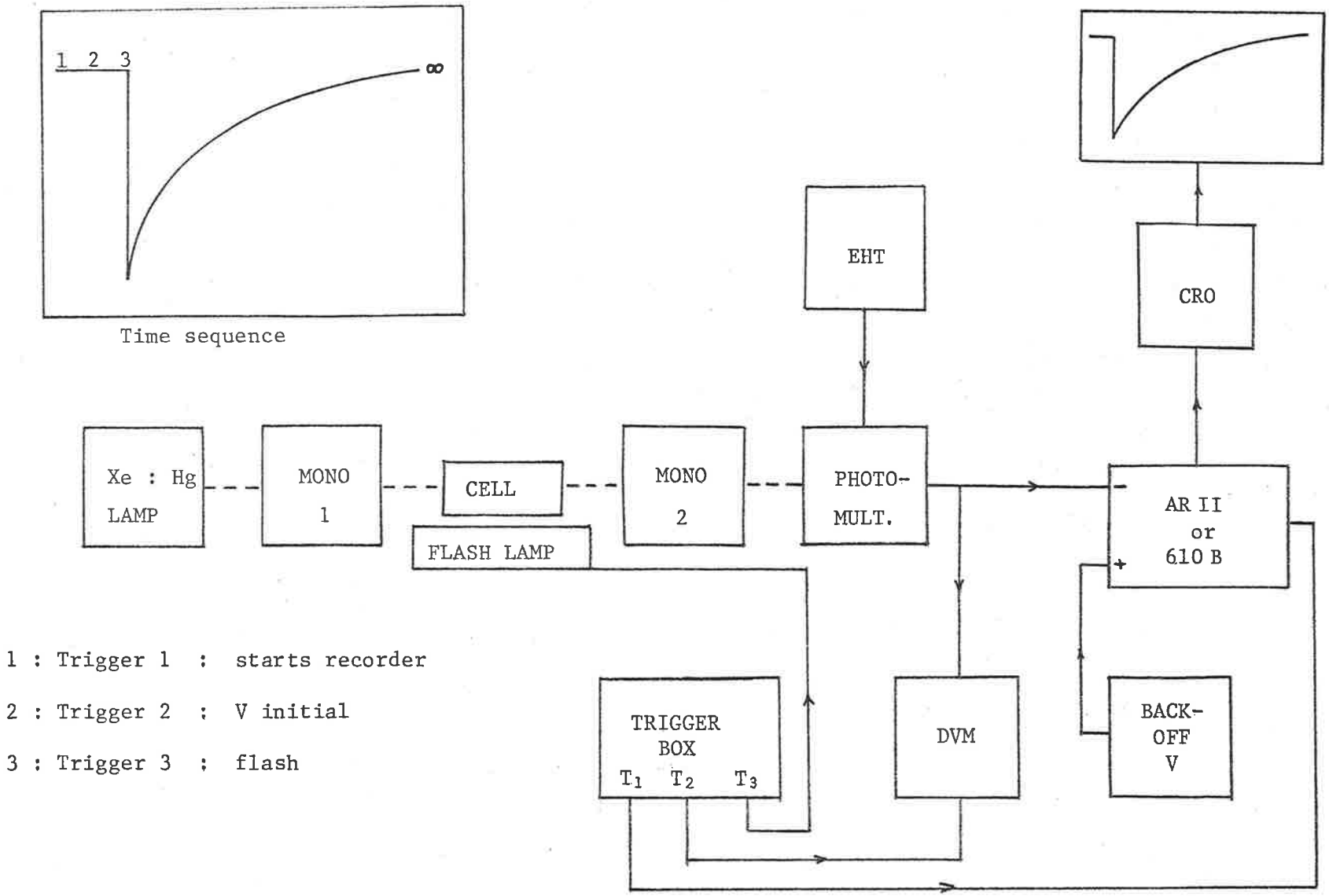
1 2 3
∞
Time sequence
EHT
CRO
Xe : Hg
LAMP
MONO
1
CELL
MONO
2
PHOTO-
MULT.
AR II
or
610 B
FLASH LAMP
1 : Trigger 1 : starts recorder
2 : Trigger 2 : V initial
3 : Trigger 3 : flash
TRIGGER
BOX
T1 T2 T3
DVM
BACK-
OFF
V

FIGURE II 6.3

equal to the respective rate constants, k_{1st} or k_{2nd}. When the reagent species is the only absorbing species at the observation wavelength, plots of $\ln OD_t$ or $1/OD_t$ are also linear, with the slope being k_{1st} or k_{2nd}/ε_1 respectively. Complication can arise if a product species absorbs significantly at the observation wavelength. If a known stoichiometric relationship exists between absorbing reactant and product species, an apparent molar absorbance may be used in second-order analysis.

In some cases in the present study, reactions were encountered whose kinetic data obeyed neither of the simple integrated rate expressions. Such reactions are referred to as 'mixed' order in the text of the thesis. This rather general term covers reactions in which:
(a) a reactant disappears by concurrent first- and second- order processes,
(b) the relative concentrations of the two reactant species are not equal (so that second-order kinetics are not obeyed), nor is one concentration in large enough excess to approximate pseudo-first order kinetics.
The former of these two classes of mixed order reaction could be analyzed using a previously written FORTRAN computer program[155] (PROGRAM FIT). Read into this program were the known value of k_{2nd} and three estimates of k_{1st}. Transient concentrations at each of many time intervals were calculated by a simple numerical integration procedure using the input rate constants. The deviation from the experimental concentrations over the time range was calculated and the interpolated value of k_{1st} which best fitted the actual results was chosen. For the latter mixed-order type of reaction, rough estimates only of rate constants could be obtained — only mechanistic inference was drawn from these mixed order reactions.

7.2 The experimental voltage versus time kinetic data were converted to absorbance (OD) readings using the expressions,

$$OD_t = \log \frac{Vo}{Vt} = \log \frac{Vo}{Vo - \Delta V_t}$$

where V_o is the initial output voltage of the monitoring beam,

V_t is the output voltage at time t after the flash/pulse

and ΔV_t is the voltage change observed at time t.

(Spectral measurements using the dual DVM set-up were conveniently carried out using the first equality above). Transient concentrations were obtained from absorbance values using the Beer-Lambert equation,

$$OD = \varepsilon.c.l$$

where ε is the molar absorbance

c is the concentration

l is the optical path length

7.3 The kinetic data from the Polaroid films was obtained using a trace reading instrument.[155] This consisted of a ruler whose movement perpendicularly across the trace on the photograph was interpreted as a digital voltage on a DVM, by attachment to a helipot potentiometer. Allowance was made for the error introduced by initial decay occurring during the transient build-up, by taking the zero-time of the decay measurement at least several μseconds after the maximum yield was reached. The kinetic analysis involved taking about 20 voltage readings over a time span covering at least two half-lives of the reaction. The decay rate considered to be characteristic of a given set of conditions was usually the average of three kinetic traces. The kinetic plots were carried out either manually onto graph paper, or using a previously written[155] computer program (PROGRAM A) which gave appropriate least-

squares error analysis. The repetitive nature of the manual calculations was facilitated in the flash work by always setting the initial photomultiplier voltage to be 4.0 volts. In such a case, a computer output had been prepared[155] for which OD_t values for a large range of ΔV_t values were tabulated. Included in these tables were the kinetic integrated simple rate law values for each voltage value.

7.4 The digitized voltage output data collected by the Biomation 610B or AR11 peripheral systems were directly amenable to kinetic analysis when transferred to the PDP-11/10 computer memory. A program KINETICS #4, written[156] in the computing language BASIC, firstly displayed the raw data on the interfaced oscilloscope. Since each of the 250 digitized data points is numbered in the memory, the data were accessible to editing routines, including the deletion of excessively noisy points, smoothing over noisy sections, or actual replacement of data points as needed. A signal averaging routine was available to improve repetitive noisy traces.

Whilst in the initial display mode, the points on the trace representing the initial and final absorbance values for kinetic analysis were chosen. Also chosen was the range of points to be covered by the kinetic analysis. The desired kinetic treatment of the data (i.e. first- or second- order) was the last specification needed to allow the kinetic analysis to proceed, after the recording specifications were entered. A least-squares regression analysis of the data using the kinetic algorithms was involved in the calculation of the experimental rate constant. The closeness of fit of the kinetic plot of the data to linearity was estimated from the calculated correlation coefficient.

Associated error analyses, and the percentage reaction covered were included in the output. The kinetic plot, with the least-squares line of best fit included, was displayed on the interfaced oscilloscope after the calculations were completed. Upon clearing the computer from this display mode, further kinetic analysis of the same data could be obtained by re-entry into the program at the appropriate place. Total clearing of the processed data from the memory allowed new data to be entered. The function of the program is represented schematically in figure II7.4

8. PRELIMINARY RESULTS

8.1 To be confident that the observed chemical effects in photolysed solution containing the bivalent macrocycles were not a consequence of complex self-absorption, some preliminary photolyses were performed. Solutions containing 50μM Ni(II)di and tet were observed immediately after the flash in neutral and acidic solution at 297 nm (within the Ni(II)L chromophore band). No photo-activity was observable. The UV spectra of multiply flashed solutions were identical to unflashed solutions.

8.2 The Ni(II)L UV-visible spectra were the same in neutral and 1M $HClO_4$ solution, indicating that there is no observable acid hydrolysis of the complexes which might complicate the results in this work.

FIGURE II 7.4

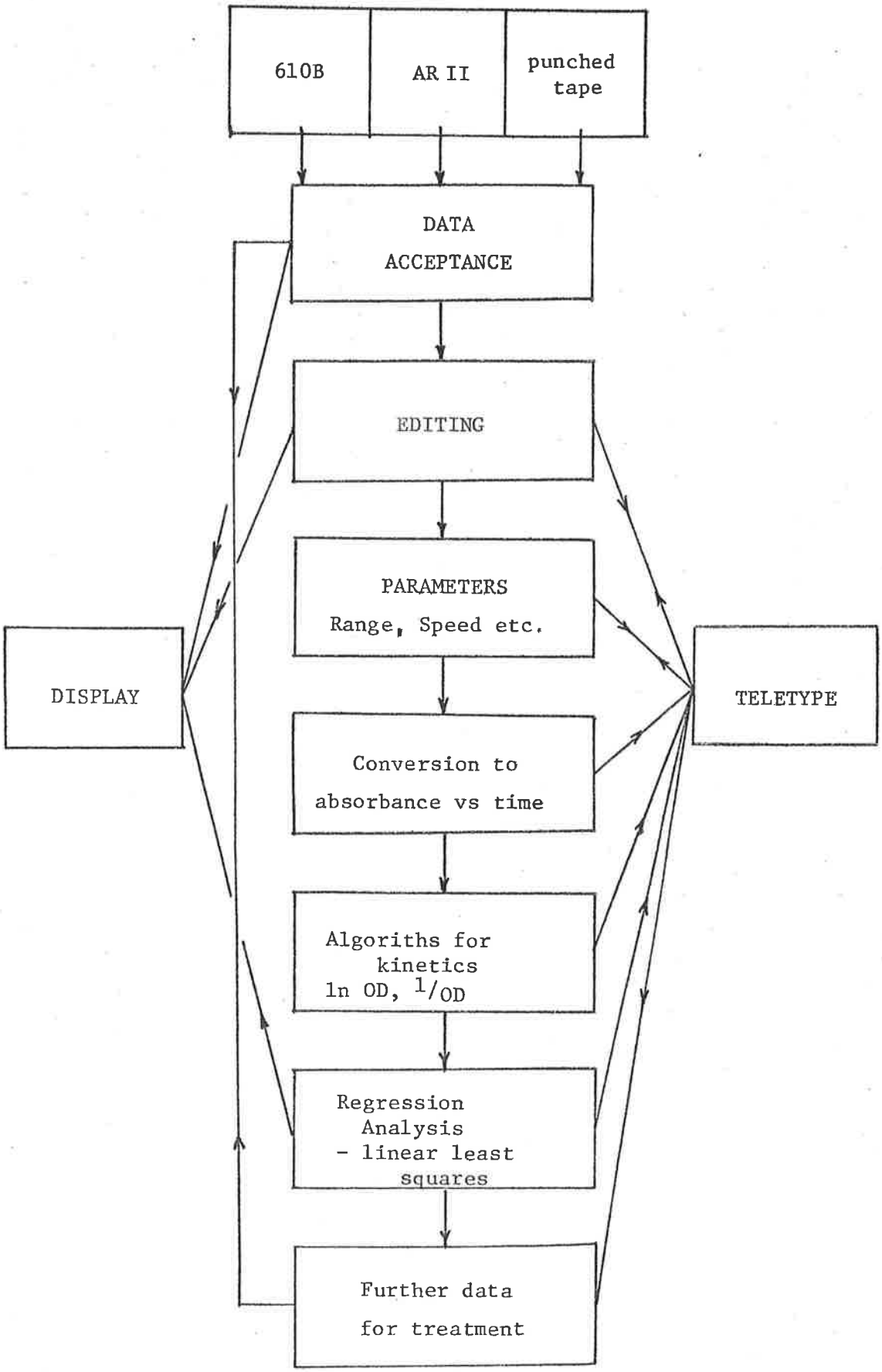
610B
AR II
punched tape
DATA ACCEPTANCE
EDITING
PARAMETERS
Range, Speed etc.
DISPLAY
TELETYPE
Conversion to absorbance vs time
Algoriths for kinetics
ln OD, 1/OD
Regression Analysis
- linear least squares
Further data for treatment

III OH AS PRECURSOR RADICAL

In this chapter, the transient characteristics of flash photolysed Ni(II)L(L = tet, di, tam), and Cu(II)di-H_2O_2 systems are investigated. The different complexes are treated separately, since although some aspects of the transient formations and decays are shared by all the complexes, notable differences do occur within the series. The Ni systems are presented in the order of increasing complexity of overall chemical behaviour.

1. Ni(II) TETENE, H_2O_2

1.1 The spectrum (shown in figure III 1.1) of the transient species produced by OH oxidation of the NI(II)tet complex was obtained from flash photolysed 20μM Ni(II)tet, 2mM H_2O_2 solution, 50 μsec after the flash. The spectral shape was independent of the pH of the solution over the range 1.0 - 5.3, and was the same in a solution 20mM in H_2O_2. The absorbance in the range 300-500nm is characteristic of trivalent nickel tetra-aza macrocycles as determined by Olson and Vasilevskis[9] in CH_3CN, and is similar to the aqueous solution spectra of non-cyclic amine Ni(III) complexes.[53,56] Absorption measurements below 300nm were not possible because of the considerable absorption of the bivalent complex chromophore in this region.

1.2 The yield of the complex transient at a given pH was dependent only on the $[H_2O_2]/[Ni(II)tet]$ ratio. This suggested a kinetic competition for the photochemically produced OH radicals between the bivalent complex and H_2O_2;

FIGURE III 1.1

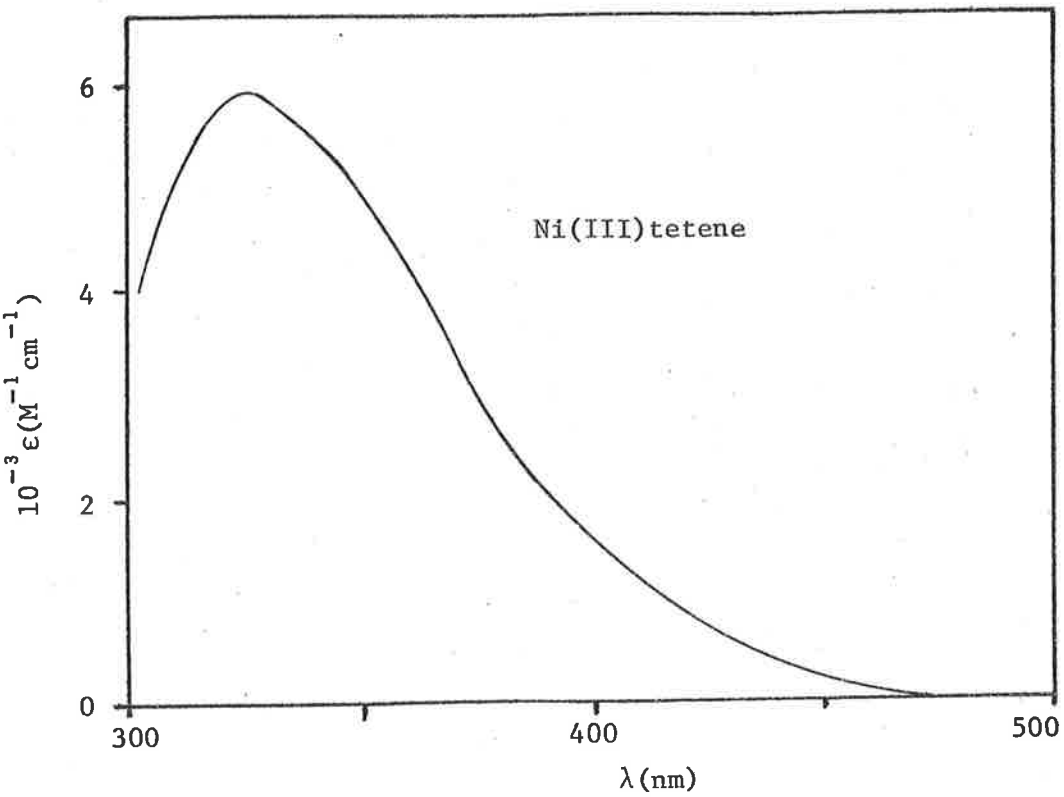

FIGURE III 1.2

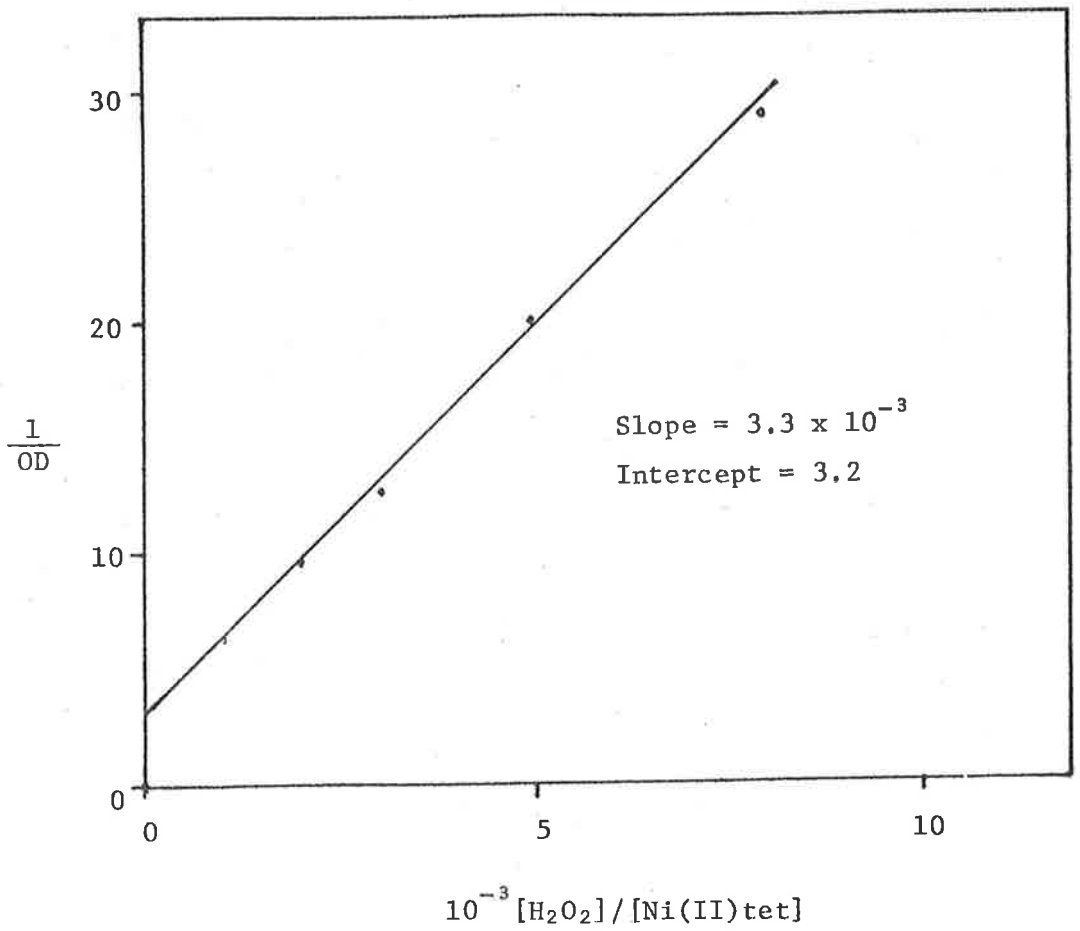

$$Ni(II)L + OH \xrightarrow{k_1} Ni(III)L + OH^-$$

$$H_2O_2 + OH \xrightarrow{k_2} HO_2 + H_2O$$

For this competition,

$$Y_{(Ni(III)L)} = Y_{(OH)} \frac{k_1 [Ni(II)L]}{k_1[Ni(II)L] + k_2[H_2O_2]}$$

where Y_x refers to the yield of species x in the photolyzed solution. Choosing a wavelength where only Ni(III)L absorbs to any considerable extent, the absorbance (OD) can be expressed by

$$OD = \varepsilon_{(Ni(III)L)} Y_{(OH)} \frac{k_1[Ni(II)L]}{k_1[Ni(II)L] + k_2[H_2O_2]}$$

and hence,

$$\frac{1}{OD} = \frac{1}{\varepsilon_{(Ni(III)L)} Y_{(OH)}} \left[1 + \frac{k_2[H_2O_2]}{k_1[Ni(II)L]} \right]$$

Provided the absorbance can be measured before any significant transient decay has occurred, a plot of $\frac{1}{OD}$ versus $[H_2O_2]/[Ni(II)L]$ should be linear, having a value of slope/intercept = k_2/k_1, where k_2 is known from the literature. At pH 2.0, the absorbances at 313nm of 10μM Ni(II)tet, 10-80mM H_2O_2 solutions were measured 50μsec after the flash. The experimental plot of $\frac{1}{OD}$ versus $[H_2O_2]/[Ni(II)tet]$ was linear (figure III 1.2) having a value of $k_2/k_1 = 1.0 \times 10^3$. Using the literature value of $k_2 = 1.2 \times 10^7 M^{-1} sec^{-1}$ (84) at this pH, $k_1 = 1.2\ (\pm 0.2) \times 10^{10} M^{-1} sec^{-1}$.

1.3 The decay rate of the Ni(III)tet species (observed at 313nm) was very pH dependent in the range 0.5 - 5.3, there being a marked decrease in rate with increased acidity.

For values of the $[H_2O_2]/[Ni(II)tet]$ ratio $\gtrsim 400$, the decay kinetics were first-order over the studied pH range, whilst an observable change to mixed order kinetics occurred for a value of the ratio <300. The observed value of the decay rate also varied with this concentration ratio, but was independent of the actual reagent concentrations for a particular value of the ratio. This result is shown in figure III 1.3 (pH4.0) for values of the ratio for which first-order kinetics prevailed. It was observed that for values of this ratio >1500, there was a pronounced levelling-off of the transient decay rate. Associated with an increase in the concentration ratio was a decrease in the observed yield of the oxidized complex.

For $[H_2O_2]/[Ni(II)tet]$ ~50, a two-step decay process was observed. At pH 5.3, each step was quite separately observable, with the primary decay being $\sim 10^3$ times faster than the secondary. However, at pH 2.0, the primary appeared as a faster initial half-life compared with the subsequent (equal) half-lives. The primary reaction at pH 5.3 was mixed order, while the secondary reaction was good first-order and independent of pH (pH range 2.0 - 5.3). The decay rate of the primary process depended on the $[H_2O_2]/[Ni(II)tet]$ ratio, while the secondary decay rate was linear in $[H_2O_2]$ and essentially independent of [Ni(II)tet] for small changes in these concentrations.

These results suggest that the decay of the Ni(III)tet complex is a bimolecular process, with the concentration of the reductant species being controlled by the $[H_2O_2]/[Ni(II)tet]$ ratio. The reductant species is thus considered to be the 'HO_2' radical, which is produced in the initial competition of the two reagents for OH radicals. The actual

FIGURE III 1.3

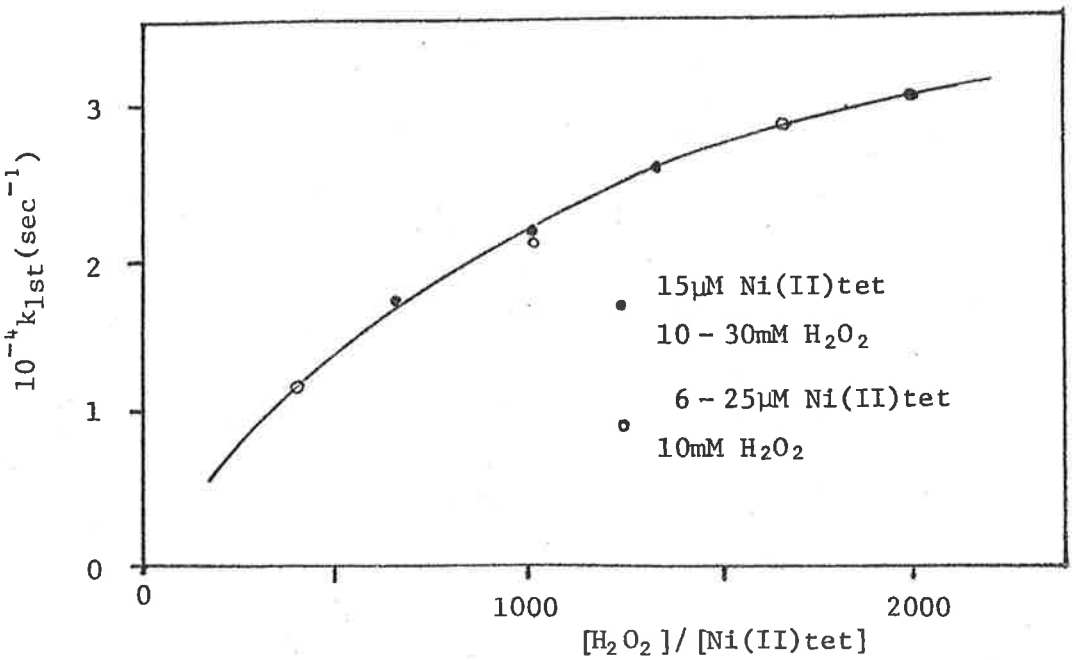

FIGURE III 1.4

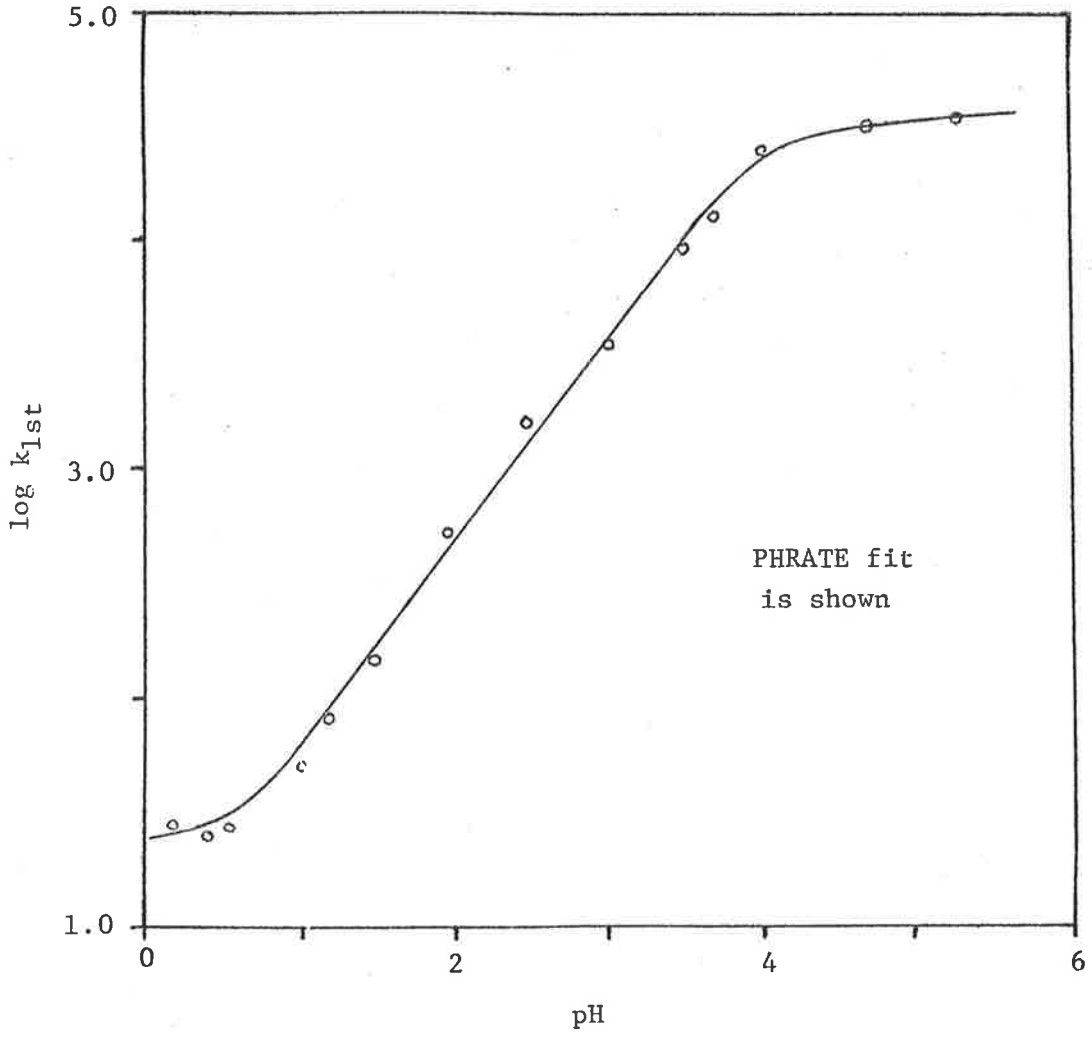

oxidized product yielded in excess in the competition depends of course on the reagent ratio. The equation for the tervalent complex reduction is

$$Ni(III)tet + 'HO_2' \longrightarrow Ni(II)tet + O_2(+H^+)$$

where 'HO_2' specifies the hydroperoxy, or superoxy radical species in either of its acid-base forms, HO_2 or O_2^-.

For values of the reagent ratio >500, 'HO_2' is produced in significant excess over Ni(III)tet, so that the observed complex decay approximates pseudo-first order. Further increases in the ratio cause the initial competition to become almost one-sided in favour of 'HO_2' production. When the ratio has a value >1500, the competition becomes so one-sided that the yield of 'HO_2' approaches the total photochemical yield of OH radicals ($Y_{(OH)}$). This is confirmed experimentally by the observed levelling-off of the transient decay rate under such conditions. This is also a consequence of $Y_{(OH)}$ being independent of $[H_2O_2]$ over a very large range.[100] The observed decrease in Ni(III)tet yield is also a consequence of the one-sided competition.

The change to mixed-order kinetics for values of the ratio <300 reflects the fact that the 'HO_2' is not produced in sufficient excess for pseudo-first-order kinetics to prevail. In the region of the ratio around 150 the kinetics of decay were approximately second-order. A further decrease in $[H_2O_2]/[Ni(II)tet]$ results in Ni(III)tet being produced in excess over the 'HO_2' concentration. Under such conditions, the complex transient reacts with the available 'HO_2', observable as the mixed order primary process in the two step decay. The excess Ni(III)tet remaining after the primary reaction depletes the $[HO_2]$ to zero,

then decays by a pseudo-first order reaction with H_2O_2. (Later evidence in section VIII 2.2, supports this conclusion on kinetic grounds). A plot of the observed first-order rate constant versus H_2O_2 for values of the reagent ratio <100 was linear, passing through the origin. The slope, which is equal to k(Ni(III)tet + H_2O_2) was 2.7 (±0.4) x $10^3 M^{-1} sec^{-1}$, independent of pH in the region 1.0 - 4.0.

1.4 The observed decay of the tervalent tetene in flash photolysed 10μM Ni(II)tet, 20mM H_2O_2 was first-order, with k_{obs} ≃3.5 x 10^4 sec^{-1} at pH 5.3 and ≃2.5 x $10^1 sec^{-1}$ at pH 0.1. pH values become rather indefinite above natural pH after the flash, since the HO_2 species deprotonates, introducing μM concentrations of H^+ into these unbuffered solutions;

viz. $HO_2 \rightleftharpoons O_2^- + H^+$ pKa = 4,88

The determination of the rate at pH 5.3 was chosen as the limit to which meaningful results could be obtained in this unbuffered system. The actual rate dependence on acid concentration, determined of the pH range 0.1 - 5.3 is shown in figure III 1.4. The ionic strength (μ) of the solution was not kept constant over the covered pH range, since at pH ≲3.5 the reactant charge product is zero, and at pH ≳3.5, where the charge product is negative, the change in μ is too small for the effect on the observed rate to be significant.

In the kinetic analysis of this system, the controversial species $H_2O_2^+$ was considered to be a possible form of the superoxy radical in acidic solution

i.e. the acid-base equilibria

$$H_2O_2^+ \overset{K_1}{\rightleftharpoons} HO_2 + H^+ \overset{K_2}{\rightleftharpoons} O_2^- + H^+$$

were considered. A Fortran computer program PHRATE (see appendix) was written, into which were substituted various values of K_1 and K_2 , and of k_1, k_2, k_3, the absolute rate constants for the reactions

$$\text{Ni(III)tet} + H_2O_2^+ \xrightarrow{k_1}$$

$$+ HO_2 \xrightarrow{k_2}$$

$$+ O_2^- \xrightarrow{k_3}$$

to give a determination of $k_{obs} = k_1[H_2O_2^+] + k_2[HO_2] + k_3[O_2^-]$. The excess '$HO_2$' radical decays unobservably at the observation wavelength via disproportionation.

i.e. $2HO_2 \longrightarrow H_2O_2 + O_2$

The total concentration of superoxy radical was set at an arbitrary, but realistic value of 20μM, with the actual concentrations of each radical form at a particular pH, being set by K_1 and K_2. The value of k_3 was in turn set at $2 \times 10^9 M^{-1}sec^{-1}$ from the observed decay rate of $\sim 4 \times 10^4$ sec^{-1} at pH 5.3 The pK_1 of the supposed $H_2O_2^+$ radical has been determined in the literature to be 1.0 (±0.4). The pK_1 used in PHRATE varied between 0.5 - 2.0 when $H_2O_2^+$ existence was considered, and was set at -6.0 when it was considered not to exist. The pK_2 value was varied between 3.7 - 5.2. The pH range covered by the program was from 0 to 5.5. The value of $k_3 = 2 \times 10^9 M^{-1}sec^{-1}$ was used with a wide variety of k_2 and k_1 values, with $k_3 > k_2 > k_1$ on electrostatic grounds. When appropriate parameters were used in PHRATE that assumed the conditions set out below, the plot of calculated log k_{obs} versus pH obtained was virtually identical to the experimental plot of the same (figure III 1.4). The conditions were;

(i) no $H_2O_2^+$ exists in the 0 - 5.5 pH range.

(ii) pKa of $HO_2 \rightleftharpoons H^+ + O_2^-$ is 4,1.

(iii) $\frac{k_3}{k_2} = \frac{k(Ni(III)tet + O_2^-)}{k(Ni(III)tet + HO_2)} \simeq 1.2\ (\pm 0.2) \times 10^3$

or with

k_3 chosen to be $2 \times 10^9\ M^{-1}sec^{-1}$

then $k_2 \sim 1.7\ (\pm 0.3) \times 10^6\ M^{-1}sec^{-1}$.

(iv) $[HO_2]$total = 20μM (estimated using SCN^- as a dosimeter solution).

(v) the disproportionation reactions of the superoxy radicals do not compete with the Ni(III)tet reaction. This assumption is quite reasonable since the second-order rate constants for the reactions $O_2^- + O_2^-$, $HO_2 + O_2^-$ and $HO_2 + HO_2$ are $<10^2$, 8.5×10^7, $7.6 \times 10^5\ M^{-1}sec^{-1}$ respectively.[102]

The difference in rate between the two forms of the superoxy radical with the Ni(III)tet complex is too large to be due to electrostatic considerations only. It appears therefore that the activation requirement for electron-transfer may be enthalpic, where HO_2 oxidation requires prior O-H bond dissociation, which is not important for the O_2^- analogue.

The most accurate determination of the pKa of the superoxy radical has been in buffered solution where a value of 4.88 (±0.10) was obtained.[102] A lower value of 4.3 (±0.2), as obtained in earlier work[104] is more consistant with the result obtained in the present work. It is presumed that factors leading to lower values of this pKa in the unbuffered determinations were operative in this work. The results also add to the number of published results that discount the existence of the $H_2O_2^+$ species in the 0-2,0 pH region.

Although the absorption spectrum of the hydroperoxy radical is known, its short wavelength absorption, and the high absorptivity of the bivalent macrocycle in the 200-300 nm region made direct observation impossible under the experimental conditions used. However, it is known that 'HO_2' reacts with TNM (tetranitromethane) in aqueous solution to produce nitroform, an intensely coloured anion, having a molar absorbance of $1.5 \times 10^4 M^{-1} sec^{-1}$ at $\lambda max = 350nm$,

i.e. $'HO_2' + C(NO_2)_4 \longrightarrow C(NO_2)_3^- (+ H^+) + NO_2 + O_2$

(TNM is used as a scavenger species for reducing radicals in general). Addition of 50μM TNM to a solution at pH 2.0 containing 20μM Ni(II)tet, 40mN H_2O_2 changed the absorbance observations at 313nm upon flashing, from a first-order decay with $k_{1st} \simeq 650 sec^{-1}$, to a first-order formation with $k_{1st} \simeq 470\ sec^{-1}$. This value of the formation rate agrees very well with that expected for these concentrations from the literature value of TNM + HO_2 at pH 2.0 of $1.0 \times 10^7 M^{-1} sec^{-1}$ viz. $5 \times 10^2 sec^{-1}$.(207) The product spectrum in the region 300-400 nm showed the characteristic absorption of the nitroform anion.

2. Ni(II)DIENE, H_2O_2

2.1 The spectrum of the intermediate produced by OH oxidation of the Ni(II)diene complex was obtained by flash photolysis of a 20μM Ni(II)di, 2mM H_2O_2 solution. The spectral shape in the observed region 300-600 nm was very pH dependent in the range 0.2 - 5.3 At a particular pH the absorbance measurements made 50μsec, 0.5 msec and 10 msec after the flash showed that the absorption in the visible region decayed more rapidly than that in the U.V. region. In the pH range

above about 3, the transient decay was faster particularly in solutions near natural pH (5.3).

Ideally, absorption measurement for transient spectral purposes should be made before any transient decay has occurred, or at least before any significant decay has occurred. The usual method of taking absorption measurements soon after the initial transient build-up during the flash was not suitable here, because the actual observed transient rate of decay depended on the observation wavelength, and, in solutions near natural pH, the decay rate was quite significant compared with the flash duration. Where transient decay was not significant during the flash time, absorbance measurements were made 50μsec after the flash was triggered. So that real comparisons between absorptions over the observed wavelength range could be made for the solutions of varying pH, values were determined by extrapolating the kinetic data ($\frac{1}{OD}$ vs t) back to t = 0. These extrapolated absorption values, ODo, have no very real physical significance, since the flash profile has a quite finite duration on the time scale considered here. Any process which completes an adjustment of transient concentration by the time of decay observation just after the flash, cannot be accounted for in the extrapolation. If the process involves an increase in the transient concentration, the extrapolated value will be an overestimate of the absorption; an under estimate would result if the process involved a decrease in the transient concentration. If the concentration adjustment was operating during the observable decay, reasonable allowance for it would be made in the extrapolation. Hence, the extrapolated absorbance values are useful for comparison at a time <u>after</u> the flash duration. They provide no information about actual transient concentrations at shorter times, unless allowance

for possible fast transient adjustment processes occurring during the flash is made. This point is relevant in terms of the mechanism of OH oxidation of the complex, discussed later.

The spectra shown for this system in figure III 2.1 are of extrapolated absorbances (where necessary) against wavelength. For reliable absorbance comparison, the spectra over the pH range 1.0 - 5.3 have been normalized to OD_{405} at pH 2.0. From the figure it is obvious that there are two separate transient species which result from OH attack on the Ni(II)diene complex immediately after the flash. The major transient observable in acidic solution has a peak at ~315 nm, with an associated broad shoulder at ~375 nm. In solutions near natural pH, the major absorption occurs in the visible region with λmax ~550 nm. Associated with this visible peak is a U.V. absorption observable below ~310 nm. A reasonably sharp isosbestic point at ~460 nm confirms that there are only two pH dependent intermediates in this system. The acid intermediate absorbs in the same spectral region as the Ni(III)tet complex, and the absorption is similar to the Ni(III)diene spectrum determined in CH_3CN.[9] The site of oxidation on the complex is thus considered to be the metal for the acid transient. The visible absorption species is not observed for the tetane analogue, but (as shown later) is again apparent for the tetramine system. This transient is considered to be the analogous coordinated ligand radical intermediate observed by Barefield[46] having λmax ~540 nm, in the base-promoted reduction of Ni(III) tetramine in non-acidic aqueous solution;

i.e.

$$\overset{III}{Ni\ NH} + H_2O \rightleftharpoons \overset{II}{Ni\ N\cdot} + H_3O^+$$

(The results presented in Barefield's work suggested the reversibility of this reaction).

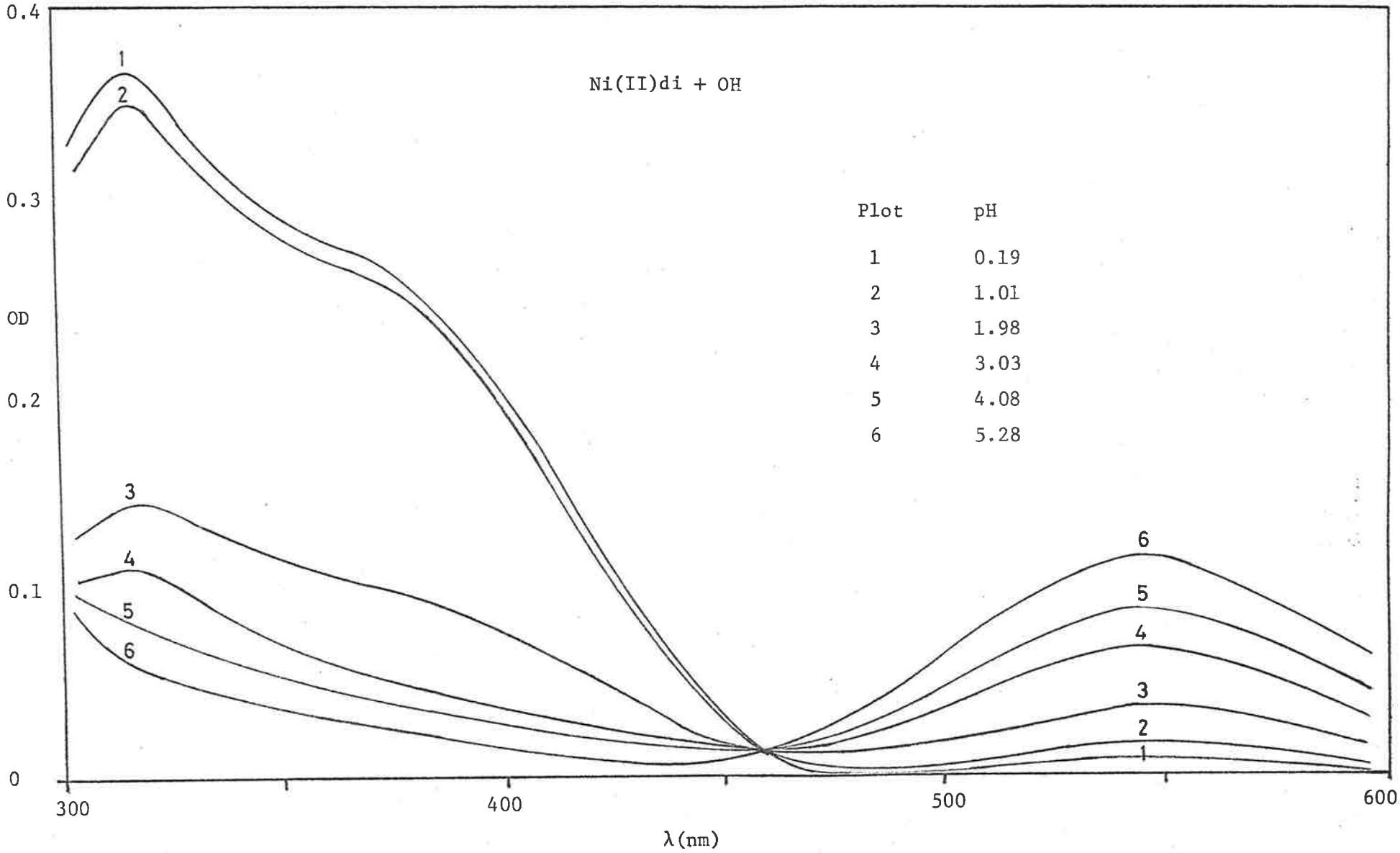

FIGURE III 2.1

2.2 The appearance of the two oxidized forms of the Ni(II)diene complex after the flash can be accounted for in two ways. For simplicity the $OH + H_2O_2$ reaction is left out of both schemes.

(i) $$Ni(II)L + OH \xrightarrow{k_1} Ni(III)L + OH^-$$
$$\searrow^{k_2} Ni(II)L^{\bullet} + H_2O$$

In this mechanism there is attack of the OH radical on both the metal centre (by electron-transfer), and on the ligand (by apparently H-atom abstraction). The pH dependence of the observed product yields is accounted for by changes of k_1 and k_2 with pH. In acidic solution it is suggested that $k_1 > k_2$, with the inverse relationship holding at natural pH.

(ii) $$Ni(II)L + OH \longrightarrow Ni(II)L^{\bullet} + H_2O$$
$$\Big\Vert\, H^+$$
$$Ni(III)L$$

OR

$$Ni(II)L + OH \longrightarrow Ni(III)L + OH^-$$
$$\Big\Vert$$
$$Ni(II)L^{\bullet} + H^+$$

This alternative mechanism suggests that OH radical attack occurs at one site only. The transient complex thus produced then undergoes a rapid equilibrium reaction to produce an equilibrium concentration of the other species. The proportion of each species in solution depends on the pH, where

$$K = \frac{[Ni(III)L]}{[Ni(II)L^{\bullet}]\,[H^+]}$$

or

$$K = \frac{[Ni(II)L^{\bullet}]\ [H^+]}{[Ni(III)L]}$$

depending on the actual site of initial OH attack.

To analyse for the more likely of these two mechanisms, observation wavelengths for each intermediate complex form were chosen. The Ni(III)L was observed at 405 nm, which is mid-range between the two regions of absorption of the other species. The ligand radical was observed at 546 nm. (Both these wavelengths correspond to intense mercury lines in the monitoring beam). The absorbances at 405 nm and 546 nm, extrapolated where necessary over the pH range 0.2 - 5.3, are shown in figure III 2.2a . The values of OD_{405} for pH >4, and of OD_{546} for pH < 1 were quite small and are thus most in error.

The absorbance values obtained are estimates of the absorbances immediately after the flash duration with due allowance for the transient decay. In considering mechanism (ii) above, it is assumed that the equilibrium has been established by the time of observation. Using the second expression for the equilibrium constant, and the Beer-Lambert equation,

$$\frac{[Ni(II)L^{\bullet}]}{[Ni(III)L]} = \frac{K}{[H^+]} = \frac{OD_{546}}{OD_{405}} \cdot \frac{\varepsilon_{405}(Ni(III)L)}{\varepsilon_{546}(Ni(II)L^{\bullet})}$$

where the ε refers to the molar absorbance of the bracketted species at the stated wavelength. Hence,

$$\log \frac{OD_{546}}{OD_{405}} = -\log [H^+] + \log\left[K \cdot \frac{\varepsilon_{546}\ (Ni(II)L^{\bullet})}{\varepsilon_{405}\ (Ni(III)L)}\right]$$

$$= pH + \text{constant}$$

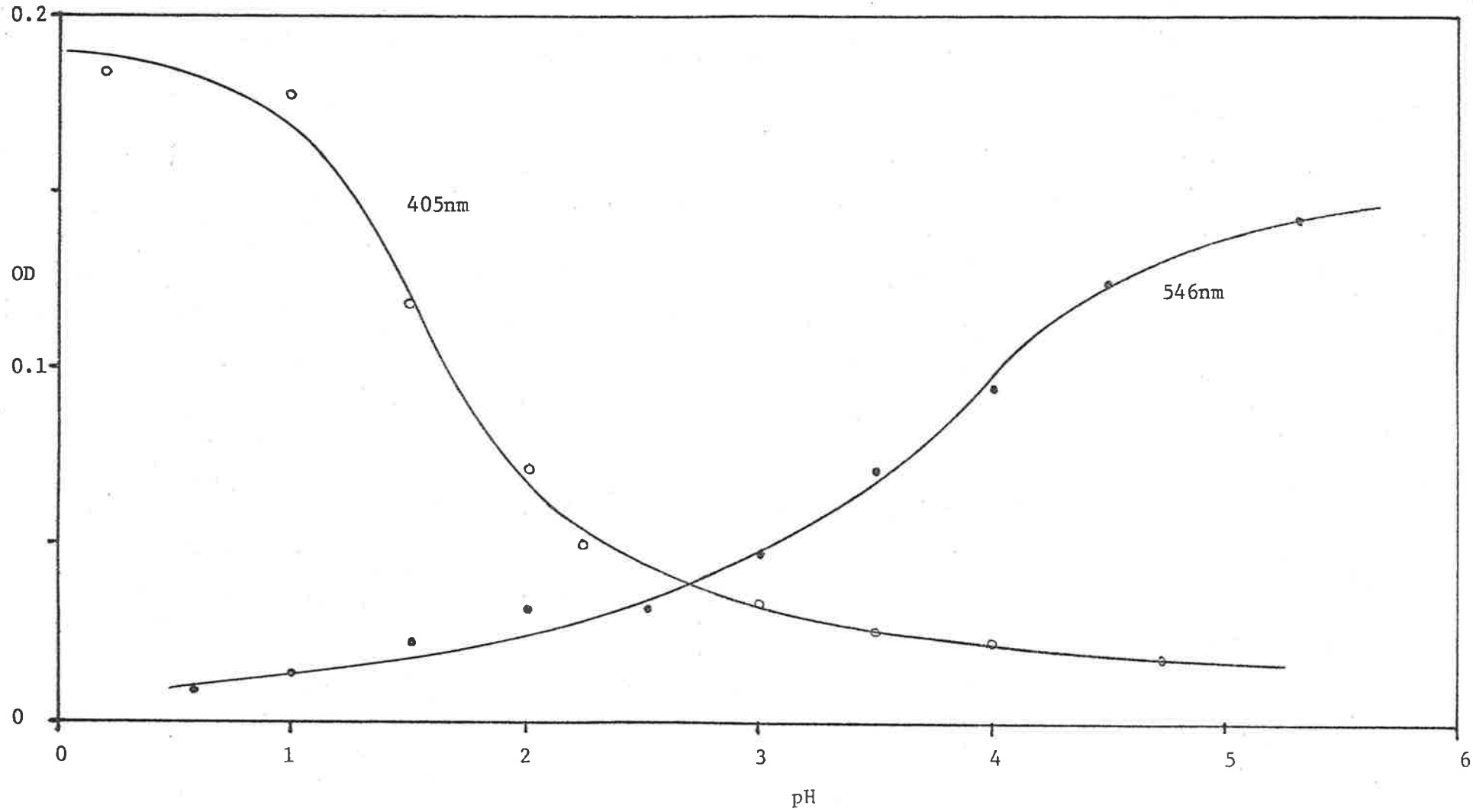

FIGURE III 2.2a

if the molar absorbances can be assumed to be independent of the pH. A plot of the logarithm of OD_{546}/OD_{405} versus pH should thus be linear with unit slope. The absorption ratio was determined over the pH region 0.5 - 5.3 for a 20μM Ni(II)diene, 2 mM H_2O_2 solution. The plot of log (OD_{546}/OD_{405}) against pH was essentially linear over this range, (figure III 2.2b) with a slope of +0.50 (±0.07), well below the anticipated value of +1.0. The effect of possible changes in the concentration of available OH radical would result in changes in the total concentration of oxidized complex, and not affect the concentration ratio of the two intermediates. The independence of the ratio on the available OH concentration was demonstrated by obtaining the same slope of the experimental plot (+0.59 (±0.06)) for a solution 10 mM in H_2O_2 in the studied pH region 0.5 - 3.0.

The results suggest that the equilibrium concentrations are not established over this wide pH range by the time of absorbance observation. i.e. no fast equilibrium exists between the two transient complexes. However, interchange between the two oxidized comples forms may occur more slowly via this mechanism: this is not observable here because of the occurrence of the fast transient decay.

2.3 Considering the initial competition for OH radicals in this system with mechanism (i) operating,

viz.

$$Ni(II)L + OH \xrightarrow{k_1} Ni(III)L + OH^-$$

$$Ni(II)L + OH \xrightarrow{k_2} Ni(II)L^{\bullet} + H_2O$$

$$H_2O_2 + OH \xrightarrow{k_3} HO_2 + H_2O$$

we have at any pH

FIGURE III 2.2b

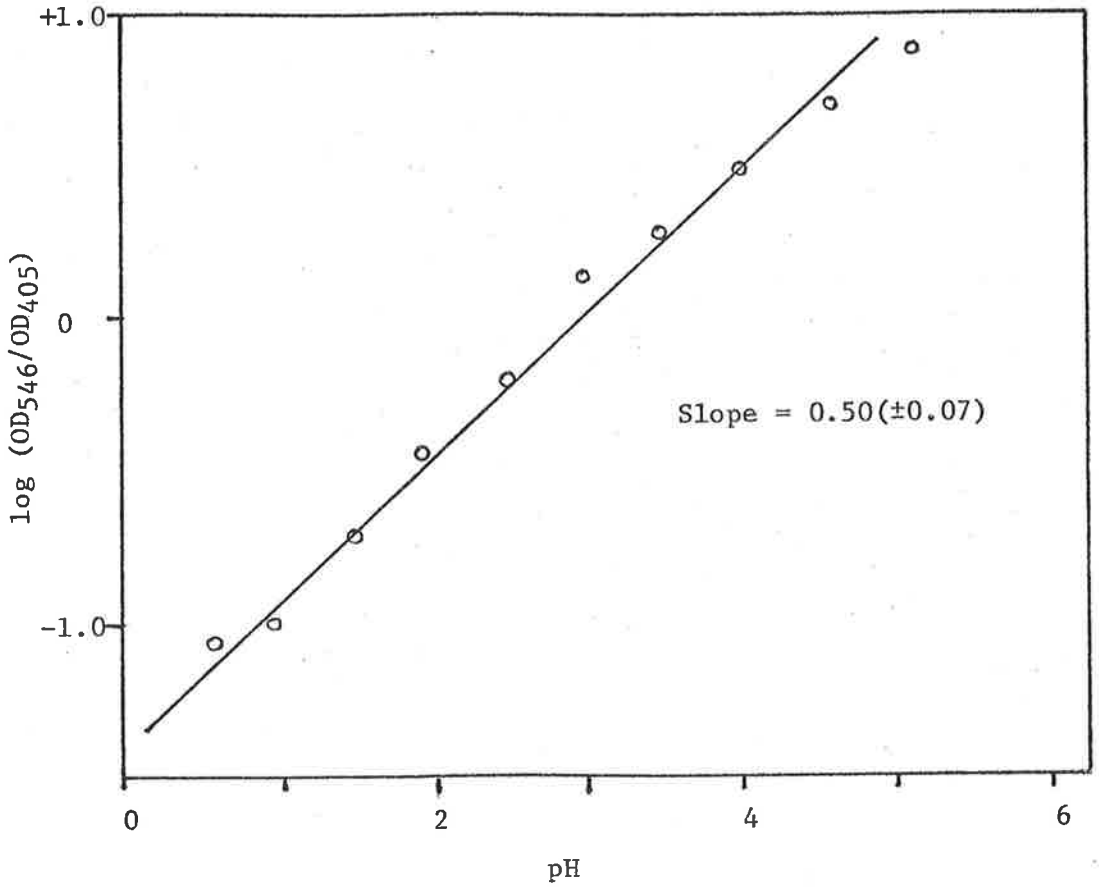

FIGURE III 2.3

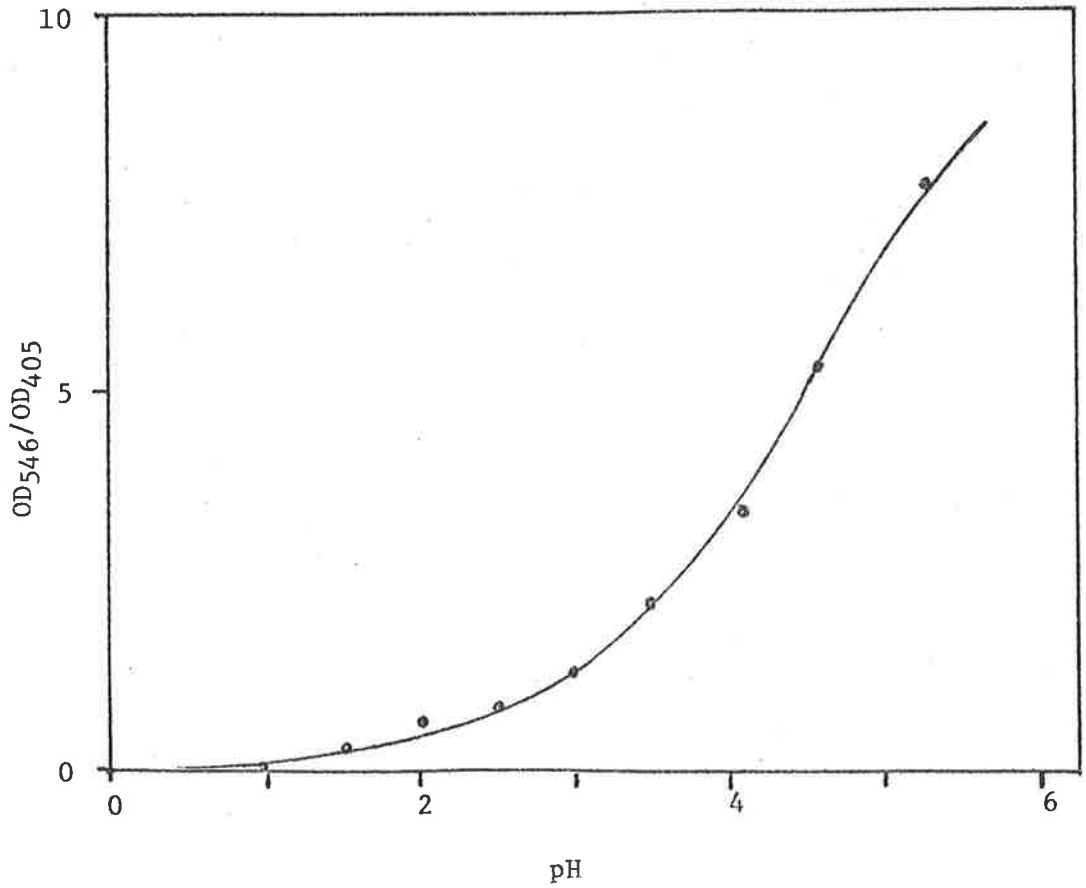

$$[Ni(III)L] = Y_{(OH)} \frac{k_1[Ni(II)L]}{(k_1+k_2)\ [Ni(II)L] + k_3[H_2O_2]}$$

and

$$[Ni(II)L^{\bullet}] = Y_{(OH)} \frac{k_2[Ni(II)L]}{(k_1+k_2)\ [Ni(II)L] + k_3[H_2O_2]}$$

where $Y_{(OH)}$ is the photolytic yield of OH radicals. Using the Beer-Lambert equation, and again assuming that only Ni(III)L absorbs at 405 nm, and $Ni(II)L^{\bullet}$ at 546 nm,

$$\frac{OD_{546}}{OD_{405}} = \frac{[Ni(II)L^{\bullet}]}{[Ni(III)L]} \cdot \frac{\varepsilon_{405}\ (Ni(III)L)}{\varepsilon_{546}\ (Ni(III)L^{\bullet})}$$

$$= \frac{k_2}{k_1} \cdot \frac{\varepsilon_{405}\ (Ni(III)L}{\varepsilon_{546}\ (Ni(II)L^{\bullet})}$$

Hence, assuming the molar absorbance ratio is independent of pH, a plot of OD_{546}/OD_{405} versus pH gives an indication of the change in the k_2/k_1 ratio over the studied pH range, independent of pH effects on $Y_{(OH)}$, $k_{ox} = k_1 + k_2$, and k_3. The plot of the absorbance ratio data obtained from 20μM Ni(II)di, 2 mM H_2O_2 solutions against pH is shown in figure III 2.3. This result suggests that there is a very large variation in the relative values of k_1 and k_2 with pH. The actual values of the molar absorbances of the two transient complexes cannot be directly determined, since the actual transient yields are not known. The molar absorbance ratio has been determined, however, from other results in section VII 3.4

viz. $\frac{\varepsilon_{405}\ (Ni(III)L)}{\varepsilon_{546}\ (Ni(II)L^{\bullet})} \simeq 1.5$

At a particular pH, the observed yield of complex transient at either wavelength was dependent on the $[H_2O_2]/[Ni(II)di]$ ratio. The Ni(II)di + OH rate was determined by competition with H_2O_2 as in the

Ni(II)tet system. Here however the rate of OH radical oxidation of the complex ($k_{ox} = k_1+k_2$) is considered to be a composite of two types of attack. Using the competition reactions in their simple form,

$$\text{Ni(II)di} + \text{OH} \xrightarrow{k_{ox}} \text{Ni(III)di, Ni(II)L}^{\bullet}$$

$$H_2O_2 + \text{OH} \xrightarrow{k_3} HO_2$$

and the Beer-Lambert equation, the expressions analogous to the tetene system are

$$\frac{1}{OD_{546}} = \left[\varepsilon_{546}(\text{Ni(II)L}^{\bullet})\ Y_{(OH)}\right]^{-1}\left[\frac{k_{ox}}{k_2} + \frac{k_3[H_2O_2]}{k_2[\text{Ni(II)L}]}\right]$$

and

$$\frac{1}{OD_{405}} = \left[\varepsilon_{405}\ (\text{Ni(III)L})\ Y_{(OH)}\right]^{-1}\left[\frac{k_{ox}}{k_1} + \frac{k_3[H_2O_2]}{k_1[\text{Ni(II)L}]}\right]$$

A plot of $\frac{1}{OD\lambda}$ versus $[H_2O_2]/[\text{Ni(II)di}]$ should be linear with a slope/intercept value equal to k_3/k_{ox}, independent of λ. Such plots at each wavelength were obtained over the concentration ratio range of 500 - 2500 at pH 1.0, 2.0, 3.0. (Extrapolation of absorbance values was necessary at 546 nm). The plots were suffficiently linear to allow for assignment of the slope/intercept values;

pH	slope/intercept (x 10^3)	
	546 nm	405 nm
1.0	1.4 (±0.3)	1.8 (±0.4)
2.0	2.3 (±0.5)	2,1 (±0.5)
3.0	2.7 (±0.6)	2.5 (±0.6)

The values obtained above are essentially independent of wavelength and pH (in this range). Using $k_3 = 1.2 \times 10^7 M^{-1} sec^{-1}$ (84) over the studied pH range, the derived value of k_{ox} is 6 (±2) x $10^9 M^{-1} sec^{-1}$ (Due to the large error limits on these results, the existence of small differences between these rates cannot be ruled out). However, from figure III 2.3 , it is apparent that although $k_1 + k_2 (= k_{ox})$ changes little over this pH range, there is a very large change in the k_2/k_1 ratio.

2.4 A possible formation mechanism that explains the observed results is as follows:

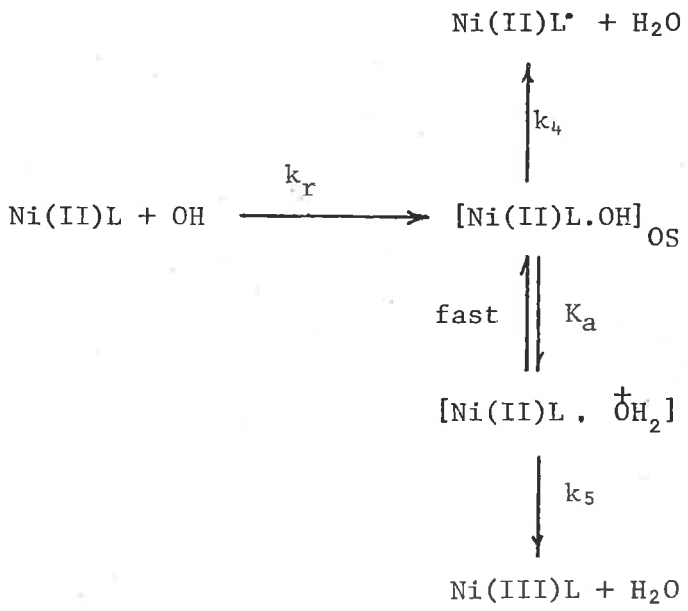

This mechanism lacks substantiating experimental evidence for the proposed intermediates, and is offered as a plausible explanation of the unusual formation characteristics. It is considered that the OH radical forms an outer-sphere complex with the bivalent macrocycle in the rate-determining step of the overall scheme. The fate of this complex is governed by the acid concentration. In acidic solution, proton addition to the complex

in a fast equilibrium step allows facile electron-transfer to occur in a subsequent step. The alternative hydrogen-atom abstraction reaction presumably has a subtle acid dependence, which is not integer in value. (The pH dependence of the OH and H atom dehydrogenations of simple amino-acids in solution has been accounted for by the relative acidities of the C-H and N-H sites along the backbone of the molecule)[208] Thus, k_4 is acid dependent, and is represented as

$$k_4 = k_4'[H^+]^{\alpha}$$

where $0<\alpha<1$.

The yield of each oxidized form of the complex is given by,

$$[Ni(II)L^{\bullet}] = \frac{k_4}{k_4 + k_5 K_a [H^+]} \cdot [Ni(II)L.OH]$$

and

$$[Ni(III)L] = \frac{k_5 K_a [H^+]}{k_4 + k_5 K_a [H^+]} \cdot [Ni(II)L.OH]$$

Choosing steady-state conditions for the outer-sphere complex,

$$[Ni(II)L.OH] = \frac{k_r [Ni(II)L]\ [OH]}{k_4 + k_5 K_a [H^+]}$$

Therefore,

$$\frac{[Ni(II)L^{\bullet}]}{[Ni(III)L]} = \frac{k_4}{k_5 K_a\ [H^+]} = \frac{k_4'[H]^{\alpha}}{k_5 K_a [H^+]}$$

$$= \frac{k_4'}{k_5 K_a} \cdot [H^+]^{(\alpha-1)}$$

and thus

$$\frac{OD_{546}}{OD_{405}} = \frac{\varepsilon_{405}(Ni(III)L}{\varepsilon_{546}(Ni(II)L^{\bullet}} \cdot \frac{k_4'}{k_5 K_a} \cdot [H^+]^{\alpha-1}$$

$$\log \frac{OD_{546}}{OD_{405}} = \text{constant} + (1-\alpha)pH$$

The previous plot in figure III 2.2b, which does not substantiate a fast equilibrium between the two complex forms, does support a mechanism similar to that proposed above.

2.5 The proposal that the saturated macrocyclic Ni complexes undergo simultaneous OH oxidation at both the metal centre and the ligand is unusual. Although OH radical attack at a ligand site of a complex is known,[209] such reactions with macrocyclics have not been studied. Electrochemical evidence for macrocycle redox of the Ni systems has only been observed for systems with extensive π-conjugation throughout the ligand[210]—metal centre redox occurred for the saturated macrocycles.[9] The π-conjugated macrocycle radical species behave similarly to porphyrin analogues.[211] The complex oxidation in this work via OH attack at the secondary coordinated nitrogen, is probably due to the strong H-atom abstracting ability of the radical, since there was no evidence for this mode of reaction with X_2^- radicals as precursor oxidants.

Flash photolysis of a 10 mM H_2O_2 solution containing 1mM diene ligand showed a very weak transient absorption in the 300-330 nm region for both acidic and natural pH solutions. There was no absorption observable in the 500-600 nm region. Reducing the macrocycle concentration to 50μM eliminated any observable absorbance. (Flashing a 1mM diene solution alone produced no observable transient in the 300-600 nm range). These results suggest that OH oxidation of the free diene macrocycle is possible. Indeed, OH oxidation of ethylenediamine and acetone, the parent reagents in macrocyclic tetramine synthesis, is known.[84]

2.6 The observed rates of decay of both the transient complexes formed by OH oxidation of Ni(II)diene in flash photolysed H_2O_2 solution were very pH dependent in the range 0,5 - 5,3. The wavelengths 405 nm and 546 nm were again chosen to observe each intermediate form. So that significant absorption of both transients could be observed, pH 2.0 was chosen to study the pH independent characteristics of the transient decay.

As with the tetene system, the decay kinetics and decay rates were dependent on the $[H_2O_2]$ / [Ni(II)di] ratio over the observed pH range, independent of whether this ratio was changed by altering $[H_2O_2]$ or [Ni(II)di]. Reasonable second-order decay kinetics were obtained at a value of this ratio ~100.# For values ≳400, reasonable first-order kinetic plots were obtained for the decays of both transient species. As expected, the decay occurred in two steps for the ratio <50 with each process being separately observable in low acid concentrations. The associated first-order dependence on $[H_2O_2]$ and the [Ni(II)di] independence of the secondary reaction, was observed under these conditions. The change in first-order decay rate at 405 nm with the $[H_2O_2]$/[Ni(II)di] ratio is shown in figure III 2.6a. The expected levelling-off of the rate occurred for values of the concentration ratio >1000. The anticipated decrease in the observed transient yields with further increase in the ratio

References throughout the text of this work to 'reasonable' or 'good' kinetic processes are based on the following:

(i) If the kinetic plot of the integrated rate equation (ln OD_t versus t for first-order, or $^1/OD_t$ for second-order) of the rate data is quite linear for two half-lives, the kinetics are referred to as 'good'.
(ii) If the kinetic plot of the experimental rate data drifts from linearity after two half-lives, the kinetics are referred to as 'reasonable'

FIGURE III 2.6a

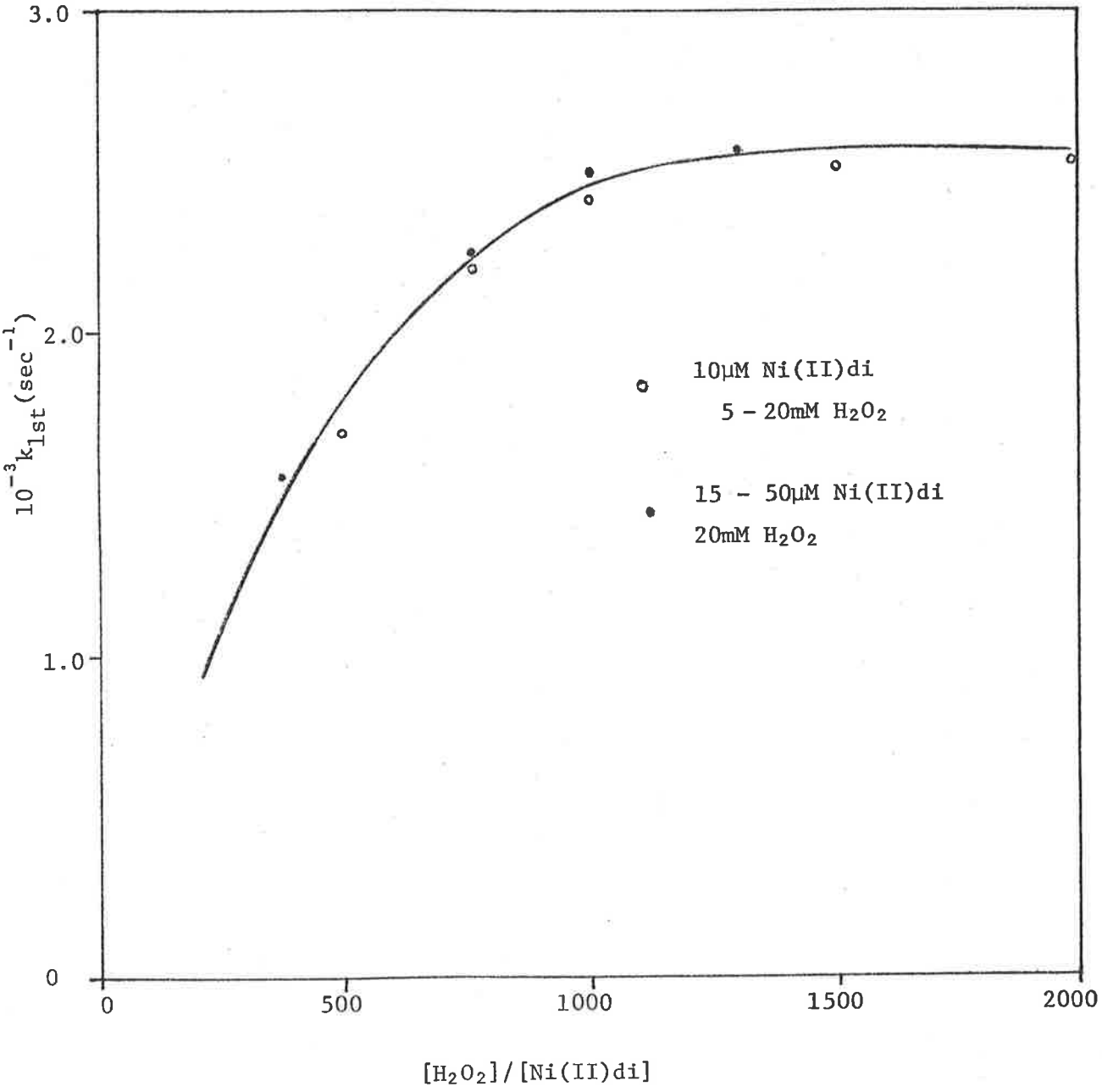

was also observed.

At pH 4.0, the addition of 35 μM TNM to a 20μM Ni(II)di, 10 mM H_2O_2 solution reduces the observed rate of decay at 546 nm (where there is no nitroform absorption) by about 45%. Taking the TNM + 'HO_2' rate of $3.2 \times 10^8 M^{-1} sec^{-1}$ at this pH,[207] this suggests a first-order rate of about 1.5×10^4 sec^{-1} for the transient decay with 'HO_2', which is confirmed in other experiments.

The similarity of the decay in this system with the tetene analogue over the studied $[H_2O_2]/[Ni(II)di]$ range, clearly indicates that for values of the ratio >100, transient reaction wholly with 'HO_2' occurs, while below this value, reaction with H_2O_2 becomes important.

The observed decay rate changes with pH for both transient species (solutions containing 10μM Ni(II)di, 20 mM H_2O_2) are shown in figure III 2.6b. (The actual yields of the two transients vary with pH as previously described). At 405 nm for pH $\gtrsim$4.5 and at 546 nm for pH <1, the absorptions of the Ni(III)L and Ni(II)L$^{\bullet}$ species respectively were too small for meaningful kinetic measurement. The plots of log k_{obs} versus pH are quite characteristic of reactions with hydroperoxy radical.

The observed decay at 405 nm, while being good first order for pH>2, showed some mixed order character below this pH. The k_{1st} values used in figure III 2.6b for pH<2 were determined from absorbance changes in the first half-life of the decay. Although $[HO_2] > [Ni(III)di] + [Ni(II)L^{\bullet}]$ under the conditions used, there is competition for the available HO_2 between both the complex transients. Below pH ~3, the rate of HO_2 reaction with Ni(II)L$^{\bullet}$ is constant and faster than that with Ni(III)L, which falls

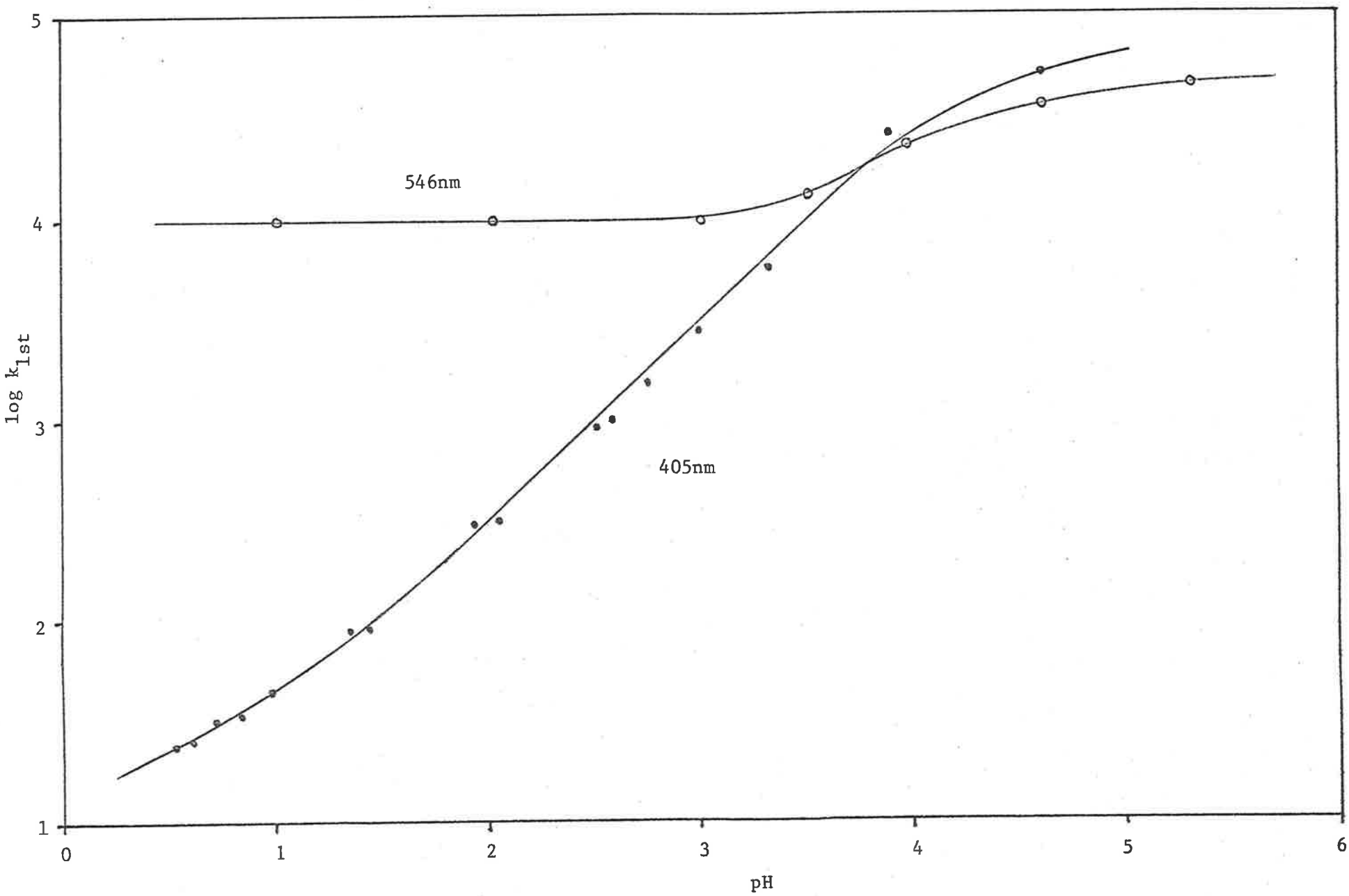

FIGURE III 2.6b

steadily as the pH decreases. The loss of HO_2 due to more efficient scavenging by Ni(II)L$^{\bullet}$ in this pH region, is enough to cause a tendency away from first-order kinetics for the observed Ni(III)di decay with HO_2.

Analysis of these results using the program PHRATE showed that the rate changes with pH were well-behaved, with

$$\frac{k(Ni(III)di + O_2^-)}{k(Ni(III)di + HO_2)} = 1.0 \ (\pm 0.2) \times 10^4 \quad \text{for } pK_a \simeq 4.3$$

and

$$\frac{k(Ni(II)L^{\bullet} + O_2^-)}{k(Ni(II)L^{\bullet} + HO_2)} = 5 \quad \text{for } pK_a \simeq 4.5$$

The best estimate of the hydroperoxy pK_a from these results in this unbuffered system is 4.4 (±0.1). The results again discounted the existence of the $H_2O_2^+$ species in acidic solution. The increased rate of reaction of Ni(II)L$^{\bullet}$ with O_2^- over that with HO_2 is probably an electrostatic effect only. The considerable difference in rate between the metal oxidized and ligand oxidized complexes with HO_2 may reflect a preference of the oxidation of HO_2 via hydrogen-atom transfer compared with electron-transfer.

i.e. $\overset{II}{Ni} - N^{\bullet} + HO_2 \longrightarrow \overset{II}{Ni} \ NH + O_2$

c.f. $Ni(III)L + HO_2 \longrightarrow Ni(II)L + H^+ + O_2$

The large difference in the observed decay rates of the two oxidized forms of the complex in acid solution supports the argument presented in section III 2.2 discounting the existence of a fast equilibrium between the species,

viz. $Ni(III)L \rightleftharpoons Ni(II)L^{\bullet} + H^{+}$

If this fast equilibrium were to occur the overall decay of each transient species would be the same and equal to the faster of the two rates with superoxy radical. (Evidence presented later (section VII) suggests that the conversion

$$Ni(III)L \longrightarrow Ni(II)L^{\bullet} + H^{+}$$

does occur with a first-order rate of ~100 sec^{-1} at pH~4).

2.7 The Ni(III)di and $Ni(II)L^{\bullet}$ reaction rates with H_2O_2 were determined from the secondary decay process observed for $[H_2O_2]/[Ni(II)di] \lesssim 80$ as in the tetene system. The second-order rates, determined from plots of the observed pseudo-first order rate against $[H_2O_2]$ were

$$k(Ni(III)di + H_2O_2) \sim 3 \times 10^3\ M^{-1}sec^{-1}$$

at pH 2.0

$$k(Ni(II)L^{\bullet} + H_2O_2) \sim 5 \times 10^2\ M^{-1}sec^{-1}$$

at pH 5.3

The first estimate agrees well with that determined accurately using Cl_2^- as the precursor oxidizing radical (see section VIII 2.2).

3. Ni(II)TETRAMINE, H_2O_2

3.1 The transient spectra obtained from a 20μM Ni(II)tam, 2 mM H_2O_2 solution are shown in figure III 3.1. The pH dependent product forms from OH oxidation of this complex were similar to those for the diene analogue. The Ni(III) tam spectrum was observed 20 msec after the

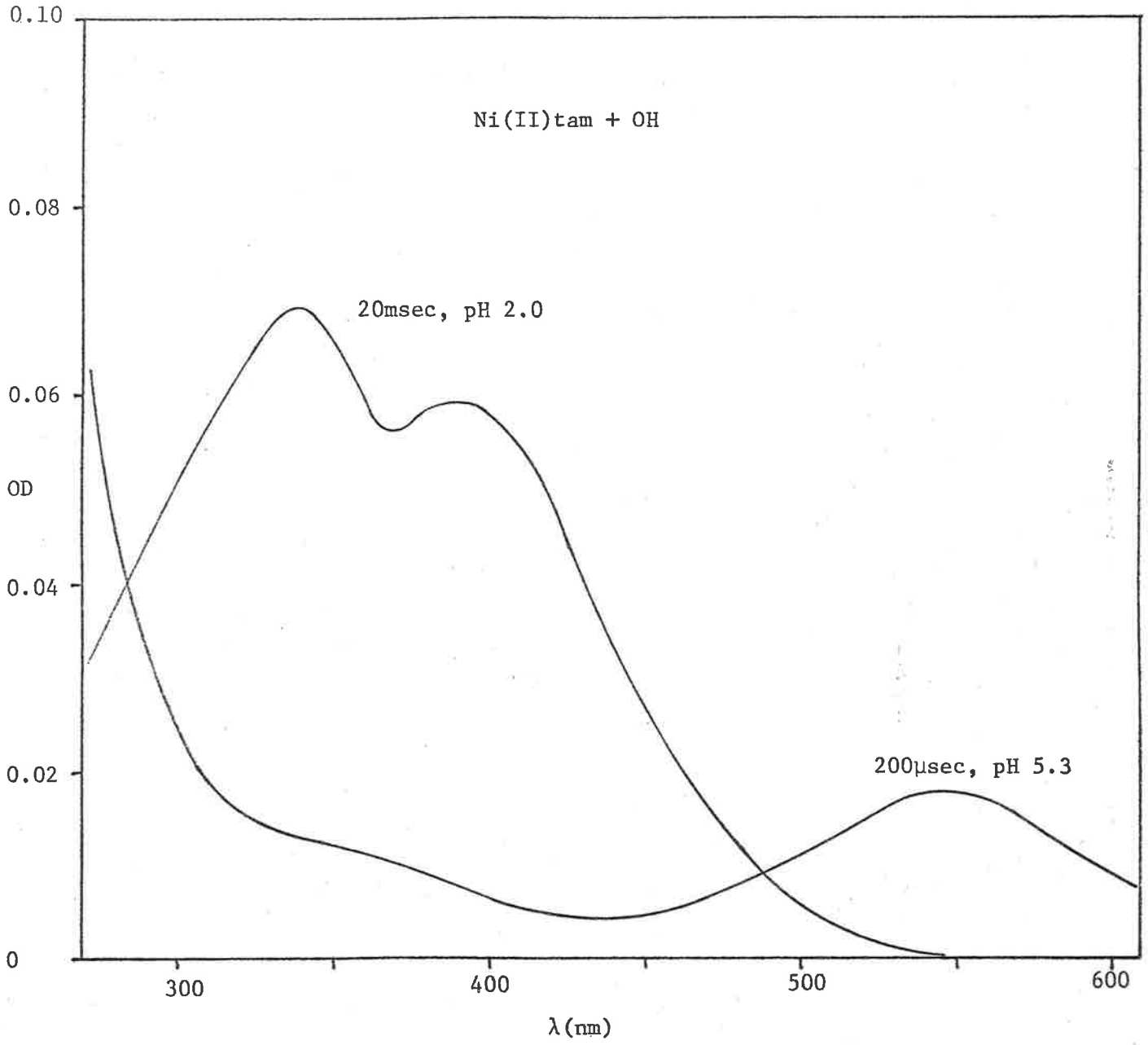

FIGURE III 3.1

flash at pH 2.0, and the ligand radical species, Ni(II)L$^{\bullet}$, 200 μsec after the flash at pH 5.3. The spectral measurements could be extended down to 270 nm in this system, because the usual high absorptivity of the bivalent macrocycle chromophore band in this region is absent for the fully saturated tam complex. The Ni(III) tam spectrum is very similar to that obtained by electrochemical means in acetonitrite.[9] Although some characteristic differences between the tervalent diene and tetramine spectra were discernable, the Ni(II)L$^{\bullet}$ spectra for both ligands were very similar. The absorption of this species below 310 nm was better observed in the tam system of course.

3.2 The absorptions at 405 nm and 546 nm were again chosen to observe the two oxidized forms of the complex. For valid comparisons between absorption values at these wavelengths, the absorptions should be extrapolated back to t = 0, under conditions where significant transient decay occurs during the time of the flash. In the pH range 0.5 - 3.0, however this extrapolation was unnecessary, and maximum absorption values after the flash were determined. The essential characteristics of the absorption changes (for comparison to the diene analogue) were clearly illustrated (figure III 3.2) over this reduced pH range. Experimental evidence here supported arguments against a possible fast equilibrium between the two oxidized forms of the complex, since the plot of log (OD_{546}/OD_{405}) versus pH (as in section III 2.2) in this pH region had a slope of 0.71 (±0.07) instead of unity.

By direct analogy to the diene system two modes of OH attack on the bivalent macrocycle are considered to be operative here. The differences in rate dependence on acid concentration are reflected in the differences

FIGURE III 3.2

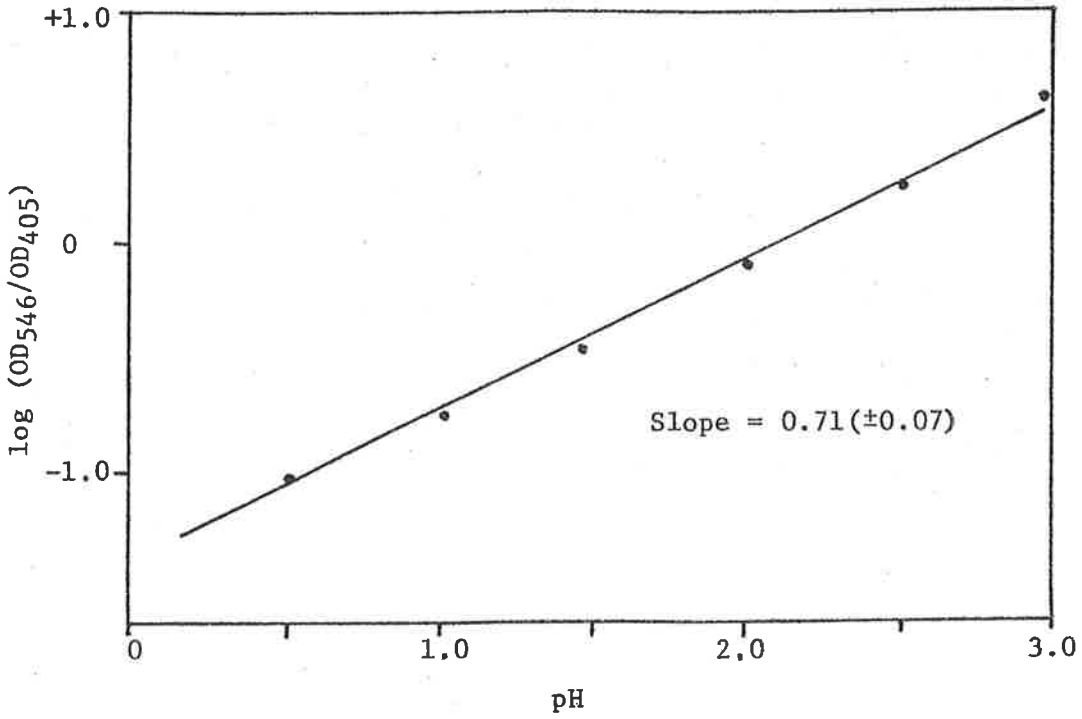

FIGURE III 3.3

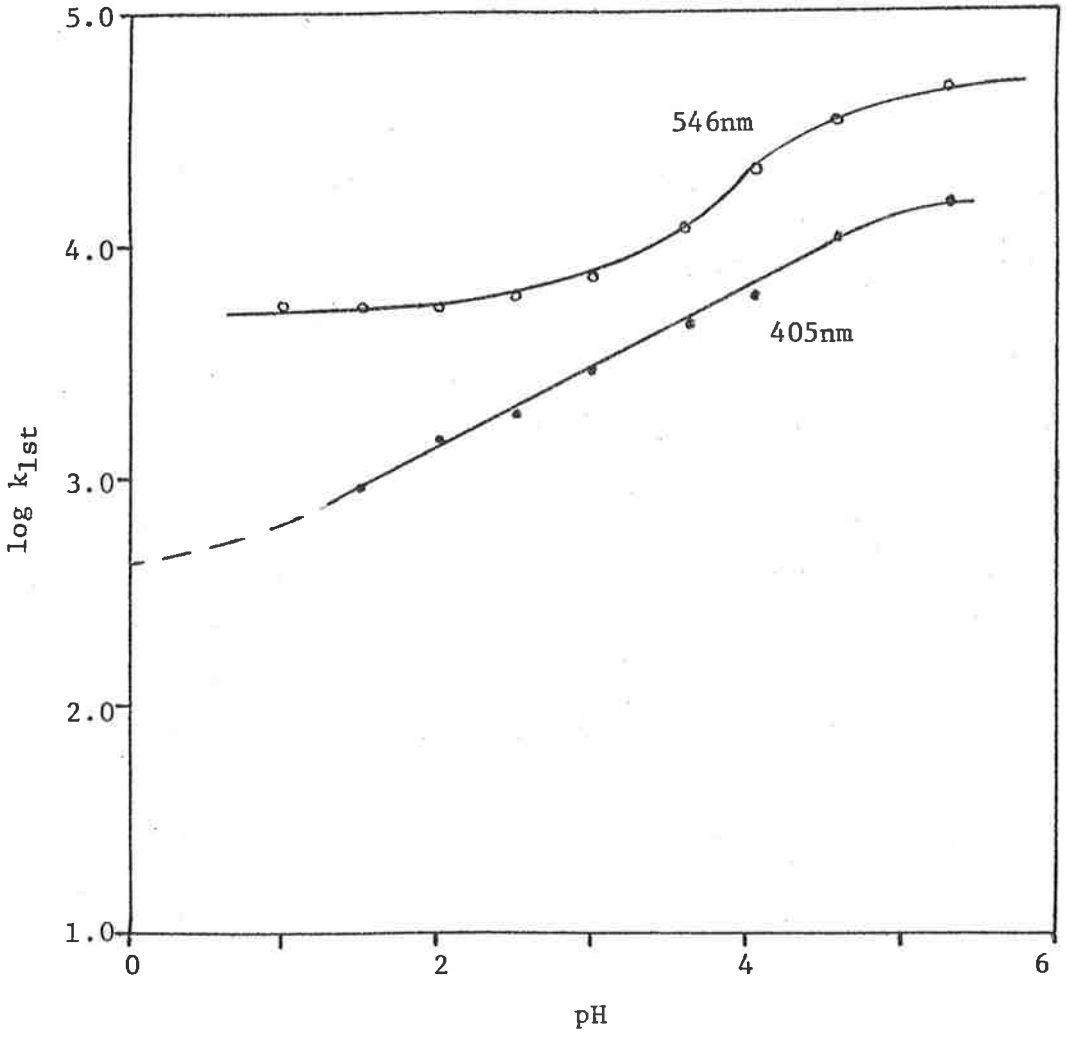

in the slopes of the log (OD ratio) versus pH plots, for which $(1-\alpha)$ is ~0.5 for diene and ~0.7 for tetramine. The value of $k_{ox} = k_1 + k_2$ was again estimated by the method of competition with H_2O_2. The values of the slope/intercept for plots of $\frac{1}{OD}$ versus $[H_2O_2]/[Ni(II)tam]$ at 405 nm and 546 nm were the same, as expected. At pH 2.0, using the $H_2O_2 + OH$ rate of $1.2 \times 10^7\ M^{-1}sec^{-1}$ (84), the value of $k_{ox} = 4.3\ (\pm 1.5) \times 10^9\ M^{-1}sec^{-1}$ was determined.

3.3 The observed decay rates at 405 nm and 546 nm for flash photolysed Ni(II)tam - H_2O_2 solutions were very pH dependent in the studied range 0.3 - 5.3. The pH independent characteristics of the decay paralleled the diene and tetene systems.

Under conditions where the oxidized complex yield was greater than that of superoxy radical, transient reactions with H_2O_2 were observable (as in the diene and tetene systems). For small changes in the $[H_2O_2]/[Ni(II)\ tam]$ ratio $\lesssim 60$, the values of these reaction rates were estimated;

$k(Ni(III)tam + H_2O_2) \sim 5 \times 10^3 M^{-1}sec^{-1}$ at pH 2.0

$k(Ni(II)L^{\bullet} + H_2O_2) \sim 1.5 \times 10^4 M^{-1}sec^{-1}$ at pH 5.3

Shown in figure III 3.3 are the actual observed rate dependences on pH at both wavelengths of a 20μM Ni(II)tam, 20 mM H_2O_2 solution over the range 1.0 - 5.3. At 546 nm for pH 1, the absorption of the $Ni(II)L^{\bullet}$ species was too small for accurate kinetic measurement. The decays observed at 546 nm and 405 nm (pH 1.5) were essentially pseudo-first order, and well behaved in terms of reaction with superoxy radical over this pH range.

3.4 The observed absorbance changes with time at 405 nm in acidic solutions (pH 0.3 - 2.0) were unusual. In figure III 3.4a is shown a plot of the difference between the absorbances measured 100 μsec and 5 msec after the flash over the pH range 0.3 - 3.0; the plot was normalized by the division of this difference by the 100μsec absorption value. (The normalization compensates for the increase in the total absorption at 405 nm with increasing acid concentration due to the more efficient OH attack at the metal centre under such conditions). For pH>2, more than 90% of the Ni(III)L absorption observable at 100μsec had decayed after 5 msec, by efficient reaction with the hydroperoxy radical. In the pH region 0.4 - 2.0 there was a considerable reduction (down to zero at pH 0.43) in the fraction of transient decay that had occurred in the time between 100μsec and 5 msec after the flash. Below pH 0.4 there was a formation occurring within the specified time. The decay of the absorption apparent 5 msec after the flash in the pH region below about 2.0 was significantly slower than the process accounting for the entire transient decay by this time above this pH.

The unusual kinetic observations are shown in figure III 3.4b. In this diagram, the time intervals 100μsec - 5 msec and 5 msec - 1.0 sec are specified as intervals (1) and (2) respectively. In interval (1) for pH>2, there was virtually complete transient decay, being first-order with $k_{1st} \simeq 1200\ sec^{-1}$. At pH 1.0 there was partial decay during interval (1) ($k_{1st} \simeq 430\ sec^{-1}$), followed by a slower mixed-order decay during interval (2). At pH 0.4 very little absorbance change occurred during (1), whilst a reasonable second-order decay was completed within interval (2). A first-order transient formation was observed in interval (1) at pH 0.3 ($k_{1st} \simeq 1700\ sec^{-1}$), followed by a good second-order decay process, $\frac{k}{\varepsilon l} \simeq 160\ sec^{-1}$, within interval (2). The observed second-order rate

FIGURE III 3.4a

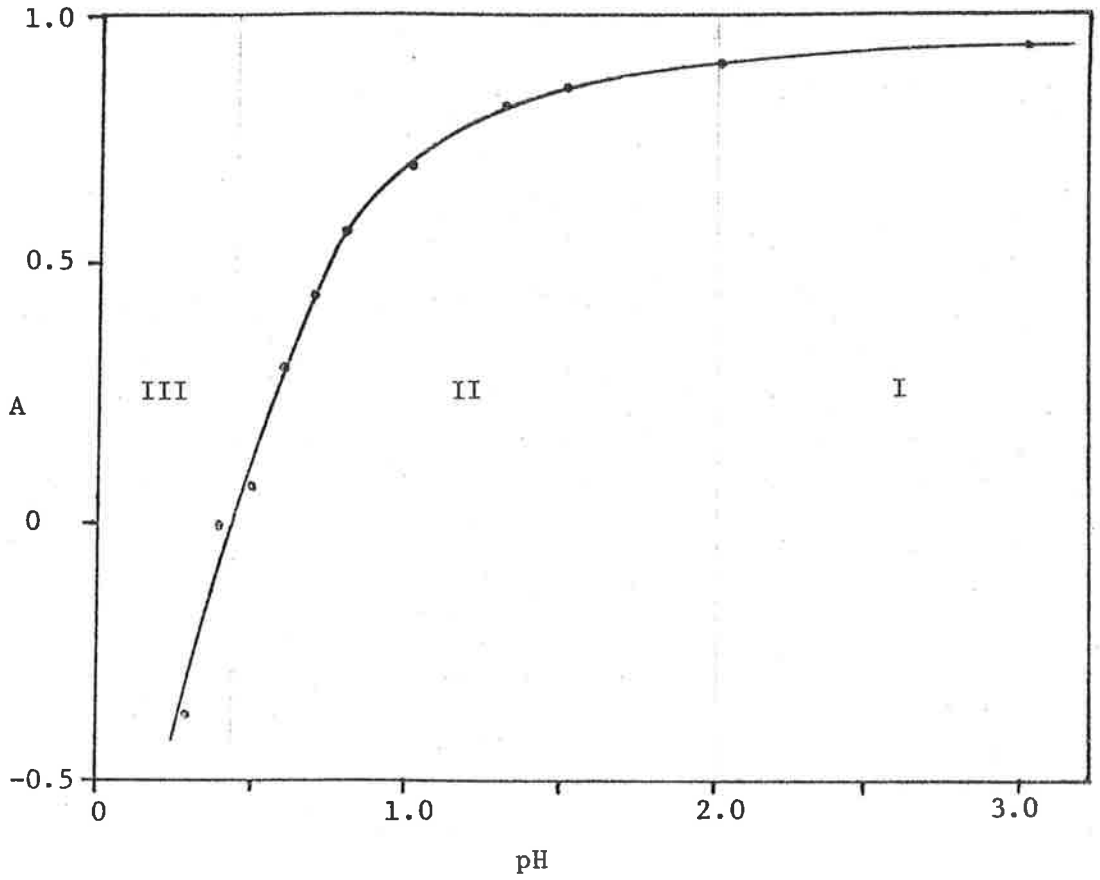

FIGURE III 3.4c

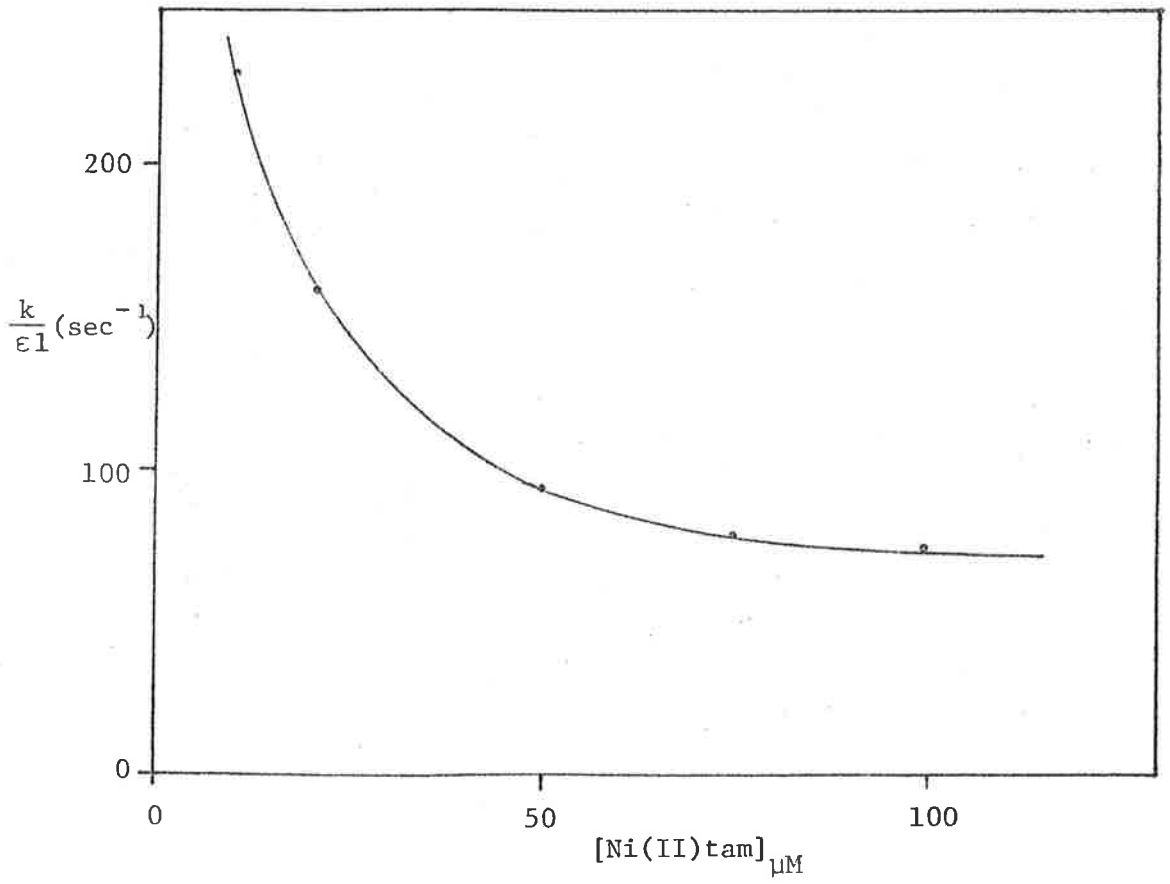

FIGURE III 3.4b

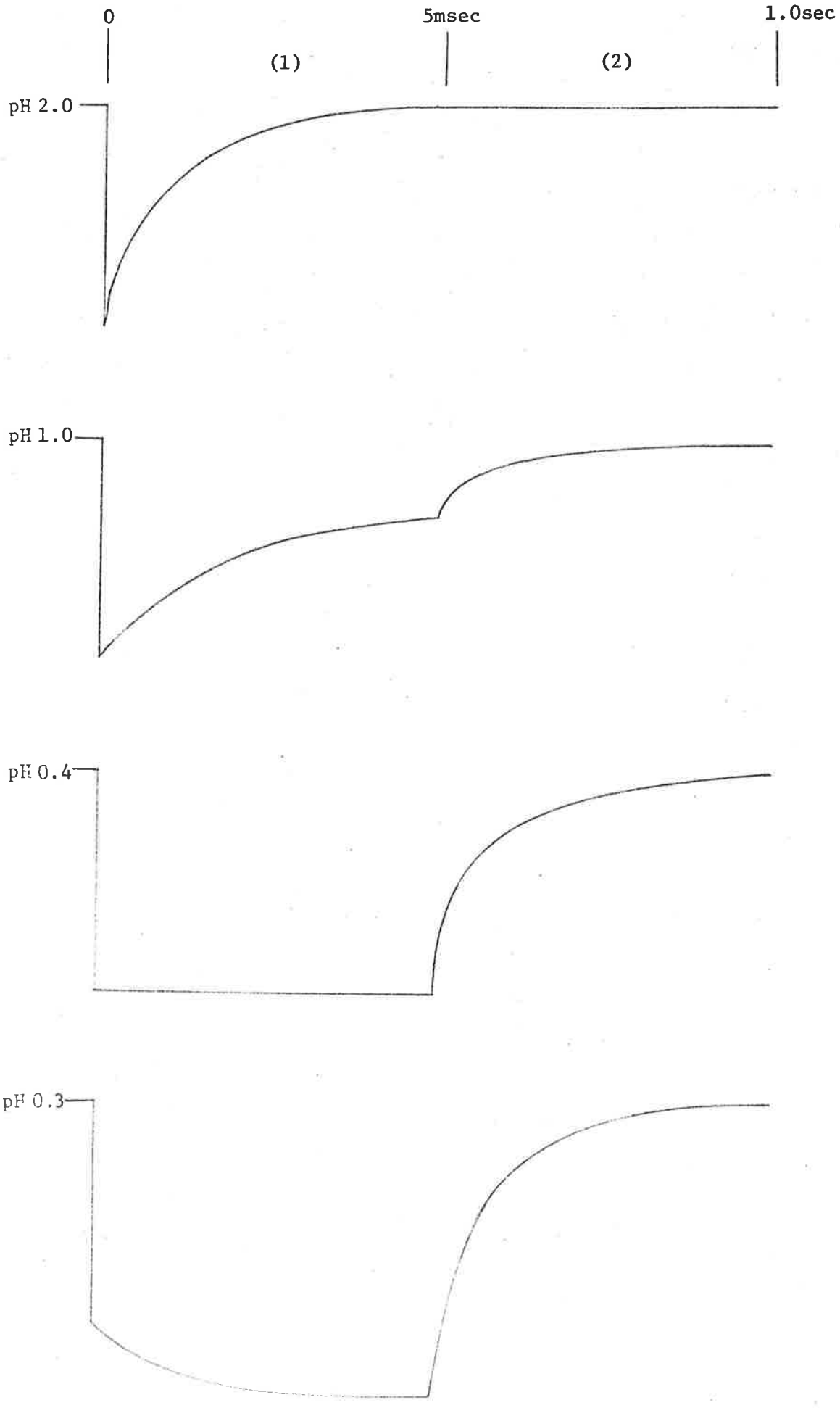

constant ($\frac{k}{\varepsilon l}$) had a negative dependence on the [Ni(II)tam] as shown in figure III 3.4c. Over the anomalous pH range, the absorbance after the overall decay returned to the initial value before the flash.

The transient spectra determined 250μsec after the flash at pH 0.5 and 1.5 were identical in shape, and characteristic of Ni(III)tam in the measured region 300-600 nm. At pH 0.7, where both processes of decay were observable, the transient spectra were measured 0.8 msec (during interval (1)) and 50 msec (during (2)) after the flash. These spectra were identical for λ>340 nm. Below this wavelength there was greater absorption down to the observation limit of 270 nm at the longer time. This is illustrated in figure III 3.4d. These spectral results suggest that the same species is produced initially after the flash at pH 0.5 and 1.5, but that an apparently different transient is produced during the time of the overall decay in these acidic solutions.

At pH 2.0, an increase in [Ni(II)tam] to 50μM resulted in a 15% decrease in the observed first-order decay rate, while at pH 0.3, such a change resulted in a 10% increase in the observed first-order formation rate. Upon increasing the [Ni(II)tam] to 100μM, a further 10% decrease in the decay rate was observed at pH 2.0, while an overall increase of 25% was apparent in the formation rate at pH 0.3 The effect on the decay rate at pH 2.0 was the same for pH up to 4.5 and can be accounted for by the availability of hydroperoxy radicals for decay with the Ni(III) tam, which is determined by the initial competition of Ni(II)tam and H_2O_2 for the photo-produced OH radicals. If the first-order processes observed at both pH 2.0 and 0.3 were rate determining steps to produce the same intermediate, which decayed very rapidly at pH 2.0, but not at 0.3, similar [Ni(II)tam] dependences would be expected at both pH values.

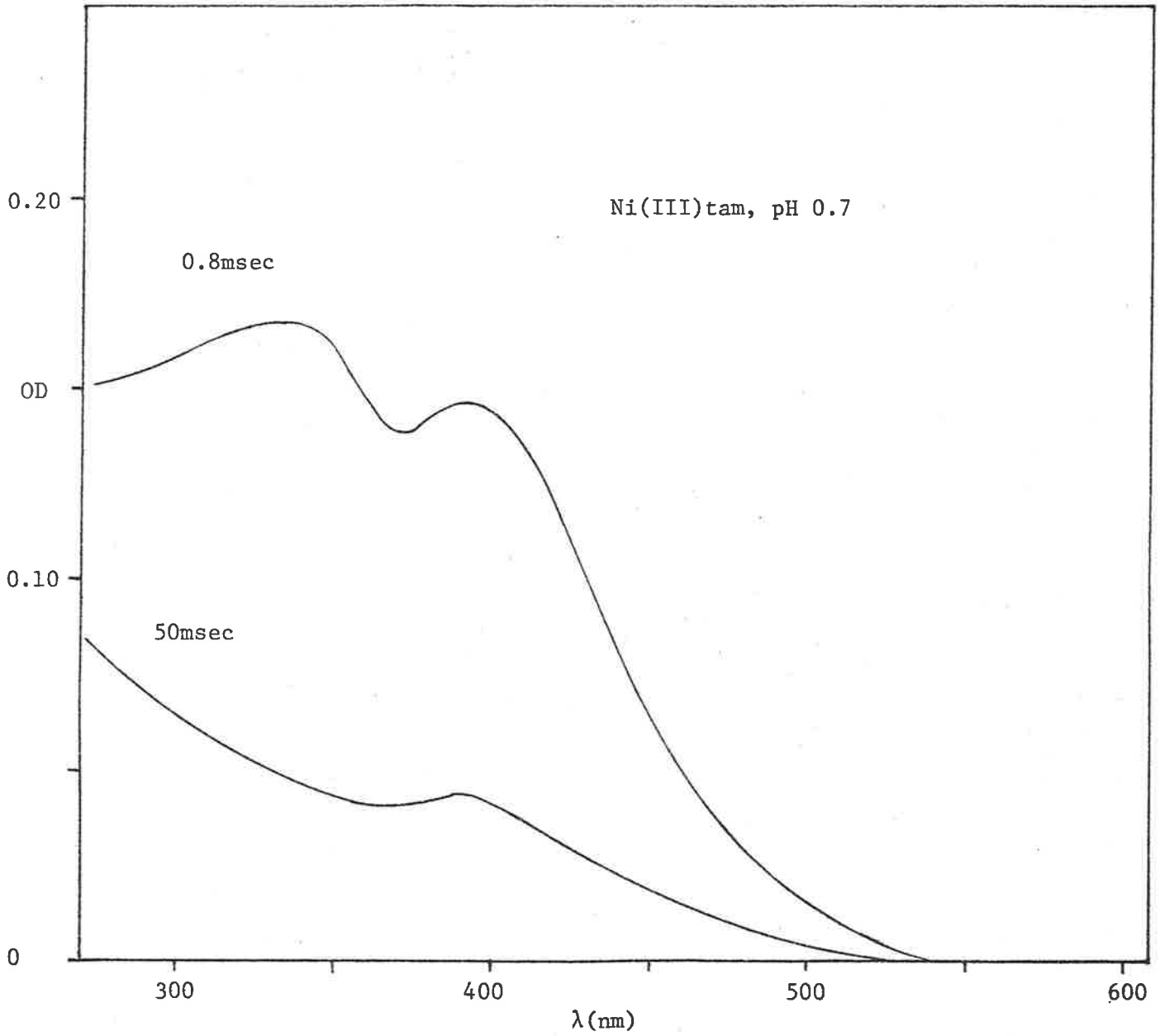

FIGURE III 3.4d

The evidence suggests that the absorbance formation at pH 0.3 is a production of tervalent mickel, which does not occur to any significant extent at pH $\gtrsim$ 2. The most probable oxidant is the HO_2 radical. This is reasonable from the observed non-linear dependence of the formation rate on [Ni(II)tam], since the effect of increasing this concentration naturally reduces the concentration of available HO_2 radicals.

The reaction of HO_2 with Ni(II) tam to produce the tervalent complex appears to occur only in acidic solution. It is known that HO_2 is a better oxidizing agent than O_2^- by ~0.3 volt, but a worse reducing agent# At both pH 2.0 and 0.3, virtually all of the hydroperoxy radicals are in the protonated form and the oxidation of Ni(II)tam might be expected to occur at both pH's. It is apparent experimentally that efficient oxidation only occurs in strongly acidic solution which suggests the involvement of an acid-catalyzed path. No observable absorption formation was detected at 546 nm at pH 0.3, suggesting that the HO_2 oxidation of the bivalent macrocycle is at the metal centre only under the experimental conditions.

The effective reduction potential of the hydroperoxy radical at a particular pH can be expressed by

$$E^{o\prime}_{HO_2} = \frac{E^o_{HO_2} + \frac{K_a}{[H^+]} E^o_{O_2^-}}{1 + \frac{K_a}{[H^+]}}$$

3.5 Although without formal computer similation analysis as verification, the following mechanism is offerred as a plausible explanation of the observed kinetic behaviour in this system for pH $\lesssim$ 2. In order to simplify the presentation of this mechanism,two separable aspects of the overall process are specified as (A) and (B). In this system the $[HO_2]$is in significant excess over [Ni(III)tam]. The scheme is;

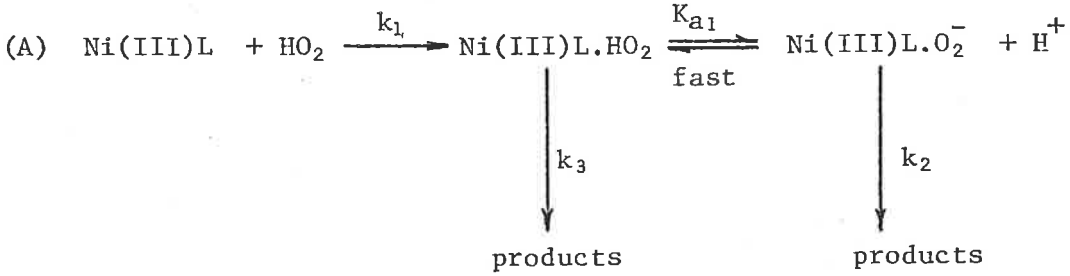

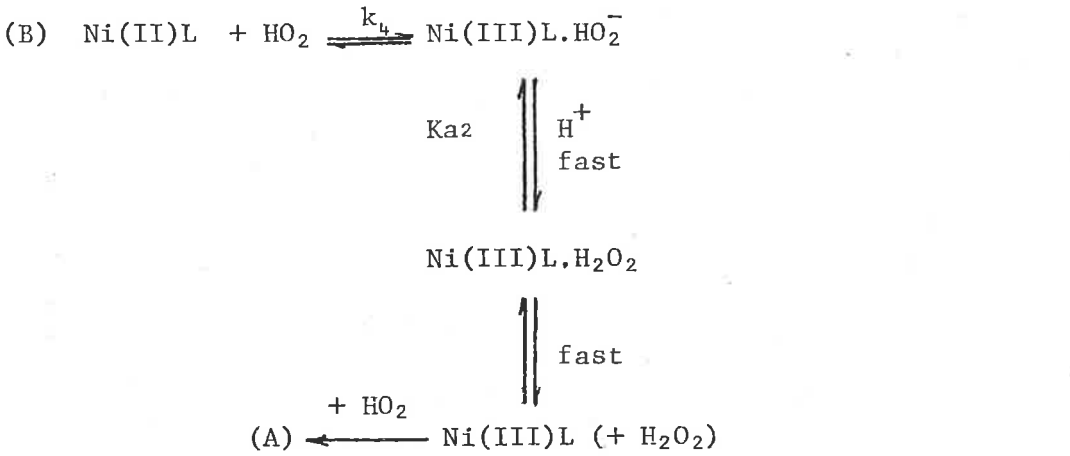

The numbered rate constants refer to the specific steps in the mechanism as shown. The Ka values are acid-base equilibrium constants.

In (A), the mechanism presumes the formation of a complex between the HO_2 radical (for pH<2 there is essentially no O_2^- present) and the tervalent macrocycle (step (1)). The complex can undergo a rapid deprotation equilibrium to produce the analogous O_2^- complex. The pKa of

the complexed HO_2 may of course be quite different from that of free HO_2. It is considered to be less than the value of pKa for free HO_2 due to the strong electron withdrawal from the acidic hydrogen atom by the tervalent metal centre. An analogy may be drawn to the increased acidity of H_2O when complexed to metal ions (e.g. $Fe^{3+}_{aq} \rightleftharpoons Fe\,OH^{2+} + H^+$, for which pKa $\simeq$ 3.2.[140]) Step (2) is a simple unimolecular electron-transfer within the O_2^- complex to yield Ni(II)L and oxygen as products. Step (3) is a second-order combination of two Ni(III)L.HO_2 complexes to produce after subsequent electron-transfer, stable 'disproportionation' products, viz. H_2O_2, O_2, Ni(II)L and $Ni(II)L_{ox}$. In the latter complexes, the ligand has achieved stability by the loss of two protons. (The nature of this product complex is inferred by analogy to be the same as that discussed in detail in section VI 5.2

In (B) more tervalent Ni is produced by HO_2 oxidation of Ni(II)L. Step (4) and the acid equilibrium have been simplified from the more rigorous form;

Step (4): $Ni(II)L + HO_2 \rightleftharpoons Ni(II)L.HO_2$

$\downarrow k_{et}$

$Ni(III)L.HO_2^-$

The kinetic analysis requires only that step (4) be rate determining in scheme (B), which is probably limited by the rate of electron-transfer, k_{et}. (The HO_2^- complexes of Mn(III), Ag(II), Co(III) and Ce(IV) are known to form very favourably in kinetic investigations of the oxidation of H_2O_2 by these metal ions).[212] The Ni(III)L produced by this process decays via the mechanism set out in scheme (A) in the presence

of excess HO_2. The equilibrium nature of each step in scheme (B) is introduced to allow for evidence of the complete reversibility of this process in the Ni(III)L + H_2O_2 reaction discussed in section VIII 2.2. The dissociation of the Ni(III)L.H_2O_2 complex after the protonation step in scheme (B) may be facilitated by the reaction

$$Ni(III)L.H_2O_2 + HO_2 \rightleftharpoons Ni(III)L.HO_2 + H_2O_2$$

The acid equilibria suggested in the overall mechanism are presumed to be faster than the other steps in the mechanism irrespective of how the rates of the various steps may change with pH.

At the observation wavelength of 405 nm only the absorbances of the free and complexed tervalent macrocycles need to considered. The superoxy-complexed macrocycles are presumed to have approximately the same absorption as Ni(III)tam above 340 nm but a greater absorption in the region below this wavelength. (This is reasonable since it is known that free 'HO_2' absorbs below 300 nm). For λ= 405 nm, therefore,

$$\varepsilon(Ni(III)L) \simeq \varepsilon(Ni(III)L.HO_2)$$

or more simply $\varepsilon_{III} \simeq \varepsilon'_{III}$

From the proposed mechanism, the rate of change of absorbance is given by the composite effect of (A) and (B);

$$\frac{-dOD}{dt} = \varepsilon_{III}\, k_1[Ni(III)L]\,[HO_2]$$

$$-\varepsilon'_{III}\, k_1[Ni(III)L]\,[HO_2]$$

$$+\varepsilon'_{III}\, k_2 \frac{Ka_1}{[H^+]}\,[Ni(III)L.HO_2]$$

$$+\varepsilon'_{III}\, k_3[Ni(III)L.HO_2]^2$$

$$-\dot{\varepsilon}_{III}\, k_4\, Ka2[H^+]\, [Ni(II)L]\, [HO_2]$$

$$= \varepsilon_{III}\Big[k_1[Ni(III)L]\, [HO_2] - k_4\, Ka2\, [H^+]\, [Ni(II)L]\, [HO_2]\Big]$$

$$+\varepsilon'_{III}\left[k_2\, \frac{Ka1}{[H^+]}\, [Ni(II)L.HO_2] + k_3\, [Ni(III)L.HO_2]^2 - k_1\, [Ni(III)L]\, [HO_2]\right]$$

This complicated expression is simplified in the pH regions >2.0 and <0.4.

At pH > 2.0, Rate (1) > Rate (4)

and Rate (2) > Rate (3) - Rate (1)

(where Rate (i) refers to the rate expression for the step (i) in the mechanism). In such a case, Rate (1) becomes rate-determining and

$$-\frac{dOD}{dt} = \varepsilon_{III}\, k_1[Ni(III)L]\, [HO_2].$$

i.e. the usual pseudo-first order decay of tervalent nickel with superoxy radical is apparent. The excess HO_2 radicals then decay unobservably by disproportionation. The value of k can be assumed to be $\gtrsim 2 \times 10^4$ sec^{-1}, which is the observed first-order decay rate at pH > 4.5, where the $Ni(III)L.O_2^-$ complex can be assumed to form by direct association.

At pH < 0.4, Rate (4) $\gtrsim$ Rate (1)

Rate (3) > Rate (2)

Rate (4) > Rate (3)

The kinetic equation thus takes the form;

$$-\frac{dOD}{dt} = (\varepsilon_{III} - \varepsilon'_{III})\, k_1\, [Ni(III)L]\, [HO_2] - \varepsilon'_{III}\, k_4\, Ka2\, [H^+]\, [Ni(II)L]\, [HO_2]$$

$$+ \varepsilon'_{III}\, k_3 [Ni(III)L.HO_2]^2$$

The first term is not observable since $\varepsilon_{III} \simeq \varepsilon'_{III}$, and the observable change is a first-order formation initially, with a [Ni(II)tam] dependence, followed by a second-order decay. Under these conditions all the available HO_2 radicals are converted to the $Ni(III)L.HO_2$ complex due to the reactions,

$$Ni(III)L + HO_2 \longrightarrow Ni(III)L.HO_2 \; (+ H_2O_2)$$

$$Ni(II)L + 2HO_2 \xrightarrow{H^+} Ni(III)L.HO_2 \; (+ H_2O_2)$$

In the pH region between the limiting values, the kinetics are very complicated and show characteristics of both the extremes to a varying degree.

The unusual kinetic behaviour encountered in the acidic tam system was not apparent for the di and tet systems. This is probably a composite effect of there being a higher pKa value of the $Ni(III)tam.HO_2$ complex, and a lower value of k_3, compared with the other complexes. For the well-behaved systems, a pH at which Rate (3) becomes comparable to Rate (2) and less than Rate (1), was not reached in the pH range studied. That only Ni(II)tam oxidation by HO_2 radical is observed is thermodynamically reasonable also. The observed absorbance change is therefore given by

$$-\frac{dOD}{dt} = \varepsilon_{III}\, k_1\, [Ni(III)L]\, [HO_2]$$

for L = di, tet over the whole of the studied pH range. The intermediate existence of the hydroperoxy complexes for these macrocycles can only be inferred by analogy to the tam system.

3.6 It is known that HO_2 radicals, produced in the presence of metal ions, generally in higher oxidation states, form complexes of the type $M\text{-}HO_2$. Such complexes in perchloric acid solution have been characterized for V(V), U(VI), Zr(IV), Th(IV), Mo(VI), Hf(IV), Ce(III), Ti(IV), Nb(V), La(III), having widely varying degrees of stability.(213) The study of these complexes was carried out in flow systems using e s r detection. $Ce(III)\text{-}HO_2$ in perchloric acid was observed spectrophotometrically.(214) For all these cations, the complex formation rate constand was $>10^5\ M^{-1}sec^{-1}$. For some of these metal ions (e.g. V(V)), the $M\text{-}H_2O_2$ complex formation was a prerequisite for $M\text{-}HO_2$ formation, while for others, Ce(III) among them, the radical complex formation was independent of such a precursor complex. In all the cases studied, the $M\text{-}HO_2$ complexes were more stable and longer lived than 'free' HO_2 and were formed with the aquo metal ions at their highest oxidaion state. The one exception was the $Ce(III)\text{-}HO_2$ complex, which decayed faster than free HO_2.(214) This was accounted for by the reactions(216)

$$Ce(III)\text{-}HO_2 + Ce(IV) \longrightarrow 2Ce(III) + O_2 + H^+$$

and $$Ce(III) - HO_2 \xrightarrow{H^+} Ce(IV) + H_2O_2$$

which are not available to the other metal ion systems (nor to tervalent nickel). The absence of observable complexation of HO_2 to the Ce(IV) ion is due to very rapid electron transfer between the reactant pair.(218)

At pH 0.3, the observed decay of the presumed $Ni(III)tam.HO_2$ complex at 405 nm was good second-order with $\frac{k}{\varepsilon l} = 160\ sec^{-1}$. Assuming $\varepsilon(Ni(III)tam.HO_2) \simeq \varepsilon(Ni(III)tam)$, which has a value determined from pulse radiolysis of $7800 M^{-1}sec^{-1}$ at this wavelength, the specific second-order rate constant is $\sim 1.2 \times 10^7\ M^{-1}sec^{-1}$. Associated with this decay process was a negative dependence of the rate on [Ni(II)tam], similar to that noted

section V 3.3, where Br^- catalysis of the tervalent macrocycle second-order decay is observed. The free HO_2 disproportionation rate in acidic solution is $7.6 \times 10^5 M^{-1}sec^{-1}$, significantly less than that observed in the tam system. The possibility of Ni(III) catalysis of the HO_2 disproportionation is unlikely in light of electrostatic considerations, and the trend noted for the other M-HO_2 complexes. It is more likely that the complexation of the tervalent macrocycle with the HO_2 species catalyses the second-order decay of Ni(III). The mechanism is tentatively presumed to be similar to that derived in section VI, where the Br^- (0.1M) catalyzed second-order rate of decay of Ni(III)tam was $2.5 \times 10^5 M^{-1}sec^{-1}$. However the suggestion of a highly reactive radical species acting as a bridge in an electron transfer reaction is quite unusual, and obviously requires further investigation.

4. Cu(II)diene, H_2O_2

4.1 The spectrum of the transient species observed 100 μsec after flashing a 50 μM Cu(II)di, 10 mM H_2O_2 solution at natural pH is shown in figure III 4.1. The same spectral shape was obtained in a solution of pH 1.0. The spectrum bears little resembelance to the Cu(III)di spectrum determined in acetonitrile via electrochemical oxidation[44] (λ max ~400 nm). The spectrum is similar, however, to those of non-cyclic Cu(III) amino complexes produced in pulse radiolysis studies.[78] In the wavelength range studied no spectral evidence for OH attack on the ligand radical was obtained.

4.2 The value of k_1 for the competitions,

FIGURE III 4.1

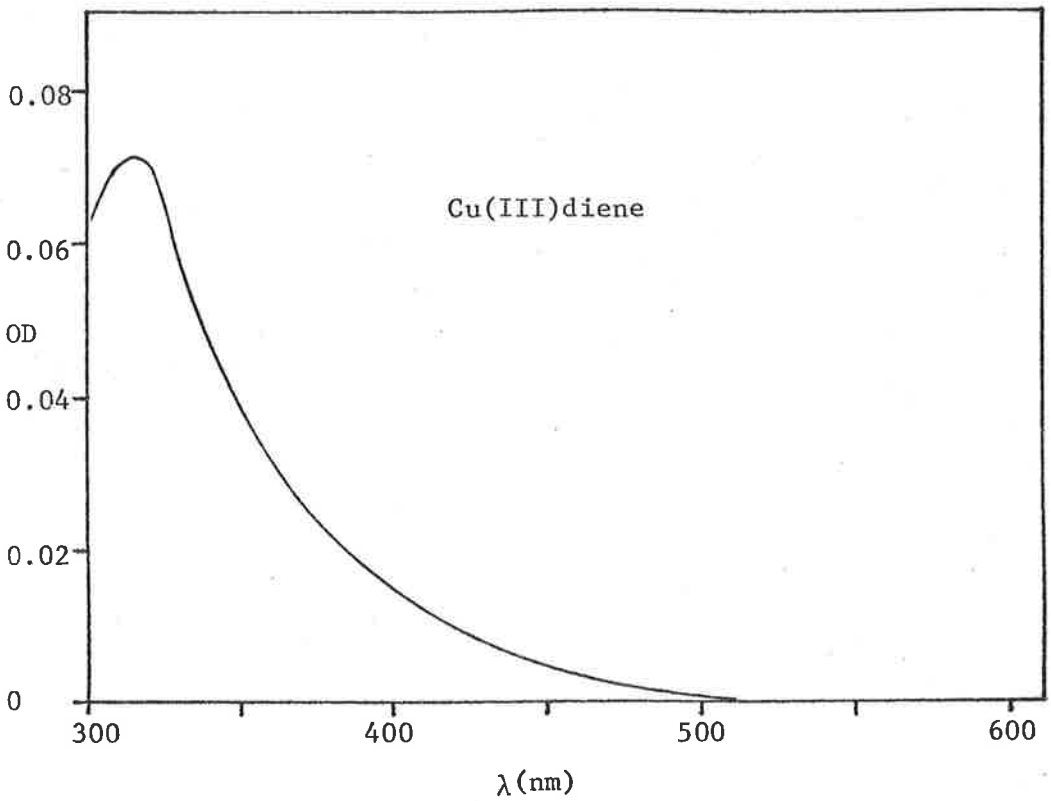

FIGURE III 4.3

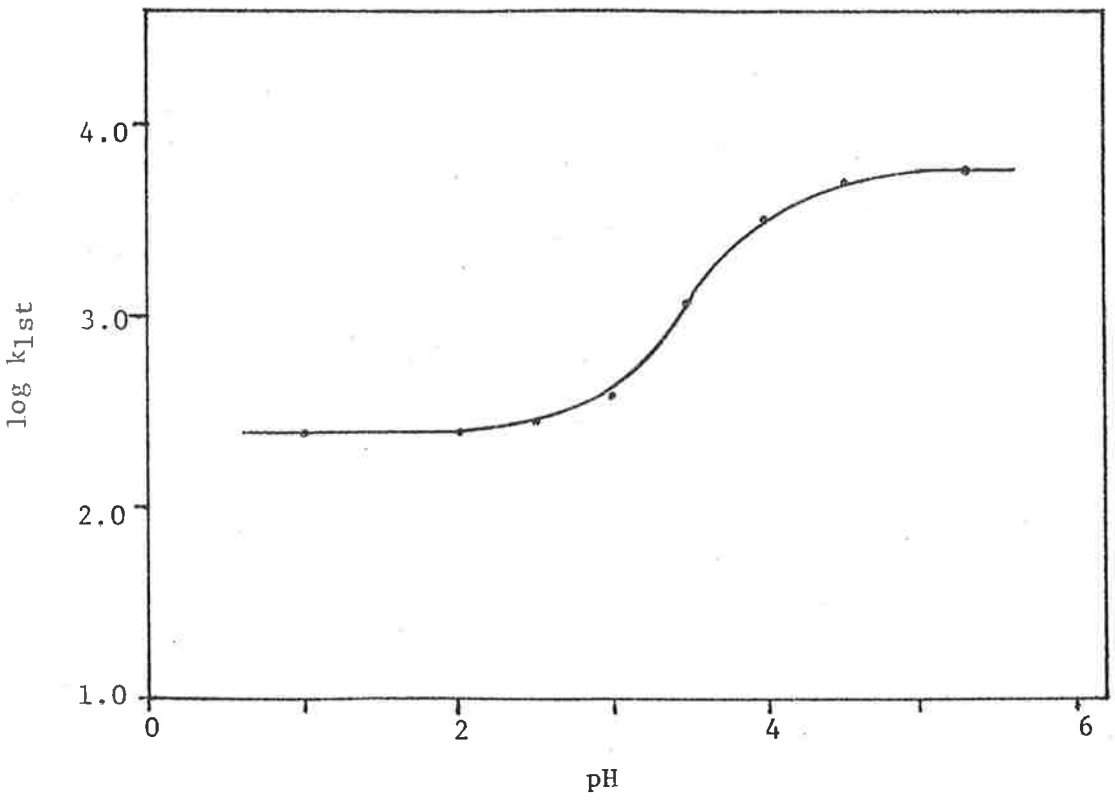

$$Cu(II)di + OH \xrightarrow{k_1} Cu(III)di + OH^-$$

$$H_2O_2 + OH \xrightarrow{k_2} HO_2 + H_2O_2$$

was determined at 313 nm in the manner used for the nickel systems, from the slope/intercept value for a plot of $\frac{1}{OD}$ versus $[H_2O_2]/[Cu(II)di]$. At pH 5.3, using a value of $k_2 = 4.5 \times 10^7 M^{-1} sec^{-1}$, the value of $k_1 = 1.5\ (\pm 0.3) \times 10^{10} M^{-1} sec^{-1}$ was determined.

4.3 As with the analogous Ni(III)L systems, the observed rate of decay at a particular pH was dependent on the $[H_2O_2]/[Cu(II)di]$ ratio, independently of how this ratio was changed. For a 20 μM Cu(II)di, 10 mM H_2O_2 solution, the observed transient decay rate at 313 nm was reasonable first order and quite pH dependent. This pH dependence was well behaved in terms of reaction between Cu(III)di and 'HO_2' (figure III 4.3).

The decay in a solution at natural pH containing 50 μM Cu(II)di and 2 mM H_2O_2 was, as expected, in two steps. The secondary process had a first-order dependence on $[H_2O_2]$ for values of $[H_2O_2]/[Cu(II)di] < 100$, with

$$k(Cu(III)di + H_2O_2) = 7.0\ (\pm 1.5) \times 10^2 M^{-1} sec^{-1}.$$

The same value for this rate was found in a solution of pH 2.0.

IV Cl_2^- AS PRECURSOR RADICAL

1. SPECTRAL PROPERTIES

The transient spectra observed 100μsec after the flash of solutions containing 20μM Ni(II)L, 0.1 M Cl^- and 5mM H_2O_2 at pH 1.0, were indistinguishable from the Ni(III)L spectra produced by OH oxidation in acid solution. The same spectra were obtained from photolysed 0.1mM $Co(NH_3)_5Cl^{2+}$ - 0.1 M Cl^- solutions containing the bivalent macrocycles. No evidence was observed for ligand radical formation when the pH was increased to 5.3; the spectral shape was independent of pH over the range 1.0 - 5.3. The identical Ni(III)L complex spectra were obtained by pulse radiolysis of 50μM Ni(II)L - 10mM Cl^- solutions at pH 3.0. Use of a SCN^- dosimeter solution allowed molar absorbance values to be determined.

2. FORMATION OF Ni(III)L

2.1 The specific rates of Cl_2^- oxidation of the bivalent Ni tetene and diene complexes were determined by competition kinetics for the radical-anions between the complexes and Fe^{2+}. The rate and mechanism of the $Fe^{2+} + Cl_2^-$ reaction is known. The mechanism involves both inner- and outer-sphere electron-transfer.[132a] (see section VI 1.1) for which the initial products after oxidation are $FeCl^{2+}$ and Fe^{3+}_{aq} respectively (The $Fe^{3+}_{aq} + Cl^-$ equilibrium is inert on the timescale of absorbance measurement in this analysis). The total rate of Cl_2^- oxidation of Fe^{2+}_{aq} is the sum of the rates via the inner- and outer-sphere paths i.e. $k_2 = k_{IS} + k_{OS}$. The $FeCl^{2+}$ system in 0.1M H^+ was chosen to produce the Cl_2^- precursor radicals. The scheme of competition is:

$$FeCl^{2+} \xrightarrow[Cl^-]{h\nu} Fe^{2+} + Cl_2^-$$

$$Ni(II)L + Cl_2^- \xrightarrow{k_1} Ni(III)L + 2Cl^-$$

$$Fe^{2+} + Cl_2^- \xrightarrow{k_2} Fe(III) + 2Cl^-; \quad FeCl^{2+} + Cl^-$$

$$Cl_2^- + Cl_2^- \xrightarrow{k_3} Cl_3^- + Cl^-$$

Any absorption in the Cl^-_{aq} CTTS band was eliminated by filtering the flash through silica. Assuming constant Cl_2^- yield from the $FeCl^{2+}$ photolysis (the Fe^{2+}_{aq} absorption in the U.V. does not inner-filter the LMCT band of the photoactive complex). The disappearance of Cl_2^- by the disproportionation reaction could be neglected in these systems. The yield of (Cl_2^-) was ~5μM, so that the initial rate of the disproportionation reaction was equivalent to a half life of 50μsec. The half life of the reaction of Cl_2^- with Fe^{2+} or Ni(II)L was ~2μsec. The effect of the metal ion competition on the yield of Ni(III)L was thus independent of this fast unavoidable reaction. At the observation wavelength (405nm) there was significant absorption due to $FeCl^{2+}$. After the flash there was a small decrease in this complex absorption due to the photolysis. This loss of absorption is considered to be constant at constant flash intensity.

Thus, the yields of Cl_2^- oxidation products can be expressed as

$$Y_{(Ni(III)L)} = Y_{(Cl_2^-)} \frac{k_1[Ni(II)L]}{k_1[Ni(II)L] + k_2[Fe^{2+}]}$$

and

$$Y_{(FeCl^{2+})} = Y_{(Cl_2^-)} \frac{k_{IS}[Fe^{2+}]}{k_1[Ni(II)L] + k_2[Fe^{2+}]}$$

where $Y_{(Cl_2^-)}$ is the yield of Cl_2^- available to the competition between Ni(II)L and Fe^{2+}_{aq}, and not the total yield from the original $FeCl^{2+}$ phot-

olysis. At 405nm, the observed absorbance change after the Cl_2^- competition is

$$OD = OD(Ni(III)L + \Delta OD\ (FeCl^{2+})$$

where $\Delta OD(FeCl^{2+})$ is a composite effect of absorbance loss due to photolysis and gain due to inner-sphere oxidation of Fe^{2+} by Cl_2^-. In the absence of added Fe^{2+},

$$OD^o = \varepsilon(Ni(III)L)\ Y^o(Ni(III)L) - \varepsilon(FeCl^{2+})\ \phi FeCl^{2+}$$

where ϕ is the primary photochemical yield. The yield value $Y^o(Ni(III)L)$ is related to to Y values of both Ni(III)L and $FeCl^{2+}$ when Fe^{2+} is in competition, by

$$Y^o\ (Ni(III)L) = Y(Ni(III)L) + \alpha\, Y(FeCl^{2+})$$

where α is the reciprocal of the ratio $k_{IS}/k_{IS}+k_{OS}$.

The absorbance change in the presence of Fe^{2+} is thus given by

$$OD = \varepsilon(Ni(III)L)\ Y(Ni(III)L) + \varepsilon(FeCl^{2+})\ Y(FeCl^{2+}) - \varepsilon(FeCl^{2+})\ \phi FeCl^{2+}$$

$$\therefore\ OD - OD^o = Y(FeCl^{2+}) \left[\varepsilon(FeCl^{2+}) - \alpha\,\varepsilon\,(Ni(III)L)\right]$$

Substituting the kinetic expression for $Y(FeCl^{2+})$,

$$OD - OD^o = Y(Cl_2^-) \left[\varepsilon(FeCl^{2+}) - \alpha\varepsilon(Ni(III)L)\right] \times \frac{k_{IS}\ [Fe^{2+}]}{k_1\,[Ni(II)L] + k_1\,[Fe^{2+}]}$$

$$\therefore \frac{1}{OD^o - OD} = \frac{1}{\text{constant}} \left[\frac{1}{\alpha} + \frac{k_1\,[Ni(II)L]}{k_{IS}\ [Fe^{2+}]}\right]$$

A plot of $1/(OD^o-OD)$ versus $[Ni(II)L]/[Fe^{2+}]$ should be linear having a slope/intercept value of $\alpha k_1/k_{IS}$. Since α is known to be 0.28 and

$k_{IS} \simeq 3.3 \times 10^6 M^{-1} sec^{-1}$ at 20^oC,[132a] the value of k_1 could be determined. Measurement of transient absorption was made 50μsec after the flash of 20μM Ni(II)tet, 0.1M Cl^-, 0.5mM Fe^{3+} solutions, varying in $[Fe^{2+}]$ from 0 - 53mM. The value of $k(Ni(II)tet + Cl_2^-)$ as determined from the appropriate plot of experimental data, was $1.2 (\pm 0.2) \times 10^{10} M^{-1} sec^{-1}$. This plot is shown in figure IV 2.1. The analogous plot for the diene complex gave $k(Ni(II)di + Cl_2^-) = 1.0 (\pm 0.2) \times 10^{10} M^{-1} sec^{-1}$.

2.3 The Cl_2^- disproportionation at 366nm in 0.1 M H^+ was observed in the presence and absence of free diene macrocycle. The decay was as usual, second-order for concentrations of diene $\lesssim$ 0.1mM, but changed to essentially first-order at 1mM, with $k_{obs} \sim 3 \times 10^4 sec^{-1}$. This result suggests that Cl_2^- oxidation of the diene macrocycle may occur with a rate $\sim 3 \times 10^7 M^{-1} sec^{-1}$. This rate is considerably slower than the Ni(II) diene rate with Cl_2^-, so that any radical attack on the coordinated ligand is considered to be negligible.

3. Ni(III) DECOMPOSITION IN ACIDIC Cl^- SOLUTION.

3.1 The mode of transient decay of the Ni(III)L complexes produced by Cl_2^- oxidation of the bivalent macrocycles was pH dependent over the pH range 1-9. The nature of the decay process occurring within this pH range depended on the actual complex considered. The decay processes in Cl^- solution at pH 1.0 are considered in this section.

3.2 The decay of the Ni(III)tet species produced by flashing a 20μM Ni(II)tet, 0.1M Cl^-, 0.1mM $Co(NH_3)_5 Cl^{2+}$ solution at pH 1.0 was slow mixed-order at 366nm. The decay was reasonable first-order after about

1½ half-lives, but had a definite faster component in its initial stages. The k_{1st} value was ≃0.03 sec^{-1}. At 0.2mM Cl^-, the decay was first-order throughout, having the same rate as at the high [Cl^-]. The decay of the tervalent diene complex was first-order having a rate constant ≃0.01 sec^{-1} independent of the [Cl^-]. No transient effects were observable at 546nm.

For the tetramine complex in 0.1M Cl^-, the flash produced a very pale yellow-green colouration of the solution. Spectral analysis showed that this species was the Ni(III)tam complex. The tervalent complex was quite stable under the experimental conditions and decayed over a period of perhaps an hour. The green colouration of the flashed solution was quickly bleached by the addition of small amounts of 0.1M I^-, SCN^- and Br^- solution, and by the addition of strong alkali.

3.3 The transient decay of the Ni(III)L complexes in 0.1M Cl^-, 1mM Fe^{3+} solutions containing 20μM Ni(II)L at pH 1.0 were observed at 405nm. The kinetics of decay of all three complexes approximated second-order for two half-lives. The second-order process appeared independent of both [Cl^-] and [Ni(II)L] for the small changes studied. Using the molar absorbance values obtained in the pulse radiolysis study at 405nm, the specific second-order rate constants for the decay reactions in this $FeCl^{2+}$ system were determined from the observed $\frac{k}{\varepsilon l}$ values (where l = 10cm).

FIGURE IV 2.1

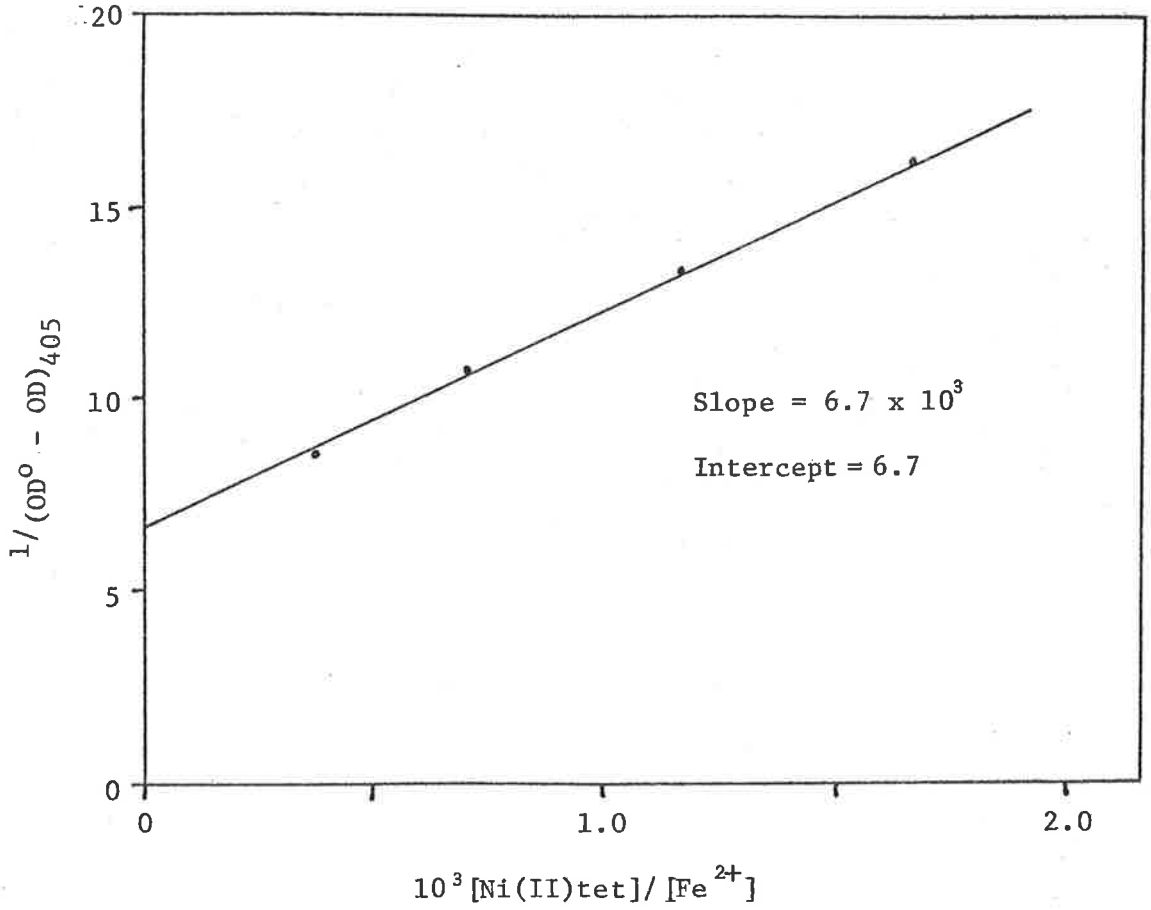

FIGURE IV 3.3

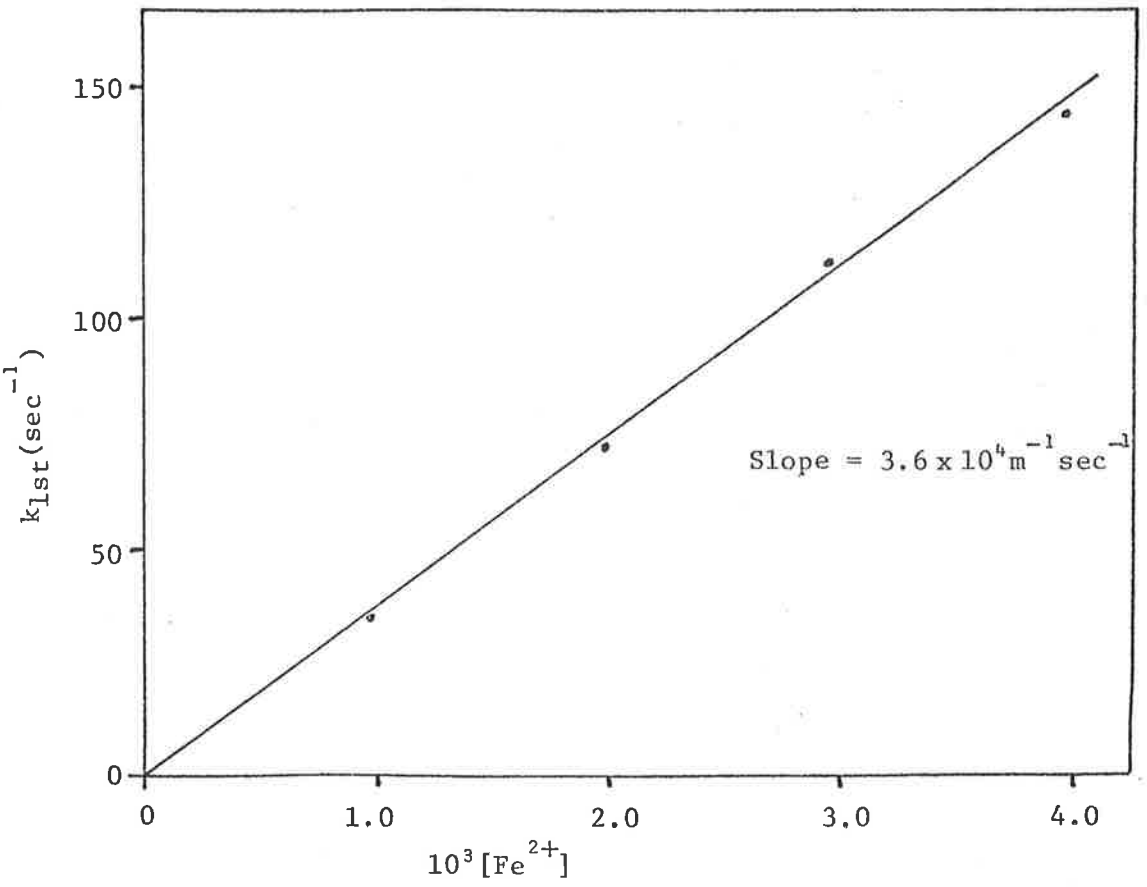

Ni(III)L	ϵ_{405} $(M^{-1}cm^{-1})$	$\frac{k_{2nd}}{\epsilon l}$ (sec^{-1})	k_{2nd} $(M^{-1}sec^{-1})$
tetene	1300	3.9	5.1×10^4
diene	4800	0.61	2.9×10^4
tetramine	7400	0.86	6.4×10^4

The error in the determined rate constants was at least 20%.

The considerable difference in the kinetics and rate of decay of the tervalent complexes between the $FeCl^{2+}$ and $Co(NH_3)_5Cl^{2+}$ systems at constant $[Cl^-]$ (particularly for the tam system) suggests that intrinsic properties of the actual solutions are responsible. The need for a reductant species present in solution in similar concentration to the tervalent intermediate in the $FeCl^{2+}$ system, is fulfilled by the photoproduction of Fe^{2+}_{aq} in the primary photolysis step;

$$FeCl^{2+} \xrightarrow[Cl^-]{h\nu} Fe^{2+}_{aq} + Cl_2^-$$

The specific rate of the Ni(III)L + Fe^{2+} reaction was determined by adding known concentraions of Fe^{2+} to the system, in which case the decay was pseudo-first order in $[Fe^{2+}]$ over the range 0.46 - 1.83mM. From the slope of plots of k_{obs} versus $[Fe^{2+}]$, the reaction rates were determined as shown below. The tetene plot is shown in figure IV 3.3.

Ni(III)L	k(Ni(III)L + Fe^{2+}) $(M^{-1}sec^{-1})$
tetene	3.6×10^4
diene	2.1×10^4
tetramine	4.2×10^4

The similarity of these second-order rates with those observed in the

$FeCl^{2+}$ system strongly suggests that the observed tervalent macrocycle decay is with photo-produced Fe^{2+} in the photolysed $FeCl^{2+}$ solution.

3.4 The yellow-green Ni(III)tam complex observed in the $Co(NH_3)_5Cl^{2+}$ system at pH 1.0, is the same colour as that reported by Barefield[46] when the perchlorate salt of the same complex was dissolved in acidic aqueous solution. No details of the UV-visible spectrum of the tervalent complex were given in this publication. The green complex was reported by Barefield to decay very slowly in perchloric acid solution by slow conversion to the ligand radical intermediate Ni(II)L$^{\bullet}$ in the rate determining step, followed by ligand fragmentation and H-atom transfer to form stable products. The evidence for ring degradation was from analysis of titratable Ni(II) using EDTA in the product solutions at neutral pH. Analysis of 'complexable' Ni(II) product in the $Co(NH_3)_5Cl^{2+}$ system using EDTA, DMG, CN^- etc.[141] was complicated by the presence of free Co^{2+}, produced from the primary photolysis. Spectral analysis of the product after several flashes was unsatisfactory because of considerable $Co(NH_3)_5Cl^{2+}$ inner-filtering of the Ni(II)tam U.V. absorption band. The decay of the tetramine tervalent complex in acidic solution is considered, without the formal proof of product analysis, to be the same as that established in Barefield's study.

In 0.1mM $Co(NH_3)_5Cl^{2+}$ soltuion, the ligand chromophore bands of the tetene and diene complexes were quite observable for [Ni(II)L] >50μM. In the region above 260nm, only the tail of the Co(III) complex absorption is important. The spectra of solutions containing 60μM (di) or 50μM(tet) Ni(II)L, 0.1mM $Co(NH_3)_5Cl^{2+}$, 0.2mM Cl^- at pH 1.0 were compared before and after multiple flashing with the spectrum in the same region of

solutions containing equal concentrations of Ni(II)L only. The test solutions were flashed until the absorption due to the Co complex was considerably depleted (10-15 flashes). The depletion of the available 0.1mM $Co(NH_3)_5Cl^{2+}$ complex by photolysis gave an indication of the transient dose; further flashing ceased when ~50μM of the Co complex was depleted. The duration between each flash was 10 minutes for the diene and 5 minutes for the tetene, to allow for complete tervalent decay to occur before the following flash. The spectra are shown in figure IV 3.4. Significant change was apparent for both complexes, with greater change occurring for the tetene. The chromophoric character was retained to a considerable degree. A quantitative analysis of the product complexes was not attempted due to the small product yields (~50μM).

The similar tervalent tet and di decompositions in this system at pH 1.0 (with the observed first-order rate being about three times faster for the tet) compared with the meta-stability of the analogous tam system, suggests that the Barefield mechanism does not occur for the unsaturated complexes. In fact, the tetene complex is incapable of conversion to the analogous ligand radical intermediate due to the absence of co-ordinated secondary nitrogen atoms. The decomposition is inferred by analogy to the tam system to involve ring rupture, with this process being catalyzed by multiple bonding within the ligand structure. It is possible that the system may proceed through a ligand radical intermediate in which the unpaired-electron is considerably more delocalized than in the tam system. An intermediate was observed (but not characterized) for the corresponding decomposition of the tervalent tetene in neutral solution, as discussed in section VII 2.4. Further kinetic and product analysis is required to understand the mechanism of this process.

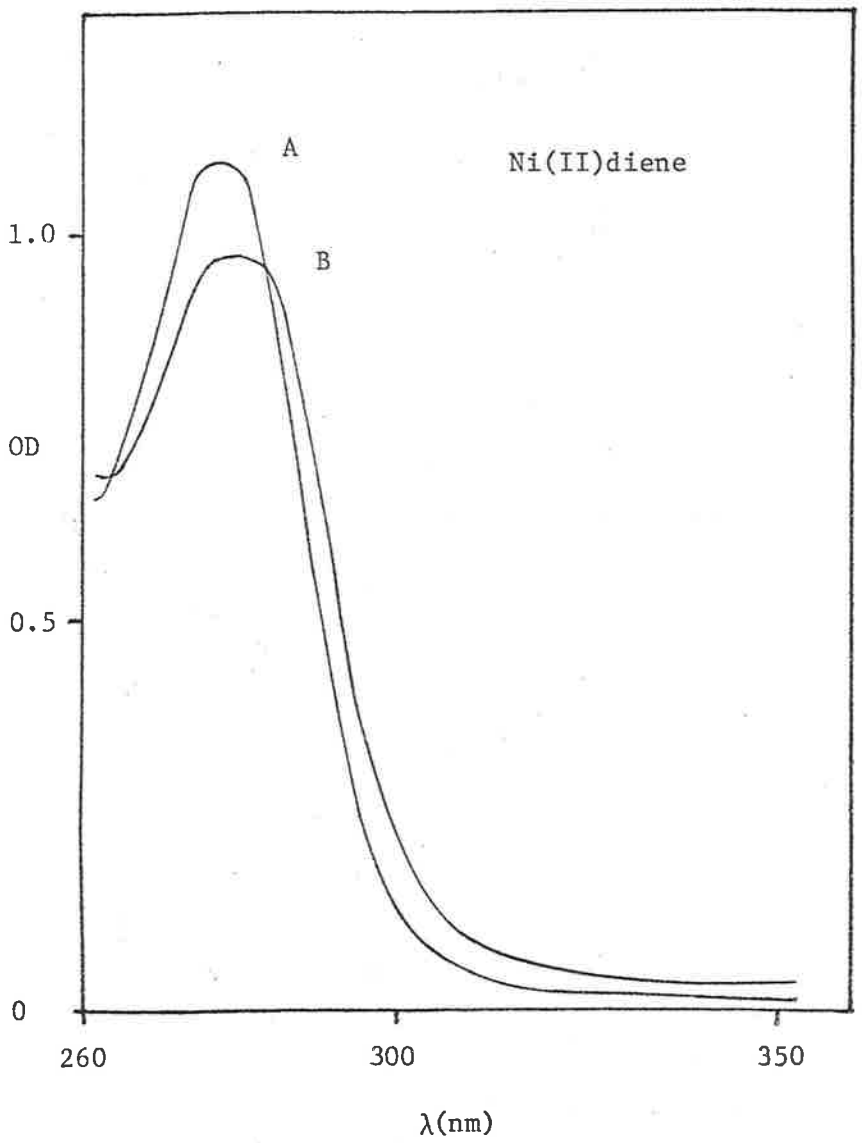

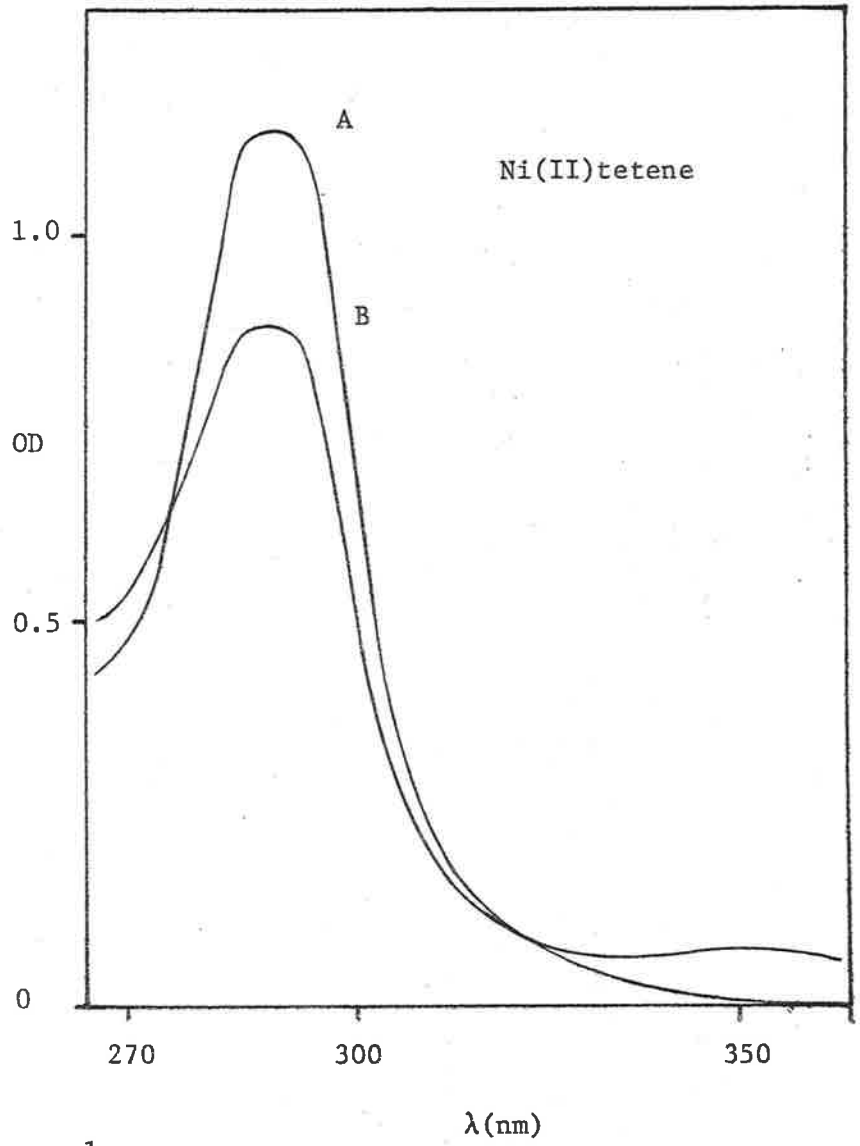

A : complex only

B : flashed complex solution

FIGURE IV 3.4

4. Cu(II)diene, Cl_2^-

4.1 The spectra observed 50μsec and 20msec after flashing a 50μM Cu(II)di, 0.1M Cl^-, 1 M Fe^{3+} solution at pH 1.0 are shown in figure IV 4.1. The initial spectrum was that of the Cl_2^- radical anion, while that observed at the later time was identical to the Cu(III)di spectrum determined previously with OH as precursor radical.

4.2 The transient decay observed at 405nm immediately after the flash was mixed order, with a tendency towards better first-order as the [Cu(II)di] increased. The kinetic data were treated according to the scheme,

$$Cl_2^- + Cl_2^- \xrightarrow{2k_1} Cl_3^- + Cl^-$$

$$Cl_2^- + Cu(II)di \xrightarrow{k_2} Cu(III)di + 2Cl^-$$

using the computer program FIT. The value of the disproportionation rate[132] used in the analysis was $2k_1 = 5.2 \times 10^9 M^{-1} sec^{-1}$, with a value of the Cl_2^- molar absorbance at 405nm of $3100 M^{-1} cm^{-1}$. The best fit of the first-order rate for each concentration of Cu(II)di in the range 20-75μM was determined by the program. The plot of the calculated first-order rates versus [Cu(II)di] is shown in figure IV 4.2, from which the value of $k_2 = k\ (Cu(II)di + Cl_2^-) = 1.5\ (\pm 0.2) \times 10^8$ was obtained from the slope.

4.3 The observed transient decay at 313nm of the Cu(III)di complex in a 20μM Cu(II)di, 0.1M Cl^-, 0.1mM $Co(NH_3)_5\ Cl^{2+}$ solution at pH 1.0 was second-order with $k/\varepsilon l \simeq 20\ sec^{-1}$. This decay process showed a negative dependence on [Cu(II)di] (figure IV 4.3) and a positive dependence on [Cl^-]; the rate of 0.3M Cl^- was 3.2 times that at 0.1M. The definite similarity

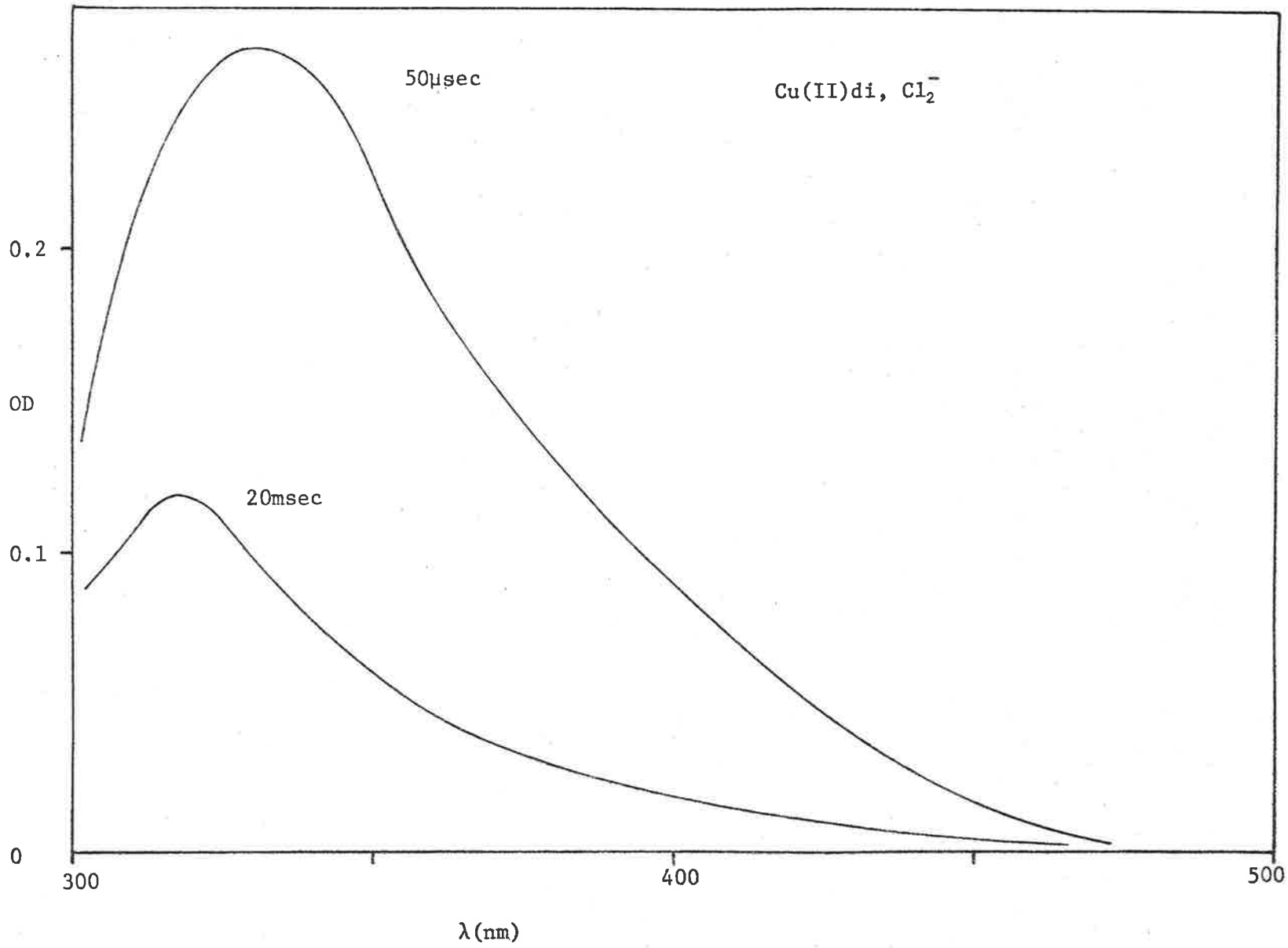

FIGURE IV 4.1

FIGURE IV 4.2

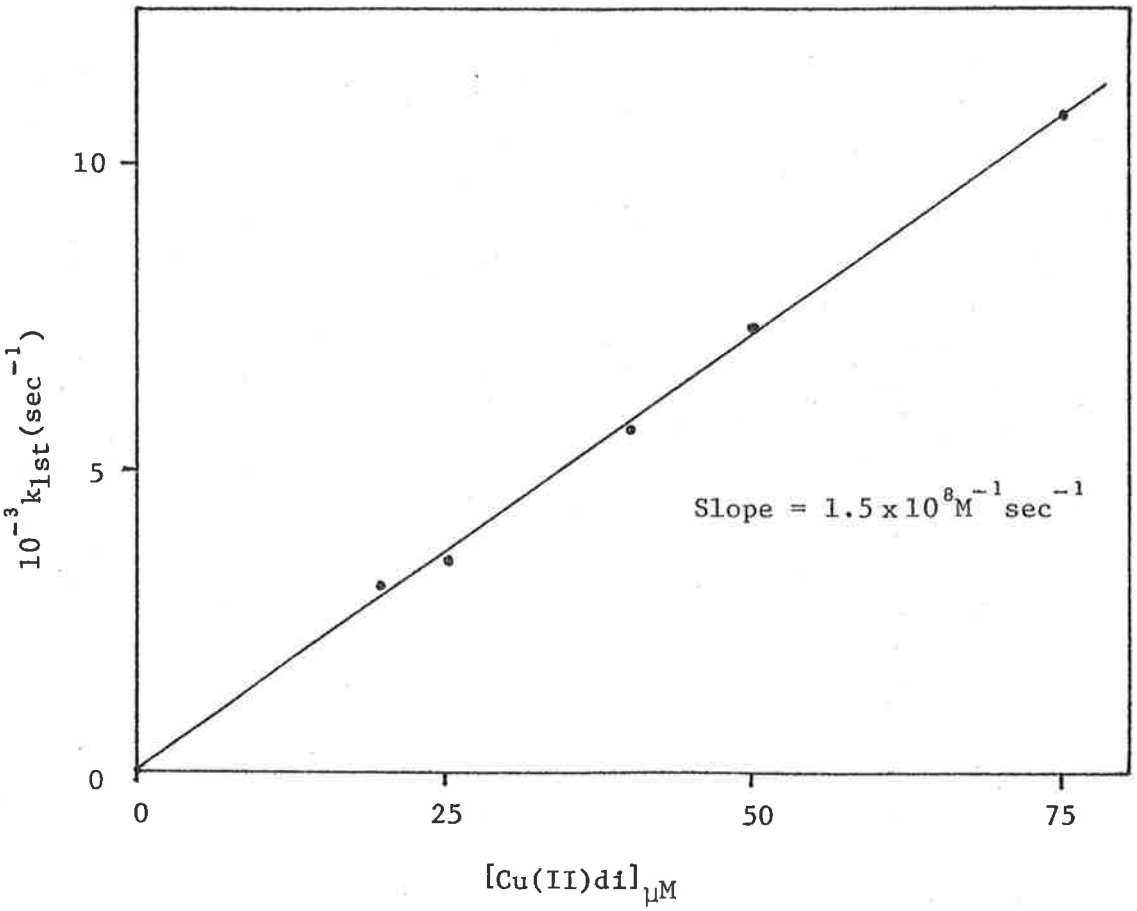

FIGURE IV 4.3

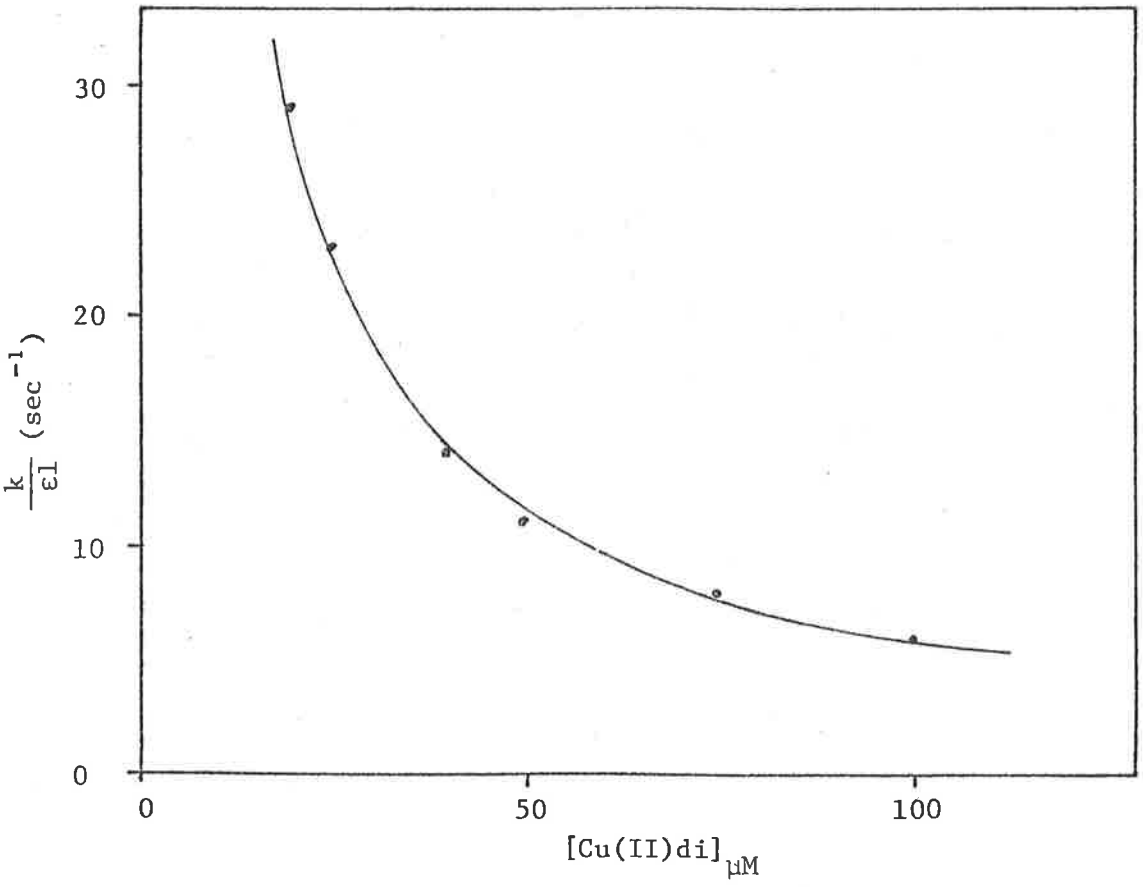

between this decay reaction and those obtained for the Ni(III)L complexes in Br^- solution, (discussed in detail in the next section) suggests that the probable mechanism of Cu(III)di decomposition is via the anion-assisted path.

The addition of N_3^- ion in solution changed the decay to pseudo-first order, with a linear dependence on $[N_3^-]$ in the range 0.8 - 4.0mM. The value of $k\ (Cu(III)di + N_3^-) = 2.5\ (\pm 0.3) \times 10^4 M^{-1} sec^{-1}$ was determined from the slope of a plot of k_{obs} versus $[N_3^-]$. (The addition of 1mM SCN^- to the reaction solution eliminated the Cu(III)di absorption upon flashing; this effect was not further investigated). The oxidation of the azide is a facile process for the highly oxidizing Cu(III)di complex, to form the stable products Cu(II)di and N_2, so that electron-transfer bridging by this anion, seen in the analogous Ni(III)L systems (section V 3.4), does not occur.

V Br_2^- AS PRECURSOR RADICAL

1. SPECTRAL PROPERTIES

1.1 The transient spectra obtained 50μsec after the flash from a 20μM Ni(II)L - 0.1M Br^- solution, are shown in figure V 1.1. The spectra determined in the 270-600nm region for L=tam, and 300-600nm region for L=di, tet, were independent of pH in the range 1.0 - 5.3 The absorbances of the transient complexes were characteristic of tervalent nickel rather than of ligand radical intermediates. The Ni(III)tet spectrum showed a significant difference from that obtained using OH radical as precursor oxidizing species. Large broad shoulders in the region >360nm were apparent in Br^- solution. The spectrum determined for the tervalent Ni diene complex was quite similar to that obtained from OH radical oxidation in acidic solution. No observable difference was apparent between the tervalent oxidation products from Br_2^-, and OH in acid, for the tam complex.

1.2 The spectral properties of the complex intermediates produced in flashed 20μM Ni(II)L, Br^- solutions at pH 1.0 containing,

(i) $FeBr_2^+$ (20mM Br^-, 0.5mM Fe^{3+})

(ii) Br_3^- (0.1M Br^-, 50μM Br_2)

(iii) $Co(NH_3)_5Br^{2+}$ (50μM $Co(NH_3)_5Br^{2+}$, 0.1M Br^-)

were all identical within experimental error to that obtained in Br^- solution alone. Insertion of pyrex or silica filters between the flash tube and sample cell, (so that absorption in the CTTS band of the Br^- was greatly diminished) resulted in complete elimination of the transient

FIGURE V 1.1

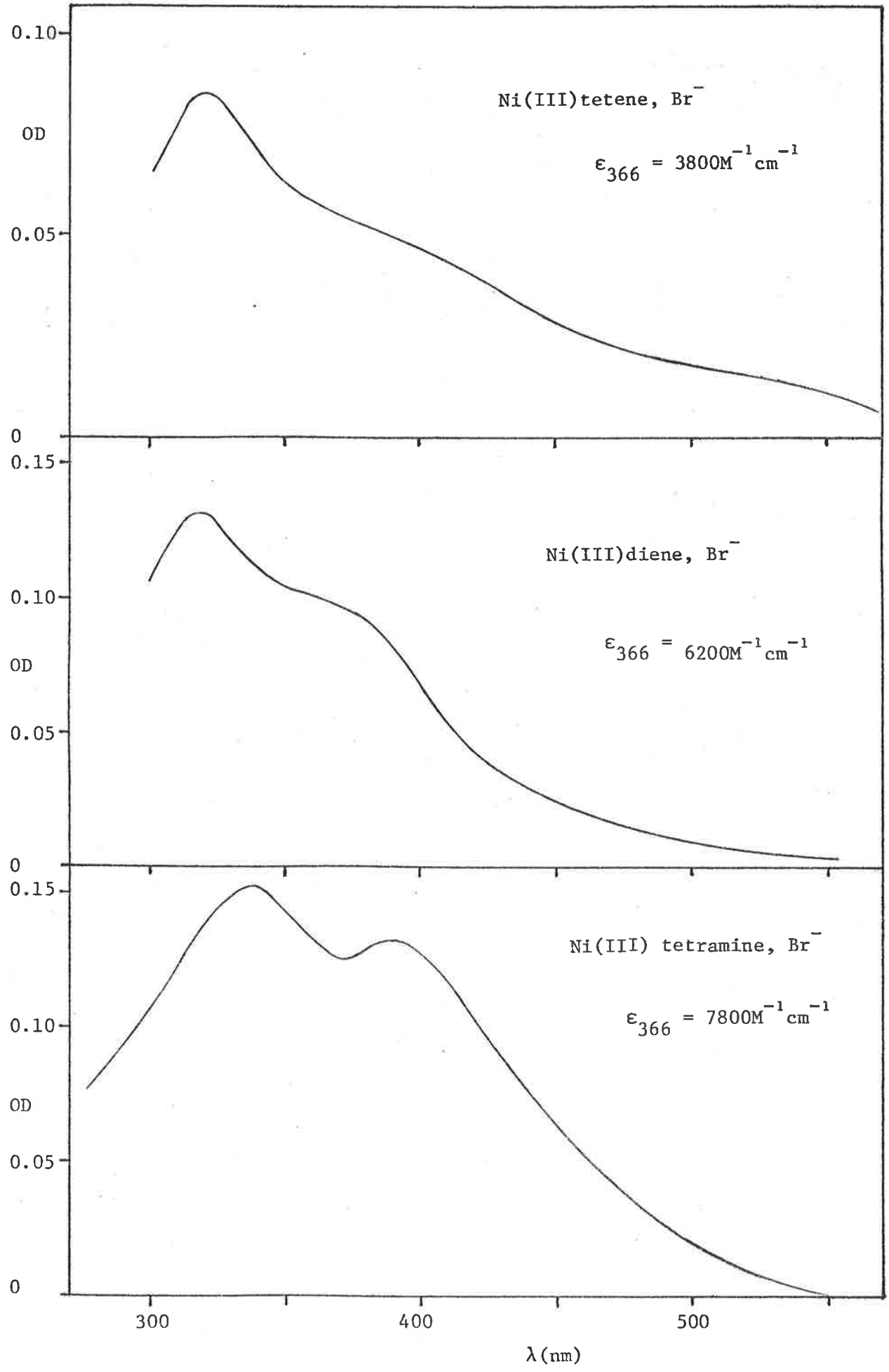
0.10
OD
0.05
0
Ni(III)tetene, Br⁻
ε366 = 3800M⁻¹cm⁻¹
0.15
0.10
OD
0.05
0
Ni(III)diene, Br⁻
ε366 = 6200M⁻¹cm⁻¹
0.15
0.10
OD
0.05
0
Ni(III) tetramine, Br⁻
ε366 = 7800M⁻¹cm⁻¹
300
400
500
λ(nm)

absorption for the Br^- only system, and unchanged spectral shape for the other systems (where photolysis occurs in bands >250nm). Pulse radiolysis of 0.1M Br^- solutions containing the bivalent complexes at pH 1.0, produced very similar spectra to those produced in the photolysis systems. Accurate measurement of the pulse dose of OH radicals (using a SCN^- dosimeter), allowed estimates of the molar absorbances of the tervalent complexes to be made.

1.3 In a 0.1mM $Co(NH_3)_5Br^{2+}$ solution, the $[Br^-]$ could be conveniently varied between 0.2mM - 0.1M without noticably affecting the quantum efficiency of the complex photolysis. At the low $[Br^-]$, the major radical species in solution after flashing is still Br_2^-, since the equilibrium constant for the process

$$Br + Br^- \rightleftharpoons Br_2^-$$

is ~2 x $10^5 M^{-1}$.(92) The tervalent macrocycle spectra were measured 250μsec after the flash for 20μM Ni(II)tet, and Ni(II)di solutions, at pH 3.0, at the low and high Br^- concentrations. At 0.2mM Br^-, the tetene spectrum was the same as that obtained from OH radical attack (in the absence of Br^-). A small but noticable increase in absorption in the 450-550nm region was observed when the $[Br^-]$ was increased from 0.2mM to 0.1M for the diene system. It can be concluded from these results that it is the presence of Br^- that affects the spectral nature of these oxidized complexes in comparison to those produced from OH oxidation, and not the fact that Br_2^- is the precursor radical in these systems. The implications of this Br^- effect were further brought out when the transient complex decompositions in Br^- solution were investigated.

2. FORMATION OF Ni(III)L

2.1 The specific rate constants of the Ni(II)L + Br_2^- reactions (L = tet, di) were conveniently determined by competition for the radical anions between the bivalent complexes and Fe^{2+}_{aq}, for which the rate and mechanism are known.[132a] The method used was analogous to that used to determine the Ni(II)L + Cl_2^- specific rate constants. For this system the Fe^{2+} + Br_2^- reaction was wholly inner-sphere, having a specific rate of $4.0 \times 10^6 M^{-1} sec^{-1}$ at 20°C.[132a] The values of the rates of Br_2^- oxidation of the Ni(II)tet and di complexes were $2.6 (\pm 0.6) \times 10^9 M^{-1} sec^{-1}$ and $2.2 (\pm 0.7) \times 10^9 M^{-1} sec^{-1}$ respectively. Evidence presented in a later section (V4.2) suggests that the Ni(II)tam + Br_2^- rate constant is $\sim 4 \times 10^9 M^{-1} sec^{-1}$. The slower specific rates of Br_2^- oxidation compared with those of Cl_2^- are considered due to the lower reduction potential of the $X_2^-/2X^-$ couple for X = Br^-.

2.2 The possibility of Br_2^- attack on the ligand was investigated by observing the effect of added 'free' diene macrocycle on the Br_2^- disproportionation rate. The second-order Br_2^- decay rate observed in a 0.1M Br^-, 50μM Br_2 solution at pH 1.0 was unchanged in the presence of 1mM diene ligand (which is about the limit of the ligand's solubility). This suggests therefore that if Br_2^- + L does occur, it has a specific rate $\lesssim 10^5 M^{-1} sec^{-1}$.

3. Ni(III)L DECAY IN Br^- SOLUTION

3.1 The transient decay process was initially observed in flashed aerated 0.1M Br^- solution containing the Ni(II) macrocycles at a concentration of 20μM. The decay rate observed at 366nm, was pH depen-

dent in the region 0.5 - 5.3, the kinetics being reasonably second-order throughout.

For the tetene complex, the observed second-order rate was virtually independent of acid concentration in the pH region 1-3, while for pH $\gtrsim$ 3, there was an increase in rate which levelled-off at pH > 5. This is shown in figure V 3.1a. The decay rate at pH 5.3 was independent of [Ni(II)tet] and [Br^-], but at pH 1.0 showed a definite positive dependence on [Br^-].

The observed second-order decay rate of the diene complex increased steadily with pH above pH 1.8, levelling off at pH > 5. (see figure V 3.1b). In the pH region 1.0 - 1.8, unusual decay characteristics were observed. The second-order plots of $^1/OD_t$ versus time had greater slopes in the initial stages of the decay. The proportion of the faster process as a fraction of the overall decay decreased as the pH fell to 1.0. Below this pH essentially linear kinetic plots for the whole decay were again obtained, with the decay rate significantly slower than that for pH > 1.8. With 50μM Br_2 in solution, no fast initial decay was observed up to pH 3.0. For the tervalent tam complex this anomalous decay effect was considerably more significant. The rate difference between the initial faster decay and the later slow decay was so considerable that the two processes were quite separately observable. In the pH region 2-3, this unusual kinetic behaviour was particularly evident. (This behaviour is discussed in detail after the more well-behaved aspects of the decay have been discussed). For both the tervalent di and tam complexes, the observed decay was independent of [Ni(II)L] and [Br^-] at natural pH, but showed a negative [Ni(II)L] dependence, and a positive [Br^-] dependence, at pH 1.0.

FIGURE V 3.1a

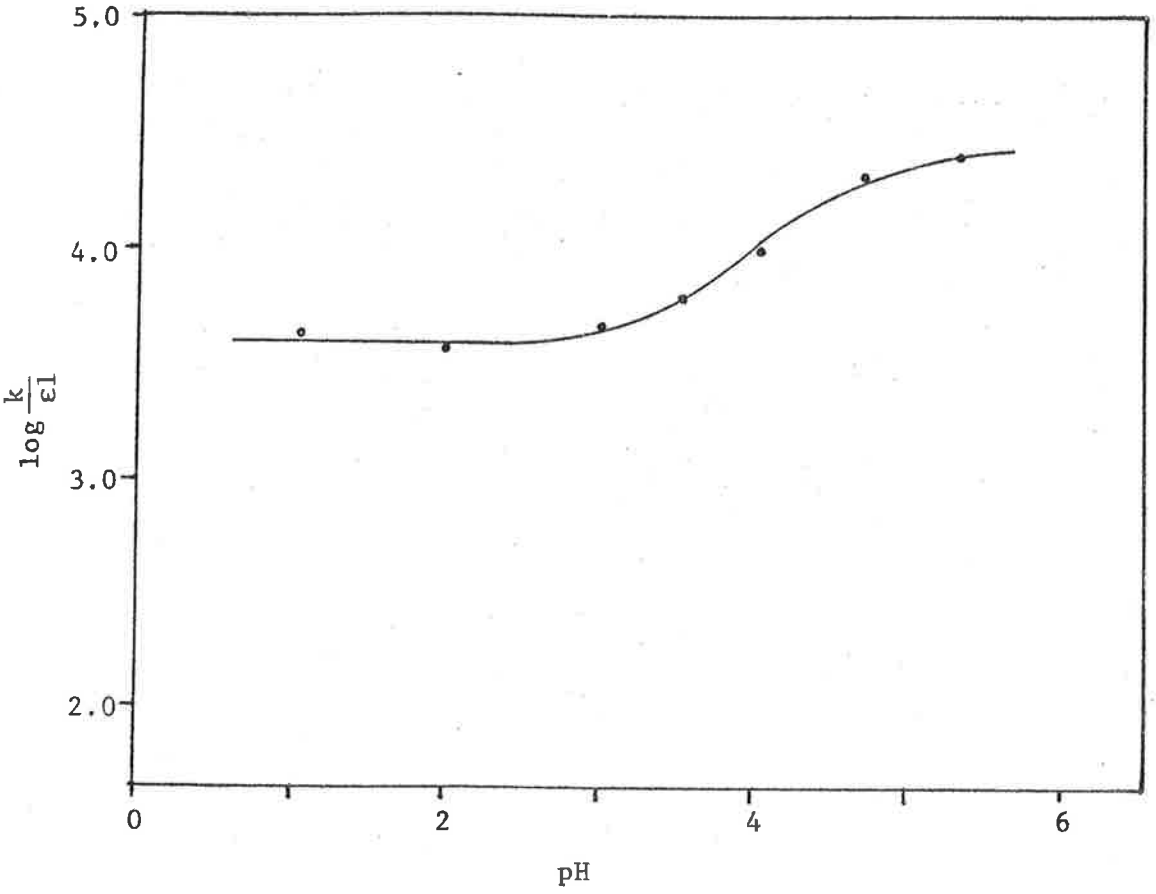

FIGURE V 3.1b

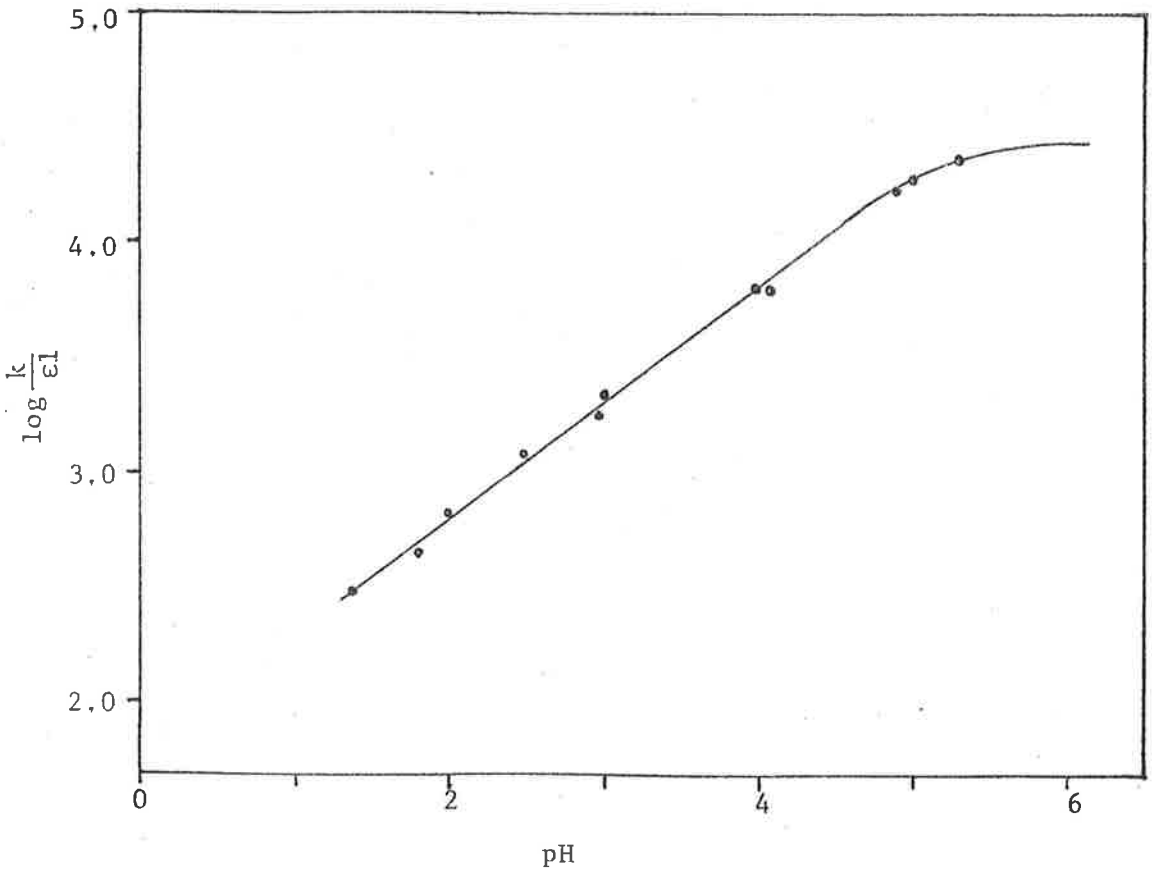

3.2 The observed decay in solutions of pH > 3 was similar in rate for the three complexes, while that in acid varied greatly in the order tetene>diene>tetramine. A significant increase in the second-order decay rate at pH 5.3 was observed when the solutions were thoroughly deaerated, whilst this had no effect at pH 1.0 for the three complexes. These results, combined with the difference in the dependences on [Ni(II)L] and [Br^-] between pH 5.3 and 1.0, suggest that the second-order decay processes are inherently different at the two pH's.

The rate change with pH of the observed decays of Ni(III)L above about 3.5 in aerated solution closely resemble those observed in the previous sections III 1.4, 2.5, 3.3, where the Ni(III)L + HO_2 reactions were established to occur. It is therefore considered that in this system, where the Br_2^- are produced from

$$Br^-_{aq} \xrightarrow[Br^-]{h\nu} Br_2^- + e^-_{aq}$$

that the e^-aq co-produced by the primary photolysis, yields superoxy radical after oxygen scavenging.

i.e. $e^-_{aq} + O_2 \longrightarrow O_2^- \ (+ H^+ \rightleftharpoons HO_2)$

or $e^-_{aq} + H^+ \longrightarrow H \ (+ O_2 \rightleftharpoons HO_2)$

depending on the pH of the solution. (These reactions are very fast, $>10^{10} M^{-1} sec^{-1}$ (84)). Second-order kinetics result for the observed Ni(III)L decay since both reactants are produced by virtually complete conversion of both the primary photolysis products under the experimental conditions. Deaeration of the solution allows e^-_{aq} to react directly with the Ni(III)L, or with Ni(II)L to produce Ni(I), which can disproportionate with the tervalent state.

i.e. $Ni(III)L + Ni(I)L \longrightarrow 2Ni(II)L$

It appears that these second-order reactions are faster than the $Ni(III)L + 'HO_2'$ reaction they replace when the solution is deaerated.

In the tetene system, addition of aqueous Br_2, $Co(NH_3)_5Br^{2+}$, or N_2O (all of which are efficient e^-_{aq} scavengers) to the aerated solution, resulted in no increase in the observed second-order rate for pH > 3. The decay rate was independent of pH over the range 1.0 - 5.3 in such cases. The situation was more complicated for the analogous diene and tetramine systems. Such an addition of e^-_{aq} scavenger did eliminate the faster second-order reaction above pH 3 but replacement by a first-order process was apparent. This aspect is dicussed later in section VII 1. The absence of dependences on [Ni(II)L] and $[Br^-]$ are expected for a reaction between Ni(III)L and the superoxy radical.

Using the molar absorbance values determined in the pulse radiolysis study for the three tervalent complexes, values of the second-order specific rate constants for the $Ni(III)L + O_2^-$ reactions were estimated in phosphate buffered solution at pH 6.2.

complex	ε_{366} $(M^{-1}cm^{-1})$	$\frac{k}{\varepsilon l}$ (sec^{-1})	k_{2nd} $(M^{-1}sec^{-1})$
tam	7.8×10^3	2.5×10^4	2.0×10^9
di	6.2×10^3	2.6×10^4	1.6×10^9
tet	3.8×10^3	2.5×10^4	1.0×10^9

These second-order rate constants are similar in value to those used in sections III 1.4, 2.5 in the program PHRATE, where estimates of $k\ (Ni(III)L + O_2^-) : k\ (Ni(III)L + HO_2)$ were determined.

3.3 The observed second-order Ni(III)L decay at 366nm at pH 1.0 was the same in solutions where the precursor Br_2^- production was via photolysis of;

Br_3^- : 50μM Br_2

$FeBr^{2+}$: 0.5mM Fe^{3+}

$Co(NH_3)_5Br^{2+}$: 0.1mM

N_2O saturated Br^- solution

for constant values of [Ni(II)L] (20μM) and [Br^-] (0.1M). The decay was independent of [Br_2] over a large range, and of [Fe^{3+}] and [$Co(NH_3)_5Br^{2+}$] over smaller ranges. (The complex yields varied with the means of Br^- production in the range 2 - 15μM). The observed dependences of the rate on [Br^-] and [Ni(II)L] were independent of the means of Br_2^- photochemical production.

The decay rate dependencies of each tervalent complex on [Br^-] were determined for flashed solutions containing 20μM Ni(II)L and 0.1mM $Co(NH_3)_5Br^{2+}$ at pH 1.0 and constant ionic strength of 0.4M. The actual magnitude and nature of the [Br^-] dependence differed for the three complexes. The observed value of $k/\varepsilon l$ for the tetene complex was almost linear in the region 0.02 - 0.15M [Br^-] with a levelling-off above and below this region. The analogous plot for the tam complex was essentially linear below 0.01M, having a pronounced level-off of rate above this value. The diene system showed characteristics similar to the tetene decay dependence, being essentially linear in the 0.01 - 0.20M region. The actual rate increases for an increase in [Br^-] from 0.01 - 0.10M were;

complex	$\frac{\text{Rate (0.10M)}}{\text{Rate (0.01M)}}$
tet	25
di	15
tam	4.2

The significant differences between the tetene and tetramine rate dependences occurred in the $[Br^-]$ region below about 0.05M. The plots of $k/\varepsilon l$ versus $[Br^-]$ for these complexes in this region are shown in figure V 3.3a. The difference in rate dependence on $[Br^-]$, particularly obvious in this region, provides the key to the mechanism of the second-order decay for the Br^- system.

The decay rate dependence of the tervalent macrocycle on the [Ni(II)L] for the diene is shown in figure V 3.3b, for flashed solutions containing 0.1M Br^-, 0.1mM $Co(NH_3)_5Br^{2+}$ at pH 1.0. For both the di and tam complexes the observed rate at 10μM Ni(II)L was 3.6 times greater than that at 100μM. The rate levelled-off for [Ni(II)L]>100μM. The Ni(III) tet decay was independent of [Ni(II)tet] over the same range.

The dependences of the transient decay rates on [Ni(II)L] and $[Br^-]$ in this system are independent of each other, and are not complementary effects as in the case of [Ni(II)L] and $[H_2O_2]$ in sections III 1.3, 2.5, 3.3. This is obvious for tetene, and is confirmed for the diene in figure V 3.3c, where quite different plots were obtained for $k/\varepsilon l$ versus $[Br^-]/[Ni(II)di]$ data determined by holding one concentration constant, while changing the other.

3.4 The apparent trend of bromide anion catalysis of the second-order decay was investigated further. The addition of either 1mM N_3^-

FIGURE V 3.3a

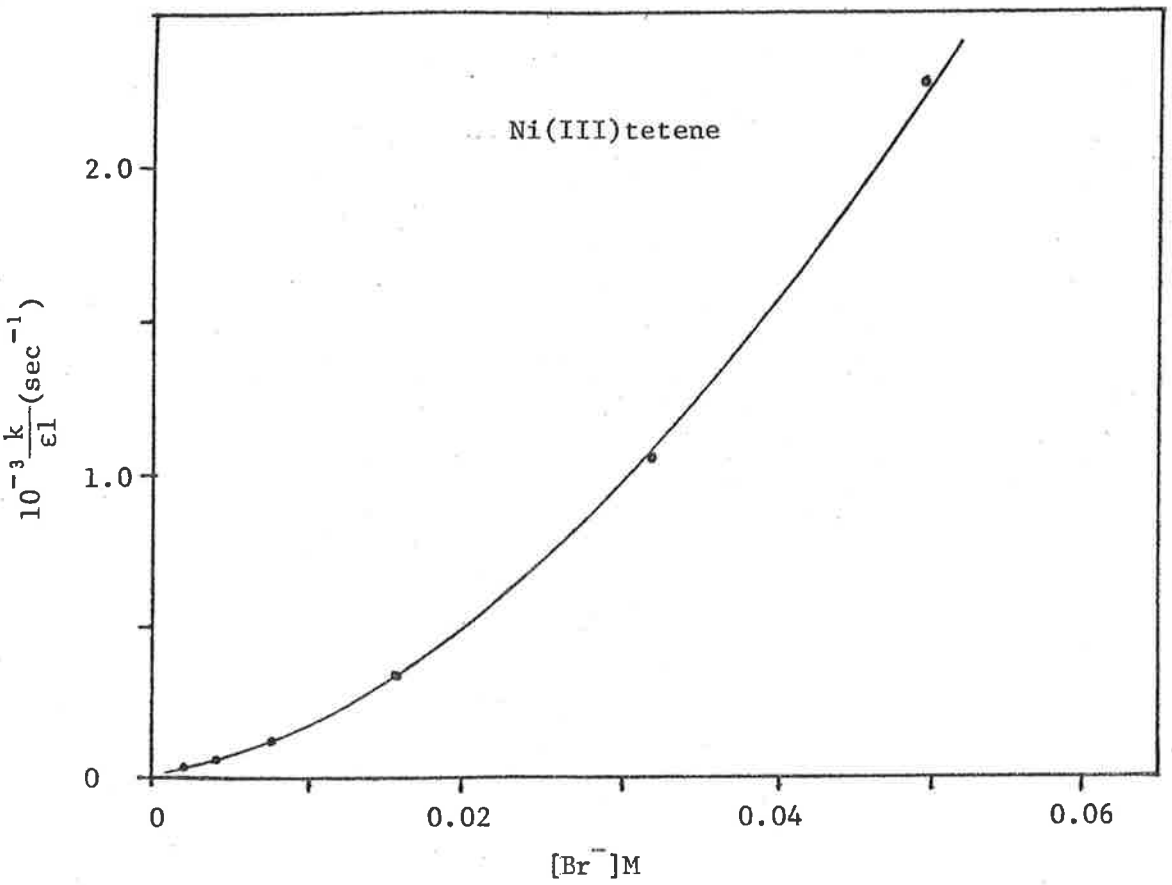
Ni(III)tetene
2.0
1.0
0
$10^{-3}\frac{k}{\varepsilon l}(sec^{-1})$
0
0.02
0.04
0.06
$[Br^-]M$

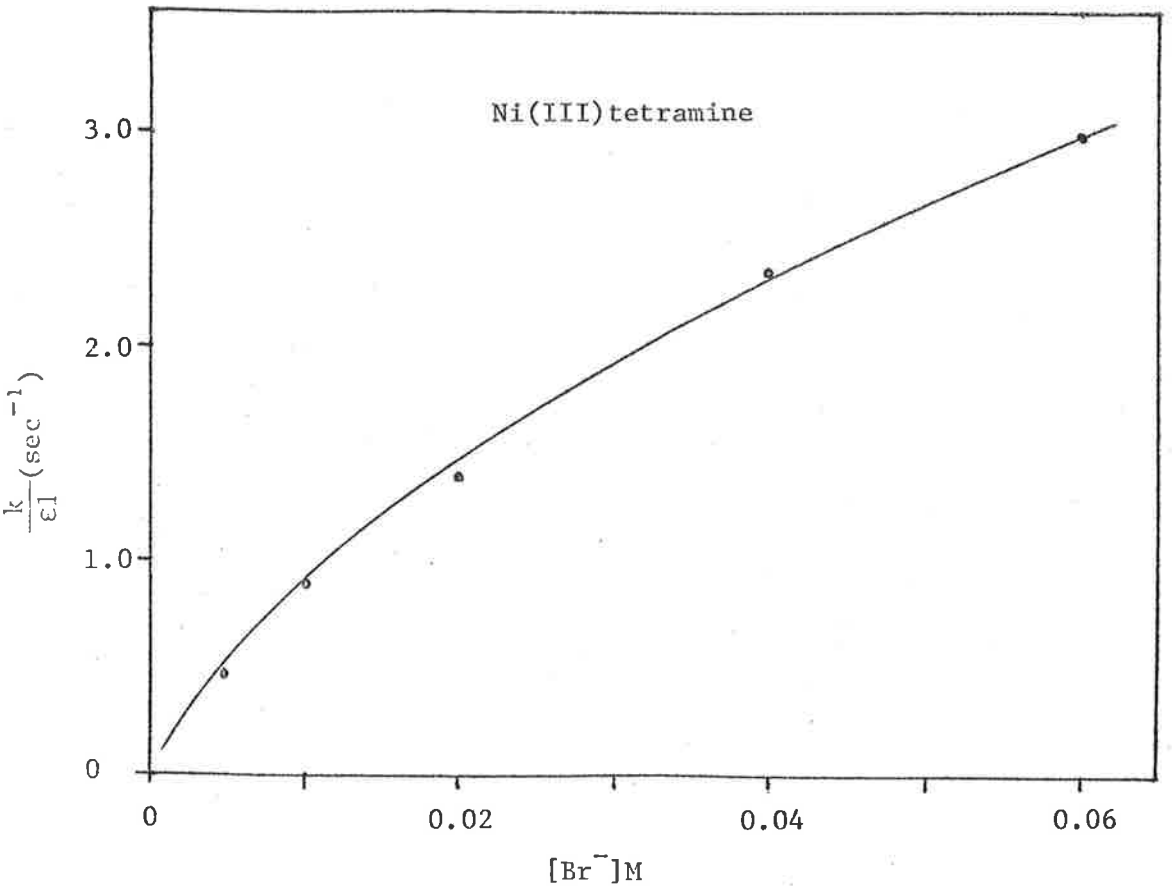
Ni(III)tetramine
3.0
2.0
1.0
0
$\frac{k}{\varepsilon l}(sec^{-1})$
0
0.02
0.04
0.06
$[Br^-]M$

FIGURE V 3.3b

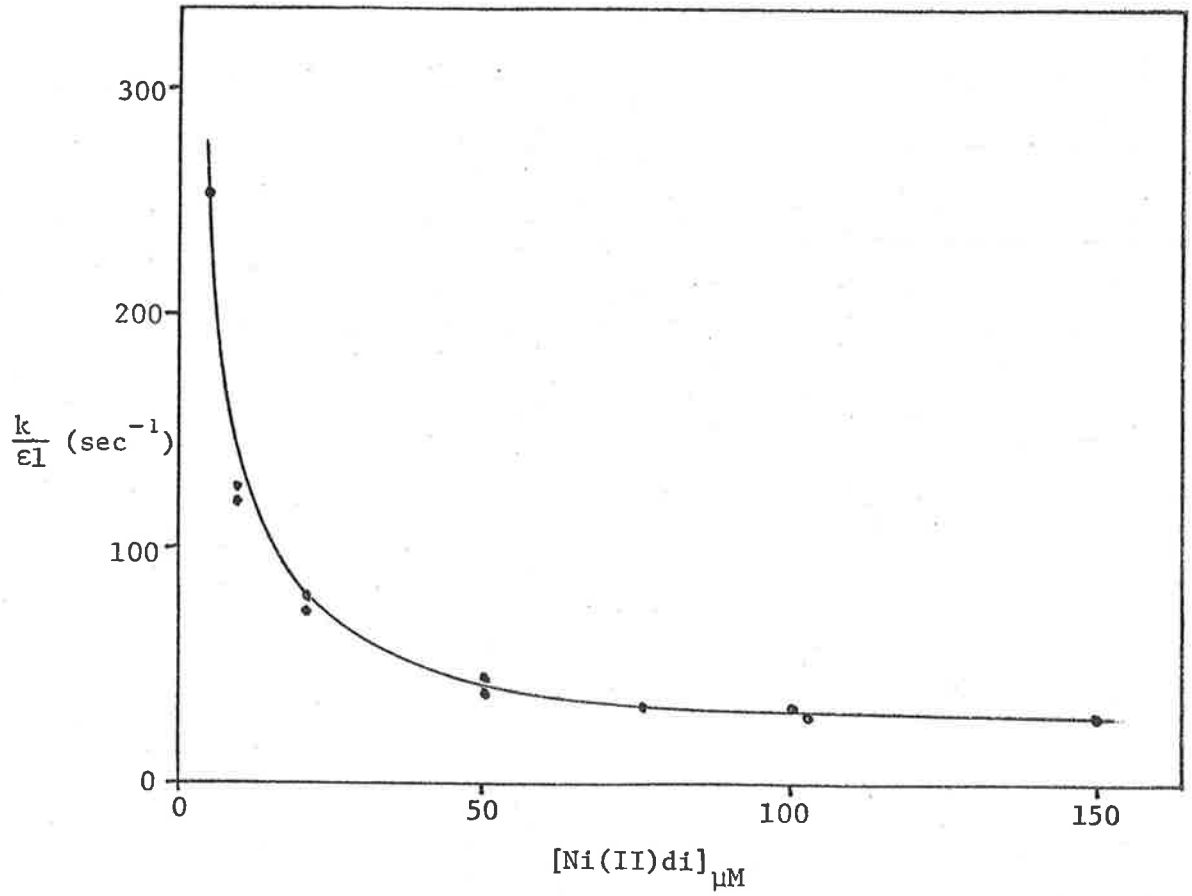

FIGURE V 3.3c

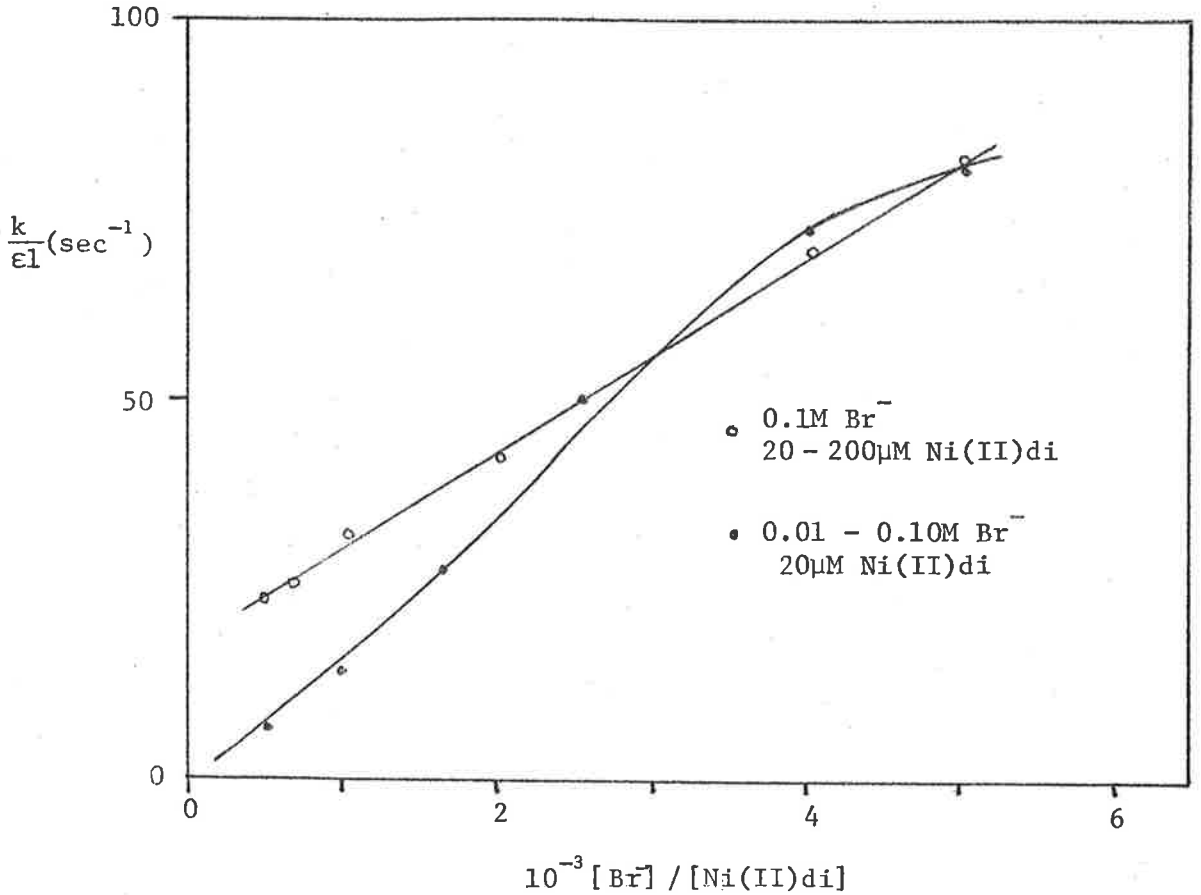

or SCN^- to the acidic solutions containing 20μM Ni(II)L and 0.1M Br^- resulted in significant increases in the observed transient decay rate at 366nm. Under these conditions, the flash is absorbed almost totally by the Br^-_{aq}, so that

$$Br^-_{aq} \xrightarrow{h\nu} Br^{\bullet} + e^-_{aq}$$

is still the primary photolytical act. It was observed that the presence of 1mM SCN^- considerably reduced the complex transient yield. This is presumed to be due to $BrSCN^-$ radical formation in competition with the usual Br_2^- formation;

viz. $Br^{\bullet} + Br^- \rightleftharpoons Br_2^-$

$Br^{\bullet} + SCN^- \rightleftharpoons BrSCN^-$

If the mixed radical is not as efficient an oxidant as the Br_2^-, (58) reduced tervalent yield may result. As shown in section VIII 1.2, the rate of reaction of $(SCN)_2^-$ with Ni(II)L is considerably less than that of Br_2^-. The actual rate increase corresponding to the addition of the pseudo-halides (1mM) to the 0.1M Br^- solutions at pH 2.0 is shown below, relative to the Br^- catalyzed reaction,

Ni(III)L	N_3^-	SCN^-
tam	6.1	2.3
di	1.6	8.4
tet	1.1	11.2

The addition of 1mM $SO_4^=$ to the tam system, considerably reduced the observed decay rate. Larger concentrations of added $SO_4^=$ were needed to show significant reductions of the di and tet decay rates. (These effects were not studied quantitatively).

3.5 The spectral and kinetic evidence obtained for the tervalent

complexes in Br^- solution suggests the possibility for an interaction between the Ni(III)L species and the anion. The observable effects of such an interaction decrease in the order tetene>diene>tetramine. To support the possibility of anion interaction with the complexes, the spectral effects of anion addition to the bivalent complexes were investigated. The UV-visible spectra of the three Ni(II)L complexes in aqueous solution were compared with those in the presence of 0.5M X^{n-}, where X^{n-} = SCN^-, Br^-, Cl^-, F^-, $SO_4^=$, using a 0.5M X^{n-} solution as a blank. The organic chromophore region of the tet and di complexes was observed as well as the d-d visible bands for 0.2mM solutions of the three complexes.

As shown in figure V 3.5, there was a significant spectral difference for the tetene complex due to the presence of SCN^-, less for Br^-, and no observable difference for Cl^-, F^- and $SO_4^=$. The interaction of the anion caused a fuller absorption in the low energy side of both peaks for the SCN^- and Br^- solutions. This spectral effect was less prominent for the diene complex and almost negligible for the tetramine. (The tam was somewhat insoluble in the 0.5M SCN^- solution).

3.6 The assumption of a complex formation between the tervalent macrocycles and Br^- enables the second-order decay mode in acidic solution to be analysed in terms of the proposed mechanism:

$$Ni(III)L + Br^- \underset{}{\overset{K_1}{\rightleftharpoons}} Ni(III)L.Br^-$$

then

(i) $$Ni(III)L.Br^- + Ni(III)L.Br^- \underset{k_{-2}}{\overset{k_2}{\rightleftharpoons}} Ni(II)L + NiL^{4+}$$

$$+2\ Br^- \downarrow k_3$$

products

FIGURE V 3.5

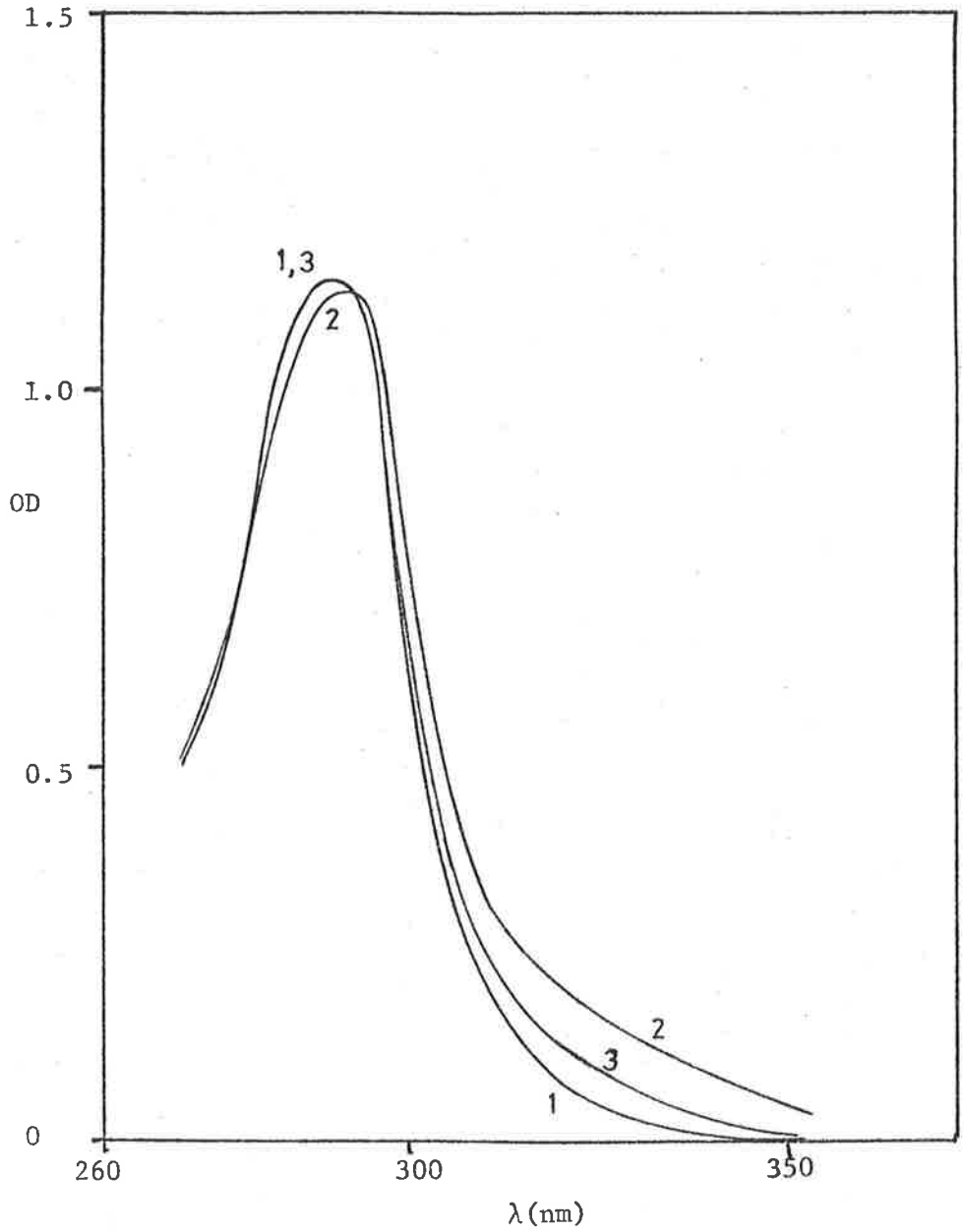

0.2mM Ni(II)tetene in

1 : water only

2 : 0.5M SCN^-

3 : 0.5M Br^-

or (ii)

$$Ni(III)L{\cdot}Br^- + Ni(III)L \underset{k_{-2}}{\overset{k_2}{\rightleftharpoons}} Ni(II)L + NiL^{4+} + Br^-$$

$$NiL^{4+} \xrightarrow{k_3} \text{products}$$

The first step involves a fast equilibrium, producing the $Ni(III)L{\cdot}Br^-$ complex. The next step can occur in two ways, involving the encounter of one complexed intermediate (i) with another, or (ii) with an uncomplexed entity, to yield the precursor complex to the activated state. After single electron transfer, the bivalent macrocycle and an unstable species, designated NiL^{4+} are produced. This short-lived product, which is two electrons short of obtaining a stable state, is presumed capable of back reaction with Ni(II)L, Competing with the back reaction is the decay of NiL^{4+} to stable products.

From the initial equilibrium, we have for the condition

$$[Br^-]_o \quad >> \quad [Ni(III)L]_o$$

$$[Ni(II)L{\cdot}Br^-] \quad = \quad K_1[Ni(III)L]\ [Br^-]_o$$

and $$[Ni(III)L]_o \quad = \quad [Ni(III)L] + [Ni(III)L{\cdot}Br^-]$$

where the non-subscripted concentrations are the equilibrium values. From these euqations,

$$[Ni(III)L{\cdot}Br^-] \quad = \quad \frac{K_1[Ni(III)L]_o\ [Br^-]_o}{1 + K_1[Br^-]_o}$$

At an observation wavelength where both Ni(III)L and $Ni(III)L{\cdot}Br^-$ absorb, the effective molar absorbance of the equilibrium mixture is given by

$$\varepsilon_{III} = \frac{\varepsilon(Ni(III)L + K_1[Br^-]_o\varepsilon(Ni(III)L{\cdot}Br^-)}{1 + K_1[Br^-]_o}$$

The two possibilities of the bimolecular encounter of the Ni(III)L species are considered separately. In the first scheme it is considered that K_1 is large enough for the major equilibrium species to be in the complexed form. The rate equation for the decay of the Ni(III)-L.Br^- complex is given by

$$-d\frac{[Ni(III)L.Br^-]}{dt} = k_2[Ni(III)L.Br^-]^2 - k_{-2}[Ni(II)L][NiL^{4+}]$$

Considering steady-state conditions for the NiL^{4+},

$$[NiL^{4+}] = \frac{k_2[Ni(III)L.Br^-]^2}{k_{-2}[Ni(II)L] + k_3}$$

Hence, the observed rate of absorbance decay is given by

$$-\frac{dOD}{dt} = \varepsilon_{III}\, k_2[Ni(III)L]_o^2 \left[\frac{K_1[Br^-]_o}{1 + K_1[Br^-]_o}\right]^2 \left[1 - \frac{k_2[Ni(II)L]}{k_3 + k_2[Ni(II)L]}\right]$$

In the alternative scheme, K_1 is considered to be smaller, so that most of tervalent intermediate is in the uncomplexed form. Hence.

$$-\frac{d[Ni(III)L]}{dt} = k_2[Ni(III)L][Ni(III)L.Br^-] - k_{-2}[Ni(II)L][NiL^{4+}]$$

Using the same derivations as in scheme (i), the rate of absorbance decay is given by

$$-\frac{dOD}{dt} = \varepsilon_{III}\, k_2[Ni(III)L]_o^2 \frac{K_1[Br^-]_o}{1 + K_1[Br^-]_o} \left[1 - \frac{k_2[Ni(II)L]}{k_3 + k_2[Ni(II)L]}\right]$$

Except for the nature of the dependence on $[Br^-]$, the kinetic equations for the rate of absorbance decay for both schemes are identical. For the larger K_1, the rate dependence is of the form,

$$\text{Rate} = A\left[\frac{K_1[Br^-]_o}{1 + K_1[Br^-]_o}\right]^2$$

while for the smaller K_1,

$$\text{Rate} = A\frac{K_1[Br^-]_o}{1 + K_1[Br^-]_o}$$

where A is a constant.

The experimental rate dependence on $[Br^-]$ data for the tetene and tetramine were fitted to the derived rate equations. For the larger K_1, it was considered that at low $[Br^-]$, $(1 + K_1[Br^-]_o)^2 \simeq 1$, so that,

$$\text{Rate} = \frac{k}{\varepsilon 1} = A\,(K_1[Br^-]_o)^2$$

or $\log(\frac{k}{\varepsilon 1}) = \text{constant} + 2\log[Br^-]_o$

The plot of $\log(\frac{k}{\varepsilon 1})$ versus $\log[Br^-]_o$ for the tetene data was linear in the region <16mM in Br^-, having a slope = 1.73 close to the expected value of 2.0. (figure V 3.6a) This plot was non-linear for the tam data. The intercept value was a function of K_1 which could not be determined in the absence of the other parameters in the constant. In scheme (ii), the rate expression can be re-arranged thus;

$$\frac{1}{\text{Rate}} = \frac{\varepsilon 1}{k} = \text{constant}\,(1 + \frac{1}{K_1[Br^-]_o})$$

A plot of $\varepsilon 1/k$ versus $1/[Br^-]_o$ for the tam rate data was linear over the studied $[Br^-]$ range, having an intercept/slope value equal to K_1 of $14M^{-1}$ (figure V 3.6b). Such a plot of the tetene data was quite non-linear.

The diene data fitted neither type of plot well, but was better fitted to the log plot. The kinetic evidence therefore suggests overall that the tervalent tetene complex decays via scheme (i) while the tetramine decays via scheme (ii). The diene is considered to decay

FIGURE V 3.6a

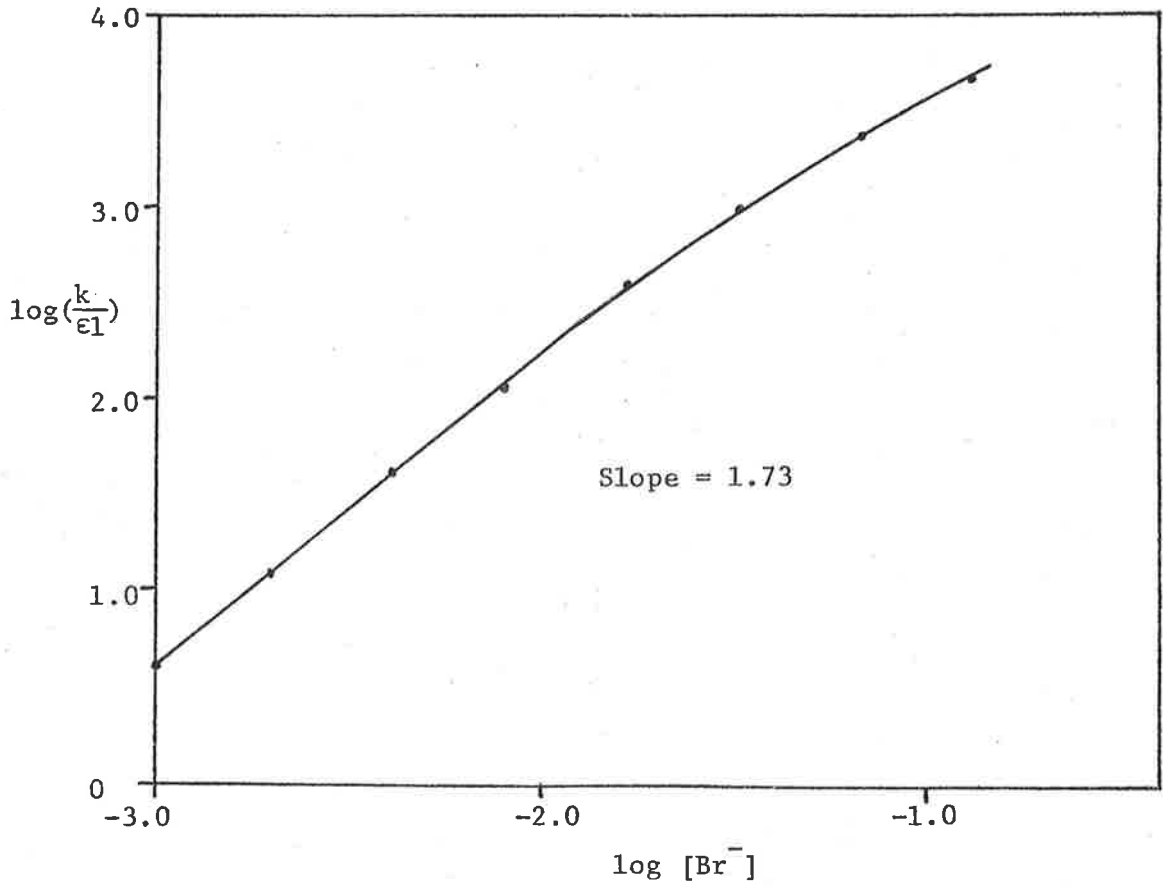

FIGURE V 3.6b

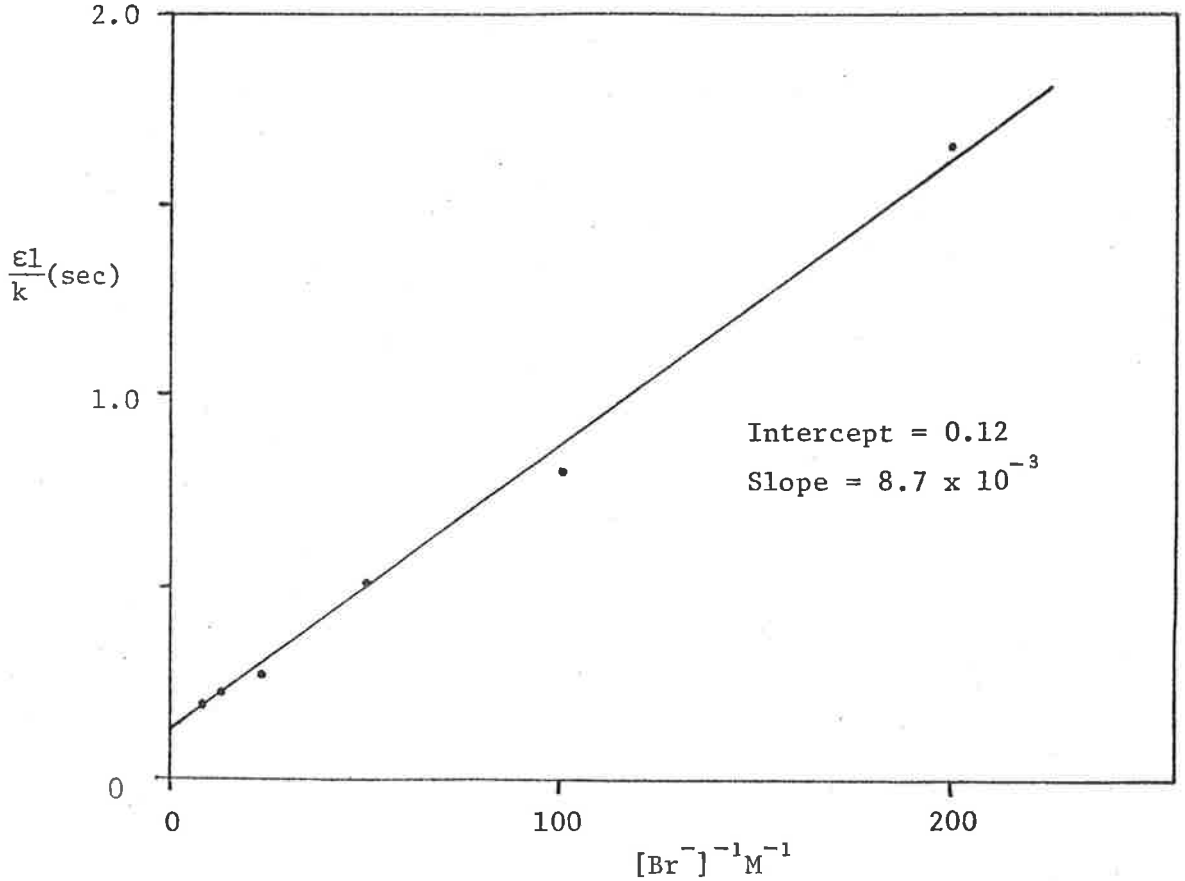

mainly by (i), but with a significant proportion of (ii) occurring also.

Recalling the expression for the effective molar absorbance in these systems,

viz. $$\varepsilon_{III} = \frac{\varepsilon(Ni(III)L + K_1[Br^-]_o\ \varepsilon(Ni(III)L.Br^-}{1 + K_1[Br^-]_o}$$

the transient spectral properties can be understood. With the larger value of K_1, as for tetene,

$$\varepsilon_{III} \simeq \varepsilon(Ni(III)L.Br^-)$$

and the spectrum of the Br^--complexed intermediate is observed. For the low K_1, as for the tetramine,

$$\varepsilon_{III} \simeq \varepsilon(Ni(III)tam)$$

and no spectral difference due to the presence of Br^- in solution is observed. The K_1 for the diene complex is considered to be mid-range between the two extremes.

The negative dependences of the tervalent complex decay rates on [Ni(II)L] are explained in the derived kinetic equations. For the di and tam complexes, $k_3 \sim k_{-2}[Ni(II)L]$ for low values of [Ni(II)L]. However, at high [Ni(II)L], the term $k_{-2}[Ni(II)L]$ becomes considerably $>k_3$ and the rate of decay consequently levels-off. For the tetene system, $k_3 >> k_{-2}[Ni(II)L]$ over the studied [Ni(II)tet] range, resulting in the observed independence of the decay rate on this concentration.

3.7 The observed transient decay at 366nm of the Ni(III)tam complex in Br^- solution at pH 1.0 and 5.3 have been explained by the previous schemes. In the intervening pH region the observed absorbance changes with time in the absence of e^-_{aq} scavengers in solution were unusual. In

figure V 3.7a is shown a plot of the difference between the absorbances measured 100μsec and 50msec after the flash over the pH range 1.0 - 5.3 of a solution containing 20μM Ni(II)tam and 0.1M Br^-. The absorbance difference at each pH was normalized by division by the 100μsec absorption value. Three pH regions are apparent from this figure. In the region ≳4, more than 90% transient decay had occurred within the time interval of absorbance observations. Between pH 4 - 2, the fraction of transient decay completed in this time fell rapidly to zero at pH ≃ 2.1. In a 0.3M Br^- solution, the pH at which no observable decay was apparent within the specified time was 2.6, as shown also in figure V 3.7a. Below pH 2.1 a transient formation was apparent for which the yield of transient product levelled-off at pH 1.0 within the specified time interval.

The actual kinetic behaviour of the system over the studied pH range is shown in figure V 3.7b for a solution 0.1M in Br^-. The two time intervals covered in the figure are (1) 100μsec - 50msec and (2) 50msec - 20sec. The overall interval covered accounts for the complete transient decay in the system and as shown, the final absorbance returned to the initial value before the flash. In time interval (1), the percentage of the overall decay proceeding via the second-order process Ni(III)tam + 'HO_2' within 50msec of the flash decreased from >90% for pH >4, to zero at pH ≃ 2.1. Second-order kinetics were only approximated for the measurable decay process in the region below pH 4. Below pH ~ 2, a first-order formation was apparent. This process was found to be pseudo-first order in [Ni(II)tam] having a specific rate constant (determined from the slope of a plot of k_{obs} versus [Ni(II)tam]) of 1.1 (±0.2) x $10^7 M^{-1} sec^{-1}$. In a 0.3M Br^- solution the formation process was faster, having a specific rate of 2.4 (±0.3) x $10^7 M^{-1} sec^{-1}$. The residual absorp-

FIGURE V 3.7a

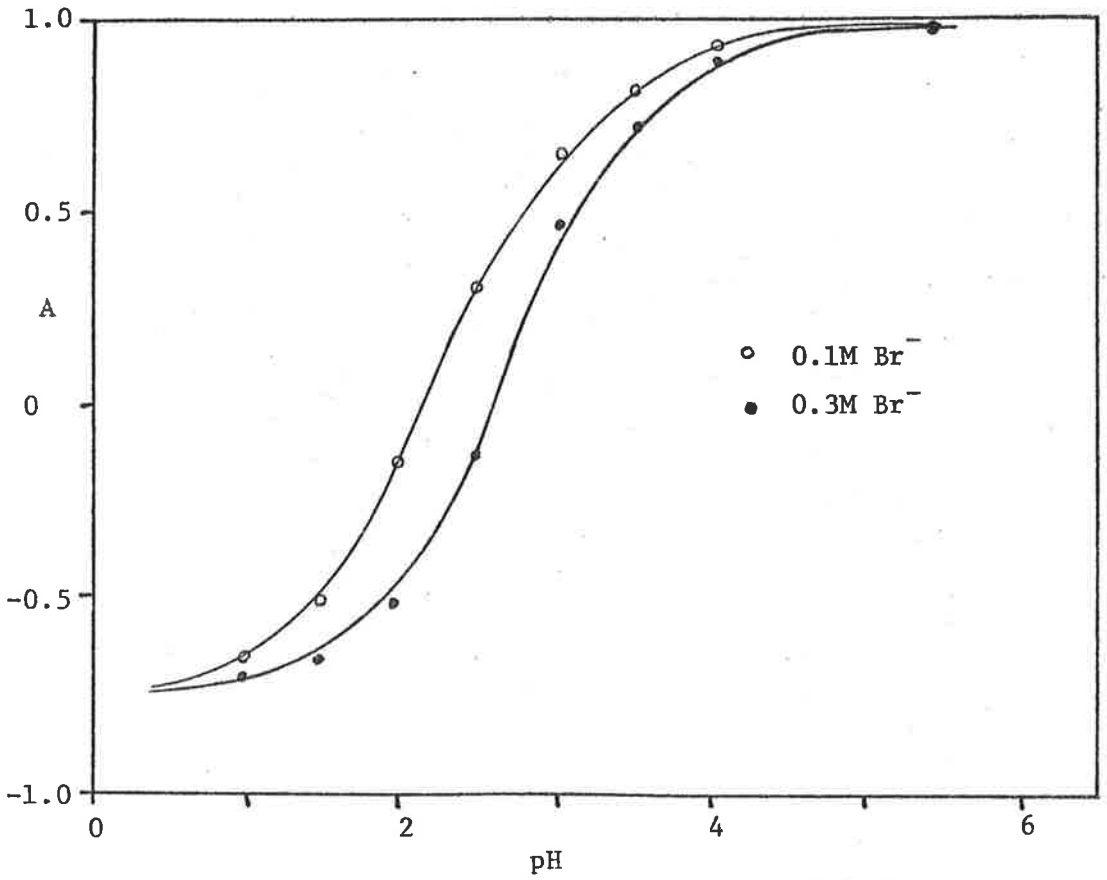

FIGURE V 3.7c

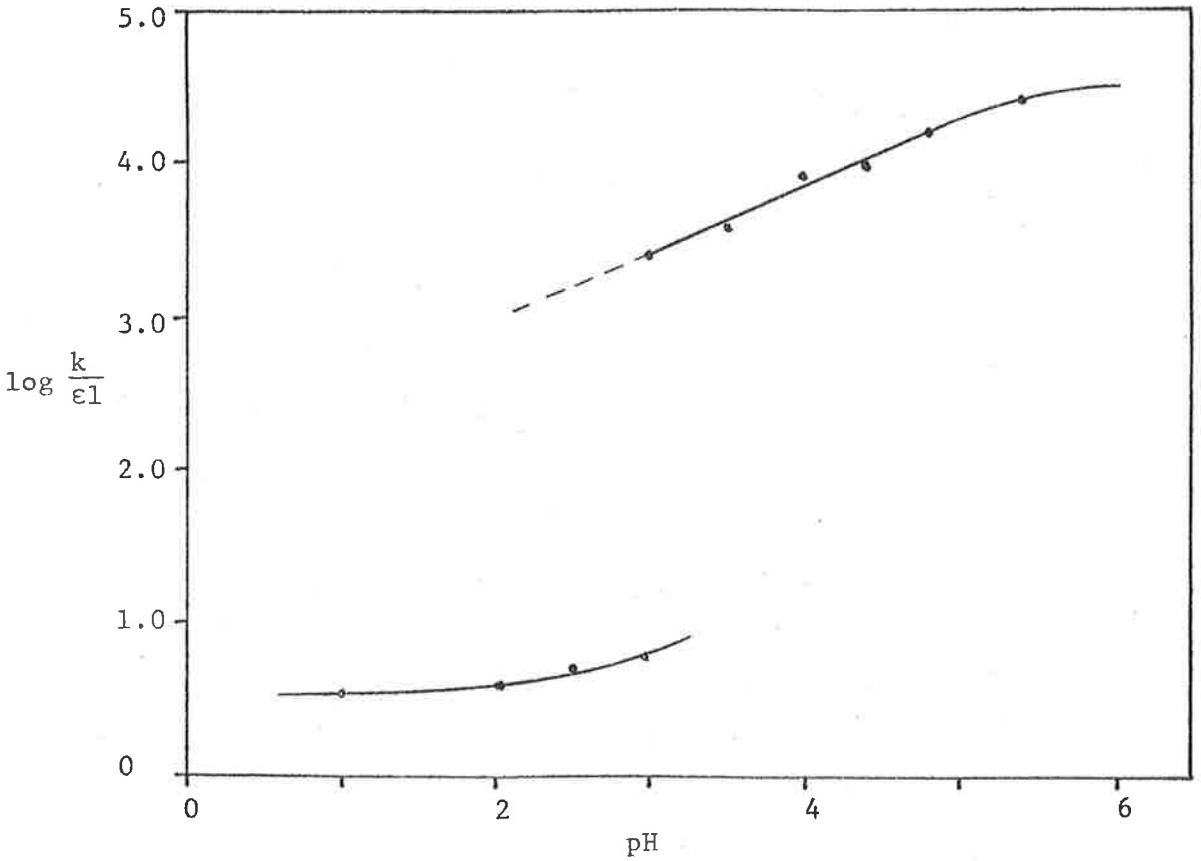

FIGURE V 3.7b

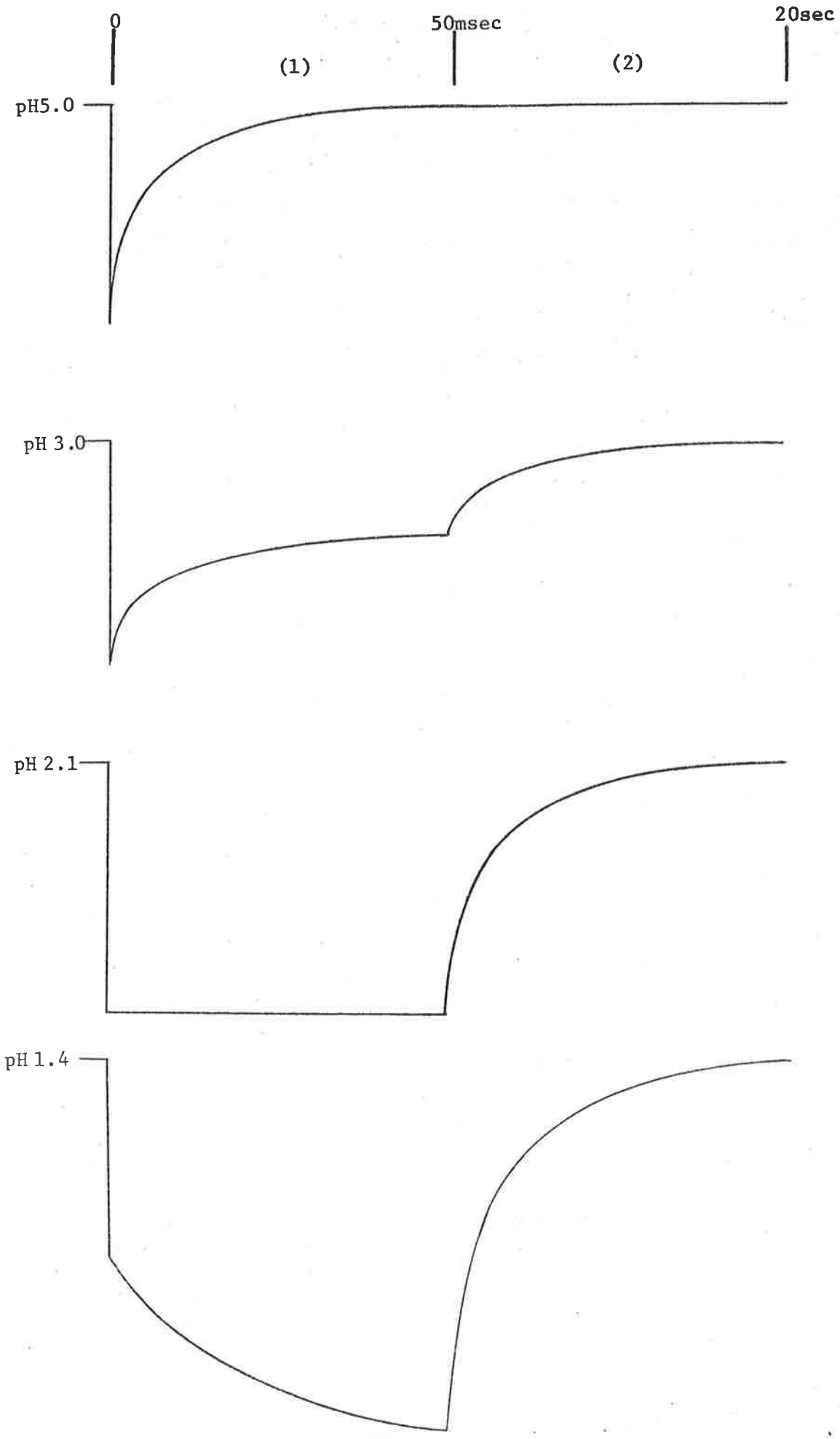

tion observable after 50msec in the studied pH range decayed by the Br^--assisted second-order process. The rate of this reaction was almost pH independent in the measured region 1.0 - 3.0. The observed second-order rates ($\frac{k}{\epsilon l}$) of both the transient decay processes are shown in figure V 3.7c.

The transient spectra were measured at pH 3.0, 1msec and 0.1sec after the flash. These spectra were identical as were those measured 100μsec and 50msec after the flash in a solution of pH 1.0. The spectra were all characteristic of Ni(III)tam which suggests that this complex is involved in both the fast and slow decay processes and is also produced in the formation process.

The considerable resemblance between this system and that discussed earlier in section III 3.5 strongly suggests that a similar mechanism is operative here. However a significant difference arises between the two systems when the pH at which the Ni(II)L + HO_2 reaction becomes apparent is considered. Whereas this process is obvious only below pH 0.4 in the absence of Br^-, it is observable below pH 2.1 in 0.1M Br^-, and below pH 2.6 in 0.3M Br^- solution. The actual rate of this reaction was observed to increase (almost linearly) with $[Br^-]$. These results suggest that Br^- is capable of more efficient catalysis of the Ni(II)tam + HO_2 reaction than is high acid concentration. The possible mechanism for this reaction is;

$$\text{Ni(II)L} + HO_2 \underset{}{\overset{k_f}{\rightleftharpoons}} \text{Ni(III)}.HO_2^- \underset{K_a}{\overset{H^+}{\rightleftharpoons}} \text{Ni(III)L}.H_2O_2$$

$$K_E \Big\| \; Br^-, H^+$$

$$\text{Ni(III)L}.Br^- + H_2O_2$$

for which the exchange equilibrium with Br^- (K_E) is a more efficient means of transfer to tervalent product in mildly acidic solution, than the acid-equilibrium (K_a) path. The K_E also has an acid dependence. Greater ease of anion exchange occurs in more acidic solution where H^+ stabilizes the released HO_2^- species.

Considering the Ni(III)tam decay in a flashed aerated solution containing only Ni(III)tam and Br^-, the overall mechanism takes the following form involving previously established reaction steps:

(A) $Ni(III)tam + Br^- \underset{\text{fast}}{\overset{K_1}{\rightleftharpoons}} Ni(III)tam.Br^-$ (1)

$Ni(III)tam\ (.Br^-) + HO_2 \xrightarrow{k_2} \text{products}$ (2)

$Ni(III)tam\ .\ Br^- + Ni(III)tam \xrightarrow{k_3} \text{products}$ (3)

(B) $Ni(II)tam + HO_2 \xrightarrow{k_4} Ni(III)tam.HO_2^-$

Br^-, H^+ ⇓ K_E, fast

(A) ⟵ $Ni(III)tam.Br^-$ (+ H_2O_2) (4)

At 366nm, where only the tervalent intermediates absorb, the rate expression takes the form,

$$-\frac{d\,[Ni(III)]}{dt} = k_3[Ni(III)L.Br^-]\,[Ni(III)L] + k_2[Ni(III)L]\,[HO_2] - k_4 K_E\,[Br^-]\,[Ni(II)L]\,[HO_2]$$

In this system, $[Ni(III)tam] \simeq [HO_2]$ after the flash.

At pH > 4, Rate (2) > Rate (4)

and >> Rate (3)

so that the Ni(III)tam + 'HO_2' reaction is observed. For pH 4 - 2 the Rate (4) term becomes steadily more comparable to Rate (2), with both Ni(III)L and Ni(II)L competing for the available HO_2 radicals. The residual tervalent species then decay via step (3). Below pH 2, Rate (4) > Rate (2); the HO_2 reacts more favourably with Ni(II)L than Ni(III)L, with the overall yield of Ni(III)L then decaying via step (3).

The same mechanism is considered to operate in the analogous diene system where unusual kinetic effects were noted in the pH region 1 - 2. The presence of HO_2 to account for these results was verified by the addition of 50μM Br_2 to the solution, Under these conditions, the observed second-order decay rate was almost independent of pH in the measured region 1 - 3; the initial fast decay in the pH region 1 - 2 was eliminated.

4. PRODUCT ANALYSES

4.1 The products of the anion-assisted second-order decay of the tervalent macrocycles were investigated, Due to the inherent low photochemical yields of the transient species in this technique (≳10μM), and the small total concentrations of Ni(II)L used (<0.1mM), extraction of primary product complex from solution was not attempted. Steady-state irradiation using either a low pressure mercury lamp or γ-radiolysis over appropriate periods was also undesirable, due to the very low transient concentrations (~10nM) inherent in these techniques. Analysis of the products of the second-order decay would be most unreliable in such a case, since other first-order modes of decay which are insiginficant at the much larger flash yields, may become dominant at the very low steady-state concentrations. Such first-order processes have been discussed in

section IV 3.2.

4.2 The normal mode of oxidation of the macrocyclic Schiff's base complexes is via oxidative dehydrogenation of the ligand, leading to the formation of coordinated imine functions. (This was discussed in Chapter I). The presence of the imine function in the trans series of these bivalent Ni macrocyclic complexes is readily detected in solutions of low concentration by UV spectrophotometry, since the imine chromophore band lies in the region 270 - 300nm having a molar absorbance $\sim 5 \times 10^3 M^{-1} cm^{-1}$. Solutions containing 40μM Ni(II)L, 0.1M Br^-, 0.5mM H_2O_2 at pH 1.0 were flashed eight times in succession. A total yield of at least around 40μM of Br_2^- could be expected from the multiple flashes. The UV spectra at wavelengths >250nm of these solutions were compared with the unflashed solutions.

For all three complexes the flashed solutions had a much stronger absorption in the 250 - 300nm region; this is shown for the tetene complex in figure V 4.2. The difference spectrum between the flashed and unflashed solutions is also shown. Addition of strong alkali solution to the stirred, flashed solution until the pH was ~7.5 resulted in the flashed spectrum returning to that of the unflashed solution. (Allowance for the small volume increase was made). The difference spectrum for a 20μM Ni(II)L solution had double the absorption in the 250 - 300nm region of the 40μM solutions.

The difference spectrum is identical with that of Br_3^- in this region. In solutions of neutral pH it is known that Br_3^- hydrolyses to the BrO^- species which does not absorb in this region.

FIGURE V 4.2

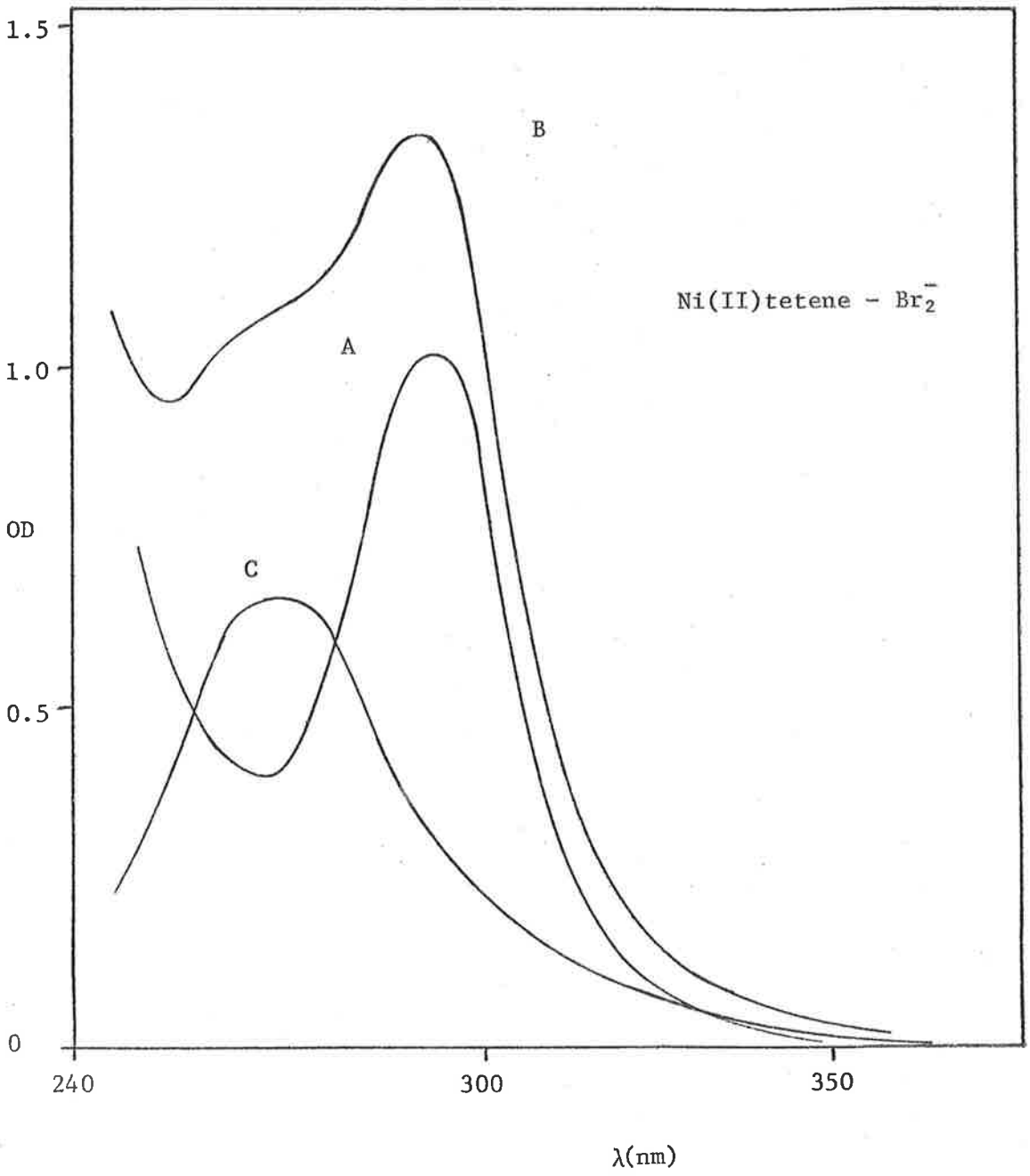

A : unflashed

B : flashed 8 times

C : difference

i.e. $Br_3^- + H_2O \longrightarrow BrO^- + 2Br^- + 2H^+$

The presence of the Br_3^- in flashed solutions is explained by the incomplete scavenging of all the photochemically produced Br_2^- by the Ni(II)L complexes after the flash. Competing with this reaction is the Br_2^- disproportionation, which yields Br_3^- as a product,

$$2Br_2^- \longrightarrow Br_3^- + Br^-$$

As expected a much larger residual absorption was produced when a solution without Ni(II)L was flashed. The yield of Br_3^- was about the same for the tet and di complexes, but less (about half) for the tam, for solutions containing 20μM Ni(II)L. This suggests that the rates of Ni(II)L + Br_2^- are similar for L = di and tet, with the tam rate being faster than both by a factor of about 2. The similarity of the reaction rate for di and tet was established in section V 2.1.

The spectral evidence here indicates that there is no difference between the original Ni(II) macrocycle and the product of the anion assisted second-order decay reaction. Of particular note was the absence of any observable imine absorption for the tam product spectrum. Further flashing (up to 12 times) failed to produce spectral evidence of imine formation with this ligand.

4.3 The spectrum and decay rate of the Ni(III)tet complex was the same in solutions containing 0.1mM Ni(II)tet, 0.1M Br^- and 1mM H_2O_2 at both pH 1.0 and natural pH. (The nature of the Ni(III)L decay changed over this pH range for the analogous di and tam systems; see section VII 1.1). The consistency of the tetene decay reaction over this pH range provided another means of product analysis for the second-order process.

The pH of an unbuffered solution initially at pH 5.6 was measured after multiple flashing; the pH was unchanged after 8 flashes. The primary ligh absorption in this system is mostly in the Br^-_{aq} CTTS band, with some absorption in the H_2O_2 UV band.

Hence,

$$Br^-_{aq} \xrightarrow[Br^-]{h\nu} Br_2^- + e^-_{aq}$$

$$H_2O_2 \xrightarrow{h\nu} 2\ OH$$

$$e^-_{aq} + H_2O_2 \longrightarrow OH + OH^-$$

$$OH + Br^- \xrightarrow[Br^-]{} Br_2^- + OH^-$$

$$Br_2^- + Ni(II)L \longrightarrow Ni(III)L + 2Br^-$$

For every Br_2^- radical produced, and therefore for every Ni(III)L species produced (if complete conversion is assumed), there is a stoichiometrically equivalent concentration of OH^- introduced into the solution. The constancy of the pH after the second-order decay suggests that one H^+ per Ni(III)L is introduced into the solution via the decay process. The same result was obtained in N_2O-saturated 0.1M Br^- solution containing 60μM Ni(II)tet. In this system, the e^-_{aq} produced by the flash is converted to OH^- by

$$N_2O + e^-_{aq} \xrightarrow{H_2O} N_2 + OH + OH^-.$$

As a further check, a solution containing 50μM Br_2 instead of N_2O was analysed. The initial pH of this solution was 4,82 (due to some Br_2 hydrolysis). After several flashes the pH of the solution fell to 4.64, indicating a significant introduction of acid into solution. This is expected since no OH^- is produced by the flash induced processes.

i.e. $Br_3^- \xrightarrow{h\nu} Br_2^- + Br^-$

$Br^-_{aq} \xrightarrow[Br^-]{h\nu} Br_2^- + e^-_{aq}$

$e^-_{aq} + Br_3^- \longrightarrow Br_2^- + Br^-$

4.3 The anion-assisted decay process therefore appears to be

$$Ni(III)tet + Ni(III)tet \xrightarrow{Br^-} Ni(II)tet + Ni(II)tet_{ox} + 2\,H^+$$

It is assumed that this process is occurring for the tetene in acidic solution also. Since all three Ni(IIIL) complexes decay by the Br^--assisted second-order reaction, differing only in rate, it is considered that acid is a product in the diene and tetramine analogues also.

5. Cu(II)DIENE, Br_2^-

The disporportionation of Br_2^- observed at 466nm for a 0,1M Br^- solution at pH 1.0 was found to be unchanged in the presence of 150μM Cu(II)di. As a result, the rate of Cu(II)di + Br_2^- may be presumed to be $\lesssim 10^8 M^{-1} sec^{-1}$.

VI BRIDGED ELECTRON TRANSFER

1. ELECTRON TRANSFER IN COMPLEXES

1.1 Electron-transfer between two metal centres can be catalyzed by the addition of anions, and it is recognized that oxidation-reductions involving metal ions and their complexes are of two main types; the so-called inner-sphere and outer-sphere mechanisms. The characteristics of these mechanisms have been discussed in several reviews and monographs.[157-165] The distinction between the two types of electron-transfer reaction lies in the nature of the interaction between the reacting species in the activated state prior to electron-transfer. The metal ions are connected by a common bridging group in inner-sphere reactions, while the coordination shells of the metal ions remain intact during outer-sphere reactions.

1.2 Several steps are involved in the anion-assisted electron-transfer mechanism in going from the initial to the final state.[162] Consider the reaction of complexes A and B in the presence of anion X. The first step involves the formation of a complex between the anion and one of the reactant complexes (the nature of this interaction is quite variable). This is followed by the formation from the reactant pair (say AX and B) of the precursor complex (AXB). No chemical bonds are made or broken in outer sphere reactions, whereas substitution is involved in inner-sphere reactions. Re-organization of the precursor complex to form the activated complex $(AXB)^{\ddagger}$, occurs in the next step. In this process, the inner-coordination shells of the reactants, as well as the polarization of the surrounding medium, adjust to the configuration appropriate to the transition state. The electron-transfer may, and

usually does, take place during the latter stages of the re-organization of the precursor complex. Following the electron-transfer is the de-activation of the activated complex to form the successor complex ($A^{-}XB^{+}$). While the electron distribution in the precursor complex corresponds to that of the reactants, in the successor complex, it corresponds to the products of the reaction. The next step involves the dissociation of the successor complex into the product pair (A^{-} and BX^{+}), while dissociation of these products to yield the final state of the system occurs in the last step.

Under conditions where one of the metal centres undergoes ligand substitution more quickly than the electron-transfer, the inner-sphere mechanism is possible. The rates of water exchange in the primary coordination sphere of many transition metal ions are known.[166] Since transfer of the bridging group from oxidizing agent to reducing agent frequently occurs in inner-sphere reactions, the immediate products of this type of mechanism are usually different from those of outer-sphere reactions. Consequently, valuable mechanistic information can be obtained from the identities of the primary products of a reaction. Since the net effect of an inner-sphere exchange is the transfer of the bridging group, they are also referred to as atom-transfer reactions.

Many complexes undergo electron-transfer more rapidly than they undergo ligand substitution. Even when one of the reactant complexes is substitution labile, if the other complex does not offer a suitable site to engage the metal centre of the labile complex, reaction by an outer-sphere activated complex will be favoured. It is considered that neither reactant complex labilizes the other for substitution. When the reactants or products undergo substitution relatively rapidly, distinction

between the reaction mechanisms becomes difficult.

Where primary bonds are affected in the course of a reaction, as in the case of the formation of the bridged activated complex for inner-sphere reactions, the geometry of the activated state is rather well defined. However, due to the variability of the interactions which distinguish one configuration from another (eg. the number of water molecules interposed between the reactant complexes) it is difficult to define the geometry of an outer-sphere activated complex.

1.3 According to the Franck-Condon principle, internuclear distances and nuclear velocities do not change during an electronic transition. Since the equilibrium configuration of the inner coordination shell of a metal complex, as well as the polarization of the surrounding medium, depend on the charge of the central metal ion, the equilibrium configurations of the coordination shells of the reactants and products of an electron-transfer will be different. If electron-transfer were to occur between reactant complexes without prior re-organization of their coordination shells, the products would be formed in highly distorted configurations. Energy conservation requires that the primary coordination shells of the reactant complexes (including the polarization of solvent medium) must rearrange to some non-equilibrium configuration before the electron-transfer takes place. When this occurs by an outer-sphere mechanism, the bond distortions at the two metal centres are not coupled. The improbability that the uncoupled events take place simultaneously when the metal centres are close enough for electron-transfer to occur, is the primary limit to the rate of the electron-transfer. In an inner-sphere mechamism, the distortions of the two metal centres are coupled through the bridging group.

1.4 Expressions for the free energy of activation for outer-sphere electron-transfer reactions, in which the potential energy changes in a continuous manner along the reaction coordinate, have been derived by Marcus[167-169] and Hush.[170] The theoretical treatment shows that the barrier to electron-transfer is made up of two parts. Difference in reaction rates may arise from differences in either or both of these contributions. The so-called intrinsic barrier is associated with the reorganization energy of reactant coordination shells and of the surrounding solvent prior to the actual electron-transfer. The thermodynamic contribution is associated with the overall free energy change for the reaction. If the reaction is electron exchange ΔG^{o} for the reaction is zero, and only intrinsic contributions are operative. When net chemical change occurs $\Delta G^{o}<0$, and thermodynamic contributions to the activation barrier may be important. (Strictly, it is the value of ΔG^{o}_{r} at a distance r between the centres of the reactants in the activated complex, that is relevant to the thermodynamic contribution to the barrier.[160])

Provided the interaction between participent complex redox orbitals is neither too large nor too small, and the differences in the stabilities of the precursor complexes may be neglected, the theoretical treatment relates the rates of exchange reactions ($\Delta G^{o}=0$) to the rates of electron-transfer reactions accompanied by a net chemical change ($\Delta G^{o}<0$). This so-called Marcus cross-relation is (provided G^{o} is not too negative),

$$k_{12} = (k_{11}\ k_{22}\ K_{12})^{\frac{1}{2}}$$

where k_{12} and K_{12} ($\alpha\Delta G^{o}$) are the rate and equilibrium constants for an electron-transfer reaction involving net chemical change, and k_{11}, k_{22} are the corresponding self exchange rate constants.[168] This relationship has proved useful in rationalizing the rates of a variety of outer-

sphere electron-transfer reactions. The theory has also been applied to inner-sphere reaction series in which bridging ligands are kept constant, but non-bridging ligands are altered.[160, 164] Such relationships, however, appear to be much less generally applicable to comparisons of rates of inner-sphere reactions in which the bridging substituent changes.

Exceptions to the correlation have been noted,[171,172] but they are not so numerous as to disqualify the correlation as a basis for normal behaviour. Significant deviations from normal behaviour have been found for the Co(III)/Co(II) couple for which drastic intrinsic reorganizational barriers exist on change in oxidation state.[162] It is a characteristic of both the heterogeneous and homogeneous reactions, that the rates of electron-transfer reactions of Co complexes are very often faster than predicted by the Marcus cross-relation.

1.5 As will be shown in the next section, the interactions that occur in the activated state between reactant complexes and assisting anions, determine to a large extent the likely path of electron-transfer. In some instances, the interactions are less specific than can be attributed to normal bonding arguments based on simple ionic or covalent influences. A more general interaction can be assumed to apply, based on conclusions drawn from an extensive categorization of bond stabilities; this is the principle of hard-soft acids and bases, devised by Pearson.[173] The principle has been used to explain interactions in electron-transfer reactions, in which the potential of a ligand to function as a bridge was assessed in terms of hard-soft acid-base considerations.[145,187] The stabilities of precursor complexes have also been discussed in terms of this principle.[174,175]

2. PRELIMINARY

In this section, explanations which have been presented to account for the reactivity patterns observed in electron-transfer reactions are introduced. The effects of metal-ion electronic configuration and bridging and nonbridging ligands on the rates of self-exchange and heterogeneous electron-transfer reactions are considered.

2.1 Information about intrinsic barriers to electron-transfer is available from self-exchange reactions. The rate constants for some self-exchange reactions of Fe(II)-Fe(III) and Ru(II)-Ru(III)(d^6-d^5), and Co(II)-Co(III)(d^7-d^6) have been measured.[161] In the former exchanges a metal t_{2g} electron is transferred while in the latter, a metal e_g electron transfers (with associated spin-multiplicity rearrangements). For the Co^{2+}, Co^{3+} metal ions, both the donor and acceptor orbitals have σ symmetry with respect to the ligand-metal axis, while π-symmetry applies for the d^6-d^5 (low spin) complex systems. This is shown schematically in figure VI 2.1. Electron transfer between metal t_{2g} orbitals is expected to be favoured by ligands having π-symmetry, whereas that between metal e_g orbitals will be facilitated by ligand orbitals having σ-symmetry. Experimentally, the d^6-d^5 systems benefit more in terms of rate enhancement of electron-transfer from the introduction of the o-phenanthroline or bipyridyl ligands (having delocalized π-systems) into their primary coordination sphere, than do the d^7-d^6 systems. The inverse is true for the σ-donating NH_3 ligands. Arguments based on orbital symmetry must be used with caution since the symmetry character of the transferring electron affects the energy requirement to reorganize the inner-coordination shells of the reactant complexes prior to the electron transfer. This is evident since removal of an electron from an e_g orbital, which is

FIGURE VI 2.1

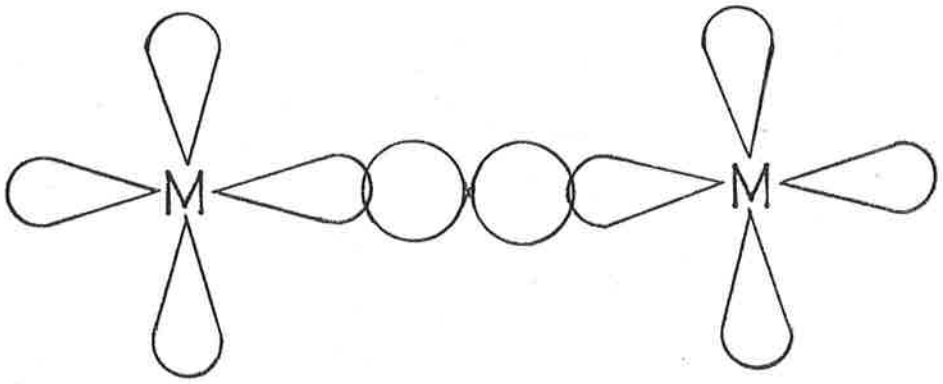

σ - overlap

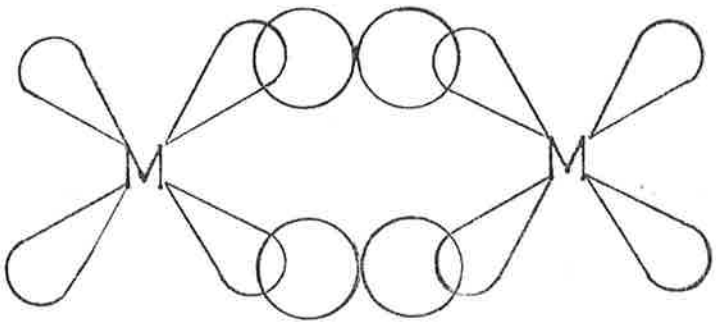

π - overlap

antibonding, will have a larger effect on bond-lengths than electron removal from a t_{2g} orbital, which is relatively non-bonding.(161)

The symmetry argument also explains the observed difference in the reactivity pattern of the inner-sphere exchange reactions,

$$Cr^{2+} + Cr\ X^{2+} \longrightarrow Cr\ X^{2+} + Cr^{2+}$$
$$Fe^{2+} + Fe\ X^{2+} \longrightarrow Fe\ X^{2+} + Fe^{2+}$$

The rates change in the order $I^- > Br^- > Cl^- > F^-$ in the former exchange, whereas the opposite trend is operative for the latter.(160) An e_g electron is transferred in the Cr exchanges, while the Fe system exchanges a t_{2g} electron. The most favourable interaction energy occurs when the redox orbitals of the metal ions have the appropriate symmetries to overlap with the orbitals of the bridging group. Hence σ-interactions with the bridge are important for Cr^{2+} as reductant, and Fe^{2+} reductions are more favoured by π-symmetrical interactions. The degree of σ-symmetrical interaction decreases with the size of the halide, while the inverse relationship holds for the π-efficiency of the halides.

2.2 The reductions of halopentamminecobalt (III) complexes, $Co(NH_3)_5X^{2+}$, by various complex reducing agents have been extensively studied.(174, 176-180) For a number of reducing agents the rate constants of the electron-transfer vary monotonically as the halide is changed from F^- to I^-. The reactivity order has come to be known as either normal or inverse, depending upon whether the rate increases or decreases with increasing atomic number of the halide. The normal reactivity order $F^- < Cl^- < Br^- < I^-$ is observed for the inner-sphere reductions by Cr^{2+} and $Co(CN)_5^{3-}$, and for the outer-sphere reductions by $Cr(bipy)_3^{2+}$ and $Ru(NH_3)_6^{2+}$. In contrast, the reductions by Eu(II) and Fe^{2+} obey the inverse order. It is difficult to generalize the reactivity trend of

the halides in different redox systems, since several factors associated with the nature of the bridging anion interaction in the activated complex may be involved. These include the relative stabilities of the anion in associating with either the reactant or product complexes, anion-orbital symmetry, and anion permeability. For different systems, one factor or another of these may be more important. The thermodynamic contribution to the reaction barrier for the Cr^{2+} and Fe^{2+} reductions favours the inverted order for both, since the stabilities of CrX^{2+} and FeX^{2+} run parallel in the series of halides and are similar in magnitude.(160) However, since the reactivity orders are opposite, intrinsic barriers associated with electron-transfer orbital symmetries are considered important here. The inner-sphere classification of the Eu(II) reduction of the $Co(NH_3)X^{2+}$ complexes was based on the observation that the reactivity order of the halides paralleled the stability of the Eu(III) halide complexes.(179)

2.3 Some mechanistic inferences have been drawn from the halide patterns of reductions of the $Co(NH_3)_5X^{2+}$ complexes. In Haim's study,(174) the reactivity orders of the halide series were correlated with the calculated stabilities of the activated complexes for a variety of reductant complexes. The criteria for mechanistic classification fell into three categories, based on the 'hardness' of the reductant complex, and the halide stabilities in the transition state. This type of systematization of rate data has proved useful for mechanistic inference, in terms of inner- and outer-sphere classification.

2.4 Interesting chemical effects have been observed when the bridging ligand is an unsymmetrical group. The transfer of an unsymmetrical group in an inner-sphere reaction may yield a product in which the

less stable end of the bridging ligand is attached to a metal centre.

e.g. $FeNCS^{2+} + Cr^{2+} \longrightarrow Fe^{2+} + CrSCN^{2+}$

The difference in rates observed with the symmetrical and unsymmetrical N_3^- and SCN^- anions as bridging groups has been used as a means of determining whether a particular reaction proceeds via an inner- or outer-sphere mechanism.(177, 180) If N-bonded SCN^- is the stable isomer to both reactant and product metal centres, and if transfer of the bridge occurs in a reaction, then an inner-sphere reaction should proceed faster when N_3^- bridges than when it is SCN^-. For example, the Cr^{2+} reduction of $Co(NH_3)_5N_3^{2+}$ proceed $\sim 2\times10^4$ times faster than the SCN^- analogue.(179) Considerations of which end of SCN^- is more stably associated with a metal complex are associated with orbital symmetry and 'hard-soft' relationships.(187) In outer-sphere reactions, SCN^- and N_3^- behave similarly, because the possibility of unfavourable S-bonding of SCN^- to a metal centre is removed, and the interactions of the similar π-systems come into play. However, if water replacement is rate determining in an inner-sphere reaction, similar effects of N_3^- and SCN^- may again be observed.(181,182)

2.5 More information about the effects of anions on the rates of outer-sphere electron-transfer reactions was obtained in a study of the reductions of $Co(phen)_3^{3+}$, $Co(en)_3^{3+}$, $Co(NH_3)_6^{3+}$ by Cr^{2+} and V^{2+}, and the oxidation of $Co(phen)_3^{2+}$ by Fe^{3+} in the presence of ClO_4^-, Cl^-, N_3^-, SCN^-.(183) With this wide variation in the type of oxidant, anion, and reductant, some general conclusions concerning anion effects were reached. With the possible exception of the reactions involving the $Co(phen)_3^{3+}$ complex, the uncatalysed rates were in good agreement with those calculated using the Marcus cross-relation. (The $Co(phen)_3^{3+}$ reactions were considered to proceed by a multistep mechanism in which the electron is transferred to the

π-system of the ligand). The ratio of the catalysed to uncatalysed rates were found to be 10^1-10^2 times larger than predicted solely by thermodynamic considerations. Greatest rate enhancement occurred in the V^{2+}-SCN^--$Co(phen)_3^{3+}$ and $CrCl^+$-$Co(NH_3)_6^{3+}$ reactions. The reactivity of these assisting anions was correlated with the symmetries of the orbitals of the electron-donor, the added anion, and the electron acceptor. For reaction with V^{2+} the electron transfers along a mostly π-symmetrical path from reductant to oxidant complex, while for the reaction with Cr^{2+} it proceeds along a totally σ-symmetrical path. This symmetry argument, (an extension of that proposed for inner-sphere bridges (184)), also holds for reactions of Fe(II) as reductant and Fe(III) as oxidant. Thus, under controlled conditions, the reactivity patterns of anions in electron-transfer reactions can be used to analyse the likely extent of orbital symmetry overlap in the activated complex.

2.6 The effect of adding anions on the observed rates of reduction by Fe^{2+} of various Fe(III) complexes has been studied,(185) in which the SCN^- catalysis of the reactions

$$Fe(phen)_3^{3+} + Fe^{2+} \longrightarrow Fe(phen)_3^{2+} + Fe^{3+}$$

and $$Fe^{3+} + Fe^{2+} \longrightarrow Fe^{2+} + Fe^{3+}$$

was compared. There was considerably more favourable SCN^- bridging in the former reaction, beyond that due to the more favourable thermodynamic contribution to the activation barrier in both reactions of $FeNCS^{2+}$ being more stable than $FeNCS^+$. The magnitude of the rate enhancement over that expected if the phen reaction was a weak interaction, outer-sphere mechanism, suggested that a different mechanism was operative in the SCN^- catalysed reduction of $Fe(phen)_3^{3+}$. (Similar effects

were noted with the anions N_3^- and I^-, and with the analogous bipy complex). The effect was interpreted in terms of SCN^- bridging through the S-atom to the phen ligand by π-electron interactions. The effect may be considered as a favourable interaction of the 'soft' S-end of the SCN^- with the 'soft' π-system of the phen ligand. By analogy, the relatively large enhancement by SCN^- of the reduction of ferricytochrome C by Cr(II) is consistent with electron-transfer through a site on the delocalized π-system of the porphyrin ring, rather than at the Fe(III) centre.(186) The reactivity pattern associated with this type of electron-transfer, viz. $Cl^- < I^- < N_3^- \sim SCN^-$, has allowed this remote attack mechanism to be attributed to the Cr(II) reductions of $Fe(phen)^{3+}$(188) and of Fe(III) complexes of octaethylporphyrin(189) and meso-tetra (4-pyridyl) porphine.(190)

2.7 The rates at which a large number of substituted carboxylato-pentamminecobalt(III) complexes are reduced by Cr^{2+} have been found to be relatively insensitive to the more ordinary inductive, conjugative, and steric effects which generally influence organic reactivities.(191,192) Suitable structural modifications of the carboxylato ligands in such complexes greatly facilitates the complex reduction by bringing into play some less usual effects, including proceeding through conjugatively stabilized radical-cation intermediates.(192) In Gould's(192,193) analysis of these systems, it was observed that electron-transfer from Cr^{2+} to coordinated Co(III) often took place readily through ligands, which when free in solution, were reducible. The ligands did not suffer a net reduction in the overall electron-transfer process. It was suggested that a remote attack followed by resonance transfer through the conjugated system was less common than radical ion formation as intermediate by ligand reduc-

tion.[193,194] The electron transfer from this intermediate radical species to the Co(III) metal centre completes the overall electron transfer in such cases. The correlation between electron-transfer efficiencies of bridging ligands and their reducibilities has not been precisely defined, and has not been extended beyond the pyridine and benzene series, nor to inorganic ligands.[193]

2.8 With this background to the mechanisms by which anion-assisted electron-transfer reactions may occur, some inference to the type of mechanism involved in the anion-assisted decay of the tervalent Ni(and Cu) macrocycles, can be made.

3. TYPE OF ANION BRIDGING

3.1 The mode of transient decay of the tervalent macrocyclic complexes depends on both the acidity of the solution and the presence of anions other than ClO_4^-. In acidic solution containing halide or pseudo- order for Br^-, N_3^-, SCN^-, while in Cl^- solution the decay is considerably slower, being first-order for the diene complex and having some second-order character for the tetene. The tam complex in Cl^- solution is meta-stable, decomposing quickly upon the addition of Br^- or SCN^- to the solution. The efficiency of the anion-assistance to the second-order rate of decay varies in the general manner $Cl^- < Br^- < N_3^- \sim SCN^-$. The actual acceleration for the added anions differs with the degree of unsaturation of the macrocyclic complex. The addition of $SO_4^=$ ion to the Br^- systems was found to decelerate the observed second-order decay rates, particularly for the tam complex. The second-order decay process was observable

in Cl^- solution for the Cu(III)diene complex only.

3.2 The kinetic and spectral evidence obtained in the Br^- systems suggested that complexation between the Ni(III) macrocycle and the anion was a necessary precursor equilibrium to the bimolecular transient decay. If the complex formation involved simply an ion-pairing interaction, where the attraction was essentially electrostatic in nature, the order of anion effect on the observed rate would be quite different. The primary consideration in such an interaction is the effective charge product of the pair, with due allowance for the charge densities of the combining species.(195) Accordingly, Cl^- would be more likely to form a stable ion-pair than Br^- or the pseudo-halide ions, and considerable ion-pairing of $SO_4^=$ would be expected. The observed anion trend suggests therefore that the interaction is more specific than simple ion-pairing. The reduction of the tam decay rate in Br^- solution by the addition of $SO_4^=$ indicates, however, that ion-pairing with this anion may impede the more specific interaction between Br^- and the tervalent complex.

3.3 It is possible that the Br^- ion can be inner-sphere substituted onto an apical position of both the tervalent (and bivalent) Ni centres of the macrocyclic complexes. The first requirement for this interaction is that the solvent substitution rate on the metal centre be sufficiently fast to allow for the observed fast rates of Ni(III)L transient decay. The water substitution rates on the Ni(II) and Ni(III) macrocycles have not been measured; on Ni^{2+}_{aq} the rate is $\sim 10^4 sec^{-1}$.(166) It is known that the presence of σ-donating amine coordination to octahedral Ni(II) (d^8) causes an acceleration of solvent exchange rates on

solvated sites — the degree of acceleration depends on the actual geometry of the ligand and the degree of σ-donation of the electons in nitrogen based orbitals to the metal centre.[196] It is thus likely that the tam complex is the most effective in its acceleration of exchange rate, since all four planar nitrogen atoms are saturated, consequently having the most extensive σ-donation of the three macrocyclic ligands. The rate of solvent exchange on the apical site of the low spin d^7 Ni(III) macrocycle is likely to be faster than on the bivalent complex, since it involves interaction with the antibonding dz^2 orbital of the metal. The degree of Jahn-Teller distortion of the apical positions of octahedral complexes explains the large exchange rates on the Cr^{2+} and Cu^{2+} metal centres.[1, 166] It has been shown on the Co(II) diene complex that marked distortion along the apical positions is apparent as a consequence of the well-defined size of the N_4 girdle of the macrocycle.[197] It may be inferred therefore that the Ni(III) macrocycles, which are isoelectronic with the Co(II) complex, also have considerable apical distortion, and hence have very rapid exchange rates in these positions. The rate on Ni(III)L is likely to be diffusion controlled. The exchange rate on Cu(III)diene, isoelectronic with Ni(II), is considered to be very fast also.

The spectral evidence for inner-sphere coordination of the X^- is indirect. The anion effects on the bivalent nickel macrocycles were observed on both the d-d and chromophoric bands on the complexes. No new peak attributable to the possible LMCT band of a Ni(III)L-Br^- interaction was observable in the high [Br^-] solution used. The effect of Br^- coordination on the transitions in the presumed $n \rightarrow \pi^*$ ligand band can be accounted for if considerable metal orbital interaction occurs in

this chromophore band. That this band is observed in the region below 230nm for the free diene ligand in solution supports such a surmise. Metal orbital interactions with the Br^- ion in the apical positions may thus be reflected in the observed imine band. The effect on the d-d bands is anomalously low however, for the type of interaction suggested, i.e. penetration of the primary coordination shell. The similarity of the type of interaction occurring on the bivalent and tervalent complexes is based on the trend of anion effect, which is not that expected for simple ion-pairing. The association is presumed to be more specific than the general effect of high concentration of inert electrolytes on the molar absorbances of ionic species.(198)

The observed trend of inner-sphere complexation of some halide and pseudo-halide ions on Ni^{2+}_{aq} is shown below;(140)

$$Ni^{2+}_{aq} + X^- \rightleftharpoons NiX^+_{aq} \qquad K_1$$

where	X^-	K_1
	Cl^-	1.7
	Br^-	0.76
	N_3^-	11
	SCN^-	15

The trend of observed complexation for the Ni(II) macrocycles is similar with respect to pseudo-halide > halide, but the inverse order of Cl^- and Br^- suggests more subtle differences in the anion interaction with the macrocyclic complex compared with the aquated complex.

Thus, if (i) simple ion-pairing can be neglected (ii) no expansion of the hexa-coordination of the Ni(III), d^7 complex occurs, nor (iii) displacement of the stable macrocycle from a coordination site occurs, several possibilities for the complex configuration in the activated state

can be considered.

3.4 The exchange rate of the anion on the apical sites of the Ni(III) macrocycle is presumed to be very large, but on a time average a finite concentration of the complexed anion is maintained. A totally inner-sphere bridging mechanism would require simultaneous insertion of the anion onto the apical positions of two Ni(III)L species. Such a requirement for activated complex formation appears too specific, considering the presumed substitution lability, and the observed efficient electron-transfer rates of decay. Formation of an outer-sphere activated complex seems reasonable in light of this. In general terms, the presence of the anion on at least one of the reactant complexes may decrease the distance between the redox centres by reducing the electrostatic repulsion, and may couple the vibratory motions of the non-bridging ligands on both metal centres. Either of these influences would facilitate electron-transfer by lowering the free energy barrier to the transition state. More specific, however, is the reactivity pattern of the various anions in assisting the observed rate of electron-transfer; this leads to considerations about the nature of the interactions involved in the activated complex.

4. THE ACTIVATED COMPLEX.

4.1 A correlation of the experimental results for the anion-assisted bimolecular decay of the M(III) complexes with the current knowledge of electron-transfer reactions of metal complexes, provides some insight into the nature of the mechanism of the observed reaction. Both intrinsic and thermodynamic factors contributing to the activation barrier

are considered. Since the Ni(III)L/Ni(II)L self-exchange rates are unknown, mechanistic inference based on Marcus theory cannot be drawn in this study.

4.2 The catalysis of the Ni(III)L decompositions was quite significant for 1mM additions of SCN^- and N_3^- to the 0.1M Br^- solutions. It is known from studies of the Cr^{2+} reduction of Fe(III) and Co(III) porphyrin complexes, that large anion catalytic effects occur when inner-sphere bonding to the metal centre of the metalloporphyrin is operative.(175) The large catalytic effects, particularly by the pseudo-halides, for the Ni(III)L decompositions, are inferred by analogy to involve inner-sphere penetration of the anion into at least one of the reactant tervalent complexes. For both the porphyrin and macrocycle systems, the inner-sphere complex is the electron-acceptor.

The acceptor orbital on the Ni(III)L metal centre is e_g having σ-symmetry. The reactivity trend of the anions however, favours π-symmetry in the activated complex, and if symmetry arguments based on intrinsic barriers are of prime importance, the symmetry of the donor orbital might be expected to have π-symmetry. This line of argument suggests that the donor orbital is not a metal e_g orbital, but a ligand orbital on the Ni(III)L complex. Since apical water on the donor complex has σ-symmetry, it is more likely that the donor orbital is on the macrocycle. This suggestion is supported by the observation that the greatest anion catalysis of the Ni(III)L electron-transfer occurs in the SCN^--assisted decay of the tetene complex, which has the most π-character of the three ligand forms. The nature of the interaction involved in the SCN^- catalysis of the unsaturated macrocycles is likened to that con-

sidered for the SCN^- catalyzed reduction by Fe^{2+} of $Fe(phen)_3^{3+}$,[185] and in the reductions of $Co(phen)_3^{3+}$ by various reducing complexes;[183] a 'soft-soft' association of the SCN^- with the orbitals of the phen ligand was considered. The redox reactions of the Fe(III)/Fe(II) cytochrome c complexes were proposed to be via remote attack of the reductant/oxidant complex on an acceptor/donor site on the exposed heme edge of the porphyrin system.[186, 199] The observed similarity of the anion reactivity pattern for the Cr(II) reduction of the ferricytochrome C complex[186] ($Cl^- < I^- < N_3^- \sim SCN^-$) is consistent with the proposition that the donor orbital of the electron-transfer in the anion-assisted decay of Ni(III)L is on the macrocycle, possibly involving the π-electrons in the imine function.

For the di and tet complexes, the greater reactivity of SCN^- over N_3^- is possibly due to the nature of SCN^- being more versatile in 'hard-soft' interactions. This anion has the ability to favourably interact with both the 'hard' metal centre through the N- atom, and with the π-system of the ligand through its S- atom. The N_3^- ion, which is probably equally 'conducting' for the donated electron, does not have the same measure of favoured interaction at the ligand. Similarly, it may be presumed that it is the greater 'softness' of Br^- that allows it more facile interaction at the ligand than Cl^-.

More difficult to rationalize in terms of intrinsic barriers however, is the observed catalysis of N_3^- in the tam decay reaction, in which the macrocycle has no unsaturated character. The interaction of N_3^- with the 'reductant' Ni(III)L complex in the activated state might still be a a ligand site, if the saturated complex is considered to offer a 'harder' site of interaction. This premise is supported by the poorer catalysis

of SCN^- for the tam complex. However, if only 'hard-soft' considerations are important in accounting for the N_3^- catalysis, little increased reactivity would be expected over that of Br^- catalysis, since both anions are intermediate 'soft' bases.

4.3 The arguments based on intrinsic barriers to activation (which involved considerations of orbital symmetry and 'hard-soft' interactions) can explain to some extent the reactivity pattern of the assisting anions. Further rationalization can be achieved by consideration of thermodynamic barriers.

The precursor complex containing the two reactant Ni(III)L species and the anion must pass through one of two possible states upon electron-transfer;

either

$$L\ Ni(III).\ X^{2-}.\ NiL^{4+}$$

or

$$L\ Ni(II).X^{\cdot}.Ni(III)L$$

The reduction of X^- by one of the reactant complexes is obviously endoergic by several volts, while the oxidation of X^- by the powerful tervalent metal centre (to effectively proceed via a coordinated $X^{\bullet}$ radical oxidation in the transition state) seems energeticlly more reasonable. The E^{o}'s for SCN^- and N_3^- have not been accurately determined, but it is considered that the value of the $SCN^{\bullet}/SCN^-$ couple is between that of $Br^{\bullet}/Br^-$ and $I^{\bullet}/I^-$.[58] The $N_3^{\bullet}$ is presumed to be a little poorer oxidant than $Br^{\bullet}$.[58]

If the activation barrier to electron transfer in this system depends on the relative 'oxidizibility' of the bridging anion, the

reactivity pattern would be $Cl^- < Br^- < N_3^- < SCN^-$. A more quantitative analysis of this thermodynamic barrier can be carried out using the Br^--bridging rate data. The barrier to the formation of the complexed $Br^\bullet$ radical in the transition state is considered. This is represented by the equilibrium,

$$\underset{\text{precursor complex}}{LNi(III).Br^-.Ni(III)L} \overset{K^{\ddagger}}{\rightleftharpoons} \left[LNi(II).Br^{\bullet}.Ni(III)L\right]^{\ddagger}$$

$$\downarrow k_{et} \quad \text{electron-transfer}$$

$$\underset{\text{successor complex}}{LNi(II).Br^- \; NiL^{4+}}$$

The value of the thermodynamic activation equilibrium constant is a function of the couples,

$$Ni(III)L + e \rightleftharpoons Ni(II)L \qquad E_1^o$$

$$Br^\bullet + e \rightleftharpoons Br^- \qquad E_2^o$$

The E^o for the activation process can be expressed as the algebraic sum of the respective couples, as

$$E^{o\ddagger} = E_1^o - E_2^o$$

Since E_2^o remains constant, while E_1^o varies by 0.18 volt[29] between tam and tet, the effective variation in $E^{o\ddagger}$ is also 0.18volt. For the one-electron transfer involved, this potential corresponds to a change in $K^{\ddagger}$ of a factor of 1.0×10^3 (using the Nernst equation). Since the rate of conversion to the successor complex is a linear function of $K^{\ddagger}$,[195] an acceleration by 1.0×10^3 would be expected in the Br^--catalysed second-order decay of the tervalent tetene over that of tetramine if the above arguments hold good. The experimentally determined rate ratio of Ni(III)tet : Ni(III)tam is 0.5×10^3, which is sufficiently close to

assume that in the decomposition process in Br^-, the major contribution to the activation barrier is thermodynamic, determined by the 'oxidizibility' of the bridging anion by the tervalent nickel centre.

Support for this mechanism of activation in bridging-assisted second-order decompositions of the M(III) complexes, comes from other experimental results.

(i) Cl^--assistance was only observed for the Cu(III)di complex, which is the most powerful of the tervalent oxidants used.

(ii) the initially discernable slow second-order character in the Ni(III) tetene decay in Cl^- solution suggests that this complex may be able to decompose to a small extent via the proposed activation step.

(iii) The faster decay of the presumed Ni(III)tam.HO_2 complex compared with the corresponding Br^- complex, can be accounted for by the lower E^o value of the O_2/HO_2 couple compared with the $Br^\bullet/Br^-$ couple. Although not an anion, the polarizable HO_2 species may act as a bridge in the electron-transfer reaction.

This argument does not explain the increased reactivity of N_3^- over SCN^- for the Ni(III)tam decay, since it is considered that SCN^- is more oxidizible than N_3^-. The anion catalysis of this reaction may involve significant intrinsic barriers to activation based on the bridge electron conducting ability, and the degree of orbital symmetry matching at the donor and acceptor sites.

If it can be assumed that the main driving force into the activated state in the Cr^{2+} reductions of carboxylatopentammine-Co(III) complexes[192, 193] is derived from the strong reducing power of the Cr(II), analogy between bridge reducibility in such systems, and bridge oxidizibility in

the anion assisted M(III) systems, may be drawn. In certain cases the intermediate existence of the coordinated reduced bridging ligand was observed.[193] No evidence for the transient existence of Ni(II)L,X$^{\bullet}$ was obtained in this study; the system merely passes through this form in the transition state.

4.4 In studies of the self-exchange rate for the low-spin Co(III) diene/Co(II) diene couple, an exceptionally low value of $10^{-9}M^{-1}sec^{-1}$ was obtained.[200] This rate contrasted markedly with that obtained for the tetene analogue of $10M^{-1}sec^{-1}$. The anomalously large Franck-Condon reorganizational barrier for the diene couple was found by structural analysis to be due to a large difference in the extent of apical distortion, ~0.5Å, between the two oxidation states.[197] The presence of the planar macrocyclic girdle has forced reorganization of bond lengths for this exchange to occur in the one direction. The difference in the apical bond lengths for the tetene analogue was considerably shorter allowing for more facile reorganization in the activated state. The anomalously slow reduction by Cr^{2+} of the Co(III) diene complex (~$10^{-8}M^{-1}sec^{-1}$) was a further example[201] of the unfavourable approach of this Co(III) centre to the activated state. Generally the anomalous reorganizational parameters were greatest for reactant pairs involving one member with one eg orbital singly occupied (Cr^{2+}, Co(II)) and the other with vacant eg orbitals (Co(III)).[202] It was noted in contrast that while the Co(II)/Co(I) couple (which is d^7-d^8, isoelectronic with the Ni(III)/Ni(II) couple) involved changes in electron density in eg orbitals, the reorganization barriers were considerably smaller, presumably because large axial distortions occur in both the oxidized and reduced species.[197, 203] No anomalous reorganizational factors due to macrocycle complexa-

tion would be expected in the activation process;

$$LNi(III).Br^- \longrightarrow LNi(II).Br^{\bullet}$$

However large effects might be expected if the energetic criterion for activation also required reorganization of the Ni(IV)/Ni(III)couple (isoelectronic with the anomalous Co(III)/Co(II) couple) in the donor macrocyclic comples. The accounting for the Br^--bridging in the system by the 'oxidizibility' argument suggests that the site of the donor orbital on the reductant Ni(III)L complex in the activated state is on the ligand, and does not involve metal centred orbitals.

4.5 It may be concluded from the preceeding discussion that the likely mechanism of electron-transfer in the anion-assisted decomposition of M(III)L, shown for nickel(III) in Br^- solutions is:

$$Ni(III)L + Br^- \rightleftharpoons LNi(III).Br^-$$

$$LNi(III).Br^- + \begin{bmatrix} LNi(III).Br^- \\ Ni(III)L \end{bmatrix} \longrightarrow LNi(III).Br.LNi(III) \text{ precursor complex}$$

$$\downarrow$$

$$\left[LNi(II).Br.LNi(III)\right]^{\ddagger}$$

$$\downarrow$$

$$LNi(II).Br.L^{(+)}Ni(III) \text{ successor complex}$$

This mechanism probably explains the observed instability of the Ni(III)-tetraphenylporphyrin complex in CH_2Cl_2 solution in the presence of Br^-.(204)

5. THE PRODUCT COMPLEX

5.1 The fate of the $Ni(III)L^{+}$ species and the nature of the return of the metal centre to the bivalent state are now considered.

The product analysis of the anion-assisted second-order decay process suggested that acid was produced in solution and that no introduction of the imine function into the macrocycle was involved. The possibility of the decay of the highly oxidized complex by reaction with water is unsatisfactory, since OH radical (the most likely product of the first step of such a reaction) would oxidize Ni(II)L to produce further Ni(III)L, i.e.

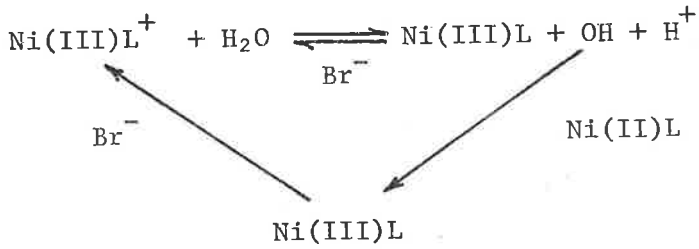

The inherent cycling in this system requires incomplete conversion at one stage for overall decay to occur. This mechanism is rejected in favour of the following.

5.2 The lack of experimental evidence for ligand fragmentation and imine formation, along with the established observation[205] that redox processes involving equal numbers of electrons and protons in solution are facile, provide the rationale for the proposed mechanism. This is illustrated for the tam and di systems on the following page, where the $Ni(III)L^{+}$ species has the form (I). In aqueous solution the $Ni(III)L^{+}$ species achieves a rapid increase in stability by deprotonation followed by intramolecular electron-transfer from the ligand to the metal centre.

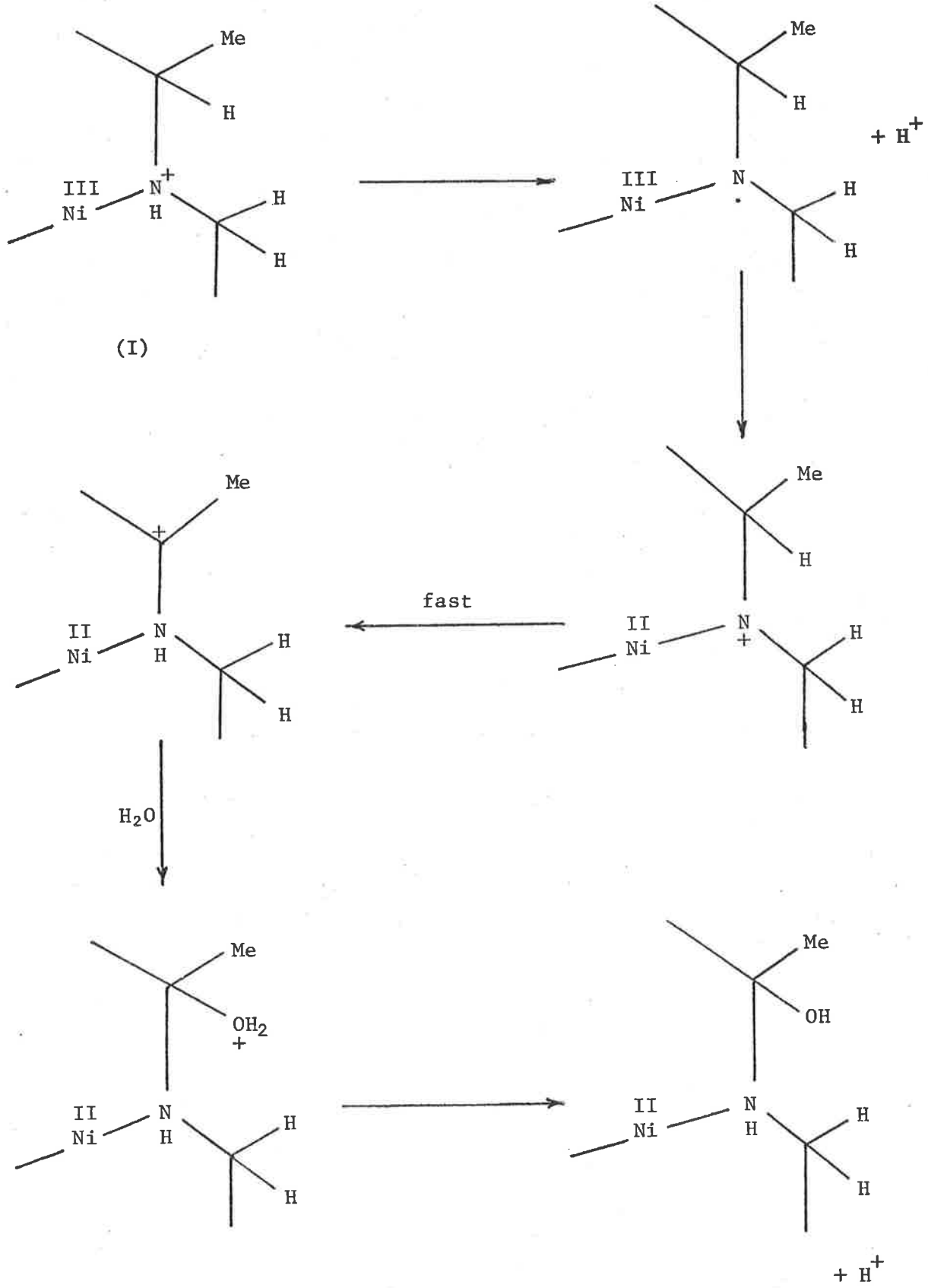
Me
H
III
Ni
N
H
H
H
(I)
+ H+
fast
II
Ni
H2O
OH2
OH

The polarity of the N-H bond would be considerably enhanced by electron withdrawal by the tervalent centre. The 'carbonium' type complex ion thus formed rapidly rearranges to a true carbonium by the placing of the charge on the less electronegative β- carbon atom. Rapid hydrolysis of the carbonium site followed by deprotonation results in the production of the hydroxy-substituted bivalent macrocyclic complex as product. The hydroxy-substitution is shown in the 6-membered ring by assuming that the quaternary β - carbonium ion is more stable than the tertiary (in the 5-membered ring).

The product of the tetene decay is also assumed to be the hydroxy-substituted complex. This point raises mechanistic complications since there is no saturated coordinated nitrogen atom to deprotonate in the first step for this complex. Perhaps deprotonation from the β-carbon due to considerable electron-withdrawal through the imine function therefore occurs. The activation barrier for the intramolecular formation of the ligand radical cation is probably larger for this complex than for the corresponding saturated complexes. However, if this barrier is smaller than the rate-determining barrier of the overall electron-transfer process it will not be kinetically noticable. Evidence for the hydroxy-substitution on the tetene complex was sought, based on the possibility of tautomerization of the product complex;

i.e.

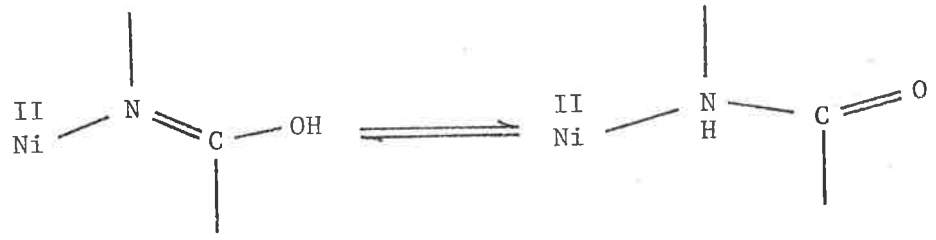

The form of the tautometric product would be expected to be pH dependent. Spectrophotometric analysis of the product solution in the UV region over the pH range 1 - 9 did not reveal any evidence for tautomerism. However if the pK_a of this conversion occurred at pH > 9, it could not be detected, since the Ni(II)tet complex is known to decompose in alkaline solution.[30]

The evidence for hydroxy-substitution onto the macrocycle is indirect and requires further product analysis, ideally using mass spectrometry and IR techniques on product samples of reasonable quantity. Such analyses were not possible on the μM solutions used in these studies.

5.3 In Barefield's[46] report on the mode of decay of Ni(III)tam in aqueous solution first-order conversion to a ligand radical intermediate occurred initially followed by ring rupture or H-atom capture; the only macrocyclic product complex was Ni(II)tam. No involvement of water (either by the production of OH or O_2) was detected in the decay process. In the presence of the anions I^- and $C_2O_4^=$ in solution, the ligand radical transient absorption was immediately quenched. In the case of I^-, I_2 was produced, indicating, along the stoichiometric evidence, that simple anion oxidation by the transient had occurred. No details of the oxalate quenching were given. It is possible in the I^- system, as in the Cu(III) diene - N_3^- system, that an initial complexation of the X^- to the tervalent complex is not followed by encounter with another M(III)L species. Instead, conversion directly to stable products occurs, as a result of the favourable E^o for X^- oxidation by the respective tervalent macrocycle.

In pyridine solution, the decay of the tam ligand radical was second-

order, producing the mono-imine macrocyclic complex as product. The imine was introduced into the 5-membered ring rather than into the 6-membered ring which is the usual mode of oxidative dehydrogenation for the tam complex.(206) Barefield proposed that when the oxidant was another ligand radical or the corresponding tervalent macrocycle, some subtle steric requirements of these oxidants might account for this anomally. In this system, it is possible that bridging between one ligand radical species and another, or with a tervalent complex, has occurred via a pyridine molecule. This molecule, having relatively low lying unoccupied orbitals, and π-delocalization would be ideally suited for a bridging group. Considerably less repulsion between the charged complexes would be expected in pyridine due to its significantly lower dielectric constant compared with water. Hence, the bridge mechanism could apply in Barefield's system in pyridine except for the fate of the presumed carbonium successor complex. In the absence of water, the process

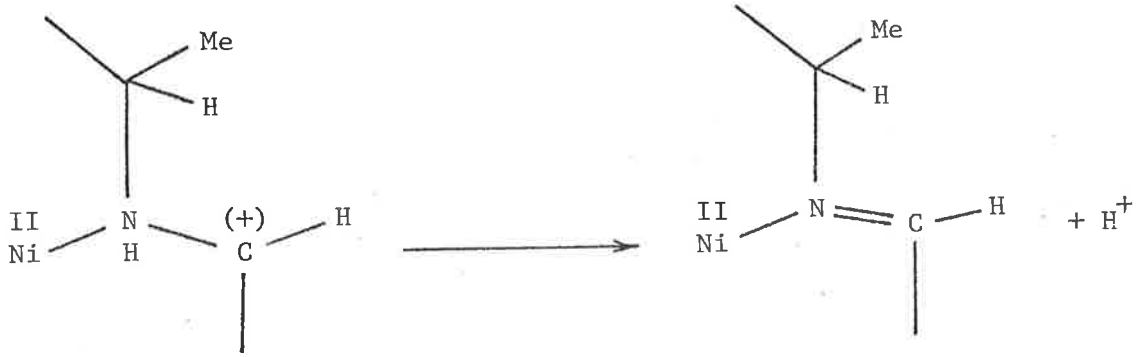

could be expected to occur. The production of the imine function in the 5-membered ring therefore presumes the carbonium ion resides on the β-carbon in this ring rather than in the 6-membered ring. (This is at variance with the expected stability of the carbonium ion on the more substituted β-carbon). It is suggested that this process must compete

with hydrolysis of the carbonium ion in aqueous solution, and that in water, the production of the hydroxy-substituted complex is the preferred path.

5.4 Hence there is no real contradiction of mechanism between this and Barefield's work, if it is considered that in aqueous solution, in the presence of bridging species

(i) transient decay via the anion-assisted second-order process is more favourable than H-atom capture or ring rupture,

(ii) hydrolysis of the carbonium-ligand successor complex is more favourable than formation of the imine function.

VII OXIDISED COMPLEX CONVERSION

1. SOLUTIONS OF NATURAL pH

1.1 The decay of the tervalent diene complex in a flashed solution containing 20μM Ni(II)di, 20mM Br^- and 10mM H_2O_2 at natural pH was observed at 366nm. The overall transient decomposition occurred in two distinct steps; the primary reaction within 0.5msec of the flash, while the secondary was complete within 50msec after the flash.

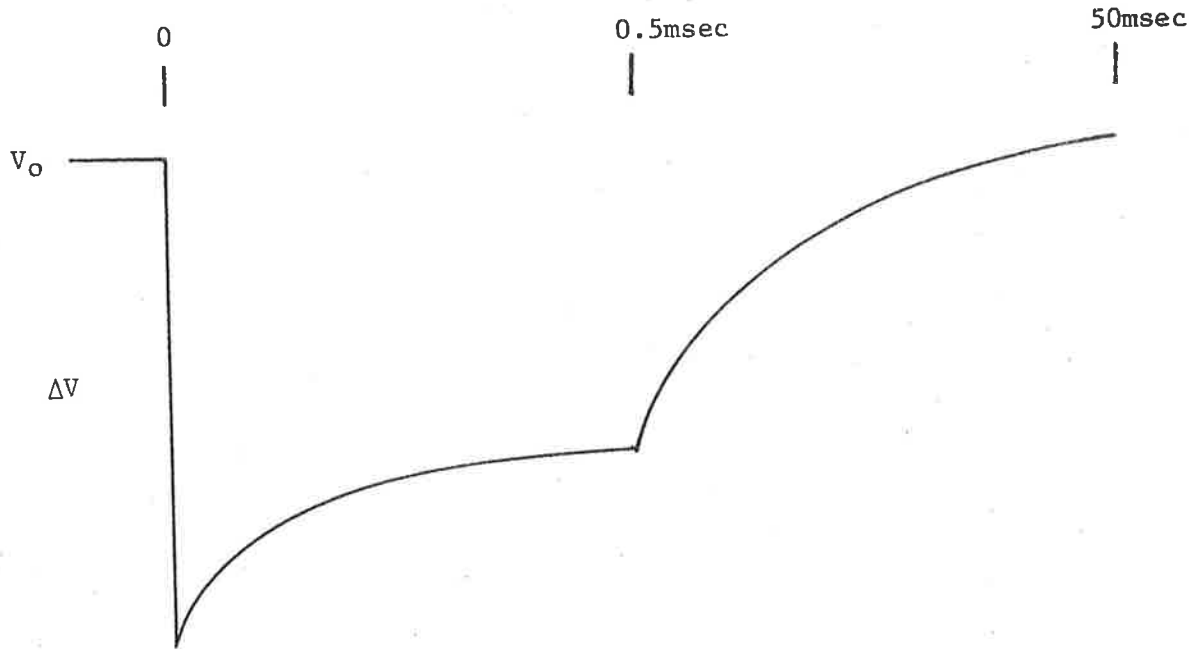

Upon changing the $[Br^-]/[H_2O_2]$ ratio, the proportion of the overall decay occurring via the two processes varied, independently of the actual values of the individual concentrations. When the $[H_2O_2]$ was decreased to 1mM only the secondary process was apparent, whilst the primary process dominated at 50mM H_2O_2. The primary step was also eliminated when the [Ni(II)di] was increased to 0.2mM. The kinetics of the primary

process were difficult to measure for $[H_2O_2] \lesssim 20mM$, due to an indefinite base-line for measurement, but appeared to be reasonable first-order at 50mM H_2O_2. The secondary process was good first-order, independent of $[H_2O_2]$ and [Ni(II)di], having a value of $k_{1st} \simeq 100sec^{-1}$.

At 546nm there was a formation process observable within about 20msec after the flash. This process had the same first-order decay rate for 1mM H_2O_2 solution as the secondary process observable at 366nm. Upon increasing $[H_2O_2]$, the significance of the formation reaction was reduced so that at 50mM H_2O_2 the process was not discernable. The decay of the 546nm absorption was found to be pseudo-first order in $[H_2O_2]$, having a specific rate constant determined from the slope of a plot of k_{obs} versus $[H_2O_2]$ over the range 5 - 20mM of 4.2 ($\pm$0.6) x $10^2 M^{-1}$ sec^{-1}.

Similar kinetic effects at both wavelengths were observed in the analogous nickel tam system, with the first-order conversion process having a rate constant $\simeq 150sec^{-1}$, independent of $[H_2O_2]$ and [Ni(II)tam]. For the tetene complex under the same experimental conditions, two steps were again apparent for the overall decay at 366nm. The primary process was the same as that observed in the diene system, being eliminated at 1mM H_2O_2 in favour of the secondary reaction. This reaction was however, good second-order (rather than first-order) in the range 1 - 4mM in H_2O_2, and showing a tendency towards pseudo-first order in $[H_2O_2]$ for values of this concentration >10mM. At 546nm, the absorption apparent after the flash decayed in the same manner as that observed at 366nm, with no observable formation process.

1.2 The transient spectra for the tet and di systems were measured 100μsec and 10msec after the flash. The initial spectrum of the diene system was that of Ni(III)di, whilst that at 10msec showed absorption in the 350-600nm region characteristic of the ligand radical species, Ni(II)L$^{\bullet}$, with $\lambda max \simeq 550nm$. The transient spectrum for the tetene system was the same in shape at both times, and was characteristic of the Ni(III)tet complex in Br^- solution. The spectral results, combined with the observed similarity of the rate of Ni(II)L$^{\bullet}$ + H_2O_2 determined in section III 2.6, and the transient decay at 546nm in this system, support the characterization of the product of the formation reaction as Ni(II)L$^{\bullet}$.

1.3 In flashed Br^- solutions containing 20μM Ni(II)L together with 50μM Br_2 or saturated with N_2O in the absence of added acid, similar kinetics were observed. For the di and tam systems at 366nm, there was one process only, this being a first-order decay with $k_{1st} \simeq 100\ sec^{-1}$. This decay was independent of [Br^-] (0.02 - 0.2M), of [Ni(II)di] (20-100μM) and of Br_2 over a large range. (The addition of acid to the solution changed the observed decay to the Br^--assisted second-order process discussed in section V 3.3). At 546nm the formation reaction was again observed with a first-order rate (under conditions of low [Br^-]) corresponding to the decay at 366nm. The apparent formation rate increased as the [Br^-] was increased to 0.1M. As [Br^-] increased, the rate of the decay process increased so much that it overlapped the first-order formation process. This leads to erroneously low values for OD_∞ for the formation step, and therefore to an apparently high value of the rate constant for the formation. The 546nm absorption subsequently decayed

by a second-order process having $\frac{k}{\varepsilon l}$ values of 21 sec^{-1} in Br_3^- solution and 13sec^{-1} in N_2O-saturated solution at 0.1M Br^-. The rate fell to 3.6sec^- in the former case when the [Br^-] was 0.01M. For the analogous tetene systems, the decay at 366nm was the same for both the Br_2 and N_2O solution, being second-order throughout with the $\frac{k}{\varepsilon l}$ value $\simeq 3.5 \times 10^3 sec^{-1}$ at 0.1M Br^-. The same decay process was observed at 546nm, with $\frac{k}{\varepsilon l} \simeq 1.7 \times 10^4 sec^{-1}$, due to the smaller molar absorbance at this wavelength.

1.4 In these systems, any e^-_{aq} produced by Br^- photolysis is scavenged by the added H_2O_2, Br_2 or N_2O. The reactions of Ni(III)L with the hydroperoxy radical which prevail in the basence of e^-_{aq} scavengers in solutions of natural pH (section V 3.2) were eliminated in these systems. In the H_2O_2 solutions, HO_2 production is possible, however, via the reaction

$$OH + H_2O_2 \longrightarrow HO_2 + H_2O$$

if [H_2O_2] is sufficiently high. In the Br^- - H_2O_2 system in the range of the [Br^-]/[H_2O_2] ratio between 0,5 - 10, where the observed decay at 366nm was via two processes, there is competition between these two reagents for the photoproduced OH radicals. The Br_2^- radical anions produced from the Br^- + OH reaction yield Ni(III)L upon reaction with the bivalent macrocycle. The observed primary reaction in this system is the subsequent reaction of the tervalent complex with the available HO_2 radical and is apparent for all three complex forms. When the available [HO_2] is zero, the slower secondary process becomes apparent. For the tetene this is the Br^- bridged second-order reaction; in the case of the saturated complexes di and tam, unimolecular conversion of the tervalent

complex to the ligand radical intermediate is observed.

i.e. $Ni(III)L \longrightarrow Ni(II)L^{\bullet} + H^{+}$

(This reaction has been established to occur for the tam complex in basic solvents by Barefield).[46] The primary decay process is absent of course in the Br_2 and N_2O systems due to the absence of HO_2 radicals; the only process observed at 366nm corresponds precisely with the secondary reaction in the Br^-, H_2O_2 system for all three complexes.

The fate of the $Ni(II)L^{\bullet}$ species for the di complex was quite similar for the three Br^- systems (Br^- and Br_2; Br^- and N_2O; Br^- and 0.5mM H_2O_2) at natural pH, this being second-order decay, with a positive dependence on $[Br^-]$. It is possible that a mechanism involving Br^- bridging (as in section VI) between two $Ni(II)L^{\bullet}$ intermediates is involved here. In solutions containing $[H_2O_2]>5mM$, reaction of the ligand radical with H_2O_2 predominates.

2. MILDLY BASIC SOLUTIONS

2.1 The transient decay reactions of the Ni(III)L complexes were observed in flashed unbuffered $Co(NH_3)_5X^{2+}$ (X = Cl, Br) solutions. In these solutions the pH rapidly increased during the time of the flash by the photoproduction of NH_3;

$$Co(NH_3)_5X^{2+} \xrightarrow[X^-]{h\nu} Co^{2+} + 5NH_3 + X_2^-$$

and $$NH_3 + H_2O \underset{}{\overset{K_b}{\rightleftharpoons}} NH_4^+ + OH^- \qquad \text{(fast)}$$

where $pK_b = 4.75$,

A solution containing 0.1mM $Co(NH_3)_5X^{2+}$ initially at natural pH had a measured pH ~ 9 after one flash. Under these conditions, therefore,

the reaction modes available to the tervalent complexes in mildly basic solution were investigated.

2.2 For a 20μM Ni(II)di, 0.1mM $Co(NH_3)_5X^{2+}$ solution, the observed decay at 366nm was very fast first-order, with considerable reaction occurring within the flash duration. The rate was independent of $[X^-]$ (0.2mM - 0.1M), having a value, $k_{1st} = 4.5(\pm 0.7) \times 10^4 sec^{-1}$. At 546nm there was a corresponding fast formation reaction observed; the transient spectrum of this rapidly formed species was identical with that of the ligand radical $Ni(II)L^{\bullet}$, in the measured region 370 - 600nm. The visible absorption subsequently decayed slowly by a first-order reaction, having $k_{1st} \simeq 4\ sec^{-1}$, independent of $[X^-]$ and [Ni(II)di].

2.3 The UV absorption spectrum of the chromophore region of the bivalent macrocycle was measured after multiple flashing and compared with the unflashed solution. Photolysis of 0.1mM $Co(NH_3)_5Cl^{2+}$ solution (containing 50μM Ni(II)di) was chosen for this analysis because of its smaller absorption in the region of spectral interest. The spectra are compared in figure VII 2.3, where it is seen that there is an increase in the absorption in the region $\gtrsim$290nm. This was independent of photolysis effects on the Co(III) complex, as determined in a blank experiment.

2.4 Whilst the effects occurring in this mildly basic solution for the diene complex were similar (but faster) to those observed for the Br_3^- etc systems at natural pH, the process occurring for the tetene system was significantly different. The transient sepctra of a 20μM Ni(II)tet, 0.1mM $Co(NH_3)_5Br^{2+}$, 0.2mM Br^- solution were measured 100μsec and 10msec

FIGURE VII 2.3

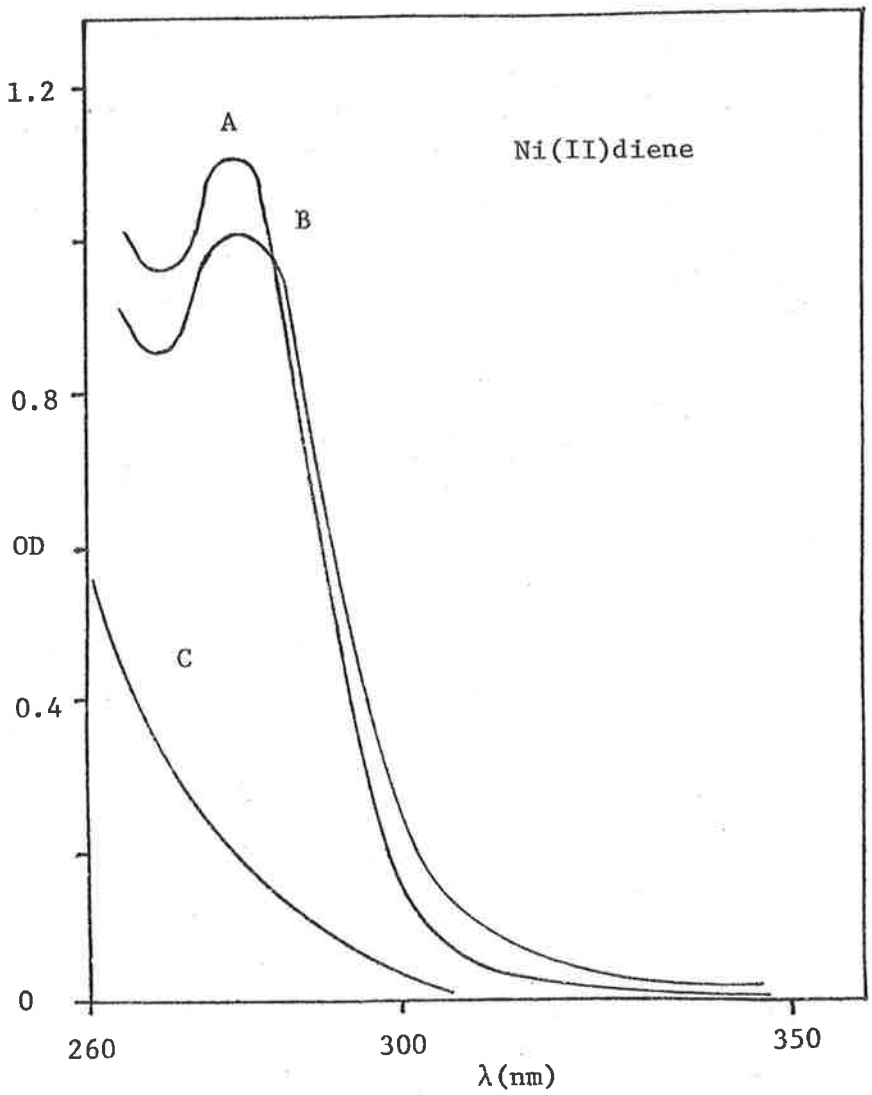

A ; unflashed solution

B : flashed solution

C : 0.1mM $Co(NH_3)_5Cl^{2+}$ alone

after the flash. These are shown in figure VII 2.4. The spectral evidence suggests that an initially formed tervalent complex transforms to another form within 10msec of the flash. Similar behaviour has been observed for the Ni(III)EDTA complex in aqueous solution.(56) Rate measurements showed that the decay observable at 366nm corresponded precisely with the formation at 450nm, this process being first-order, $k_{1st} \simeq 200sec^{-1}$. This modified form of the tervalent complex then decayed by a slow first-order process to products, $k_{1st} \simeq 8sec^{-1}$. The same kinetic observations were obtained in the analogous Cl^- system. These processes were not exclusive to flashed $Co(NH_3)_5X^{2+}$ solutions, as Br^- solutions containing 1mM H_2O_2 or dissolved N_2O, adjusted to pH~9 prior to flashing, produced the same results.

Measurement of the UV chromophore band of a multiply flashed tetene solution (50μM, with 0.1mM $[Co(NH_3)_5Cl]Cl_2$) revealed considerable difference between the product solution and the unflashed solution. The actural spectral change was very similar to that observed at pH 1.0 in section IV 3.4, where very slow first-order transient decay was observed. On the basis of this product analysis, it is considered that the same process of tetene decay is operating at pH 1 and 9, with this reaction being base catalyzed and observable in two steps at the high pH.

2.5 Comparison with Barefield's results(46) on the mechanism of Ni(III)tam decay in aqueous solution would suggest that for the diene system, ring rupture occurs after conversion to the ligand radical intermediate in the primary step. This conversion which proceeds through the deprotonation of the secondary coordinated amine nitrogen cannot occur for the tetene. The observation of a conversion to an intermediate for

FIGURE VII 2.4

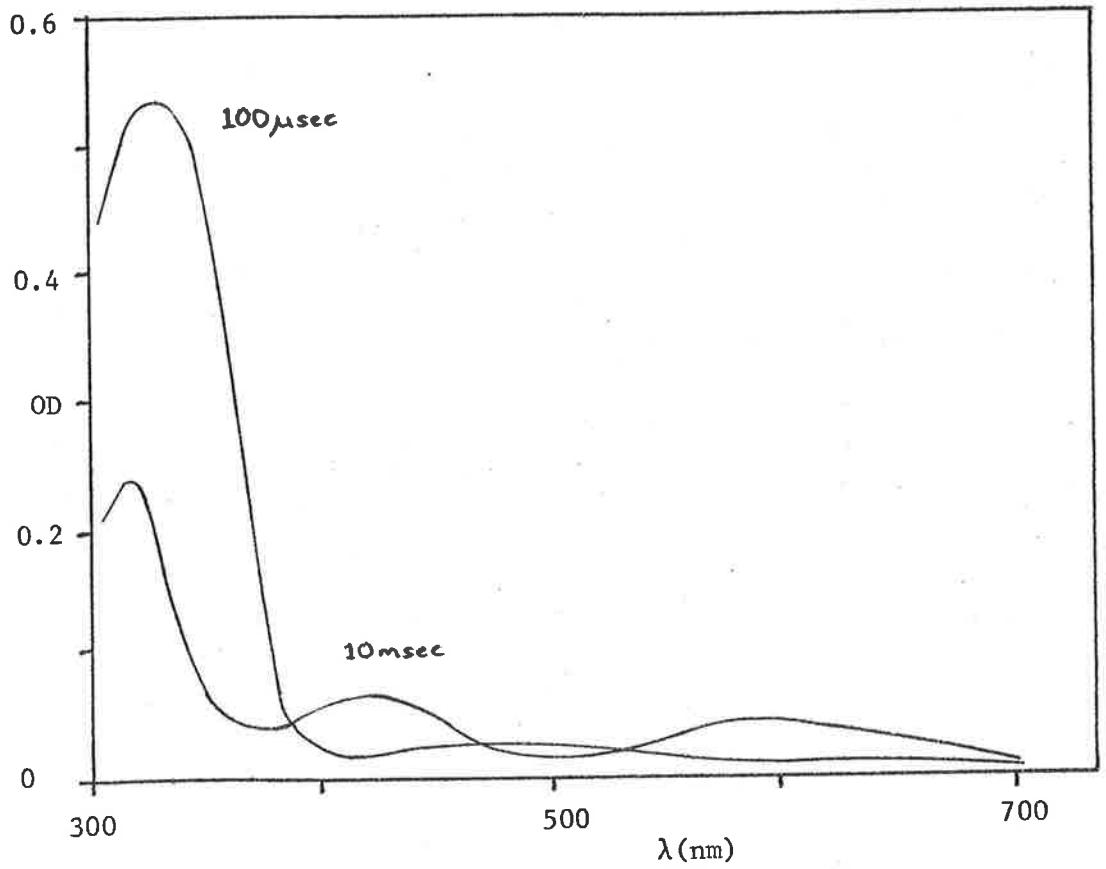

FIGURE VII 3.1

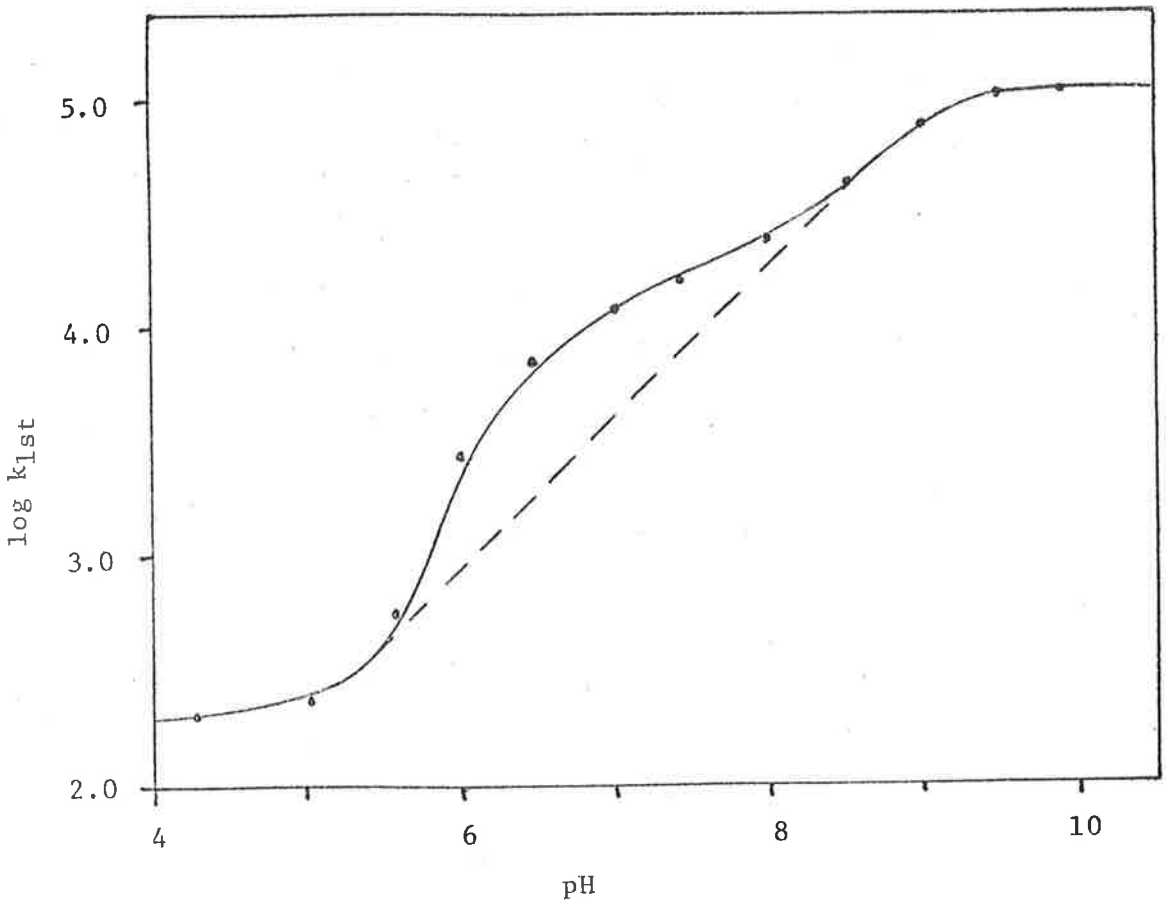

this complex, in which an unpaired electron may be considerably more delocalized than in the saturated complex analogue, suggests that attainment of stability by ring rupture is probable for the tetene as well as the diene. The retention of the chromophoric band in the product solutions suggests that the imine functions coordinated to the metal centre remain intact.

3. THE OVERALL pH RANGE 1-9

3.1 The apparent increase in the rate of conversion of Ni(III)L to Ni(II)L$^{\bullet}$ at pH 9 compared with pH 5 for the saturated complexes was further investigated. The first-order rate was measured as a function of pH in the range 4.0 - 9.8 for a flashed 20μM Ni(II)L (di, tam), 0.1M Br^- and 1mM H_2O_2 solution at 366nm. The pH dependence of the rate in this range for the tam complex is shown in figure VII 3.1 for unbuffered solutions. The pH was measured prior to flashing of the reaction solution. The decay was good first-order in the measured regions 4.0 - 5.5 and 8.5 - 9.8. However, in the region 5.5 - 8.5, usual decay characteristics were observed.

The observed reaction rate fell-off as the reaction proceeded. The first-order value of the rate shown in figure VII 3.1 is an apparent value measured for the first half-life of the decay. This decay reaction, which was particularly anomalous for solutions initially around pH 7, did not fit second-order kinetic analysis. When the reaction solution was buffered at pH 6.5 (using phosphate buffer) the decay was good first-order throughout, having a $t_{\frac{1}{2}}$ significantly slower than the initial $t_{\frac{1}{2}}$ of the unbuffered reaction at the same pH.

This anomalous kinetic effect in unbuffered solution is explained by the rapid introduction of OH^- into the solution during the flash by the reactions,

$$OH + Br^- \xrightarrow{Br^-} Br_2^- + OH^-$$

and

$$e^-_{aq} + H_2O_2 \longrightarrow OH + OH^-$$

Immediately after the flash, therefore, the pH of the solution is more basic by a few μM in $[OH^-]$ than the initial pH before flashing. The Ni(III)L thus decays in its initial stages more quickly than expected at the initial pH, and since this reaction involves the introduction of H^+ into solution, the basicity falls-off as the reaction proceeds; this causes the rate to fall accordingly. In the pH regions beyond this near-neutral range, the acid/base concentrations are high enough to buffer the flashed solutions for the small pH changes induced by the transient reactions. The presumed real pH dependence of the rate has been indicated by the dashed line in figure VII 3.1.

The diene complex showed an identical reactivity pattern to tam in the pH range 4.2 - 9.9. The tetene analogue displayed its first-order mode of decay for pH > 5.5 for which the observed rate was almost independent of pH up the measured limit of 9.2.

3.2 The pH dependence of the conversion of the Ni(III)L complex for di and tam to the ligand radical Ni(II)L$^{\bullet}$, is difficult to rationalize. A mechanism involving

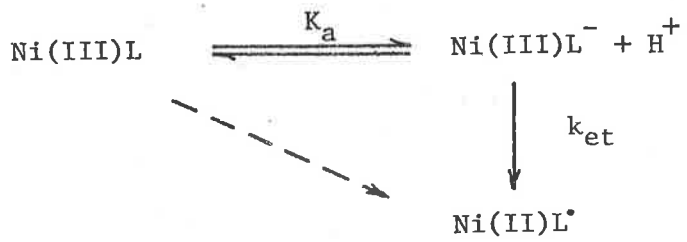

as suggested by Barefield,[46] does not satisfactorily explain the levelling-off of the rate at both the extremes of the pH range 4 and 9. The dependence apparently indicates that a direct path of conversion proceeding independently of the deprotonation equilibrium may be operative in the lower pH region.

3.3 Below pH 5.5, the transient decay in the tetene system observed at 366nm became mixed-order, and was good second-order below pH 4.5, this being the Br^- assisted decay mechanism discussed in section VI. For the diene complex the decay at 366nm was first-order at pH 4 but was second-order at pH 2, having the established characteristics of the Br^- assisted mechanism.

The transition between the first-order conversion process at pH>4, and the Br^- assisted decay studied at pH 1.0 for the tam complex was investigated further in 20μM Ni(II)tam, 0.1M Br^-, 50μM Br_2 solutions in the pH range 4.7 - 1.0. A plot of the difference in absorbance measured 0.5msec and 50msec after the flash, normalized by division of this difference by the 0.5msec absorption, is shown over the pH range in figure VII 3.3a. Within this range, the overall decay of the tervalent tam at 366nm was in two steps, the proportion of each step varying with increasing $[H^+]$ from being almost totally first-order at pH 4.7 with $k_{1st} \simeq 150sec^{-1}$ to second-order at pH 1.0 with $\frac{k}{\varepsilon l} \simeq 3.5sec^{-1}$. The characteristics of the overall decay are shown in figure VII 3.3b. At pH 3.0, the

FIGURE VII 3.3a

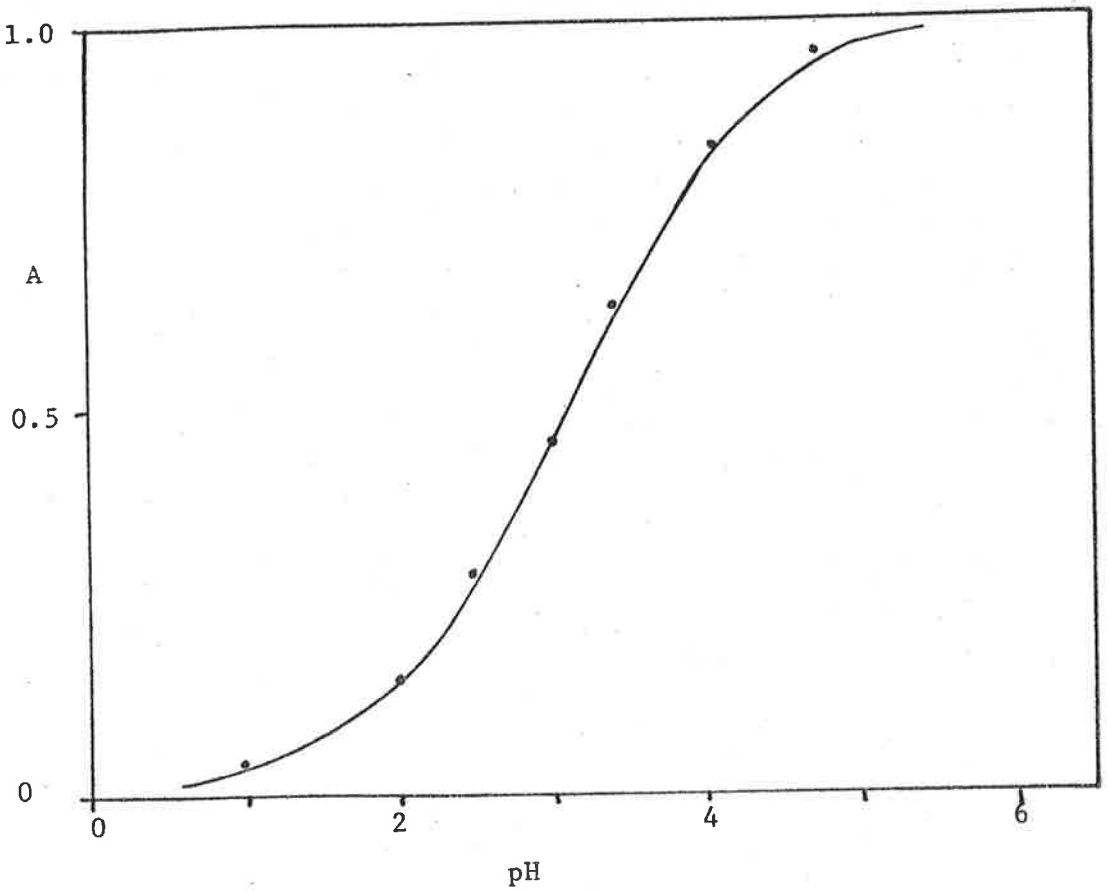

FIGURE VII 3.4

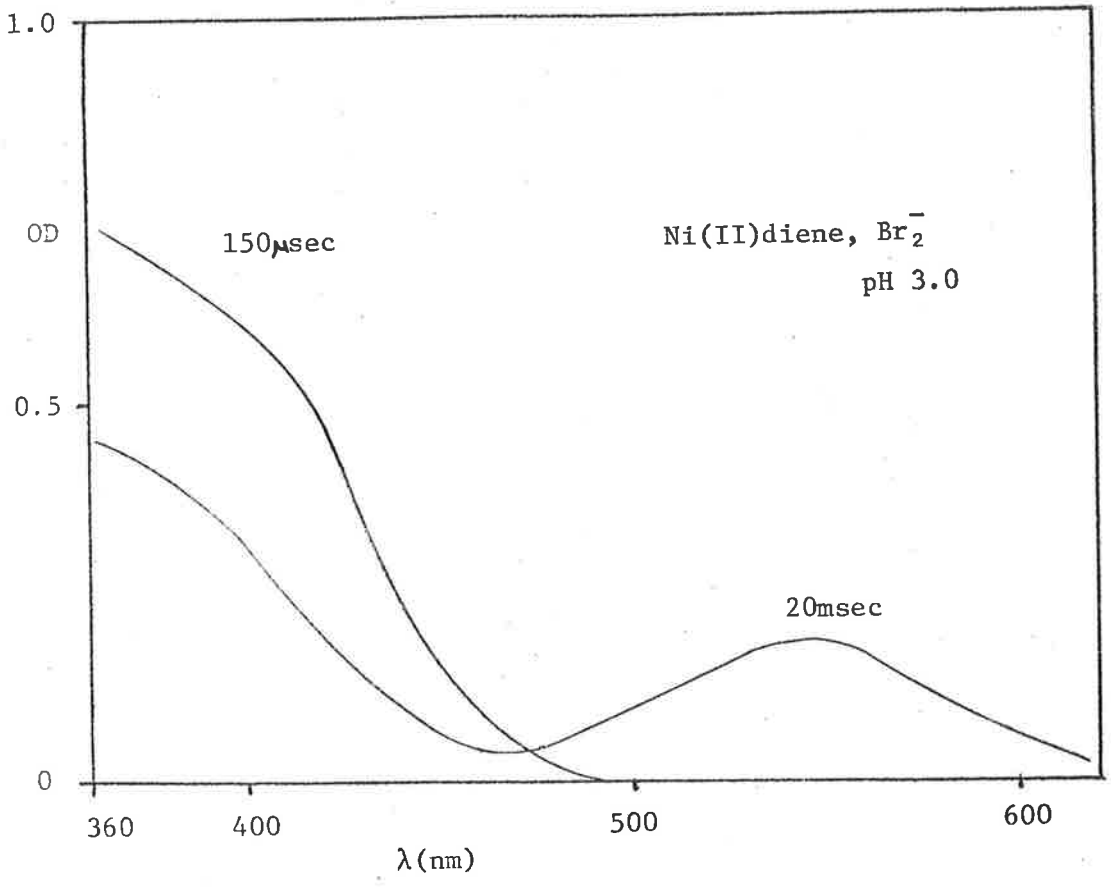

FIGURE VII 3.3b

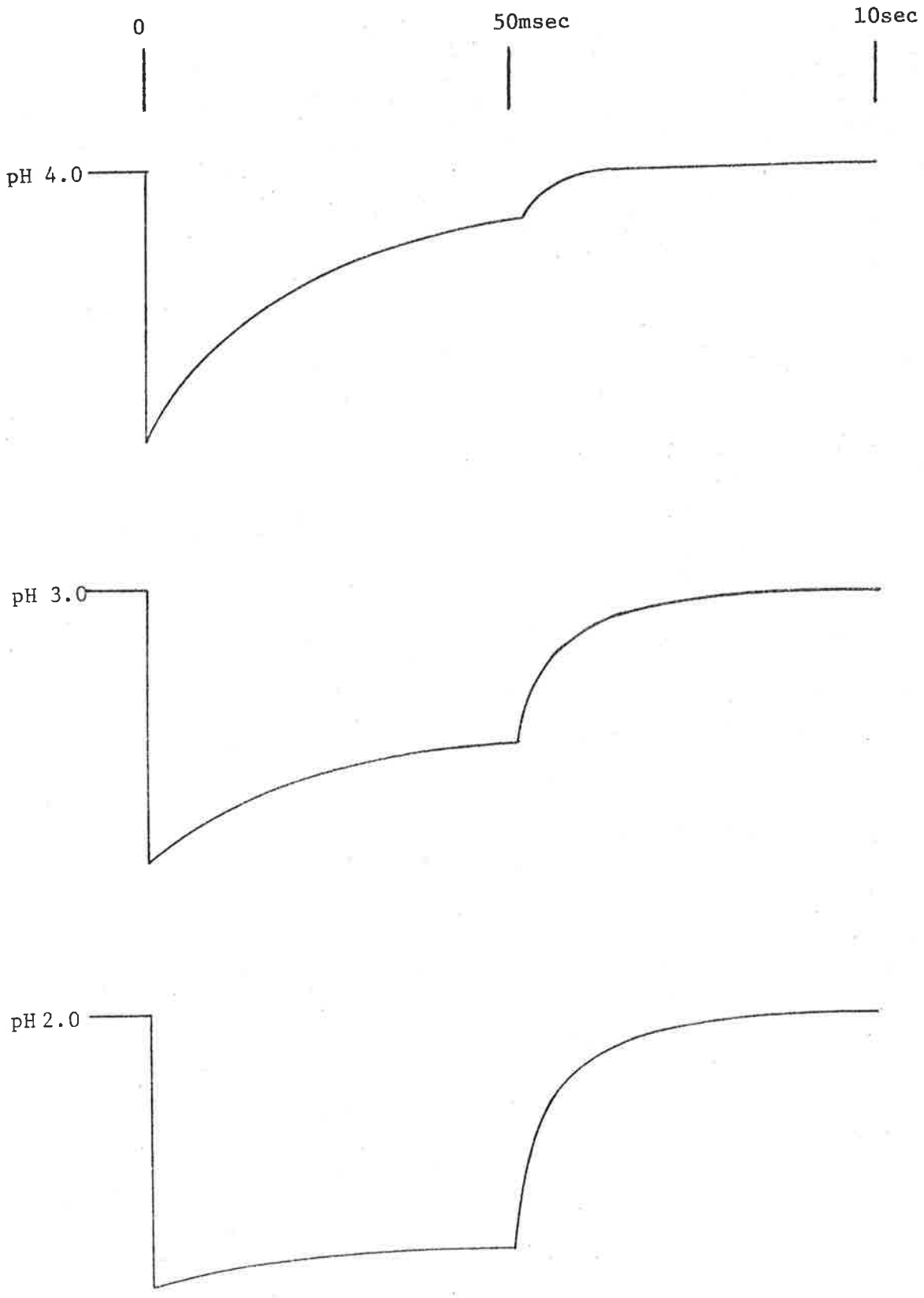

primary first-order process accounted for about half the overall decay, and had a rate similar to that at pH 4.7. The gradual elimination of this reaction as an observable process as the pH decreases below pH 4.7 is thus not due to a decrease in this rate constant. The gradual replacement of this reaction by the almost pH independent second-order Br^- assisted process cannot be explained at present. The mechanism is possibly similar to that presented in section III 3.5, where similar unusual effects were observed.

3.4 The probable equilibrium nature of the Ni(III)L $\rightarrow$ Ni(II)L$^\bullet$ + H^+ reaction was studied at pH 3.0 in a flashed 20μM Ni(II)di, 0.1mM $Co(NH_3)_5Br^{2+}$, 0.2mM Br^- solution. The transient spectra were measured 150μsec and 20msec after the flash in the region 360-600nm. The initial spectrum was that of tervalent Ni diene only, while that observed 20msec after the flash showed significant absorption characteristic of both Ni(III)L and Ni(II)L$^\bullet$ co-existing in solution (figure VII 3.4). The decay at 405nm was in two stages; the primary reaction was first-order with $k_{1st} \simeq 100sec^{-1}$, corresponding exactly to a formation at 546nm. The decay of the residual absorption after the conversion process had been completed was slow first-order at both wavelengths, with $k_{1st} \simeq 5sec^{-1}$.

These results suggest that the Ni(III)L complex produced by the flash undergoes an equilibrium conversion to the Ni(II)L$^\bullet$ intermediate, with the rate of approach to equilibrium being $\simeq 100sec^{-1}$ and with about half the original [Ni(III)L] converting at this pH. Once the equilibrium is established, the Ni(II)L$^\bullet$ species then decays via a first-order process to stable products. Since the equilibrium is labile on this time scale, the Ni(III)L complex observed at 405nm, appears to decay at the same rate

by proceeding through the Ni(II)L$^{\bullet}$ intermediate. Since the loss of the [Ni(III)L] in attaining the equilibrium corresponds to the increase in the [Ni(II)L$^{\bullet}$], the $\varepsilon_{546}/\varepsilon_{405}$ ratio can be determined from $\Delta OD_{546}/\Delta OD_{405}$ at the time of establishment of the equilibrium (20msec after the flash). From figure VII 3.4, $\varepsilon_{546}/\varepsilon_{405} \simeq 0.65$. (This result is significant to section III 2.3).

VIII SUPPLEMENTARY STUDIES

1. OTHER PRECURSOR OXIDANTS

1.1 I_2^- : The observed disproportionation rate of I_2^- at 366nm in a flashed 0.1M I^- solution at pH 1.0 was unchanged by the addition of 100μM Ni(II)L or Cu(II)di, suggesting that the rates of M(II) + I_2^- are $\lesssim 5 \times 10^7 M^{-1} sec^{-1}$. (This and the other estimates presume that a M(II)L + X_2^- rate $\gtrsim$10% of the X_2^- + X_2^- rate would be observable.)

1.2 $(SCN)_2^-$: The effect of added M(II)L on the observed disproportionation of $(SCN)_2^-$ at 485nm in 1mM SCN^-, 2mM H_2O_2 solutions were determined at pH 1.0. For the bivalent nickel di and tam complexes, the decay changed to reasonable pseudo-first order, having a corresponding formation at 366nm with the same rate. By varying [Ni(II)L] over the range 20 - 100μM, the specific second-order rates were estimated:

$$k(Ni(II)tam + (SCN)_2^-) \sim 2 \times 10^8 M^{-1} sec^{-1}$$

$$k(Ni(II)di + (SCN)_2^-) \sim 6 \times 10^8 M^{-1} sec^{-1}$$

The disproportionation reaction at 485nm was unaffected by the presence of 150μM Ni(II)tet or Cu(II)di, suggesting that the rate of M(II)L + $(SCN)_2^-$ is $\lesssim 10^8 M^{-1} sec^{-1}$ for these complexes.

The decay of the tervalent tam and di complexes in this system was second-order, having values of $\frac{k}{\varepsilon l}$ at 366nm similar to those determined in section III 3.4, where 1mM SCN^- was added to 0.1M Br^- solutions. Further kinetic analysis was not attempted.

2. THE Ni(III)L + H_2O_2 REACTIONS

2.1 The reaction of tervalent nickel with H_2O_2 was observed at 366nm in flashed solutions containing 20μM Ni(II)L, 0.1M Cl^- and $[H_2O_2]$ in the range 1 - 6mM, generally over the pH range 0.5 - 4.0. The specific rates of Ni(III)L + H_2O_2 were determined from plots of the observed pseudo-first order rate constants against $[H_2O_2]$.

In this system, the photo-produced OH radicals were scavenged almost entirely by the Cl^- to produce the precursor oxidizing radicals Cl_2^-. Although the specific rate of Cl^- + OH falls-off with increasing pH by a factor of about 10^3 between pH 1.0 and 4.0[84], it can be considered that ≳80% of the OH radicals react with Cl^- in the low acid solutions.

2.2 For the tetene complex, the specific rate of the tervalent reaction with H_2O_2 was almost independent of pH in the region 0.5 - 4.0, increasing by a factor of only 1.9 over this range; the value of

$$k(Ni(III)tet + H_2O_2) = 3.3\ (\pm 0.4) \times 10^3 M^{-1} sec^{-1}$$

was determined at pH 0.5. The rate increase may be presumed to be due to medium effects. The decay process was independent of [Ni(II)tet] (10 - 50μM) over the pH range studied. Addition of 50μM TNM to the solution at pH 4.0 resulted in a 30% reduction in the observed pseudo-first order decay rate at 1mM H_2O_2.

The tervalent diene complex rate of reaction with H_2O_2 was pH independent in the region 1.0 - 3.0, with

$$k(Ni(III)di + H_2O_2) = 2.3\ (\pm 0.3) \times 10^3 M^{-1} sec^{-1}$$

FIGURE VIII 2.2a

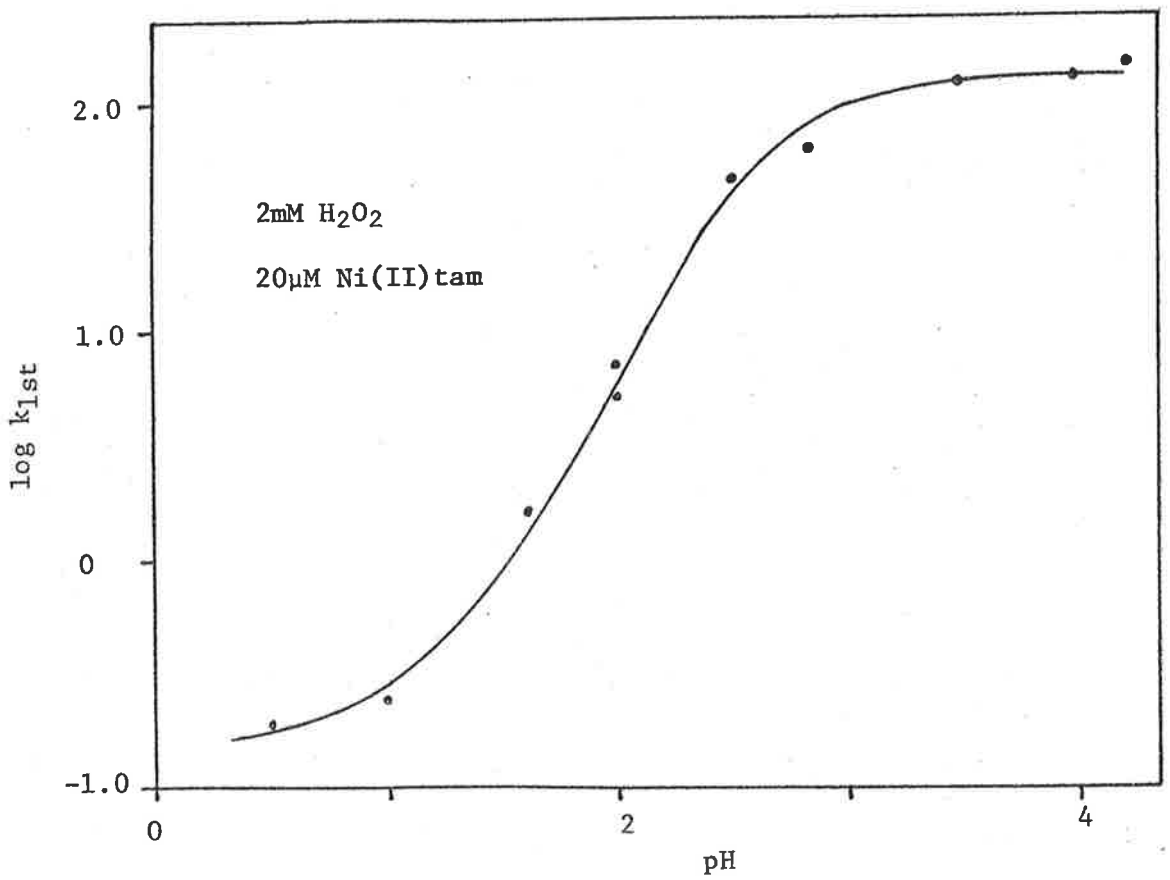

FIGURE VIII 2.2b

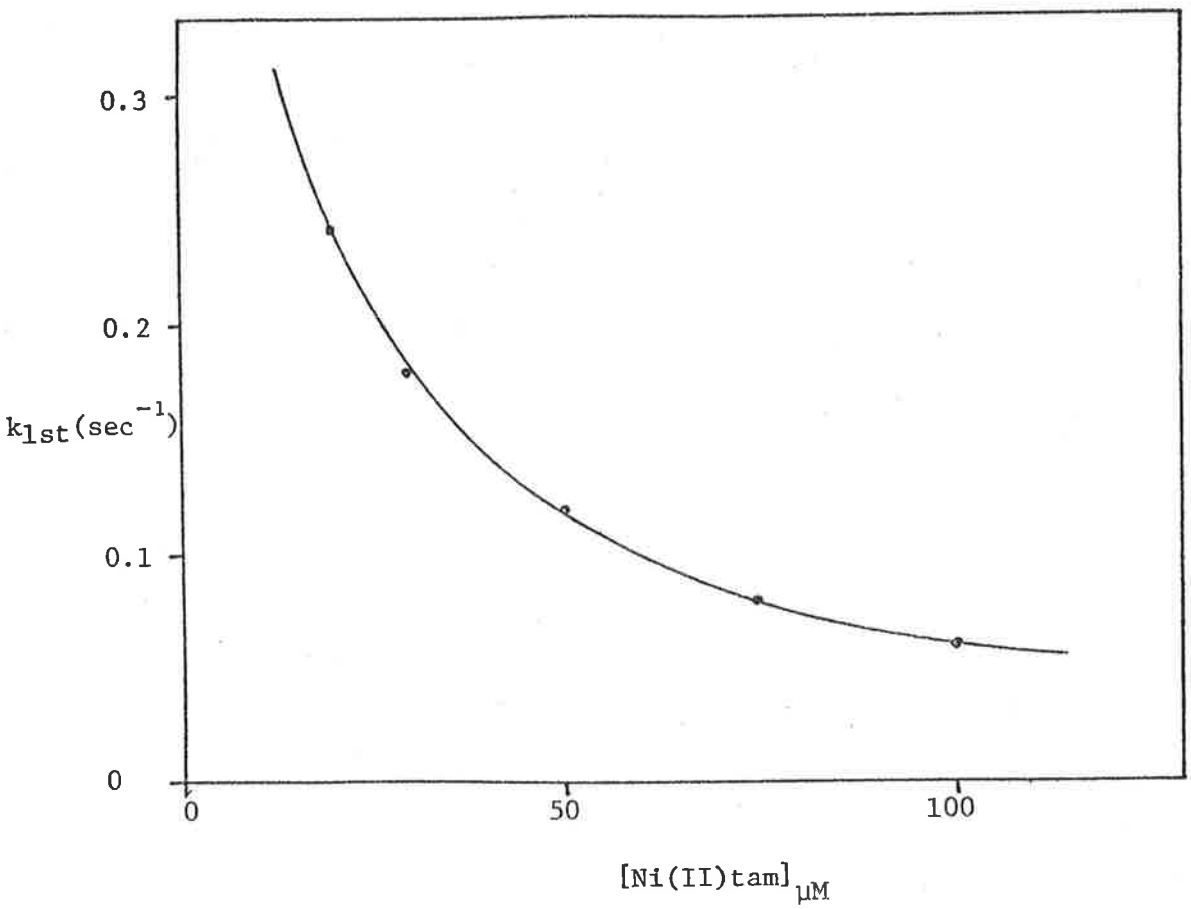

At pH 0.5, the specific rate constant was 1.4 (±0.2) x $10^3 M^{-1} sec^{-1}$.

The observed rate of the Ni(III)tam + H_2O_2 reaction was very pH dependent in the range pH 0.5 - 4.0, as shown in figure VIII 2.2a. The pseudo-first order decay rate observed for a 2mM H_2O_2 solution was independent of [Ni(II)tam] at pH 3.0, but showed a definite inverse dependence on this concentration at pH 1,0 (figure VIII 2.2b).

2.3 The oxidation of H_2O_2 by metal ions has been studied for Ce(IV), Ag(II), Co(III), Mn(III), Fe(III),[212] and Ru(III).[215] The stoichiometric equation,

$$2M^{n+} + H_2O_2 = 2M^{(n-1)+} + O_2 + 2H^+$$

for the overall reaction has been found to be made up of basically two processes, the former being rate determining;

$$M^{n+} + H_2O_2 \longrightarrow M^{(n-1)+} + HO_2 + H^+$$

$$M^{n+} + HO_2 \longrightarrow M^{(n-1)+} + O_2 + H^+$$

Kinetic spectrophotometric investigations suggest that the reactions of Mn(III), Ag(II), Fe(III), Ce(IV) and Co(III) are inner-sphere reductions involving cation-HO_2^- complexes in the first step.[212] In the Ce(IV), H_2O_2 system, the complex intermediate Ce(III)-HO_2 is considered to form; this species is capable of back reaction to H_2O_2 in sulphuric acid solution.[216] The absence of the back reaction in perchloric acid is due to the higher E^o for the Ce(IV)/Ce(III) couple in this acid, by ~0.17 volt, compared with sulphuric acid.[217]

Considering this mechanism for the Ni(III)L reactions with H_2O_2, i.e.

$$Ni(III)L + H_2O_2 \underset{k_{-1}}{\overset{k_1}{\rightleftharpoons}} Ni(II)L + HO_2 + H^+$$

$$Ni(III)L + HO_2 \xrightarrow{k_2} Ni(II)L + O_2 + H^+$$

in which the back reaction is included in the first-step, the rate equation for tervalent Ni decay has the form

$$-\frac{d[Ni(III)L]}{dt} = \frac{2k_1k_2[Ni(III)L]^2[H_2O_2]}{k_{-1}[Ni(II)L] + k_2[Ni(III)L]} \quad \ldots(1)$$

assuming steady-state conditions apply for the HO_2 concentration.

$$\text{i.e.} \qquad [HO_2] = \frac{k_1[Ni(III)L]\ [H_2O_2]}{k_{-1}[Ni(II)L] + k_2[(Ni(III)L]}$$

In the presence of HO_2 scavenger, S, another term is introduced into the scheme

viz. $$S + HO_2 \xrightarrow{k_3} \text{products}$$

(i) If $k_2[Ni(III)L] >> k_{-1}[Ni(II)L]$, rate equation (1) above simplifies to

$$-\frac{d[Ni(III)L]}{dt} = 2k\,[Ni(III)L]\,[H_2O_2] \quad \ldots \quad (2)$$

With HO_2 scavenger present, this equation takes the form.

$$-\frac{d[Ni(III)L]}{dt} = (1 + A)\,k\,[Ni(III)L]\,[H_2O_2]. \ldots \quad (3)$$

where

$$A = \frac{k_2[Ni(III)L]}{k_2[Ni(III)L] + k_3[S]}$$

This mechanism, in the form of the rate expression (2), satisfactorily applies for the tetene and diene systems. Support for the

mechanism comes from the observed decrease in the tetene rate in TNM solution for which rate expression (3) applies. The fall-off in the rate of the diene reaction below pH 1.0, may be due to the increasing significance of the back reaction in the first step under such conditions.

(ii) If k_{-1} Ni(II)L cannot be considered to be $<< k_2[Ni(III)L]$, rate expression (1) can be rearranged to the form,

$$\frac{1}{k_{obs}} = \frac{1}{2k_2[Ni(III)L]} \left[1 + \frac{k_{-1}[Ni(II)L]}{k_2[Ni(III)L]} \right]$$

For the tam system at pH 1.0, where the observed rate had a negative dependence on [Ni(II)tam], a plot of the experimental data according to the above expression, viz. k_{obs}^{-1} versus [Ni(II)L], was linear with an intercept, as expected if [Ni(III)L] can be assumed constant. This result, which indicates the reversibility of the first-step of the Ni(III)tam + H_2O_2 reaction, confirms the evidence presented in section III 3.4, in which a negative dependence of the rate of Ni(III)tam + HO_2 in acidic solution was observed.

It is apparent that the Ni(II)L + HO_2 reaction only occurs with any measurable efficiency for the tam complex in acidic solution. This is a consequence of the HO_2 being a powerful enough oxidant to efficiently oxidize only the tam complex of the ligand series. The increased efficiency of this reaction with increased acidity of the solution accounts for the observed fall-off in the specific rate of the Ni(III)tam + H_2O_2 for pH $\lesssim$ 3.0. The acid-catalyzed mechanism of the Ni(II)tam + HO_2 reaction has been discussed previously in section III 3.5.

2.4 The Cu(III) di + H_2O_2 rate was measured at 313nm in a 100μm Cu(II)di, 0.1M Cl^- solution at pH 1.0 over a range of $[H_2O_2]$ of 8-22mM;

$$k(Cu(III)di + H_2O_2);\ 6.2\ (\pm 0.8) \times 10^2 M^{-1} sec^{-1}$$

3. REACTIONS WITH ADDED METAL IONS.

3.1 The rates of reaction of Ni(III)L with some oxidizible metal ions were determined. In these systems Cl_2^- and Br_2^- were used as the precursor oxidizing radicals. The Ni(II)L and metal ion concentrations were adjusted so that the majority of the photo-produced radical anions reacted with the bivalent macrocycle. The reactions of the Ni(III)L complexes with the added substrates were observed under pseudo-first order conditions, so that plots of k_{obs} versus [metal ion] were linear; the specific second-order rate constant was determined from the slope of the plot. (Unless otherwise stated the linear plot passed through the origin). The addition of the bivalent metal ions to the halide solutions resulted in no complication due to MX^+ formation, since the formation constants for such complexes are quite low.(140)

3.2 Fe(II): The specific rate of Ni(III)di + Fe^{2+} was determined at 405nm to be the same irrespective of the precursor X_2^- radical.

(i) In 20μM Ni(II)di, 0.1M Br^- solutions at pH 1.0, with $[Fe^{2+}]$ between 0.43 - 1.83mM, the derived rate was 2.4 (±0.3) x $10^4 M^{-1} sec^{-1}$.

(ii) In 20μM Ni(II)di, 0.1M Cl^-, 1mM Fe^{3+} solutions at pH 1.0, over the same $[Fe^{2+}]$ range, the rate constant was determined to be 1.8 (±0.2) x 10^4 $M^{-1} sec^{-1}$ (see figure IV 3.3).

The Ni(III)tet and tam rates of Fe^{2+} oxidation were determined using Cl_2^- as precursor radical in systems analogous to (ii) above (as mentioned in section IV 3.3). The specific rates determined from the pseudo-first-order plots were;

$k(Ni(III)tet + Fe^{2+}) : 3.6(\pm0.4) \times 10^4 M^{-1} sec^{-1}$

$k(Ni(III)tam + Fe^{2+}) : 4.2\ (\pm0.6) \times 10^4 M^{-1} sec^{-1}$

3.3. Mn(II): Addition of 10mM Mn^{2+}_{aq} to 20μM Ni(II)L (where L = di, tam), 0.1M Cl^-, 1mM Fe^{3+} solutions at pH 1.0 resulted in no observable increase in the slow second-order decay of the tervalent complexes at 405nm (see section IV 3.3). This suggests that if these Ni(II)L + Mn^{2+} reactions do occur, their specific rates of reaction are $\lesssim 10 M^{-1} sec^{-1}$.

The addition of Mn^{2+} to the tetene analogue resulted in a change of the decay process to pseudo-first order kinetics. The Ni(III)tet + Mn^{2+} rate was determined from the rate analysis over the $[Mn^{2+}]$ range 0-16.4mM. The plot is shown in figure VIII 3.3. From the slope,

$k(Ni(III)L + Mn^{2+}) : 1.5\ (\pm0.2) \times 10^2 M^{-1} sec^{-1}$

(The presence of an intercept in the absence of added Mn^{2+} is a consequence of the residual reaction of Ni(III)tet with the photoproduced Fe^{2+} in solution).

3.4 Co(II): The addition of 20mM Co^{2+} to solutions at pH 1.0 containing 20μM Ni(II)L and either (i) 0.1M Br^- or (ii) 0.1M Cl^-, 1mM Fe^{3+}, showed no change in the corresponding Ni(III)L decay rates for each system. Thus the specific rate of the Ni(III)L + Co^{2+} reaction, should it occur, is $\lesssim 1 M^{-1} sec^{-1}$.

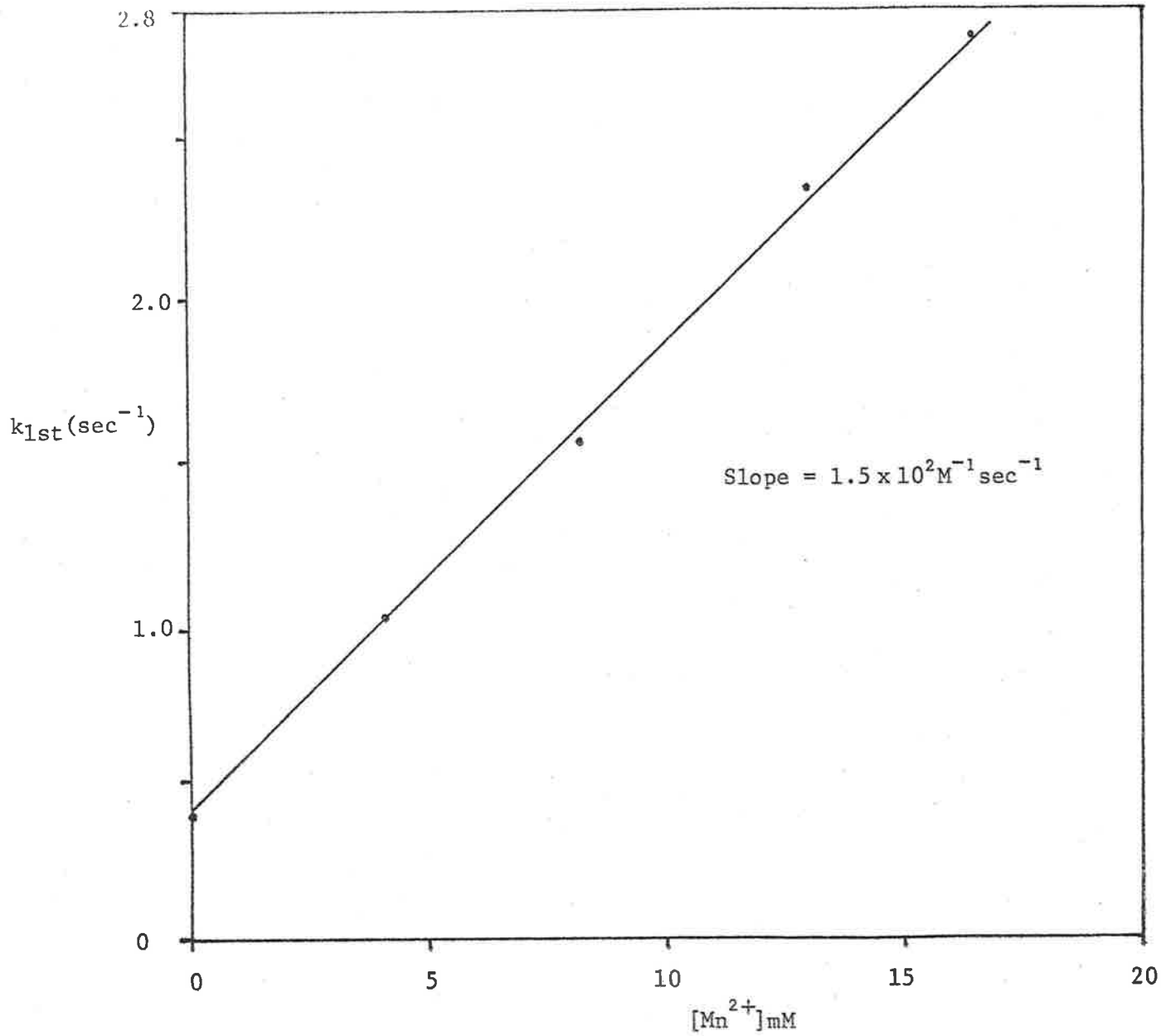

FIGURE VIII 3.3

REFERENCES

1. F.A. Cotton, G. Wilkinson
   Advanced Inorganic Chemistry, Third edition, John Wiley, New York (1972)

2. L. Mond
   J. Soc. Chem. Ind. 49T, 371 (1930)

3. R.S. Nyholm
   Chem. Revs, 53, 263 (1953)

4. W. Levason, C.A. McAuliffe
   Coord. Chem. Rev. 12, 151 (1974)

5. J.A. Howard, J.H.B. Chenier
   Can. J. Chem. 54, 382 (1976)

6. A.V. Babaeva, I.B. Baranokskii, G.G. Afanas´eva
   Russ. J. Inorg. Chem. 10, 686 (1965)

7. N.F. Curtis, D.F. Cook
   Chem. Commun. 962 (1967)

8. E.K. Barefield, D.H. Busch
   Chem. Commun., 523 (1970)

9. D.C.Olson, J. Vasilevskis
   Inorg. Chem. 8, 1611 (1969)

10. R.S. Nyholm
    J. Chem. Soc. 2602 (1951)

11. G.A. Barclay
    Rev. Pure Appl. Chem. 4, 77 (1954)

12. G.A. Barclay, A.K. Barnard
    J. Chem. Soc. 4269, (1961)

13. K.A. Jensen, B.Nygaard, C.T. Petersen
    Acta Chem. Scand. 17, 1126 (1963)

14. G.E. Wymore, J.C. Bailar
    J. Inorg. Nucl. Chem. 14, 42 (1960)

15. G.R. van Hecke, W.D. Horrocks
    Inorg. Chem. 5, 1968 (1966)

16. J.J. Born, P.J.M.W.L. Birker, J.J. Steggerda
    Inorg. Chem. 10, 1202 (1971)

17. A.L. Balch, R.H. Holm
    J. Am. Chem. Soc. 88, 5201 (1966)

18. A.H. Maki, N.Edelstein, A. Davison, R.H.Holm
J. Am. Chem. Soc. 86, 4508 (1964)

19. E.I. Stiefel, J.H. Waters, E. Billig, H.B. Grey
J. Am. Chem. Soc. 87, 3016 (1965)

20 R.H. Holm, A.L. Balch, A. Davison, A.H. Maki, T.E. Barry
J. Am. Chem. Soc. 89, 2866 (1967)

21. W. Klemm, W. Brandt, R. Hoppe
Z. Anorg. Allg. Chem. 308, 179 (1961)

22. E.S. Gore, D.H. Busch
Inorg. Chem. 12, 1 (1973)

23. P. Kriesman, R. Marsh, J.R. Preer, H.B. Gray
J. Am. Chem. Soc. 90, 1967 (1968)

24. V.M. Peshkova, V.M. Savostina
"Analytical Chem of Nickel"
Israel Prog. for Scientific translations, pg 27 (1967)

25. K.A. Jensen, B. Nygaard
Acta Chem. Scand. 3, 481 (1949)

26. E.G. Vassian, R.K. Murmann
Inorg. Chem. 6, 2043 (1967)

27. I. Fried, D. Meyerstein
Israel J. Chem. 8, 865 (1970)

28. I. Fried, D. Meyerstein
Electoral. Chem and Interfacial Electrochem 29, 429, (1971)

29. F.V. Lorecchio, E.S. Gore, D.H. Busch
J. Am. Chem. Soc. 96, 3109 (1974)

30. N.F. Curtis
Coord Chem. Rev. 3, 3 (1968)

31. J.C. Dabrowiak, F.V. Lovecchio, V.L. Goedken, D.H. Busch
J. Am.Chem. Soc. 94, 5502 (1972)

32. E.K. Barefield, D.H. Busch
Inorg. Chem. 10, 108 (1971)

33. V.L. Goedken, D.H. Busch
J. Am. Chem. Soc. 94, 7355 (1972)

34. C. Hipp, D.H. Busch
Inorg. Chem. 11, 1983 (1972)

35. G.N. Schrauzer, E. Deutch
J. Am. Chem. Soc. 91, 3341 (1969)

36. K. Farmery, D.H. Busch
Inorg. Chem. 11, 2901 (1972)

37. G. Costa, G. Mestroni, E. Savorguani
Inorg. Chem. Acta. 3, 323 (1969)

38. D.H. Busch
Science, 171, 241 (1971)

39. D. Dolphin, R.H. Felton, D.C. Bry, J. Fajer
J. Am. Chem. Soc. 92, 743 (1970)

40. C. Hipp, D.H. Busch
J. Chem. Soc, Chem. Commun. 737 (1972)
Inorg. Chem. 12, 894 (1973)

41. J.L. Karn, D.H. Busch
Inorg. Chem, 8, 1149 (1969)

42. E.K. Barefield, F.V. Lovecchio, N.E. Tokel, E. Ochiai, D.H. Busch
Inorg. Chem. 11, 283 (1972)

43. N.F. Curtis
J. Chem. Soc. 2644 (1964)

44. D.C. Olson, J. Vasilevskis
Inorg. Chem. 10, 463 (1971)

45. F.P. Hinz, D,W. Margenum
J. Am. Chem. Soc. 96, 4993, (1974)

46. E.K. Barefield, M.T. Mocella
J. Am. Chem. Soc. 97, 4238 (1975)

47. M.O. Kestner, A.L. Allred
J. Am. Chem. Soc. 94, 7189 (1972)

48. M.T. Mocella, E.K. Barefield
Inorg. Chem. 12, 2829 (1973)

49. N.F. Curtis, T.N. Milestone
Aust. J. Chem. 28, 275 (1975)

50. J.M. Palmer, E. Papaconstantinou, J.F. Endicott
Inorg. Chem. 8, 1516 (1969)

51. A.V. Babaeva, J.B. Baranovskii, G.G. Afanas´eva
Russ. J. Inorg. Chem. 13, 660 (1968)

52. D. Meyerstein
Inorg. Chem. 10, 638 (1971)

53. J. Lati, D. Meyerstein
Inorg. Chem. 11, 2393 (1972)

54. J. Lati, D. Meyerstein
Inorg. Chem. 11, 2397 (1972)

55. J. Lati, D. Meyerstein
Israel J. Chem. 10, 735 (1972)

56. J. Lati, D. Meyerstein
Int. J. Radiat. Phys. Chem. 7, 611 (1975)

57. A.T. Thornton, G.S. Laurence
J. Chem. Soc. Dalton, 1632 (1973)

58. S.D. Malone, J.F. Endicott
J. Phys. Chem. 76, 2223 (1972)

59. B. Falcinella, P.D. Felgate, G.S. Laurence
J. Chem. Soc. Dalton. 1367 (1974)

60. R.C. Wright, G.S. Laurence
J. Chem. Soc. Chem. Commun. 132 (1972)
and papers referred to therein.

61. D. Lachenal
Inorg. Nucl. Chem. Letters 11, 101 (1975)

62. M. Anbar
Advan. Chem. Ser. 49, 126 (1965)

63. T.J. Truex, R.H. Holm
J. Am. Chem. Soc. 94, 4529 (1972)

64. D.F. Mahoney, J.K. Beattie
Inorg. Chem. 12, 2561 (1973)
and references therein

65. L.F. Lindoy
Chem. Soc. Rev. 4, 421 (1975)

66. E.K. Barefield
Ph.D. Thesis, Ohio State University (1969)

67. A.S. Ghosh-Mayumdar, E.J. Hart
Adv. Chem. Ser. 1968, 81, 193

68. N.F. Curtis, Y.M. Curtis, H.K.J. Powell
J. Chem. Soc. A. 1015 (1966)

69. L.G. Warner, D.H. Busch
J. Am. Chem. Soc. 91, 4092 (1969)

70. J.G. Mohanty, A. Chakravorty
Inorganica Chimica Acta 18, L33 (1976)

71. G.C. Allen, K.D. Warren
Inorg. Chem. 8, 1895 (1969)

72. P.T. Beurskens, J.A. Cras, J.J. Steggerda
Inorg. Chem. 7, 810 (1968)

73. L. Janovsky,
Z. Anorg. u. Allgem. Chem. 307, 208 (1961)

74. M.W. Lister
Canad. J.Chem. 39, 2330 (1961)

75. T.L. Allen
J. Am.Chem. Soc. 77, 2306 (1951)

76. C.E. Bawn, D. Margerison
Teans. Farad Soc. 51, 925, (1955)

77. F. Feigl
'Chemistry of Specific and Sensitive Reactions' p.130,
Acedemic, N.Y. 1949

78. D. Meyerstein
Inorg. Chem. 10, 2244 (1971)

79. M. Anbar, R. Munoz, P. Rona
J. Phys. Chem. 67, 2708 (1963)

80. M. Anbar, A. Levitzki
Radiat. Res. 27, 32 (1966)

81. A. Levitzki, M. Anbar
J. Am. Chem. Soc. 89, 4185 (1967)

82. G.E. Adams, L.M. Dorfman,
Nat. Bur. Stud.
Nat. Ref. data Series No 43 (1973)
and references contained therein

83. G. Semerano
Coord. Chem.Rev. 16, 185 (1975)

84. M. Anbar, P. Neta
Int. J. App. Radiat. Isotopes 18, 493 (1967)

85. R.L. Wilson, C.L. Greenstock, G.E. Adams, R. Wageman, L.M. Dorfman
Int. J. Radiat. Phys. Chem. 3, 211 (1971)

86. L. Grossweiner, M. Matheson
J. Phys. Chem. 61, 1089 (1957)

87. A. Fudge, K. Sykes
J. Chem. Soc. 119 (1952)

88. P. Carter, N. Davidson
J. Phys. Chem. 56, 877 (1952)

89. L. Grossweiner, M. Matheson
J. Chem. Phys. 23, 2443 (1955)

90. E. Gusarski, A. Treinin
J. Phys. Chem. 69, 3176 (1965)

91. M.S. Matheson, W.A. Mulac, J. Rabani
J. Phys. Chem. 67, 2613 (1963)

92. A.T. Thornton
PhD. Thesis Univ. of Adelaide (1973)

93. J. Baxendale, P. Bevan, D. Stott
Trans. Farad. Soc. 64, 2389 (1968)

94. M. Anbar, J. Thomas
J. Phys. Chem. 68, 3829 (1964)

95. G. Adams, J. Boag, B. Michael
Trans. Farad. Soc. 61, 1674 (1965)

96. B. Cercek, M. Ebert, C. Gilbert, A. Swallow
'Pulse Radiolysis' Acedemic Press New York, pg 83 (1965)

97. J. Thomas
Trans. Farad. Soc. 61, 702 (1965)

98. D. Behar, P. Bevan, G. Scholes
J. Phys. Chem. 76, 1537 (1972)

99. D. Behar
J. Phys. Chem. 76, 1815 (1972)

100. J.H. Baxendale, J.A. Wilson
Trans. Farad. Soc. 53, 344 (1957)

101. G. Czapski
Anna. Rev. Phys. Chem. 22, 191 (1971)

102. D. Behar, G. Czapski, L.M.Dorfman, J. Rabani, H.A. Schwarz
J. Phys. Chem. 74, 3209 (1970)

103. A. Samuni, G. Czapski
In. J. Chem. 7, 361 (1969)

104. K. Sehested, O.L, Ramussen, H. Fricke
J. Phys. Chem. 72, 2 (1969)

105. J. Pucheault, C.Ferradini, A. Buu
Int. J. Radiat. Phys. Chem. 1, 209 (1969)

106. C. Ferradini, C. Seide
Int. J. Radiat. Phys. Chem. 1, 219 (1969)

107. B.H.J. Bielski, H.A. Schwarz
J. Phys. Chem. 72, 3836 (1968)

108. G. Czapski, D. Meisel
Int. J. Radiat. Chem. (1971)

109. F. Haber, R. Willstatter
Chem. Ber. 64, 2844 (1931)

110. F. Haber, J. Weiss
Proc. Royal Soc. A147, 332 (1934)

111. T. Anderson, T.R. Byberg, K.J. Olsen
J. Phys. Chem. 71, 4129 (1967)

112. I. Fridovich
Accounts Chem. Res. 5, 321 (1972)

113. D. Ballou, G. Palmer, V. Massey
Biochem. Brophys. Res. Commun. 36, 898 (1969)

114. P. Airey
A.A.E.C. Lucas Heights - private communication

115. J.M. Pink
Canad. J. Chem. 48, 1169 (1970)

116. V. Balzani, V. Carassiti
'Photochemistry of Coordination Compounds'
Academic press, New York (1970)

117. E. Rabinowitch
Rev. Mod. Phys. 14, 112 (1942)

118. M. Evans, N. Uri
Nature 164 , 404 (1949)

119. M. Evans, M. Santappa, N. Uri
J. Plymer. Sci. 7, 243 (1951)

120. R.C. Wright, G.S. Laurence
Chem.Commun. 132 (1972)

121. M.E. Langmuir, E.J. Hayon
J. Phys. Chem. 71, 3308, (1967)

122. G. Caspari, R.G. Hughes, J.F. Endicott, M.Z. Hoffman
J. Am. Chem. Soc. 92, 6801 (1970)

123. T.L. Kelly, J.F. Endicott
J. Am. Chem. Soc, 92 5733 (1970)
J. Am. Chem. Soc. 94, 1797 (1972)

124. N. Uri
Chem. Rev. 52, 375 (1952)

125. K.J. Ellis, G.S. Laurence
Trans. Farad. Soc. 63, 91 (1967)

126. M. Evans, N. Uri
Symposium #5 'Co_2 fixation and Photosynthesis'
Soc. for exptal biol. Sheffield, 1950.
Cambridge Uni Press, Cambridge (1951)

127. R. Betts, F. Dainton
J. Am. Chem. Soc. 75, 5721 (1953)

128. A.T. Thornton, G.S. Laurence
J. Chem. Soc. Datton, 1632 (1973)

129. J.F. Endicott, M.Z. Hoffman
J. Am. Chem. Soc. 87, 3348 (1965)

130. A.W. Adamson
Disc. Farad Soc. 29, 163 (1960)

131. L. Moggi, N. Sabbatini, V. Balzani
Gazz. chim ital 97, 980 (1967)

132. A.T. Thornton, G.S.Laurence
J. Chem. Soc, Dalton, 805 (1973)
ibid 1637 (1973)
ibid 1142 (1974)

133. J.H. Baxendale
Radiat. Res. Suppl. 4, 114 (1964)

134. J.H. Baxendale, M.D. Ward, P. Wardman
Trans. Farad Soc. 67, 2532 (1971)

135. L.E. Bennett
Progr. Inorg. Chem. 18, (1973)

136. D. Meisal, G. Czapski
J. Phys. Chem. 79, 1503 (1975)

137. P.S. Rao, E. Hayon
J. Phys. Chem. 79, 397 (1975)

138. S.D. Malone, J.F. Endicott
J. Phys. Chem. 76, 2223 (1972)

139. D.P. Rillema, J.F. Endicott, N.A.P. Kane-Maguire,
J. Chem. Soc. Chem. Commun. 495 (1972)

140. L.G. Sillén, A.E. Martell
Stability constants of Metal-ion Complexes
Chem. Soc. Special Publication No 25 (1971)

141. A.E. Vogel
Quantitative Inorganic Analysis
Longmans, London (1962)

142. A. Henglein, J. Langhoff, G. Schmidt
J. Chem. Soc. 63, 980, (1959)

143. G. Schlessinger
Inorg. Synth. 6, 180 (1960)

144. H. Diehl, H. Clark, H.M. Willard
Inorg. Synth. 1, 186 (1939)

145. G.A.K. Thompson, A.G.Sykes
Inorg. Chem,15, 638 (1976)

146. N.F. Curtis, Y.M. Curtis, H.K.J. Powell
J. Chem. Soc. A, 1015 (1966)

147. L.G. Warner, N.J. Rose, D.H. Busch
J. Am. Chem. Soc. 90, 6938 (1968)

148. N.F. Curtis
J. Chem. Soc. A, 2834 (1971)

149. N.F. Curtis
J. Chem. Soc. 2644 (1964)

150. N. Sadisivan, J.F. Endicott
J. Am. Chem. Soc. 88, 5468 (1966)

151. E. Hart, M. Anbar
The Hydrated Electron
Wiley Interscience (1970)

152. H. Stephen, T. Stephen
Solubilities of Inorganic and Organic compounds.
Pergaman Press, 1963.

153. G. Porter, M.A. West
Flash photolysis in G.G. Hammes (Ed.) Technqiues of chemistry vol VI Part II
Wiley-Interscience 1974 pg 367

154. L.M. Dorfman
Pulse Radiolysis in ibid, pg. 463

155. A.T. Thornton
PhD. Thesis, University of Adelaide (1973)

156. G.S. Laurence, A.T. Thornton
University of Adelaide; unpublished information.

157. H. Taube
Advan. Inorg. Chem. Radiochem 1, 1 (1959)

158. J. Halpern
Quart. Rev. (London) 15, 207 (1961)

159. N. Sutin
Ann, Rev. Nucl. Sci. 12, 285 (1962)

160. N. Sutin
Acc. Chem. Res. 1, 225 (1968)

161. N. Sutin
Chem. Brit. 8, 148 (1972)

162. H. Taube
'Electron Transfer Reactions of Complex Ions in Solution'.
New York Acedemic 1970

163. A.G. Sykes
A.W. Inorg. Chem, Radiochem, 10, 153 (1967)

164. N. Sutin
A, Rev. Phys. Chem. 17, 119 (1966)

165. H. Taube
Pure Appl. Chem, 44, 25 (1975)

166. J.P. Hunt
Coord. Chem. Rev. 7, 1 (1971)
and references therein.

167. R.A. Marcus
Discussions Farad. Soc. 57, 557 (1961)

168. R.A. Marcus
J. Chem. Phys. 44, 679 (1965)

169. R.A. Marcus
Ann. Rev. Phys. Chem. 15, 155, (1964)

170. N.S. Hush
Trans. Farad. Soc. 57, 557 (1961)

171. J.F. Endicott, H. Taube
J. Am. Chem. Soc. 86, 1686 (1964)

172. R.J. Campion, N. Purdie, N. Sutin
Inorg. Chem. 3, 1091 (1964)

173. R.G. Pearson
J. Am. Chem. Soc. 85, 3533 (1963)
and Science 151, 172 (1965)

174. A. Haim
Inorg. Chem. 7, 1475 (1968)

175. R.F. Pasternack
Inorg. Chem. 15, 1475 (1968)

176. A.E. Ogard, H. Taube
J. Am. Chem. Soc. 80, 1084 (1958)

177. D.L. Ball, E.L. King
J. Am. Chem. Soc. 80, 1091 (1958)

178. J.P. Candlin, J. Halpern
Inorg. Chem. 4, 766 (1965)

179. J.P. Candlin, J. Halpen, D.L. Trimm
J. Am. Chem. Soc. 86, 1019 (1964)

180. J.H. Espenson
Inorg. Chem. 4, 121 (1965)

181. B. Baker, M. Orhanovic, N. Sutin
J. Am. Chem. Soc. 89, 722 (1967)

182. M. Orhanovic, N. Sutin
J. Am. Chem. Soc. 90, 4286, (1968)

183. T.J. Przystas, N. Sutin
J. Am. Chem. Soc. 95, 5545 (1973)

184. J.A. Stritar, H. Taube
Inorg. Chem. 8, 2281 (1969)

185. A. Forman, N. Sutin
J. Am. Chem. Soc. 93, 5274 (1971)

186. D.P. Fay, N. Sutin, J. Yandell
J. Am. Chem. Soc. 95, 1131 (1973)

187. D.P. Fay, N. Sutin
Inorg. Chem. 9, 1291 (1970)

188. J.S. Littler, I.G. Sayce
J. Chem. Soc. 2545 (1964)

189. C.E. Castro, H.F. Davis
J. Am. Chem. Soc. 91, 5405 (1969)

190. P. Hambright, E.B. Fleisher
Inorg. Chem. 4, 912 (1965)

191. R.T.M. Fraser
J. Am. Chem. Soc. 84, 3436 (1962)

192. E.S. Gould, H. Taube
J. Am. Chem. Soc. 86, 1318 (1964)

193. E.S. Gould
J. Am. Chem. Soc. 87, 4730 (1965)

194. D.K. Sebera, H.Taube
J. Am. Chem. Soc, 83 1785 (1961)

195. A.A. Frost, R.G. Pearson
'Kinetics and Mechanisms' second addition Wiley, N.Y. 1962

196. R.J. West
PhD. Thesis, University of Adelaide (1973)

197. M.D. Glick, W.G. Schmonsees, J.F. Endicott
J. Am. Chem. Soc. 96, 5661 (1974)

198. G. Stein, A. Treinin
Trans. Farad. Soc. 56, 1393 (1960)

199. B.S. Brunschwig, N. Sutin
Inorg. Chem. 15, 631 (1976)

200. J.F. Endicott, R.R. Schroeder, D.H. Chidester, D.R. Ferrier
J. Phys. Chem. 77, 2579 (1973)

201. D.P. Rillema, J.F.Endicott
Inorg. Chem. 11 2361 (1972)

202. D.P. Rillema, J.F. Endicott
Inorg. Chem. 15, 1459 (1976)

203. M.D. Glick, J.M. Kuszaj, J.F. Endicott
J. Am. Chem. Soc. 95, 5097 (1973)

204. D. Dolphin, T. Niem, R.H. Felton, I. Fujita
J. Am. Chem. Soc. 97, 5288, 1975

205. G.A. Hamilton
'Progress in Bioorganic Chemistry' Ed.E.T. Kaiser, F.J. Kezdy
Wiley N.Y. Vol 1 pg 83 (1971)

206. N.F. Curtis
Chem. Commun. 881 (1966)

207. J. Rabani, W.A. Mulac, M.S. Matheson
J. Phys. Chem. 69, 53 (1965)

208. P. Neta, M. Simic, E. Hayon
J. Phys. Chem. 74, 1214 (1970)

209. M.Z. Hoffman, M. Simic
J. Am. Chem. Soc. 92, 5533 (1970)

210. M. Millar, R.H. Holm
J. Am. Chem. Soc. 97, 6052 (1975)

211. A. Wolberg, J. Manassen
J. Am. Chem. Soc. 92, 2982 (1970)

212. C.F. Wells, M. Husain
Trans. Farad. Soc. 67 760 (1971)
and references therein

213. A. Samuni
J. Phys. Chem. 76, 2207 (1972)
and references therein

214. G. Czapski, A. Samuni
Israel J. Chem. 7, 361 (1969)

215. C. Creutz, N. Sutin
Proc. Nat. Acad. Sci, 72 2858 (1975)

216. A. Samuni, G. Czapski
Israel J. Chem. 8, 551 (1970)

217. C.F. Wells, M. Hussain
J. Chem. Soc. A, 1013 (1970)

218. M.S. Bains, J.C. Arthur, O. Hinojosa
Inorg. Chem. 9, 1570 (1970)

APPENDIX

```
      PROGRAM PHRATE(INPUT,OUTPUT,TAPE5=INPUT,TAPE6=OUTPUT)
      DIMENSION HH(50),H(50),DENOM(50),CH2O2P(50),CHO2(50),CO2M(50)
      DIMENSION OBSK(50),XLOGK(50), PH(50),AH(50)
   10 READ(5,1) EK1,EK2,RK1,RK2,RK3,IPH,N,IND
      IF(N.EQ.1)2,3
    2 READ(5,4) CTOT
    3 CONTINUE
      JPH=2*IPH
      DO 5 I=1,JPH
      HH(I)=10.0**(-I+1)
      AH(I)=-ALOG10(HH(I))
      PH(I)=0.5*AH(I)
      H(I)=10.0**(-PH(I))
      DENOM(I)=1.0+EK1/H(I)+EK2*EK1/H(I)**2
      CH2O2P(I)=CTOT/DENOM(I)
      CHO2(I)=CH2O2P(I)*EK1/H(I)
      CO2M(I)=CHO2(I)*EK2/H(I)
      OBSK(I)=RK3*CH2O2P(I)+RK2*CHO2(I)+RK1*CO2M(I)
    5 XLOGK(I)=ALOG10(OBSK(I))
      PEK1=-ALOG10(EK1)
      PEK2=-ALOG10(EK2)
      WRITE(6,6)PEK1,PEK2,RK1,RK2,RK3
      WRITE(6,7)
      DO 9 I=1,JPH
    9 WRITE(6,8)  PH(I),OBSK(I),XLOGK(I)
      IF(IND.EQ.0) GOTO 10
      STOP
    1 FORMAT(5E10.3,2X,I2,2X,I1,2X,I1)
    4 FORMAT(E10.3)
    6 FORMAT(1H1,//,35X,*PK1 = *,F5.2,/,35X,*PK2 = *,F5.2,//,40X,*RATE K1 = *
     11 = *,E10.3,/,40X,*RATE K2 = *,E10.3,/,40X,*RATE K3 = *,E10.3,///)
    7 FORMAT(30X,*PH*,15X,*OBSERVED RATE*,15X,*LOG(RATE)*,//)
    8 FORMAT(29X,F4.2,16X,E10.3,18X,F5.3)
      END
```

IX. SUMMARY

1.1 The normal mode of oxidation of the bivalent macrocyclic amine complexes is via oxidative dehydrogenation, leading to the introduction of coordinated imine functions into the ligand structure.[30] Chemical oxidations of the 14-membered cyclam series to produce imine unsaturation have been performed under conditions of acidic aqueous medium in the presence of anions having poor electron-transfer bridging character. These reactions, which are believed to proceed via the tervalent state of the metal centre, occur in solution where there is an excess of oxidizing reagent. In the free radical oxidations of the present study, the low oxidant concentration compared with that of the bivalent complex, puts these systems in the same class as the reactions studied by Barefield.[46] In these, solid Ni(III) complexes were dissolved in various solvents and the subsequent changes followed.

1.2 In this free-radical redox study, where no product evidence of further ligand unsaturation was obtained, aspects of Barefield's preceding work were significantly enlarged upon. Of particular interest was the development of the importance of the presence of bridging anion species in soltuion upon the mode of tervalent complex decomposition. The observed rate of the electron-transfer in the anion assisted disproportionation reaction, between the two reactant tervalent nickel macrocycles, was found to be a function of both thermodynamic and kinetic characteristics of the complex-bridge interaction in the activated state. Facile electron-transfer was determined to be dependent on the complex oxidizing power, the bridge oxidizibility, and the degree of orbital symmetry matching of the reactant species in the transition state. The observed trends of the second-order rates, viz $Cl^- < Br^- < N_3^- \sim SCN^-$ for the anions studied, and tam < diene < tetene for the nickel macro-

cycles suggest π-symmetrical character as the important intrinsic parameter to facile transition through the activated state. The observed anion catalysis only by Cl^- for the Cu(III) diene, combined with the satisfactory rate conelation with the nickel complex and Br^- redox couplex, lend strong support to the importance of the thermodynamical factors. Indeed, the kinetic and thermodynamic effects are not totally separable, and the specific arguments tailored to fit the observed trends of reactivity do overlap. However, a composite of each activation factor is capable of explaining the character of the catalytic bridging species in a qualitative way.

1.3 In aqueous solution, in the presence of poor bridging species (Cl^-), the next available means of transient complex decay leads to still different products. Barefield has suggested that slow ligand rupture occurs in acidic solution for the tam complex, which apparently applies in the present study. However, an apparent catalytic effect on this type of ligand degradation derives from the presence of imine functions in the ligand structure. Although this aspect was not thoroughly investigated, it is a further illustration of the diversity of the means of the Ni(III) macro-cycle decay.

1.4 The current evidence therefore suggests that the overall mode of M(II) macrocyclic amine oxidation (and hence the nature of the products) depends on such factors as the relative concentration of oxidant, specific metal-ligand interactions, anion effects, and solvent and medium effects.

2.1 The ability of the OH radical to react at different sites on free organic amines under different medium conditions is known,[208] as is the capability of its reaction at two sites on a coordinated ligand species under one set of reaction conditions.[219] However, the dual

modes of OH attack on both the metal and ligand centred sites of the saturated Ni(II) macrocyclic amines, as proposed in this study, is the only such case yet presented.

Complexation of organic ligand species to metal centres is known to be capable of changing ligand reactivity to radiation induced radical attack. The initiated attack of radiation produced OH radical is generally at the metal centre, with the fate of the oxidized metal deciding the nature of the ligand sensitization or protection.[53,54,78,79,220] Hence, the type of dual OH attack proposed in this study is unusual and is therefore of significance in this important field of radiation chemistry.

2.2 The need for the coordinated nitrogen atom of the Schiff-base macrocyclic complexes to be protonated is the prime requirement when considering the formation of the coordinated ligand radical species. This is the case for the nickel complexes whether the complexed radical intermediate is produced by OH radical attack on the bivalent macrocycle, or by the intra-molecular conversion of the site of oxidation onto the ligand from the tevalent metal centre. In this latter case, Barefield has suggested on equilibrium nature to the pH dependent inter-conversion, which is confirmed in this work. However, the present study shows that the process involves more than the consequent steps of ligand deprotonation (of the secondary amine) and electron-transfer. Direct conversion involving the intermediate formation of an H atom from the tervalent complex appears to be a possibility. The results presented in this work thus expand on the complexity of the process, and offer insight into the types of consequent investigation needed to allow some measure of generalization in this field of metal-ligand electron-transfer.

No evidence has been presented for intra-molecular ligand-to-metal electron-transfer from coordinated amine functions on the tervalent nickel

ammonia,[53] ethylenediamine, and glycine complexes.[54] These Ni(III) complexes decay via disproportionation processes to yield stable oxidized free ligand products. This reactivity trend is the same for the tervalent ammonia and en complexes of copper,[78] but it was found that the amino acid complexes of Cu(III) decayed via an intramolecular LMCT in the first-step to produce a non-coordinated organic radical species. The transfer was presumed to come from the carboxyl group rather than the amino function however. A fast conversion process, believed to be structural rearrangement rather than electron-transfer has been found for the Ni(III) EDTA complex immediately after OH oxidation of the bivalent complex.[56] Hence, it is probable that the observed intramolecular electron-transfer process of the saturated nickel macrocycles is a unique property of their cyclic nature.

2.4 Another interesting aspect of the interconversion process comes from a combination of the results of this work and previously published information.[33,58] Of the saturated macro-cycle systems (in particular the diene complexes) that have been studied in aqueous solution, interchange of the site of complex oxidation, viz $M(III)L \rightarrow M(II)L^{\bullet}$, can be considered to occur for the iron ($d^5 - d^6$) and nickel ($d^7 - d^8$) systems, whilst there is no evidence for this process for the cobalt ($d^6 - d^7$) and copper ($d^8 - d^9$) metal centres. (This type of process is assumed to occur for Cu(III)tam in acetonitrile, however.[44]) These results suggest that the energy barrier to the intra-molecular electron-transfer is probably not thermodynamic, since the available information[30,31,44] suggests that the reduction potentials of the Fe, Co complexes are significantly less than those of Ni, Cu. The activation barrier is most probably related to the intrinsic characteristics of the metal-amine bonds in the cyclic structure. In the Co and Cu systems, higher activation for the reaction may be associated with larger reorganizational

requirements in the metal-ligand bond lengths for the $d^6 - d^7$ and $d^8 - d^9$ exchanges involved.[202]

3.1 The tervalent state of nickel is a moderately powerful oxidant in aqueous solution. Reactions of the tervalent macrocycles with H_2O_2 and Fe^{2+} were observed; Mn^{2+} was oxidized only by the most powerful member of the nickel series, namely the tetene. The specific rate of oxidation of Fe^{2+} was found to be essentially independent of the degree of unsaturation on the macrocyclic ligand. This independence of the rate on the redox potentials of the Ni(III)L complex suggests an inner-sphere path is operative in the electron-transfer, since the Marcus theory[167-169] for an outer-sphere process would predict a rate increase of $\sim 10^3$ from the tam to the tet complex. Since the water exchange rate on Fe^{2+}_{aq} is significantly faster (being $\sim 10^6$ sec^{-1})[166] than the observed rates of oxidation, the results suggest that the water exchange on the tervalent metal centre is rate determining. The rate of water exchange on the Ni(III) macrocycles (presumed to be low-spin by analogy to the iso-electronic Co(II) complexes)[139] can thus be assumed to be of the order of 10^4 sec^{-1}, the rate of observed Fe^{2+} oxidation. Reasonable confirmation of this estimate might be derived from a water exchange study on the stable Co(II) macrocyclic analogues, the rate constants for which are presently unknown. The presumed rate of water exchange of $\sim 10^4$ sec^{-1} on the tervalent nickel complexes is fast enough to confirm the possibility of inner-sphere bridging by anions in the catalyzed disporportionation reactions. The oxidation of H_2O_2 by the Ni(III)L complexes apparently followed the well-established two-step mechanism derived for the oxidation by Ce(IV)[221] in acidic aqueous solution.

3.2 There has been considerable recent interest in the reactivities of O_2^- and HO_2 radicals in systems related to the biologically significant superoxide dismutase.[101] The rigorously studied reactions of the tervalent

Ni and Cu macrocyclic amines with the superoxy radical are the first detailed report of this important radical species reacting with highly unstable metal centres in simple inorganic analogues to the biological tetra-aza macrocyles.

For the systems studied, changes in the observed decay rate of the M(III)L species with pH could be quote satisfactorily correlated with the single acid-base equilibrium of the superoxy radical, viz, $HO_2 \rightleftarrows O_2^- + H^+$. Results in this work suggest the precussor formation of a superoxy-complexed metal macrocycle species prior to the intramolecular electron-transfer. The O_2^- species has been shown to be significantly more reactive towards M(III)L than its protonated analogue HO_2. This has been interpreted as due to large differences in enthalpic barriers to the electron-transfer for the two radical species. An apparent preference of HO_2 to reduce the coordinated ligand radical species on nickel via H-atom transfer, rather than electron-transfer was also observed. In addition to the hydroperoxy radical acting as a facile reduction agent of the oxidized complexes, evidence was found to suggest the ability of this radical to oxidize the Ni(II)tam complex. The dual redox nature of this radical may be of intrinsic importance in its biological redox reactions.

References

219. J.C. Sullivan et al.
Inorg. Chem. 15, 2864 (1976).

220. J.C. Brodovitch et al.
Int. J. Radiat. Phys. Chem. 8, 465 (1976).

221. G. Czapski, B.H.J. Bielski, N. Sutin
J. Phys. Chem. 67, 201 (1963).